State Estimation for Nonlinear Dynamic Systems - Some Contributions

Thesis Submitted

By

Nilanjan Patra

Doctor of Philosophy (Engineering)

Department of Electrical Engineering,
Faculty Council of Engineering &Technology
JADAVPUR UNIVERSITY,
Kolkata-700032, India.

2019

JADAVPUR UNIVERSITY
KOLKATA-700032

Index No. 151/13/E

1. Title of the thesis: "*State Estimation for Nonlinear Dynamic Systems - Some Contributions"*

2. Name, Designation & Institution of the Supervisors:

Prof. SMITA SADHU,
Professor
Department of Electrical Engineering,
Jadavpur University, Kolkata-700 032, India.

&

Prof. TAPAN KUMAR GHOSHAL,
Honorary Emeritus Professor
Department of Electrical Engineering,
Jadavpur University, Kolkata-700 032, India.

3. List of Publication:

International Journal

1. Nilanjan Patra, Smita Sadhu, Tapan Kumar Ghoshal, "Adaptive State Estimation for Tracking of Civilian Aircraft," *IET Science, Measurement & Technology*, Volume 12, Issue 6, April 2018, pp. 777 – 784.

2. Nilanjan Patra, Smita Sadhu, Tapan Kumar Ghoshal, "Performance Evaluation of a Novel Adaptive Variable Structure State Estimator," Journal of Aerospace Engineering ***(Under review)***

3. Nilanjan Patra, Smita Sadhu, Tapan Kumar Ghoshal, "Pragmatics for Tuning State Estimators for a Class of Nonlinear Systems," Transactions of the Institute of Measurement and Control ***(Under review)***

4. Nilanjan Patra, Smita Sadhu, Tapan Kumar Ghoshal, "An Adaptive Minimal Model IMM Estimator for Aircraft Tracking" IET ***(Under review)***

4. List of Patents: Nil

5. List of Presentations in National/International Conferences:

1. Patra, Nilanjan, Smita Sadhu, and Tapan Kumar Ghoshal. "Adaptive state estimation for ballistic object tracking with nonlinear model and state dependent process noise." *IEEE International Conference on Power Electronics, Intelligent Control and Energy Systems (ICPEICES)*. IEEE, 2016

2. Patra, Nilanjan, Smita Sadhu, and Tapan Kumar Ghoshal. "Pragmatics for tuning aircraft tracking estimators." *Power Electronics, Intelligent Control and Energy Systems (ICPEICES), IEEE International Conference on. IEEE, 2016*

3. Patra, Nilanjan, and Smita Sadhu. "Adaptive Extended Kalman Filter for the state estimation of Anti-Lock Braking System." *India Conference (INDICON), 2015 Annual IEEE*, 2015

CERTIFICATE FROM SUPERVISORS

This is to certify that the thesis entitled "*State Estimation for Nonlinear Dynamic Systems - Some Contributions*" submitted by ***Nilanjan Patra***, who got his name registered on *28th March 2013* (*Ref. No.: D-7/E/211/13 dated on 28th March 2013*, Index No. *151/13/E*), for the award of Ph. D. (Engineering) degree of Jadavpur University is absolutely based upon his own work under the supervision of ***Prof. Smita Sadhu*** & ***Prof. Tapan Kumar Ghoshal*** and that neither his thesis nor any part of the thesis has been submitted for any degree /diploma or any other academic award anywhere before.

1.----------

(Signature of the supervisor and date with Office Seal)

Prof. Smita Sadhu,
Professor,
Dept. of Electrical Engineering,
Jadavpur University,
Kolkata, India.

2.----------

(Signature of the supervisor and date with Office Seal)

Prof. Tapan Kumar Ghoshal
Professor,
Dept. of Electrical Engineering,
Jadavpur University,
Kolkata, India

Abstract

This dissertation addresses the problem of state estimation of dynamic systems which remains an active research area. Formally, 'State Estimation' may be defined as a technique to estimate the unmeasured states of a dynamic system by using the model of the system and all or some of the measured (output) variables.

Observers as state estimators, though have been used fairly extensively, suffer from two shortcomings: firstly, the design methods of observers do not take cognisance of measurement noise; secondly, the accuracy of the (state) estimation may be severely affected if the dynamics of the actual system differs from what has been assumed or some of the excitation inputs are inaccessible. These shortcomings are overcome in stochastic state estimators (of which, the Kalman Filter (KF) is considered to be the most well-known). Stochastic state estimators take care of measurement noise by filtering it out to the extent possible and also admit modeling inaccuracies, which are treated as a different variant of noise, called "process noise". Kalman filter and its descendants have built-in mechanisms to trade-off components of estimation error due to measurement inaccuracy and due to process model inaccuracy.

The present work evaluates Kalman filters and its extensions for nonlinear models as well as their adaptive counterparts for practical problems and also proposes novel extensions. The nonlinear counterparts of KF include Extended Kalman Filter (EKF), Unscented Kalman Filter (UKF), Central Difference Filter (CDF), Divided Difference Filter (DDF), Gauss Hermite Filter (GHF). The present work also employs variants and extensions of *Variable Structure Filter* (VSF).

In particular, adaptive nonlinear state estimators such as Adaptive Extended Kalman Filter (AEKF), Adaptive Unscented Kalman Filter (AUKF), Adaptive Divided Difference Filter (ADDF) and Adaptive Gauss Hermite Filter (AGHF) have been evaluated for aircraft tracking scenarios under model uncertainty and unknown noise statistics. Evaluations are carried out with fairly extensive Monte Carlo simulation and with a number of numerical metrics like time averaged RMS error, peak RMS error and rms of RMS error. For qualitative appreciation, time plots of RMS errors are also provided.

The following modified and improved nonlinear state estimators have been proposed, characterized and evaluated (by cross-comparisons of performance) for civil aircraft tracking scenarios. These are: (i) A sigma point variant of Smooth Variable Structure Filter (SVSF) (ii) An adaptive version of Smooth Variable Structure Filter (ASVSF) (iii) An adaptive version of Interacting Multiple Model Filter (AIMM).

Monte Carlo simulation and the metrics mentioned above have been used for evaluating the proposed novel filters. Performance of the proposed enhanced state estimators have been compared with the existing EKF, UKF, DDF, GHF, SVSF and Interacting Multiple Model (IMM) state estimator.

Salient contributions of the work of this dissertation are summarised as follows:

- A systematic survey of current literature on nonlinear state estimation, including adaptive state estimator and variable structure state estimators were done. Also carried out a systematic study of the estimation of aircraft tracking scenarios which involve mode switching between linear and non-linear models.

- The estimation performance of some standard linear and non-linear state estimators have been characterised, evaluated and benchmarked against, for single model adaptive estimator in tracking scenarios.

- Evaluation of Adaptive nonlinear state estimators such as AEKF, AUKF, ADDF and AGHF has been carried out for tracking scenarios under model uncertainty and unknown noise statistics.

- The following modified, enhanced and improved nonlinear state estimators have been proposed, characterized and evaluated (by cross-comparisons of performance) for civil aircraft tracking scenarios/ These are:

    i. A sigma point variant of Smooth Variable Structure Filter (SVSF)

    ii. An adaptive version of Smooth Variable Structure Filter (ASVSF)

    iii. An adaptive version of Interacting Multiple Model Filter (AIMM)

Acknowledgment

I take this opportunity to express my deepest gratitude to my supervisors Professor Smita Sadhu and Professor Tapan Kumar Ghoshal for their continuous support, patience, advice and encouragement during the whole period of my Ph. D. work and the writing of this dissertation.

I am extremely thankful to all the members of the respected Doctoral Committee for the valuable internal reviews and suggestions they provided regarding the work which was pivotal in giving a perfect blend to the thesis.

I am grateful to the Head of the Electrical Engineering Department for providing the necessary laboratory (Centre for Knowledge Based System) and library facilities during my course of work. I would like to extend my heartfelt gratitude to all faculty and non-teaching staffs of this department for their helpful attitude and constant encouragement.

The entire work of this dissertation has been supported and funded by Council of Scientific & Industrial Research (CSIR), India.

I express my heartfelt gratitude to Late Professor Kalyankumar Datta for motivating me to start my Ph. D. work.

I am thankful to my colleagues Sayanti Chatterjee, Aritro Dey, Manasi Das, Sudeshna Dasgupta, Rudrashish Majumdar for their love and support.

I would like to make special mention and thank Rajiv Mishra and Avijit Sur for their constant support and encouragement.

I would also like to express my gratitude to my parents, Narendranath Patra and Niyati Patra and brother, Nirvik Patra for their constant support throughout my career. Without loving support of my fiancée Swagata Maji this work would not have been possible.

Table of Contents

List of Figures

List of Tables

1 Introduction

1.1 Background

The problem of state estimation of a dynamic system remains an active research area in the domain of control systems since about half a century. A state feedback controller needs the information of the states of the system to be controlled. However, only a subset of the states could be directly available by measurement. This is because of the cost, physical accessibility and/or space constraints. To utilize the design freedom of state feedback based control, the non-measured states need to be estimated and made available to the controller to apply such control laws. State estimators have been found to be very useful for controlling many complex plants like chemical process, spacecraft, ships, manufacturing process etc.

More formally, 'State Estimation' may be defined as a technique and implementation to estimate the unmeasured states of a dynamical system by using the dynamic model of the system and all or some of the measured (output) variables specific algorithms are required to "reconstruct" the states.

State estimators may be broadly classified into deterministic and stochastic. Deterministic state estimators, generally called (state) observers do not specifically take into account the fact that measurements may often be noisy. Luenberger observer (Ogata and Yang 2002) is a popular state estimator for linear systems whereas 'sliding mode observers' (Floquet, Edwards and Spurgeon 2007) and 'Walcott-Zak observers' (Xiang, Su and Chu 2005) are well known nonlinear observers. Most state observers themselves are (simulated) dynamic systems which are excited by functions of estimation error as shown in (Ogata and Yang 2002).

Observers as state estimators, have been used extensively though they have some shortcomings. The first one alluded above is that the design methods of observers do not take cognizance of measurement noise. The second one is that observers are designed based on a defined (nominal) model of the system dynamics (say a nominal state variable model), further, the excitation input to the system needs to be used by the observer. The accuracy of the (state) estimation may be severely affected if the dynamics of the actual system differs from what has been assumed or some of the excitation inputs were inaccessible. Observer design steps do not generally have inbuilt mechanisms to take care of inaccurate model of the dynamic systems. It is generally accepted that some trade-off mechanism is required to balance the component of estimation error due to measurement inaccuracy and the component for process model inaccuracy. In other words, some optimization is required.

Stochastic state estimators intrinsically take care of measurement noise and reduce such disturbances which are 'filtered out' probably, for this reason, state estimators are also called "filters". With such filtering, the performance of state feedback based controllers generally improves.

Further, stochastic state estimators can also admit modeling inaccuracies, which they treat as a different variant of noise, called "process noise".

Kalman Filter (KF) (R. E. Kalman 1961) is considered to be most well-known and also one of the best optimal state estimator for linear systems in presence of noisy measured data and inaccurate process model (Grewal 2011). A salient feature of Kalman Filter and its 'descendants' is the modeling and quantification of the inaccuracy in the process model by the so-named 'process noise' and its covariance respectively, as mentioned above. This feature would be discussed and utilized rather extensively in the present work. Though a time-continuous domain description of Kalman filter is available, the more popular version is the discrete time domain (Simon 2006) (Anderson and Moore 1979) (Grewal 2011). In this dissertation, only the discrete time form of the Kalman and succeeding filters would be discussed. It may be noted in passing that the Kalman filter has also been used for interpolation, smoothing and prediction of data sequences (like future courses of dynamic systems like trajectories of celestial bodies, prices of traded commodities, flows of the river during flood etc. (Zarchan 2005) (Grewal 2011) .

Extensions of Kalman Filter have occurred in several directions, namely, for robust filtering (Xie, Chai Soh and Souza 1994) (Xie and Chai Soh 1994) (Gandhi and Mili 2010), for adaptive filtering (Das, et al. 2015) (Das, Sadhu and Ghoshal 2013) (Dey, Sadhu and Ghoshal 2014) (Dey, Sadhu and Ghoshal. 2013), for coordinating distributed measurement (federated Kalman filter) and also for nonlinear plants by the so-named Extended Kalman Filter (EKF) (Felter 1990).

In the direction of extension of Kalman Filter for nonlinear plants, several extensions of the KF are available in the literature, some of which are enumerated in the following table.

Table 1.1 Extensions of Kalman Filters

	Estimators	Proposed by	Text Book/ Recent publication
1	Unscented Kalman Filter UKF	Julier and Uhlman (Julier and Uhlmann 1997)	(Ristic, Arulampalam and Gordon 2004)
2	Central Difference Filter, CDF/DDF-1	Tor Steinar Schei (Schei 1997)	(NøRgaard, Niels K, & Ravn, 2000)

3	Divided Difference Filter DDF-2	NøRgaard, Niels K, & Ravn (NøRgaard, Niels K, & Ravn, 2000)	(Ahmadi, Khayatian and Karimaghaee 2012)(NøRgaard, Niels K, & Ravn, 2000)
4	Gauss Hermite Filter (GHF)	Kazufumi Ito and Kaiqi Xiong (Ito and Xiong 2000)	(Ito and Xiong 2000)
5	Gaussian Sum Filter QKF	Alspach, Daniel, and Harold Sorenson. (Alspach 1972)	(Arasaratnam, Haykin and Elliott 2007)
6	Cubature Quadrature filter (CQF)	Ienkaran Arasaratnam and Simon Haykin (Arasaratnam and Haykin 2009)	(Jia, Xin and Cheng 2013) (Bhaumik 2013)

Apart from the above, several more approaches have been suggested to improve the accuracy of such estimators (i) to increase the robustness (ii) for a system with grossly inadequate modeling information etc.

The present work also employs variants and extensions of Variable Structure Filter (VSF) and adaptive state estimators, discussed briefly below.

Sliding mode observers (Floquet, Edwards and Spurgeon 2007), based on the concept of Sliding Mode Control (Utkin 1993) have been found to possess robustness against modeling errors but do not explicitly take care of measurement noise. Another variant called VSF (Habibi, Burton and Chinniah 2002) is structured in the predictor-corrector format (like Kalman Filtering technique) for the robust state estimation of dynamic system. It was first introduced in the literature in 2002 (Habibi and Burton 2002) for linear discrete-time system and has been subsequently extended in other publications discussed in later chapters.

Adaptive State Estimators (Mohamed and Schwarz 1999) are useful when the process noise covariance or/and measurement noise covariance. Recently some extensions of adaptive estimators for nonlinear systems have also been published (Cao and Kai 2016) (Das, et al. 2015).

The literature survey chapter of this dissertation will review some of the above types of nonlinear filters with adaptivity and/or robustness as also some applications.

Such estimators are used in numerous complex applications, such as object tracking, control and navigations, guidance, fault-tolerant systems, automotive system etc. to estimate state and parameters.

1.2 Motivation

The original broad motivation of the present worker had been to contribute to the body of knowledge in nonlinear state estimation specifically for cases where the model error is present i.e. knowledge of the process is not accurately known. This is because a number of nontrivial and interesting applications could be found in literature where an accurate model of the plant is not available. The unknown and inaccurate process models in such cases have been characterized by state variable models with unknown parameters and/or unknown process noise covariance.

Regarding inaccurate model, there could be two possible situations; in first case an accurate model is too complex and unwieldy for state estimation, in second case the dynamics of the plant cannot be completely modeled due to the very nature of the problem. Example of the second type of situation is tracking of manned (by a remote pilot or a pilot in the cockpit) aircraft where the inputs by pilots cannot be modeled a priori. Though one may try out "unknown input observers" for such situations, practical applications do not seem to favor such approach due possibly to the inherent shortcomings of nonlinear observers.

For systems with unknown process noise, the classical approach had been to manually tune the state estimators. To explore this approach, a systematic tuning exercise was carried out on Kalman filters for aircraft tracking scenario (as described in a later chapter) which provided some valuable insight into the tracking problem. From the study, it has been found that proper tuning of process noise covariance (Q) is required to handle model error or uncertainty to improve estimation accuracy. This motivated the present worker to study and explore the possibility of using Q-adaptive state estimators to handle such a situation.

In the course of literature survey, further interesting patterns emerged. In contrast to linear problems, tuning of nonlinear estimators appeared to be rather problematic. On the other hand, adaptive estimators which automate the tuning process did not appear to be as developed as linear adaptive estimators. So designing nonlinear adaptive observers suited to the particular application also appeared to be challenging.

Adaptive Extended Kalman Filter (AEKF) (Almagbile, Jinling, & Weidong, 2010). (He, Xiong, Zhang, Sun, & Fan, 2011), Adaptive Unscented Kalman Filter (AUKF) (Jiang, Song, He, & Han, 2007) (Song & He, 2009), Adaptive Divided Difference Filter (ADDF) (Dey, Sadhu and Ghoshal. 2013) (Das, Sadhu, & Ghoshal, 2013) are some of the nonlinear adaptive filters exist in the literature. These nonlinear adaptive estimators are single model adaptive estimators which adapts noise covariance automatically.

Further, the aircraft tracking problem is also considered from the viewpoint of hybrid systems where the plant model varies following unknown sequences. Hybrid systems are generally defined by a known or unknown sequence of modes, each having potentially different dynamics. An Aircraft tracking system with an unknown sequence of mode changes (or a switched system) suffers from a more complex form of model uncertainty and poses further challenges.

Several approaches have been taken for such system whose states are to be estimated. Interacting Multiple Model (IMM) (Bar-Shalom, Chang, & Blom, 1989) state estimator is one of the popular state estimators for such switched system (or, Hybrid system). IMM estimators are sometimes referred as multiple-model (adaptive) state estimators. Also, several types of other multiple-model (adaptive) state estimators have been proposed and evaluated for tracking aircraft targets. Subsequent to the maturity of the Interactive Multiple Model algorithm several types of new nonlinear estimators have been proposed. Some of these estimation algorithms are claimed to be robust. Other estimators can apparently be cast in the form of single model adaptive state estimators. However, such recently proposed nonlinear state estimation methods have not been sufficiently characterized for systems with inadequate or inaccurate dynamic model or for hybrid systems.

Thus the above challenges and "grey areas" in nonlinear state estimation for hybrid systems with inaccurate dynamic model motivated this worker to carry out further research so as to be able to make non-trivial contribution in this area.

1.3 Objective

The objective of the present work may be articulated as follows:

1. To evaluate existing nonlinear state estimators like robust (e.g. SVSF) state estimators, single model adaptive estimators and Interactive Multiple Model (IMM) estimators for (hybrid) systems with inaccurate process model as exemplified by maneuvering aircraft tracking problems.

2. To enhance SVSF and IMM estimators so as to obtain better state estimation performance.

3. To evaluate and compare the performances of the enhanced estimators with the already reported state estimators mentioned in (1) above.

1.4 Contribution

Salient contributions of the work of this dissertation are as follows:

- A systematic survey of current literature on nonlinear state estimation, including adaptive state estimator and variable structure state estimators. Also carried out a systematic study of the estimation of aircraft tracking scenarios which involves mode switching between linear and nonlinear models.

- The estimation performance of some standard linear and nonlinear state estimators have been characterized and evaluated and benchmarked against for single model adaptive estimator in tracking scenarios.

- Evaluation of Adaptive nonlinear state estimators such as AEKF, AUKF, ADDF and AGHF has been carried out for tracking scenarios under model uncertainty and unknown noise statistics.

- Following modified, enhanced and improved nonlinear state estimators have been proposed, characterized and evaluated (by cross-comparisons of performance) for civil aircraft tracking scenarios. These are:

    i. A sigma point variant of Smooth Variable Structure Filter (SVSF)

    ii. An adaptive version of Smooth Variable Structure Filter (ASVSF)

    iii. An adaptive version of Interacting Multiple Model Filter (AIMM)

1.5 Organization

Rest of this dissertation is organized as follows:

The literature survey is presented in the next chapter. The 3rd chapter discusses model and case studies. Existing adaptive Q Adaptive Filters are evaluated with the case studies in the 4th chapter. Algorithm of Sigma-Point Variable Structure Filter was presented in chapter-5. Adaptive Smooth Variable Structure Filter is presented in the 6th chapter. Adaptive Interacting Multiple Model is presented in chapter-7. Conclusion and discussions of the work are given in the last chapter. Appendix section provides (i) pragmatics for process noise tuning in linear and nonlinear estimators (ii) parameter estimation by linear and nonlinear state estimators.

2 Literature Survey

2.1 Chapter Introduction

This chapter provides a brief review of recent literature on state estimators and also selected problem domains, both of which form the core of the present work. Established state estimation methods available in textbooks are mostly skipped and the emphasis has been on nonlinear Adaptive and Robust estimators.

After a subsection on general aspects of nonlinear state estimation, adaptive state estimators are surveyed in the next section, which is followed by Variable Structure Filters in section 2.3. Interacting Multiple Model (IMM) state estimators are covered in section 2.4. and problems of tracking of maneuvering targets are reviewed in the section 2.5. Finally, salient findings from the survey have been mentioned in section 2.6.

2.1.1 Problem Formulation

State estimation is carried out on the basis of known, nominal or approximate dynamic model of the plant or system. The objective, of course is to estimate the values of the state variables at time instants, given the sequence of measurements up to the present.

For linear systems, the equations describing the system take the form:

$$x_{k+1} = F_k x_k + G_k\left(u_k + w_k\right) \tag{2.1.1}$$

$$y_k = H_k x_k + v_k \tag{2.1.2}$$

where, $x_k \in R^{n_x}$ is the continuous vector-valued state vector at time step k and $y_k \in R^{n_y}$ is the vector-valued noisy measurements at each time step k. The vector $u_k \in R^{n_u}$ represents the (known, deterministic) input u_k. The uncorrelated white Gaussian process and measurement noise are represented as $w_k \in R^{n_u}$ and $v_k \in R^{n_y}$ with their covariances Q_k and R_k respectively.

The optimal state estimators for such system is the well-known Kalman Filter (Simon, 2006) (Grewal, 2011). Literature survey about state estimation must begin with the recursive Kalman filter which may be shown to be optimal for the linear model with Gaussian noise. Even for non-Gaussian noise, a KF happens to be the best linear filter (Anderson & Moore, 1979). Target tracking community had earlier

used weaker forms of KF called alpha-beta filter, alpha-beta-gamma filter (Brookner, 1998) and fading memory filter. Though proposed in 1960, the Kalman filter is still popular as a practical and viable method for many systems which were not strictly within the linear Gaussian domain.

For linear systems with Gaussian noise, the estimated states would also have a Gaussian distribution. This permits description of the estimate in terms of mean, which is called "the estimated value of state" and the covariance which is called error covariance P.

The commonly used nonlinear discrete state equation with additive inputs is represented as

$$x_{k+1} = f_k(x_k) + g_k(u_k, w_k) \tag{2.1.3}$$

$$y_k = h_k(x_k) + v_k \tag{2.1.4}$$

The functions $f_k(\bullet), g_k(\bullet,\bullet), h_k(\bullet)$ may depend on the time step *k*. For time-invariant functions, the subscripts may be omitted. In subsequent developments, the known input u_k is omitted.

The generic family tree for state estimators is shown in Fig 2.1, which is applicable to both linear and nonlinear systems. The first branch of the tree is called 'known model'. Here, both the plant dynamic model and the noise statistics are assumed to be known. The other branch includes situations where the plant dynamic model is approximate and/or noise statistics are not known. The unknown model situation may be handled by one of the alternatives, viz., robust filters and adaptive filters. Robust filters may produce acceptable state estimation even if the modeling (both dynamics and noise model) is inaccurate. Adaptive filters, on the other hand, adjust filtering parameters (as in single model adaptive filters) or equivalent means (as in multiple model adaptive filters) to evolve and provide an acceptable estimation.

While the adaptive and robust filters would be discussed in greater details in subsequent sections of this chapter, we continue this discussion assuming the model and the covariances are known. It may be pointed out that nonadaptive (single model) estimators form the kernel of most adaptive estimators (Fig 2.3). Hence these are very briefly reviewed before taking up robust and adaptive filters.

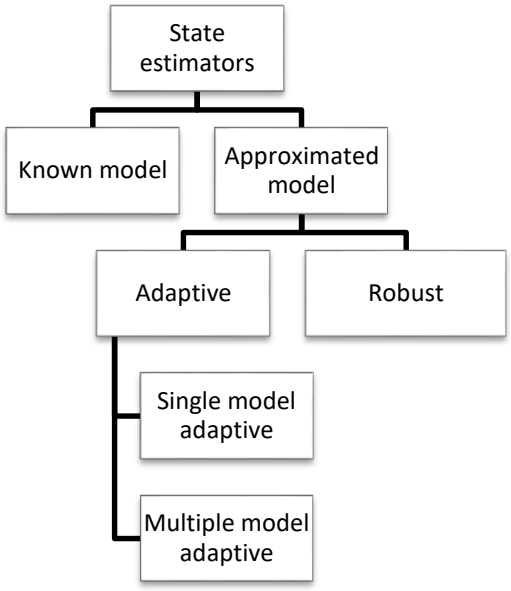

Figure 2.1 Generic family tree for state estimators

2.1.2 General Aspects of Nonlinear State Estimators

Even when the parameters of the dynamics and the noise statistics are known, nonlinear system poses several other problems. Firstly, for nonlinear systems even with Gaussian noise, the probability distribution of the error is usually non-Gaussian. This must be taken into account in state estimator for nonlinear systems. Secondly, the steps of state estimation are more involved as shown below.

As the probability distribution of error is most likely to be non-Gaussian, one should strictly know the probability distribution by applying the Bayes' Theorem. In fact, many of the nonlinear state estimation methods, especially the numerical integration based types may be appreciated in the light of Bayes' Theorem (Anderson & Moore, 1979) (Ristic, Gordon, & Arulampalam, 2004) (Afshari, 2014). Though Kalman filter may be derived without taking recourse to the Bayes Theorem, it may be shown that KF may also be derived, albeit more rigorously, from Bayes' Theorem.

With Bayesian paradigm the state estimation problem is formulated as the determination of conditional a posteriori probability density of the states denoted by $p(x_{k+1} \mid Z_{k+1})$, where $Z_{k+1} = \{y_1, y_2, \ldots, y_{k+1}\}$ is the sequence of noisy measurements. This can be recursively carried out in two steps using the state *a priori* PDF $p(x_k \mid y_k)$. {Starting with the initial PDF of the state $p(x_0) = p(x_0 \mid y_0)$}. The two steps are variously known as prediction and update or time projection and measurement update. The time update of the PDF for the estimated state is given by the Chapman-Kolmogorov equation as

$$p(x_{k+1} \mid Z_k) = \int p(x_{k+1} \mid x_k) p(x_{k+1} \mid Z_k) dx_k \quad (2.1.5)$$

Note that for Kalman filter, as the distribution is known to be Gaussian, the above step consists of time update of mean and covariance $x_{k+1|k}$ and $P_{k+1|k}$.

The first term in the above integrand can be obtained using the system model. The second term is obtained from the previous (k^{th}) step following the process shown below.

The measurement update step can be obtained from

$$p(x_{k+1} \mid Z_k) = \frac{p(Z_{k+1} \mid x_{k+1}) p(x_{k+1} \mid Z_k)}{p(Z_{k+1} \mid Z_k)} \quad (2.1.6)$$

The first term in the numerator is the likelihood function and can be obtained from the measurement equation. The second term in the numerator is the time update PDF described above whereas the denominator is the normalizing constant given by

$$p(x_{k+1} \mid Z_k) = \int p(Z_{k+1} \mid x_{k+1}) p(x_{k+1} \mid Z_k) dx_k \quad (2.1.7)$$

From the above *a posteriori* PDF, a theoretically optimal state estimate may be computed by minimum mean square error (MMSE) method (Ristic, Gordon, & Arulampalam, 2004) (Afshari, 2014) or by maximum *a posteriori* (MAP) method.

However, the integration involved in Bayes Theorem for nonlinear systems often become intractable, and approximations may have to be carried out to perform those integrations. A very powerful method of state estimation which has almost no restrictions has recently been proposed and it goes by the name of particle filters (Ristic, Gordon, & Arulampalam, 2004). Another closely related method is approximate grid based filters (Bhaumik, 2013). In this literature survey, we would skip discussions about these two types of state estimators which are extremely numerically intensive (except for in the context of some applications) and not suitable for on-board applications.

Approximations may be carried out by adopting one of several possible approaches. The first approach is local linearization where the nonlinear equation is approximated by a few terms of Taylor series or equivalent methods like Sterling interpolation formula (Ito & Xiong, 2000). This approach assumes that the distributions remain close to Gaussian despite such nonlinearity and leads to several estimation techniques such as the extended Kalman filter (EKF), and the central difference filter (CDF). Simplest

among this class is EKF (Simon, 2006) (Ristic, Gordon, & Arulampalam, 2004) and its variants like second order EKF (Simon, 2006) (Anderson & Moore, 1979), iterated EKF (Ristic, Gordon, & Arulampalam, 2004), linearized approximation (Brown & Hwang, 1992).

Another approach is approximating the non-Gaussian PDF into a sum of several Gaussian PDFs. This class of filter is known as the Gaussian sum filter. In Gaussian sum filters (Anderson & Moore, 1979), the posterior densities are approximated by a series of Gaussian distributions with different covariances. A version of the same is called statistically linearized filter (SLF) (Sarmavuori & Sarkka, 2012). The third alternative is carrying out a numerical integration by deterministic or statistical approximations.

Nonlinear filters with known model may be classified in many different ways (Ristic, Gordon, & Arulampalam, 2004) (Afshari, 2014) but for the present literature survey, the classification (which is different from other publications) as in Fig 2.2 would be more appropriate. The simplest among this class is the function approximation based filter. The "function" might mean the combination of the state model and the measurement model. approximation of this "function" corresponds to the previously described EKF family and the DDF family. The "function" may also mean the probability distribution function and the approximation for the same may be carried out with the help of so-named sigma point (Julier & Uhlmann, 1996) (Julier & Uhlmann, 1997) (Julier, Uhlmann, & Durrant-Whyte, 2000) (Julier S. J., 2002) . It has been shown (Lefebvre, Bruyninckx, & Schuller, 2002), (Lefebvre, Bruyninckx, & Schutter, 2004)that both these forms are equivalent and the sigma point filters are, in effect, statistical linear regression of the state and measurement dynamics and the common term linear regression Kalman filter (LRKF). Accordingly, in this survey, no distinction would be made between LRKF and sigma point Kalman filter (SPKF) families.

It may be noted that LRKF/SPKF types of state estimators had been introduced to overcome the main drawbacks of EKF and EKF family-based approaches viz., the requirement for calculating derivatives, filter divergence, inconsistency (Zarchan, 2005) including optimistic estimation of error covariance. Accordingly LRKF/SPKF groups of estimators are also called derivative free (NøRgaard, Niels K, & Ravn, 2000) nonlinear state estimators. According to (Sarmavuori & Sarkka, 2012), many of such LRKF based methods can also be interpreted as numerical approximations to the statistically linearized filter (SLF). Another possible approach is by extending the SLF method as in Fourier-Hermite Kalman filters (Sarmavuori & Sarkka, 2012) to improve estimation accuracy for more severe nonlinearity.

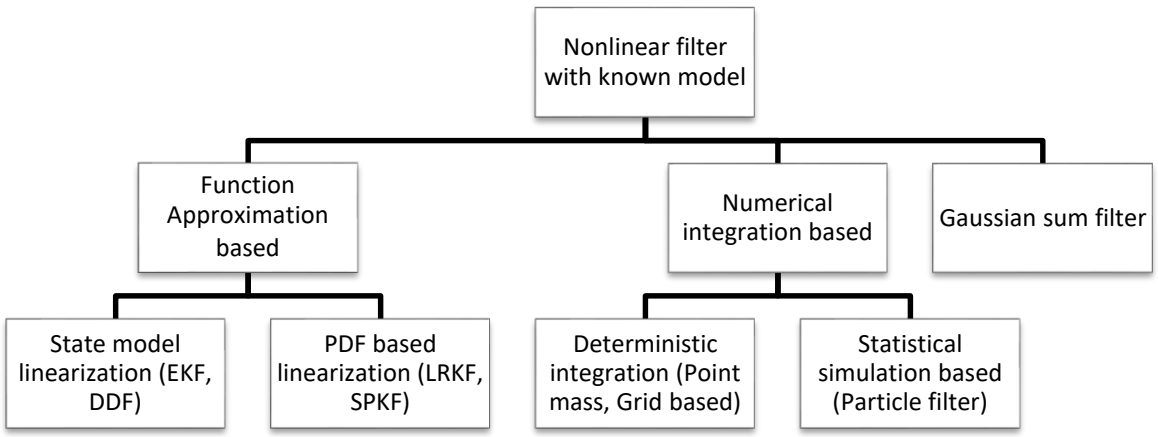

Figure 2.2 Nonlinear filters with known model

Not included in the family tree is (a) variable structure filter (VSF) including smooth variable structure filter (SVSF) (b) ordinary multi-model filters (Li & Bar-Shalom, 1993) (Mazor, A., Averbuch, & Dayan, 1998)and interacting multiple model (IMM) filters. Interestingly, both types of multiple model filters are sometimes called "variable structure filter" (Gadsden, Habibi, & Kirubarajan, 2014) (Gadsden, Habibi, & Kirubarajan, 2012)and "adaptive filter" (Das, Sadhu, & Ghoshal, 2013) (Dey, Das, Sadhu, & Ghoshal, 2015).

2.2 Adaptive State Estimation of Nonlinear Systems

Adaptive state estimators are generally designed to adapt the parameters used in the estimator's algorithm according to the unwanted changes in the actual systems or measurement. Plant noise, or process noise and measurement noise have been major consideration for optimal filters like Kalman Filter. The adaptive state estimators are focused to adapt the mainly the noise statics of process and measurement.

Broadly adaptive filters are classified into two categories: (i) adaptation of noise statistics and (ii) adaptation of the structure of estimators also called Multiple Model Estimator

The noise adaptations are done based on (a) innovation or (b) residual. The method is applied to estimate the noise covariances of the measurement or the system. To realize that, a moving window is set to store the previous instances of the sequence of innovation or residual to calculate the estimated noise covariances. Some methods are available to adjust process and measurement noise based on fuzzy logic.

On the other hand, Multiple Model Estimators are based on more than one filter running in parallel in different mode to match the statistical information of the truth model.

However, in this work the adaptive state estimators are basically referred to adapt the unknown or inaccurately known noise statistics only.

Figure 2.3 Generic diagram for an adaptive filter

2.2.1 Process noise and measurement noise adaptation

2.2.1.1 Linear Estimators

In (Sage & Husa, 1969) some preliminaries algorithms for linear adaptive state estimators are reviewed. In 1972, R K Mehera explains the four categories of adaptive estimators: Bayesian, maximum likelihood (ML), correlation and covariance matching (Mehra R. , 1972). Also in (Mehra R. , 1972) new algorithms of adaptive estimation of optimal Kalman Gain when process noise covariance (Q) is not known accurately have been proposed. An Adaptive Extended Kalman Filter was proposed in (Maybeck, Jensen, & A. Harnly, 1981) for target tracking applications. Next year, in (Stallard, 1982) process noise adaptation for Kalman Filter was demonstrated and evaluated in a Ship tracking case. An approach of robust estimation of Kalman Filter by noise covariance adaptation was presented in (Tsai & Kurz, 1983). ML-based process and measurement noise covariance estimation for Extended Kalman Filter to estimate the attitude of spacecraft were presented in (Mehra, Seereeram, Bayard, & Hadaegh, 1995). Adaptive Kalman filtering for linear system was summarised and applied to Inertial Navigations System in (Mohamed & Schwarz, 1999).

2.2.1.2 Nonlinear and Sigma Point estimators

Adaptive Extended Kalman Filter was experimentally validated for localization of mobile robot in (Jetto, Longhi, & Venturini, 1999) . R-Adaptive Extended Kalman Filter was applied to estimate the state of the charge of lead-acid batteries in (Han, Kim, & Sunwoo, 2009). Evaluation of the performance

of residual and innovation based adaptive Kalman filter for R and Q based on ML and scaling factor provided in (Almagbile, Jinling, & Weidong, 2010).

Applications of adaptive EKF to estimate state of charge in lithium battery are found in (He, Xiong, Zhang, Sun, & Fan, 2011), (Xiong, H., F., & K, 2013), (Xiong, X., C. C., & F, 2013), (Sepasi, Ghorbani, & Yann Liaw, 2014).

The extension of noise statistics adaptation to the nonlinear sigma point filters such as Unscented Kalman Filter (UKF) was presented in (Jiang, Song, He, & Han, 2007) . Fading factor based adaptive Unscented Kalman Filter was presented in (Soken & Hajiyev, 2009). Some nonlinear applications of adaptive Unscented Kalman Filter were found in (Han, Song, & and He, 2009), (Song & He, 2009), (Wu, Ma, & Tian, 2010), (Bisht & Singh, 2014), (Partovibakhsh & Liu, 2015), (Zhang, Shi, & Ma, 2015), (Dróżdż & Szabat, 2016), (Cao & Kai, 2016). Joint estimation of state and parameter for a nonlinear system with Q-adaptive Divided Difference Filter (ADDF) was proposed by (Dey, Sadhu, & Ghoshal., 2013). Residual and innovation based adaptive sigma point filters, AUKF and adaptive Central Difference Filter (ACDF) were evaluated in (Das, Sadhu, & Ghoshal, 2013). The adaptive Gauss Hermite Filter was proposed by (Dey, Sadhu, & Ghoshal, 2014) to estimate time-varying parameter of the system with unknown process noise. Adaptive Square-Root Cubature–Quadrature Kalman Particle Filter was proposed by (Kiani & Pourtakdoust, 2014) for satellite attitude determination using vector observations. The extension of noise covariance adaptation to Unscented Information Filter was presented in (Dey, Das, Sadhu, & Ghoshal, 2015). R adaptive CDF was proposed in (Das, Dey, Sadhu, & Ghoshal, 2015) for state and parameter estimation of ballistic target tracking problem for unknown measurement noise.

2.2.1.3 Some Recent developments

An enhanced adaptive unscented Kalman filter (AUKF) based on adaptive Kalman filter combined with particle swarm optimization for fault detection of actuators onboard satellites, proposed in (Rahimi, Dev Kumar, & Alighanbari, 2015). A new covariance matching based AUKF for INS/GNSS system for adaption of process noise was presented in (Meng, Gao, Zhong, Hu, & Subic, 2016). An estimation scheme based on AUKF and least-square support vector machines (LSSVM) was proposed in (Meng, Luo, & Gao, 2016) to estimate the state-of-charge of lithium polymer battery. A novel robust Masreliez–Martin UKF which can provide reliable state estimates in the presence of both unknown process noise and measurement noise covariance matrices was proposed in (Li, Sun, Jia, & Du, 2016). A hybrid robust fault tolerant control based on adaptive joint unscented Kalman filter for robotic manipulator was presented in (Hagh, Asl, & Cocquempot, 2017). A new approach was proposed in

(Rahimi, Dev Kumar, & Alighanbari, 2017) for improving parameter estimation with adaptive unscented Kalman filter by adapting the covariance matrix to the faulty estimates using innovation and residual sequences combined with an adaptive fault annunciation scheme.

2.2.2 Multiple Model State Estimator

Multiple Model (MM) state estimators were introduced to adapt structural and parameter changes in the system. Multiple Model estimation algorithms (Jitendra K, 1982) had a fixed structure initially. The approach is a model based hybrid state estimation technique where more than one model is used in the filter algorithm for state estimation of a dynamical system whose behaviour changes rapidly. The Interacting Multiple Model (IMM) estimator consists of running a standard filter for each model (mode), a model probability evaluator, and an estimate combiner at the output of the filters. Each filter of IMM uses a mixed estimate at the beginning of each cycle (Bar-Shalom, Chang, & Blom, 1989). Detailed literature survey of IMM is given in the section 2.4.

2.3 Variable Structure State Estimators

2.3.1 Early forms of V S State estimators

Based on the concept of variable structure observers the so-named Variable Structure Filter (VSF) were introduced 2002 (Habibi, Burton, & Chinniah, 2002). The departure from the observer format was characterized by two important criteria. (i) Recognition of process noise and measurement noise in the plant. (ii) The filter algorithm cast into the familiar predictor-corrector format (like Kalman Filtering technique). This type of filter was described in (Habibi, Burton, & Chinniah, 2002) (Habibi & Burton, 2002) for a linear discrete-time system.

The main objective was to estimate the states of a linear dynamical system from noisy measurements and also in the presence of process noise. VSF assumes the noise sequences of the system are uncorrelated but the theory doesn't prescribe to be normal distributions. The problem is described by the following set of the equation where w_k and v_k represent respectively process and measurement noise sequences. The discrete variables x_{k+1}, z_k, as also the matrices *A*, *B* and *C* have their usual meanings.

$$x_{k+1} = Ax_k + Bu_k + w_k \tag{2.3.1}$$

$$z_k = Cx_k + v_k \tag{2.3.2}$$

Like Kalman Filter it uses a similar strategy of using *a priori* $\hat{x}_{k|k-1}$, *a posteriori* $\hat{x}_{k|k}$ states and *a priori* measurement $\hat{Z}_{k|k-1}$ for the calculation of gain $K_{k+1|k+1}$ for corrections for a given linear system described in Equation.

$$Kalman\ gain:\ K_{k+1|k+1} = P_{k+1|K} H^T \left[H P_{k+1|K} H^T + R \right]^{-1} \tag{2.3.3}$$

$$VS\ gain:\ K_{k+1|k+1} = \left(YC^{-1} \left| e_{z\,K+1|k} \right|_{ABS} + \left(I + \left| A^{-1} \right|_{ABS} \right) C^{-1} V_{\max} + \left| A^{-1} \right|_{ABS} R_{\max} \right) \circ \operatorname{sgn}\left(e_{z\,K+1|k} \right) \tag{2.3.4}$$

In the sliding mode *control* a switching gain is used to push the system's state towards a surface called 'sliding surface' (a hyperplane) and after reaching the surface the states start sliding along it to converge to the operating point within a finite time.

Whereas, the Variable Structure Filter uses a 'discontinuous component' which differs from the previously reported sliding mode observers (Habibi & Burton, 2002). The corrective gain is a function of the *a priori* output estimation errors, the modeling uncertainties, and the initial conditions (Fig 2.4). The calculation of gain considers upper bound for the unmodeled dynamics in the system.

The stability of the VSF with the derivation of correction gain and an application of the algorithm to an uncertain linear system are also provided in (Habibi & Burton, 2002).

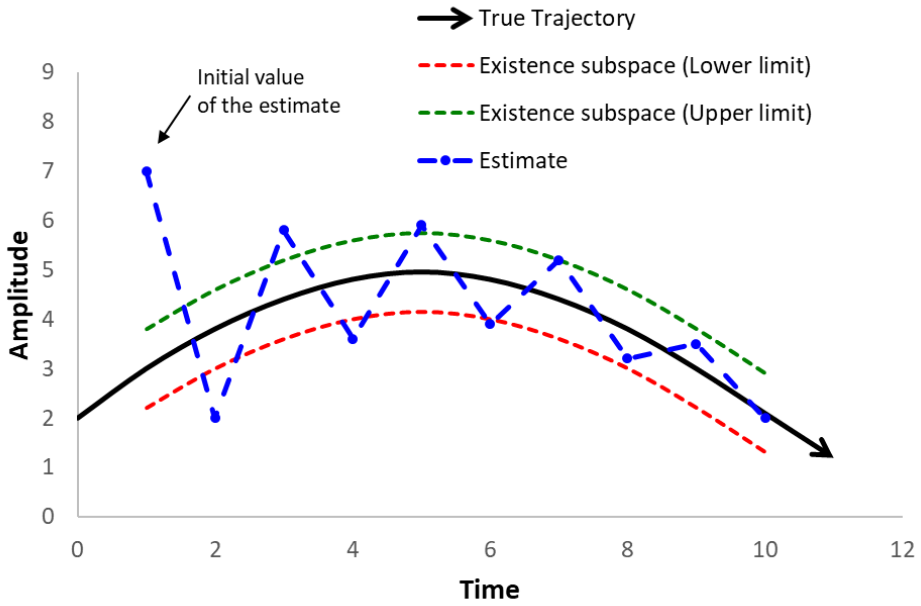

Figure 2.4 SVSF Concept

However, VSF suffers from a few disadvantages. The estimator can only be applied for the linear systems. VSF yields non-optimal results and often produces chattering in the estimates, which may be undesirable for certain applications (Gadsden & Hamed, 2015).

2.3.2 Extended Variable Structure Filter

The Variable Structure Filter described above has been developed for linear plants. The next big development comes in 2007 with the introduction of Extended Variable Structure Filter (Habibi S. , 2006). The EKVSF is the extension of VSF for the state estimation of nonlinear systems.

A nonlinear system can be described as

$$x_{k+1} = f(x_k, u_k) + w_k \tag{2.3.5}$$

$$y_{k+1} = h(x_{k+1}) + v_{k+1} \tag{2.3.6}$$

Where f and h are system and measurement functions respectively. w and v are representing the process and measurement noise.

In (Habibi S. , 2006) the nonlinear system equations have been linearized for the use in EKVSF estimator. The nonlinear approximation has been done by taking Jacobian of the nonlinear functions *f* and *h* described in the equations (2.3.7) and (2.3.8). The Jacobians are computed as given in the as follows

$$\hat{F}_k = \left.\frac{\partial f(x)}{\partial x}\right|_{x=\hat{x}_{k|k}, u_k} \tag{2.3.7}$$

$$\hat{H}_{k+1} = \left.\frac{\partial h(x)}{\partial x}\right|_{x=\hat{x}_{k+1|k}} \tag{2.3.8}$$

EKVSF also considers the system to be observable and the nonlinear function to be smooth and differentiable. It also assumes the output matrix to be constant in its linearized form, i.e., $H_k = H$. The computation process of the corrective term of EKVSF is similar to VSF. The main advantage of the EKVSF is that it can be applied to the nonlinear system. The disadvantages of EKVSF are found to be similar to Extended Kalman Filter (EKF). The nonlinear approximation (truncating the higher order terms of Taylor series) makes the estimate inaccurate as compare to VSF. Numerical computation of Jacobians increases the complexity of the algorithm. The stability condition and the proof are also given

in the paper. The application of the algorithm is demonstrated by applying the algorithm to a nonlinear robotic arm.

2.3.3 Smooth Variable Structure Filter (with boundary layer)

The smooth variable structure filter was presented in (Habibi S. , 2007). The name 'smooth' refers to the smooth nonlinear dynamical system. The smooth variable structure filter (SVSF) can be applied to both linear and nonlinear systems. The SVSF has a secondary performance indicator for detecting modeling errors. Like VSF, SVSF also uses the predictor-corrector format. A 'smoothing boundary layer' is used for the discontinuous function of the gain term. The chattering is filtered out by using a smoothing function with a known boundary layer around the switching function.

The replacement of $sign(vec)$ by a smoother function $sat(vec,\psi)$ in the gain of the estimator is also suggested for the SVSF. The choice of width of the smoothing boundary layer (ψ) is important as chattering depends on it. If the width of the smoothing boundary layer (ψ) is greater than the existence boundary layer (β) then the effect of chattering is removed and for $\psi < \beta$ chattering increases. One conservative choice of ψ would be assigning the value of the upper bound of the existence subspace i.e. $\psi = \beta$.

The corrective gain for SVSF was derived by following the condition given in Eq 2.3.9

$$\left|e_{z_{k|k-1}}\right|_{ABS} \leq \left|\hat{H}K_k\right|_{ABS} < \left|e_{z_{k|k-1}}\right|_{ABS} + \left|e_{z_{k-1|k-1}}\right|_{ABS} \tag{2.3.9}$$

Where,

$$e_{z_{k|k}} = z_k - \hat{z}_{k|k} \tag{2.3.10}$$

$$e_{z_{k|k-1}} = z_k - \hat{z}_{k|k-1} \tag{2.3.11}$$

Note that the above condition assumes the output matrix (H) to be linear or has been linearized. The usual practice has been to keep H as a square and identity matrix, where the number of states (n) is equal to the number of measurements (m). But in real applications, there are scenarios where the available measurements are fewer than the number of states, i.e. $m < n$. In (Habibi S. , 2007) the SVSF methodology has been demonstrated for a case where $m < n$ by using Luenberger reduced order observer additionally to get the output matrix full rank.

In (Habibi & Burton, 2007) application of SVSF for state and parameter identification of electrohydraulic actuator with linear measurement has been presented. A comparative study of SVSF and Extended Kalman Filter for nonlinear system model was demonstrated in (Wang, Habibi, & Burton, 2008). The method of transformation in order to obtain the full state observer form of SVSF was also given in (Wang, Habibi, & Burton, 2008). The performance of SVSF has been shown to be more robust than EKF (Wang, Habibi, & Burton, 2008). SVSF was applied to a target tracking application (Gadsden & Habibi, 2009) for both linear and nonlinear estimation problem and performance has been evaluated in the presence of an outlier. SVSF was used for the robust estimation of sideslip angle of lateral dynamics of the vehicle in (Huang & Wang, 2013).

2.3.4 Variable Structure Filter combined with other Estimators

Variable structure Filter (VSF) is found to be more robust against modeling uncertainty and disturbances (Habibi S. , 2007) as compared to the Kalman Filters for linear systems. On the other hand Kalman Filters are optimal for a known linear system. Utilizing the robustness of VSF and optimal estimation of KF, the effort was given to form a combined structure for robust estimators with improved accuracy.

In (Habibi S. , 2008) VSF was combined with EKF for improved performance and applied to a parameter tracking problem in a noisy and uncertain system. A user-defined boundary layer was introduced to make a decision to use estimator's gain (either VSF or EKF) to be used for the state estimation. If a large error occurs (due to model error or uncertainty) in *a priori* and *a posteriori*, the VSF dominates and for lesser error EKF's gain used in the correction term.

2.3.5 Derivation of Covariance in SVSF

Kalman filter (KF) needs *a priori* covariance, $P_{k+1|k}$ for the derivation of Kalman gain (Simon, 2006). Kalman Gain equation, for instance, is as follow

$$K_{k+1} = P_{k+1|k} H^T \left[H P_{k+1|k} H^T + R_{k+1} \right]^{-1} \tag{2.3.12}$$

Where, R_{k+1} refers to the measurement noise covariance of the system.

For SVSF, there has been no requirement of $P_{k+1|k}$ for calculating gain or corrective term. In 2010 *a priori* covariance was first derived for SVSF (Al -Shabi & Habibi, 2010) for linear system. The derivation of $P_{k+1|k}$ for linear system found similar to the KF.

$$P_{k+1|k} = E\left\{\left(x_{k+1} - \hat{x}_{k+1|k}\right)\left(x_{k+1} - \hat{x}_{k+1|k}\right)^T\right\} \quad (2.3.13)$$

However, Stability of SVSF for the linear system was not affected after deriving covariance. The update of *a posteriori* covariance $P_{k+1|k+1}$ was also given in the same paper (Al -Shabi & Habibi, 2010). It is interesting to note that the gain equation of SVSF was still unchanged, meaning that it did not use $P_{k+1|k}$ and hence the performance of SVSF (with covariance derivation) was not improved as compared to the previously reported SVSF without covariance derivation. The objective of deriving covariance was to open the possibility of combining Interacting Multiple Models (IMM) technique with SVSF.

2.3.6 Derivation of time-varying optimal boundary layer width for SVSF

SVSF had been using smoothing boundary layer (ψ) defined by the upper bounds of the model uncertainties present in the system since its first introduction in 2007 (Habibi S. , 2007). The concept of optimal boundary layer width was first presented in (Gadsden, Mohammed, & Habibi, 2011) by solving partial derivative of the $trace\{P_{k+1|k}\}$ with respect to ψ for a linear system. The derivation of the optimal boundary layer width assumes the existence of boundary layer for each state trajectory. The time-varying optimal boundary layer ψ_k is a function of $P_{k+1|k}$, $e_{z_{k|k}}$ and $e_{z_{k|k-1}}$. The paper (Gadsden, Mohammed, & Habibi, 2011) suggested that for the implementation of optimal boundary layer, one needs to create a full measurement matrix for a case where $m < n$. Some methods have been suggested to create a full measurement matrix, typically an identity matrix for a system where $m < n$ as given in (Habibi S. , 2007).

For a linear system, the gain of SVSF with optimal boundary layer is found to be identical to Kalman Filter (KF) within the boundary of the *saturation* in the gain equation (Gadsden S. A., 2011).

SVSF using data association technique for target tracking application was presented in (Attari, Gadsden, & Habibi, 2013).

2.3.7 Combining SVSF with other filters

SVSF is said to be robust but not optimal for the estimation of state and parameter. Time-varying optimal boundary layer makes SVSF optimal within the saturation limit but it loses robustness to some extent (Gadsden S. A., 2011). It has also been reported that the KF, EKF and UKF are more accurate than SVSF for linear as well as nonlinear systems where on uncertainty and disturbance were present (Fig 2.5).

The combined structure of SVSF with other optimal filters aimed at improving the estimation accuracy of SVSF without compromising robustness.

In (Gadsden, Habibi, & Kirubarajan, 2012) the particle filter was combined with SVSF for nonlinear state estimation. Robustness of EKF has been increased after combining with SVSF utilizing the effect of chattering (Al-Shabi, Gadsden, & Habibi, 2013).

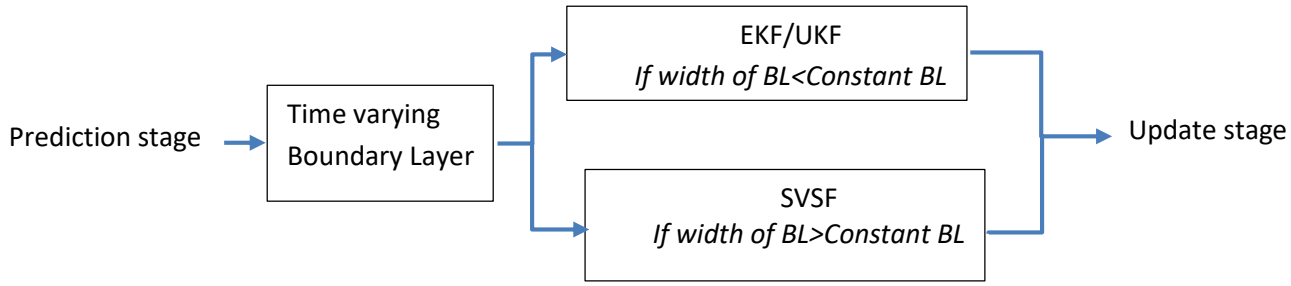

Figure 2.5 Combined structure of SVSF and other nonlinear filters

Optimal boundary layer has also been used for the detection of uncertainty or fault present in the system. Based on the width of the optimal boundary layer, one can choose robust SVSF gain or optimal EKF/UKF gain for a combined approach of state estimation. EKF and UKF were combined with SVSF to construct EK-SVSF and UK-SVSF for target tracking application based on the width of the boundary layer in (Gadsden, Habibi, & Kirubarajan, 2014). Cubature quadrature Kalman Filter was also combined with SVSF for nonlinear robust estimation in (Gadsden, Al-Shabi, Arasaratnam, & Habibi, 2014). A good review of SVSF has been presented in (Gadsden & Hamed, 2015). A comparative study of SVSF combined with other sigma point filters have been carried out for the application of robotic arm (Al-Shabi M. , 2017).

2.3.8 Recent advances of SVSF

2.3.8.1 Second order Smooth Variable Structure Filter

A second order Variable structure state estimator for linear and nonlinear system was presented in (Afshari, 2014). Like SVSV, second order SVSF is also a model based estimation method which additionally benefits the chattering suppression and robustness characteristics of second order of sliding mode system. Derivation of gain and the stability analysis are also given in (Afshari, 2014).

2.3.8.2 Continuous time Variable Structure Filter

First continuous-time variable structure filter was presented in (Gadsden, El Sayed, & Habibi, 2011). The algorithm was proposed for a linear system. A comparable result with performance analysis was given with Kalman Filter for a case study of the linear second order system.

2.3.8.3 Unscented Smooth Variable Structure Filter

Recently a novel boundary layer for SVSF based on sigma point has been presented in (Al-Shabi & Hatamleh, 2014). The same has been applied to the nonlinear system with linear measurement. However, Stability and proof of robustness have not been given in the same paper.

2.3.8.4 Square root formation of SVSF

Square root formulation of SVSF for improved numerical stability was proposed in (Gadsden & Lee, 2017). The algorithm has used two-pass smoother SVSF gain for a linear system. The same has been evaluated in a case study of a linearized system.

2.3.9 Some of the gaps observed in the literature survey

i. The variable structure filters in its early form have been demonstrated for a linear system. The EKSVSF was the first extension of SVSF to a nonlinear system by linearizing the system and measurement matrix. However, taking Jacobian of the nonlinear system equation often produces inaccurate result. The SVSF with time-varying boundary layer always assumes the measurement equation to be linear and invertible. However, additional techniques are to be followed where the measurement matrix is not linear or square.

ii. The Sigma point SVSF as presented in (Al-Shabi & Hatamleh, 2014) calculates only the boundary layer based on the Sigma-points. The sigma point formulations of the output equation are however yet to be explored. Stability and robustness of such cases need to be established. In (Al-Shabi & Hatamleh, 2014) a novel boundary layer based on unscented Sigma-point has been presented, but the derivation of such layer was not presented.

iii. The measurement equation for SVSF in most cases considers as a linear one. For a nonlinear measurement equation, the SVSF linearizes and inverts the output equation.

iv. SVSF with optimal boundary layer always considers the output matrix to be linear and of full rank. In practical scenarios, situation may arise when this assumption may not always true. SVSF with optimal boundary layer assumes noise statistics of process and measurement noise

to be known properly. However, for robust application, where the system has model error the knowledge of noise statistics may be unavailable.

v. The measurement noise covariance corresponding to the artificial measurements as provided in (Gadsden S. A., 2011) (Gadsden, Habibi, & Kirubarajan, 2014) is a point of concern.

vi. Computation of inverse function in the gain term and in boundary layers may produce numerical instability.

2.4 Interacting Multiple Model Estimators

Interacting Multiple Model (IMM) approach is a model based hybrid state estimation technique where more than one model is used in the filtering algorithm for state estimation of a dynamical system whose behaviour changes rapidly (Mazor, A., Averbuch, & Dayan, 1998). A finite number of models with different dynamics are used in the estimators operating in different modes. Main advantage of IMM is its ability to estimate the states of a system which has several modes and can switch from one to another. The system model for IMM is represented by these equations (Bar-Shalom, Rong Li, & Kirubarajan, 2001):

$$x(k+1) = F\left[M(k+1)\right]x(k) + v\left[k, M(k+1)\right] \tag{2.4.1}$$

$$y(k+1) = H\left[M(k+1)\right]x(k+1) + w[k+1, M(k+1)] \tag{2.4.2}$$

where, $x(k+1)$ and $y(k+1)$ are state vector and measurement vector respectively. Variable v and w represent the corresponding process noise and measurement noise of the system. Here $M(k)$ denotes the mode or model at the time k. The mode at time k is considered to be among the possible r modes.

$$M(k) \in \left\{M_j\right\}_{j-1}^{r} \tag{2.4.3}$$

It is assumed that the mode (model) switching or the mode jump process is a Markov chain process with known mode transition probability.

$$p_{ij} \triangleq P\left\{M(k) = M_j \mid M(k-1) - M_i\right\} \tag{2.4.4}$$

The IMM estimator at time k computes the state estimate under each possible current model using r filters, with each filter using a different combination of the previous model-conditioned estimates (Bar-Shalom, Rong Li, & Kirubarajan, 2001).

Multiple Model (MM) state estimators were introduced in the mid-1960s (Magill, 1965) to adapt structural and parameter changes in the system. A survey on various suboptimal state estimations and structure detection of the system was presented in (Jitendra K, 1982). However, initially the Multiple Model estimation algorithm has a fixed structure. MM estimation with the variable structure as proposed by Xiao-Rong Li (Li X. R., 1994) uses a set of models to represent the possible behavior pattern of the system were considered in the design of the estimator. The state estimation of hybrid stochastic system by variable structure MM estimator has been demonstrated in (Li & Bar-Shalom, 1996). In (Li X. R., 1998) a process of choosing estimate optimally in the MM estimation with uncertain parameters has been presented.

The Interacting Multiple Model (IMM) estimator consists of running a standard filter for each model (mode), a model probability evaluator, and an estimate combiner at the output of the filters. Each filter of IMM uses a mixed estimate at the beginning of each cycle (Bar-Shalom, Chang, & Blom, 1989). In IMM estimator 2 or 3 'mode matched' filters (model based) run in parallel exchanging information in each step (sample) based on mode transition probability and combine the overall estimate and covariance at the end of the cycle. A good study of IMM implemented in stochastic hybrid system, civilian aircraft tracking system provided in (Li & Bar-Shalom, 1993). Several practical issues have been discussed in (Kirubarajan & Bar-Shalom, 2003) on when to choose IMM over Kalman Filter.

Target tracking has been seen to be one of the major application areas of IMM since last two decades. A good review of IMM estimator with the application in target tracking problems has been given in (Mazor, A., Averbuch, & Dayan, 1998). Numerically robust implementation of MM and IMM has been presented in (Li & Zhang, 2000) by overcoming the numerical problems with the standard implementation. Performance of static MM, dynamic MM and IMM in solving Air Traffic Control (ATC) tracking problem has been evaluated in (Bar-Shalom, Rong Li, & Kirubarajan, 2001). A comparative study of Multiple Model algorithms for maneuvering target tracking is given in (Pitre, Jilkov, & Li, 2005). Performance of different versions of IMM has been compared and analyzed for maneuvering target tracking applications in (Hong-Quan & Shao-Hong, 2008).

However, IMM estimators while combining a number of mode-matched filters which would fit the desired target model to estimate lags the choice of estimators to enhance robustness. Optimal filters if used inside the IMM filters are sensitive to process and measurement noise. An effort was put (Gadsden, Habibi, & Kirubarajan, 2010) to combine robust smooth variable structure filter with other optimal filters in the IMM algorithm to enhance the robustness of IMM. Recently in (Gao, Gao, Zhong, Hu, & Gu, 2017)IMM was constructed with robust and adaptive (based on fading factor) unscented Kalman Filter.

2.5 Tracking of Maneuvering targets

Tracking of maneuvering target is a good application area to evaluate the performance of the estimators. A two-dimensional target tracking form of Air Traffic Control (ATC) scenario has been discussed in (Bar-Shalom, Rong Li, & Kirubarajan, 2001). A good review about the dynamic models of target maneuvering system is discussed in (Li & P. Jilkov, 2003). Some important ballistic target models are reviewed in (Li & P. Jilkov, 2001). Review of measurement models of maneuvering target is discussed in (Li & Jilkov, 2001). A good review and evaluation of Multiple Model in maneuvering target tracking are given in (Pitre, Jilkov, & Li, 2005) (Hong-Quan & Shao-Hong, 2008).

2.6 Conclusion of the Literature Survey

This chapter provided a comprehensive description of the popular optimal/suboptimal Kalman Filter based estimators. The merits and shortcomings are also provided for the number of filters/estimators. Emphasis has been given mainly on nonlinear state and parameter estimation. The recent development of adaptive nonlinear state estimators and robust estimators have been thoroughly studied. Some of the gaps for conventional estimators on the robust application, variable Structure Filters and Multiple Model State Estimators have been identified and discussed. The main focus of this research is to deal with model error or process noise adaptation to improve the performance of some recently developed nonlinear estimators for a class of nonlinear hybrid system.

3 Models and Case Studies

3.1 Why case studies?

The case studies are important for evaluation of the performance of the proposed estimators or the estimation scheme. The simulation studies are to be carried out for the performance evaluation and comparison considering different environmental scenarios or conditions. State estimators which are designed for the estimation of the system's states or parameters of the noisy system are required to be evaluated under different noise sequences (known as Monte Carlo simulation). Case studies are therefore essential practice to test the efficacy of the algorithm in the field of estimation and control. Another major aspect is to perform the comparative study of the proposed estimators with others keeping the simulation environment unchanged. It also helps one to understand and assess the effect of assumptions and consideration of certain parameters' value that were made while constructing the algorithm.

3.2 Overview of Case Studies

This section demonstrates case study of (a) tracking scenarios of a civilian aircraft, (b) Ballistic object tracking and (c) road-tire friction estimation.

The 2-D motion models have been chosen for the simulation. Commonly known as 'Uniform Motion' (linear) and 'Coordinated Turn' (nonlinear) model are taken into consideration of modeling the aircraft's trajectory. Process noise and measurement noise have also been considered for the evaluation of the estimators. Tracking of a falling object is considered as the model of ballistic object tracking. Longitudinal and lateral dynamical model with popular friction model has been considered for modeling an anti-lock braking system.

3.3 Civil aircraft Models and Tracking

3.3.1 The Literature on Models and Tracking

Ground-based radar tracking of aircraft is an important task of air traffic control system. Estimation of position, velocity, mode, altitude etc. of the aircraft needs truth models of the trajectory tracking system. Modeling a maneuvering target involves combination of linear and nonlinear modes of the target. Two basic modes of the flight are considered: uniform motion (UM) which involves straight path with constant moving and the coordinated turn (CT) which involves maneuvering. Some CT models are validated and compared in (Nabaa & Bishop, 2000). A two-dimensional planar model describing

uniform motion and coordinated turn model is given in (Li & Bar-Shalom, 1993). Models for the target tracking system and navigation system are given in (Yaakov, X, & Kirubarajan, 2001). Tracking and estimation of Similar two-dimensional models are also presented in (Wang, Kirubarajan, & Bar-Shalom, 1999) (Pitre, Jilkov, & Li, 2005) (Mazor, A., Averbuch, & Dayan, 1998) (Gadsden, Habibi, & Kirubarajan, 2014) (Crouse, 2015). A survey on dynamical models used for target tracking is presented in (Li & P. Jilkov, Survey of maneuvering target tracking. Part I. Dynamic models, 2003). (Yuan, Han, Duan, & Lei, 2005) presents the choice of models for tracking the maneuvering targets with CT models. The measurement models for tracing and maneuvering have been discussed in (Li & Jilkov, 2001). The ballistic target models are surveyed by (Li & P. Jilkov, 2001). A three-dimensional airborne maneuvering target tracking problem has been presented in (Moose, Vanlandingham, & McCabe, 1979).

3.3.2 Two Dimensional Planar Motion

3.3.2.1 Uniform Motion

The discrete state equations of the model for uniform motion is represented as given in (Yaakov, X, & Kirubarajan, 2001) (Gadsden, Habibi, & Kirubarajan, 2014)

$$\mathbf{x}_{k+1} = \begin{bmatrix} 1 & 0 & T & 0 \\ 0 & 1 & 0 & T \\ 0 & 0 & 1 & 0 \\ 0 & 0 & 0 & 1 \end{bmatrix} \mathbf{x}_k + \begin{bmatrix} 0.5T^2 & 0 \\ 0 & 0.5T^2 \\ T & 0 \\ 0 & T \end{bmatrix} \mathbf{w}_k \tag{3.3.1}$$

where T is the sampling interval, and the state vector $\mathbf{x}_k$ is defined as

$$\mathbf{x}_k = \begin{bmatrix} \zeta_k & \eta_k & \dot{\zeta}_k & \dot{\eta}_k \end{bmatrix}' \tag{3.3.2}$$

with, ζ_k and η_k representing the position of the aircraft along the X and Y direction respectively; $\dot{\zeta}_k$ and $\dot{\eta}_k$ represent the corresponding linear velocities. Here $\mathbf{w}_k$ represents the discrete equivalent of noise in the acceleration in the X and Y directions with covariance Q_{UM}.

$$\mathbf{Q}_{UM} = \begin{bmatrix} \frac{T^3}{3} & 0 & \frac{T^2}{2} & 0 \\ 0 & \frac{T^3}{3} & 0 & \frac{T^2}{2} \\ \frac{T^2}{2} & 0 & T & 0 \\ 0 & \frac{T^2}{2} & 0 & T \end{bmatrix} .L_1 \tag{3.3.3}$$

Where L_1 is the power spectral density of corresponding continuous domain noise for linear acceleration and angular acceleration.

3.3.2.2 Coordinated Turn

The coordinated turn model (Gadsden, Habibi, & Kirubarajan, 2014) (Yaakov, X, & Kirubarajan, 2001) contains an additional state variable, viz., the turn rate Ω, which is nominally an unknown constant. For this model, the state vector $\mathbf{x}_k$ is defined as $\mathbf{x}_k = \begin{bmatrix} \zeta_k & \eta_k & \dot{\zeta}_k & \dot{\eta}_k & \Omega \end{bmatrix}'$

$$\mathbf{x}_{k+1} = \begin{bmatrix} 1 & 0 & \frac{\sin(\Omega_k T)}{\Omega_k} & -\frac{1-\cos(\Omega_k T)}{\Omega_k} & 0 \\ 0 & 1 & \frac{1-\cos(\Omega_k T)}{\Omega_k} & \frac{\sin(\Omega_k T)}{\Omega_k} & 0 \\ 0 & 0 & \cos(\Omega_k T) & -\sin(\Omega_k T) & 0 \\ 0 & 0 & \sin(\Omega_k T) & \cos(\Omega_k T) & 0 \\ 0 & 0 & 0 & 0 & 1 \end{bmatrix} \mathbf{x}_k + \begin{bmatrix} 0.5T^2 & 0 & 0 \\ 0 & 0.5T^2 & 0 \\ T & 0 & 0 \\ 0 & T & 0 \\ 0 & 0 & T \end{bmatrix} \mathbf{w}_k \tag{3.3.4}$$

Here $\mathbf{w}_k$ represents the discrete equivalent of noise in the acceleration in the X and Y directions with covariance Q_{CT}. The measurement noise covariance is defined as

$$\mathbf{Q}_{CT} = \begin{bmatrix} \mathbf{Q}_{UM} & \mathbf{0}_{4X1} \\ \mathbf{0}_{1X4} & \frac{L_2}{L_1} T \end{bmatrix} .L_1 \tag{3.3.5}$$

L_1 and L_2 are the power spectral densities of corresponding continuous domain noise for linear acceleration and angular acceleration respectively as given in (Gadsden, Habibi, & Kirubarajan, 2014).

3.3.3 Measurement models

Two types of measurement models are considered, namely the linear Cartesian measurement model and the nonlinear polar (r,θ) measurement model (also called range-bearing model). Both these models are applicable for CT and UM model cases. While the range-bearing model is more natural for a simple radar tracker, the simpler linear Cartesian measurement model is included to facilitate comparative study.

3.3.3.1 Cartesian

It is assumed that the tracker is stationed at the origin to measure the position along the X and Y directions. The measurement for the UM model is

$$\mathbf{y}_k = \begin{bmatrix} 1 & 0 & 0 & 0 \\ 0 & 1 & 0 & 0 \end{bmatrix} \mathbf{x}_k + \mathbf{v}_k \tag{3.3.6}$$

The corresponding measurement model for CT is

$$\mathbf{y}_k = \begin{bmatrix} 1 & 0 & 0 & 0 & 0 \\ 0 & 1 & 0 & 0 & 0 \end{bmatrix} \mathbf{x}_k + \mathbf{v}_k \tag{3.3.7}$$

3.3.3.2 Polar Measurement

The polar measurement model (Shi, Han, & Liang, 2009) is defined as

$$y_k = \begin{bmatrix} r_k \\ \theta_k \end{bmatrix} = \begin{bmatrix} \sqrt{\zeta_k^2 + \eta_k^2} \\ \tan^{-1}\left(\eta_k / \zeta_k\right) \end{bmatrix} + \begin{bmatrix} v_{rk} \\ v_{\theta k} \end{bmatrix} \tag{3.3.8}$$

3.3.4 **Civilian Aircraft 2-D Trajectories**

3.3.4.1 Test trajectory-1 ('s')

Trajectory-I can be described as follows: The aircraft starts flying from its initial position of [25,000m, 10,000m]. The fight trajectory without considering process noise has been shown in Fig 3.1. From the initial point it flies westward (along X direction) with a constant velocity of 120m/s for 125s. Then it takes a coordinated turn with a turn rate of $1^\circ/s$ in anti-clockwise direction for 90s. Next, it flies southward for another 125s at a constant velocity of 120m/s. Then it takes another coordinated turn for 30s at $3^\circ/s$. Finally, it reaches the destination after taking a straight path to the westward direction at

120m/s for 120s. The trajectory marked true has been corrupted by an instance of the process noise. For both the Cartesian and the Polar measurement cases, the sensing radar is located at (0, 0).

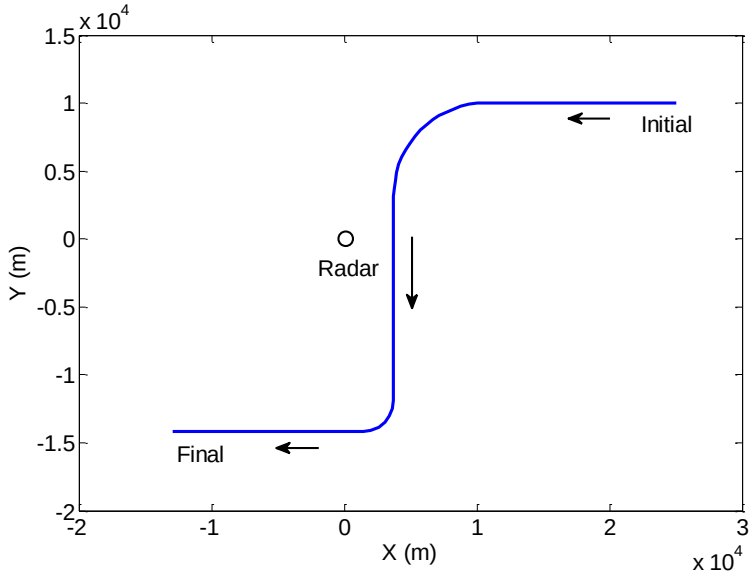

Figure 3.1 Nominal trajectories (not corrupted with process noise) of the aircraft for 's' trajectory

3.3.4.2 Test trajectory -2 (zigzag)

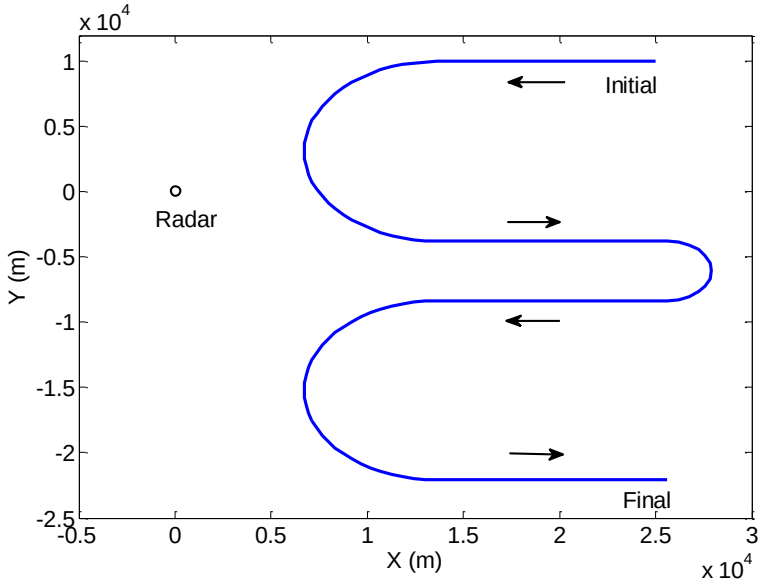

Figure 3.2 Nominal trajectories (not corrupted with process noise) of the aircraft for 'zigzag' trajectory

Trajectory – II which is more severe than the previous one is employed to further contrast the performance of non-adaptive and adaptive state estimators. This is a relatively zigzag trajectory. The initial position of the aircraft is [25,000m, 10,000m]. It travels eastward for 100s along X direction with a velocity of 120m/s. Then it takes a coordinated 'U' turn for 180s with a turn rate of $1^{\circ}/s$ to return back

towards east. Then it maintains a constant speed of 120m/s for 100s. The aircraft then takes a second turn with different turn rate $3^{\circ}/s$ for 60s to fly back westward. It then repeats the same trajectory for next 100s with uniform motion and 180s with coordinated turn ($1^{\circ}/s$) and terminates after a uniform motion segment with a constant speed of 120m/s. The trajectory marked true has been corrupted by an instance of the process noise.

3.4 Ballistic object tracking

3.4.1 Literature

Ballistic object tracking is one of the major application areas for estimators. It is often used as a test field to evaluate performance or the characterization of the estimators. A nonlinear model of target motion of ballistic object in the re-entry phase is developed by (Farina, Ristic, & Benvenuti, 2002) . A one-dimensional vertical motion model with unknown ballistic coefficient was presented in (B., Farina, Benvenuti, & Arulampalam, 2003) analyzing the posterior Cramer-Rao lower bounds. The system is mainly nonlinear due to the presence of drag. Drag parameter is one of the major concerns for the state estimation. Sequential Monte Carlo-based filter was proposed by (Angelova, Simeonova, & Semerdjiev, 2003) for tracking nonlinear ballistic object with uncertain drag parameter. Several non-linear estimation schemes for ballistic object tracking have been discussed in (Ristic, Arulampalam, & Gordon, 2003). State and parameter estimation by Unscented Kalman Filter for tracking ballistic object was demonstrated in (Liu, 2011). Estimation scheme of target landing point during re-entry phase and its accuracy was proposed in (Farina, Benvenuti, & Ristic, 2002). Applications of nonlinear adaptive filters on tracking of the ballistic object are given in (Dey, Sadhu, & Ghoshal, 2013), (Dey, Das, Sadhu, & Ghoshal, 2015).

3.4.2 System Model

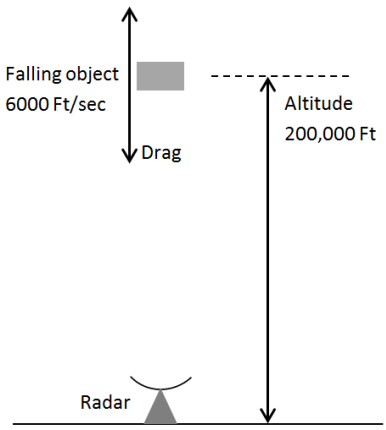

Figure 3.3 Free body diagram of a falling object

The free body diagram of a ballistic object is shown in figure 3.3, which starts falling from an altitude of 200,000 Ft from the ground (Zarchan, 2005). The dynamics of the system is given as

$$\ddot{x} = drag - g = \frac{Q_p g}{\beta} - g \tag{3.4.1}$$

Where, x is the distance from the radar to the object, β is the ballistic coefficient of the object and Q_p is the dynamic pressure. The ballistic coefficient, which is considered to be a constant in this problem, is a term describing the amount of drag acting on the object. Small values of β indicate high drag, and high values of β indicate low drag. Setting β equal to infinity eliminates the drag. The dynamic pressure Q_p is given as

$$Q_p = 0.5\rho\dot{x}^2 \tag{3.4.2}$$

Where, ρ is representing the air density. For this problem it is assumed that the air density is an exponential function of the altitude (Zarchan, 2005).

$$\rho = 0.0034e^{-x/22000} \tag{3.4.3}$$

Therefore, the equation expressing the acceleration acting on the object is to be expressed as the nonlinear second-order differential equation having two states, position and velocity $\begin{bmatrix} x & \dot{x} \end{bmatrix}^T$. Only the position is considered as measurement of the system. The time evolution of the states of the system is shown in Fig 3.4 and Fig 3.5

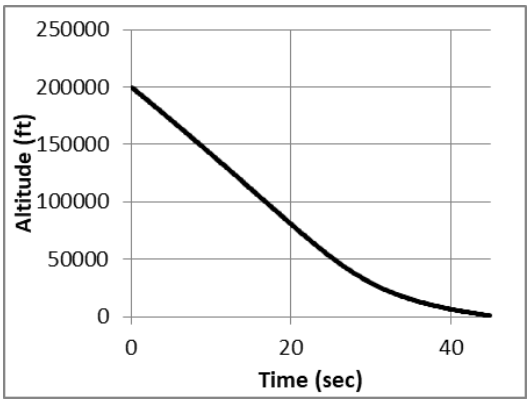

Figure 3.4 Altitude

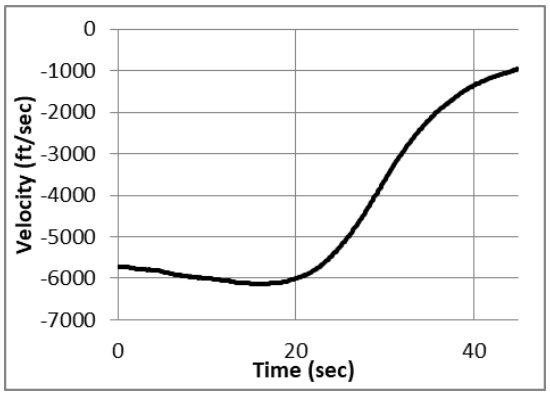

Figure 3.5 Velocity

The fundamental matrix of the system by taking two-term Taylor-series approximation is given as

$$\Phi_k = I + FT_s \tag{3.4.4}$$

In the above equation, $F = \begin{bmatrix} 0 & 1 \\ f_{21} & f_{22} \end{bmatrix}$ where, $f_{21} = \frac{-\rho g x^2}{44{,}000\,\beta}$ $f_{22} = \frac{\rho g \dot{x}}{\beta}$

The process noise was derived as given in (Zarchan, 2005)

$$Q_k = \Phi_s \begin{bmatrix} \frac{T^2}{3} & \frac{T^2}{2} + f_{22}\frac{T^2}{3} \\ \frac{T^2}{2} + f_{22}\frac{T^2}{3} & T + f_{22}T^2 + f_{22}^2\frac{T^2}{3} \end{bmatrix} \tag{3.4.5}$$

where Φ_s is the noise spectral density of the system assumed to be on the acceleration and T is the sampling interval. The measurement noise given as $R = \sigma_v^2$ where σ_v^2 denotes the variance of the altitude noise. The linear measurement matrix is defined as $H = \begin{bmatrix} 1 & 0 \end{bmatrix}$. The plots in figure 3.6 show the dynamics of the elements of covariance matrix Q.

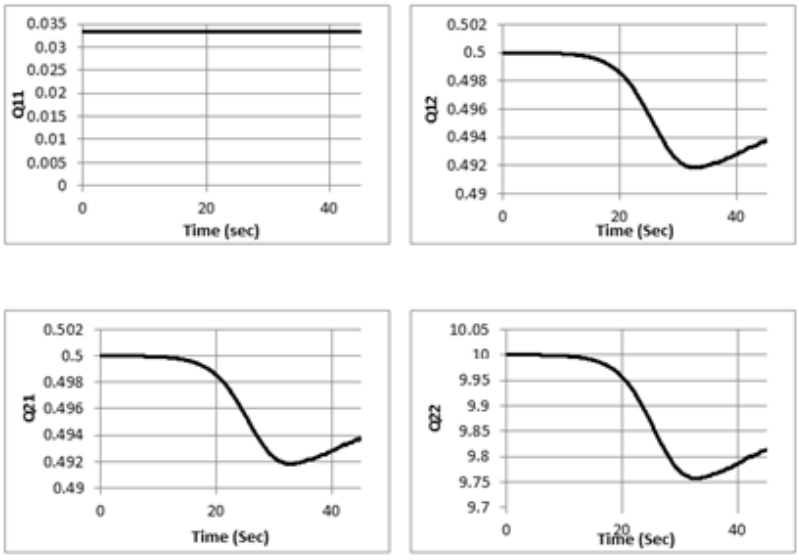

Figure 3.6 Process noise covariance

3.5 Tire friction estimation case study

3.5.1 Literature

The characteristics of Anti-lock Braking System (ABS) rely strongly on the tire-friction model which introduces non-linearity into the system dynamics of ABS. Numerous research papers are available which are based on the designing and modelling ABS controllers such as (Amodeo, Antonella, Riccardo, & Claudio, 2010) (Villagra, D'Andréa-Novel, Fliess, & Mounier, 2011) (Park & Lim, 2008) (Unsal & Kachroo, 1999) (Köppen, Küpper, & Makarenkov, 2017). The state and parameters are estimated by observer or estimator to increase the efficiency of the controller. Several estimation scheme such as sliding mode observer (Baffet, Charara, & Lechner, 2007) (Baffet, Charara, & Lechner, 2009) (Amodeo, Antonella, Riccardo, & Claudio, 2010), Kalman filters (Imsland, Grip, Johansen, Fossen, Kalkkuhl, & Suissa, 2007) (Dakhlallah, Glaser, Mammar, & Sebsadji, 2008) or other non-linear observers (Doumiati, Victorino, Charara, & Lechner, 2010) etc. The development of state estimators are mainly on vehicle velocity, lateral forces (Nam, Hiroshi, & Yoichi, 2012), longitudinal or lateral slips (Antonov, Fehn, & Kugi, 2011) (Sebsadji, S., S., & J, 2008), some parameters such as road-tire friction cornering stiffness are estimated for ABS controller, are given in (Dakhlallah, Glaser, Mammar, & Sebsadji, 2008) (Rajamani, Piyabongkarn, & Lew, 2012) (Ahn, Peng, & Eric Tseng, 2013) (Zong, Song, & Hu, 2011) .

3.5.2 System Model

The control systems of an automotive application broadly depend on the vehicle handling dynamics. Therefore, the system is to be modeled to apply control laws. The main focus of the area of this work is to design estimation based control scheme which for the following applications:

The anti-lock braking system (ABS) is a system to ensure the vehicle stability and motion control while a hard brake is pressed. The brake pressure is to be applied smoothly on the wheel such that the wheels don't get locked after the application of hard brake in an emergency situation. The slip value is an important parameter for the ABS system, which is to maintain at an optimum level such that the vehicle can be operated at in a stable zone. The tire force on the other hand, is dependent on the surface of the road. The road surface may change time to time which results the tire force to change as the friction coefficient between road and tire changes with the change of road asphalt. The propagation of the tire force and the sensing of the tire force is the most important part of the slip controller as the brake pressure depends on it. The propagation of the tire force depends on the tire characteristics. Thus modeling the tire and the vehicular system needs to be done for the application of estimation and control methodologies.

3.5.2.1 Quarter car model

A simple quarter car model (Mirzaeinejad & Mirzaei, 2010) (Anwar, 2006) (Park & Lim, 2008) (Unsal & Kachroo, 1999) is considered here which holds necessary characteristics of the whole vehicle dynamics. As the comprehensive vehicle model is much complex this simplified single-wheel model is taken for controller design purpose. Fig 3.7 shows the free body diagram of the wheel.

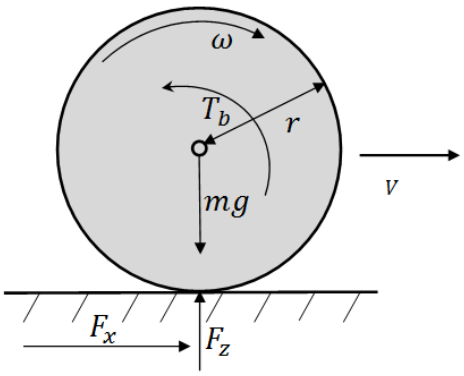

Figure 3.7 Free body diagram of the quarter car model

The equations of motion of the vehicle can be written as follows:

$$\dot{V} = \frac{-F_x}{m_t} \tag{3.5.1}$$

$$\dot{\omega} = \frac{1}{I_t}\left(RF_x - T_b\right) \tag{3.5.2}$$

Where m_t is Total mass of the quarter vehicle, F_x is longitudinal tire force, V Longitudinal velocity of the vehicle, ω is wheel's angular velocity, I_t represents total moment of inertia of the wheel, R represents the radius of wheel, T_b is the braking torque.

The total mass of the quarter vehicle is given by

$$m_t = \frac{1}{4}m_{vs} + m_w \tag{3.5.3}$$

Where, m_{vs} is the vehicle sprung mass and m_w is the mass of the wheel.

The longitudinal force acting on the tire depends on the load which has two components: a static component for vehicle mass and a dynamic component for load transfer during braking. The tire normal force is given by

$$F_z = m_t g - F_L \tag{3.5.4}$$

$$F_z = m_t g - \frac{m_{vs} h_{cg}}{2l} \ddot{x} \tag{3.5.5}$$

Where g is the gravitational acceleration, F_L is the dynamic load transfer, h_{cg} represents height of the sprung mass c.g., Longitudinal acceleration is denoted by $\ddot{x}$ and wheelbase is represented as l.

3.5.2.2 Longitudinal dynamics

The vehicle model of a quarter car has been described in the previous section. For developing an anti-skid controller for vehicle so it is important to measure wheel longitudinal slip (Mirzaeinejad & Mirzaei, 2010), (Smith & Starkey, 1995). During vehicle acceleration, a positive torque is applied to the wheel. If this applied torque exceeds the tire-road friction force to the wheel, the wheel starts rotating and moves the loaded mass. Similarly, the wheel along with the vehicle speed decreases during braking after a braking torque is applied to the wheel. When the vehicle moves with a constant velocity, the vehicle speed and the tire longitudinal speed are of same value. However, if a driver presses the brake pedal in order to reduce the speed of the vehicle, the braking pressure increases the braking torque which decreases the angular velocity of the wheel. In this time slip between tire and road occurs at the contact surface of tire and road because the wheel longitudinal velocity and the tire longitudinal velocity are not same.

The longitudinal slip, λ of the wheel is the relative difference between the driven wheel angular velocity and the vehicle absolute velocity

$$\lambda = \frac{V - R\omega}{V}, \quad V < R\omega,\ \omega \neq 0,\ acceleration \tag{3.5.6}$$

$$\lambda = \frac{V - R\omega}{V}, \quad V > R\omega,\ V \neq 0,\ braking \tag{3.5.7}$$

Differentiating with respect to time gives

$$\dot{\lambda} = \frac{\dot{V}(1-\lambda) - R\dot{\omega}}{V} \tag{3.5.8}$$

Substituting this equation into vehicle motion equation gives

$$\dot{\lambda} = \frac{1}{V}\left(\frac{F_x}{m_t}(1-\lambda) + \frac{R^2 F_x}{I_t}\right) + \left(\frac{R}{VI_t}\right)T_b \tag{3.5.9}$$

Where T_b is Braking torque

The traction force depends on the slip ratio and the normal force acting on the wheel.

$$F_x = \mu(\lambda)F_z \tag{3.5.10}$$

The traction force or the friction force F_x comes from the wheel-road contact surface and strongly depends on the modeling of the wheel-friction. The wheel-friction models give the typical relationship between wheel slip ratio (λ) and the friction force (F_x) of the tire or the relationship between the slip ratio (λ) and friction coefficient (μ). A typical tire-road friction curve with respect to slip ratio is shown in the Fig 3.8.

Eq 3.5.9 and 3.5.10 are two governing equations of motion. In state space form the vehicle velocity, V and the wheel slip ratio, λ are two state variables. The control variable is barking torque T_b is to control the wheel-slip at the desired state.

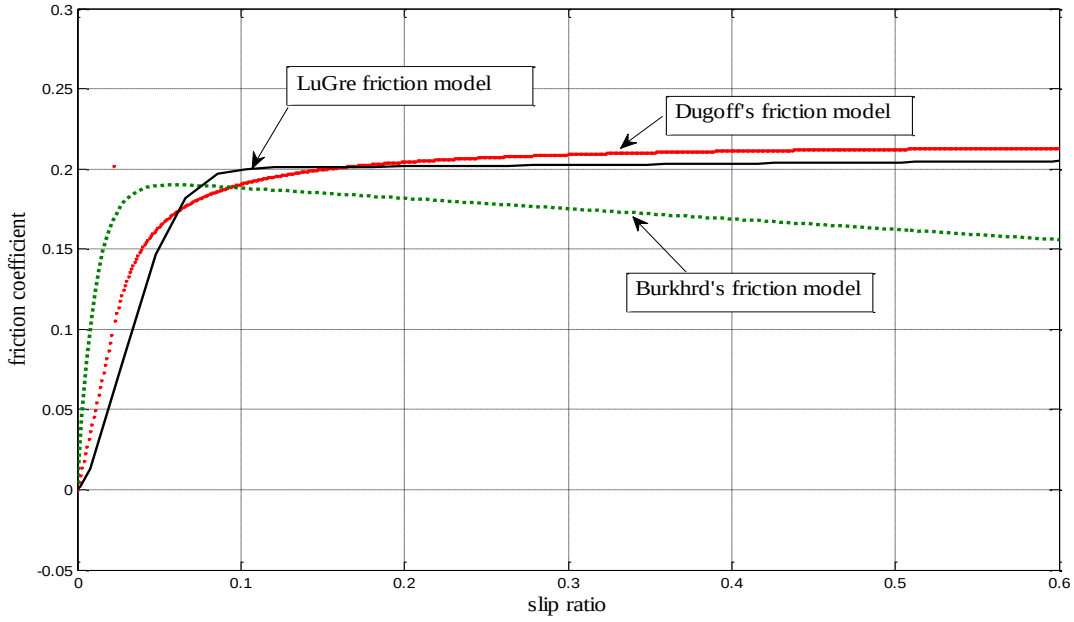

Figure 3.8 Slip – friction characteristics (simulated for snow asphalt only)

The tire longitudinal force F_x is a function of wheel-slip λ. Due to the saturation property of tire forces the $F_x - \lambda$ relationship is nonlinear for the higher value of slip ratio λ. At the low slip ratio this relationship is linear before reaching the maximum value of tire longitudinal force. Several tire models are there in the literature describing the $F_x - \lambda$ characteristics. Some popular tire models are discussed later in this chapter.

3.5.2.3 Lateral dynamics

Free body diagram of the bicycle model of a ground vehicle is shown in Figure 3.8 to demonstrate lateral dynamics of the vehicle (Ahn, Peng, & Eric Tseng, 2013).

The motion equation can be described as

$$m\left(\dot{v}_y + v_x r\right) = F_{yf} + F_{yr} \tag{3.5.11}$$

$$I_z \dot{r} = aF_{yf} - bF_{yr} \tag{3.5.12}$$

Here, m is the mass of the vehicle, v_x is the longitudinal velocity, v_y is the lateral velocity, F_y is the frictional force of the tire for front and rare wheel, r is the yaw rate, I_z is the moment of inertia, a and b are the length of the front wheel and rear wheel from the centre of gravity of the vehicle.

Slip angle of the front wheel α_f and the rear wheel α_r can be written as

$$\alpha_f = \frac{v_y + ar}{v_x} + \delta \tag{3.5.13}$$

$$\alpha_r = \frac{v_y + br}{v_x} \tag{3.5.14}$$

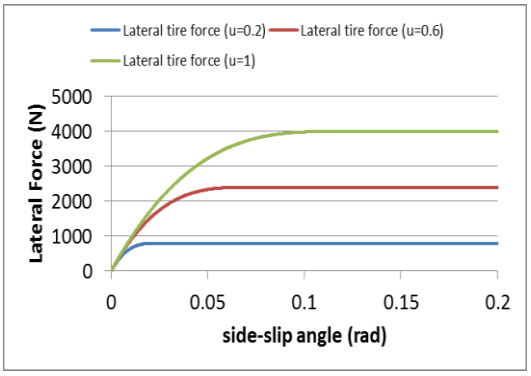

Figure 3.9 Lateral Force of the tire

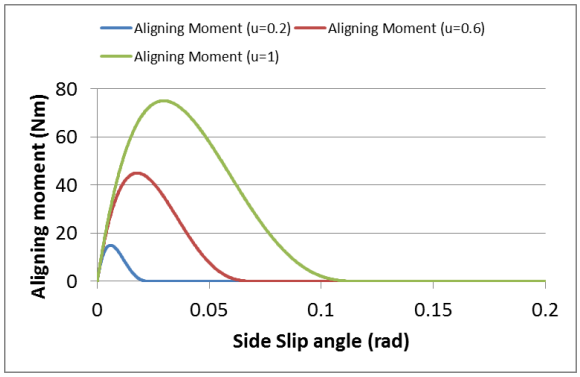

Figure 3.10 Aligning Moment of the tire

3.5.2.4 Road tire friction model

Modeling of anti-lock braking system requires the vehicle model which longitudinal slip dynamics and the tire model which characterizes frictional forces. The longitudinal and lateral vehicle dynamics have been discussed earlier. It requires the model of the tires which would relate the force to slip or friction to slip characteristics. The friction models are discussed in this section. Three popular road-tire friction models have been considered here for the purpose of designing anti-lock braking system. Dugoff's friction model, LuGre tire model and Burckhardt tire model are discussed here. It is important to study the longitudinal force and friction characteristics of the tire. The slip ratio λ depends on the current road friction which is faced by the wheel's contact surface area. It is required to operate the friction in the linear range of λ so that the system becomes stable. The longitudinal force curve of the wheel

therefore changes according to the surface condition of the road. The peak of the $F_x - \lambda$ curve shifts from left to right.

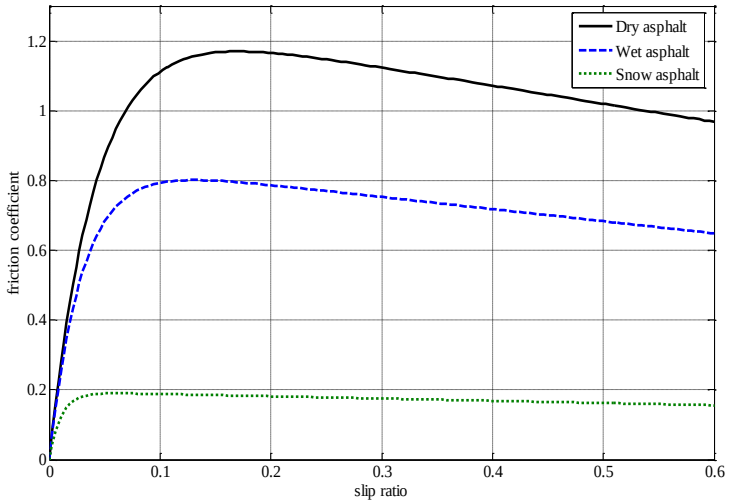

Figure 3.11 Friction coefficient characteristics in different road conditions

It is also important to have the maximum friction coefficient since the maximum braking performance is related to the maximum road-tire friction coefficient.

$$\mu_{\max} = \left.\frac{F_x}{F_z}\right|_{\max} \tag{3.5.15}$$

$F_x|_{\max}$ Can be achieved from the peak value in the $\mu - \lambda$ curve.

Dugoff's friction model

The Dugoff's friction tire model (Dugoff, 1969) is the critical factor during emergency maneuvering. Linear tire model is not always sufficient for accurate maneuvering. To account for the nonlinearity due to saturation property of the tire force, the non-linear Dugoff's tire model has been studied. It can calculate pure longitudinal and lateral tire forces and side slip ratio of the wheel. Dugoff's tire model says uniform vertical pressure distribution on the tire contact patch which is based on friction ellipse concept. Comparing to the other model it is fast and gives more transparent equations for maximum friction coefficient from longitudinal force- slip dynamics.

The relation of the longitudinal force of the tire is given as follows

$$F_x = \frac{C_i}{1-\lambda} f(s) \tag{3.5.16}$$

Where,

$$f(s) = \begin{cases} s(2-s), \ if \ \ s < 1 \\ 1, \ if \ \ s > 1 \end{cases} \tag{3.5.17}$$

$$s = \frac{\mu F_z \left(1 - \varepsilon_r V \sqrt{\lambda^2 + \tan^2 \alpha}\right)(1-\lambda)}{2\sqrt{C_i^2 \lambda^2 + C_\alpha^2 \tan^2 \alpha}} \tag{3.5.18}$$

Where, C_i is the longitudinal stiffness of the tire, C_α is the cornering stiffness of the tire, F_z represents normal load of the tire and ε_r represents road adhesion factor.

In the figures below the tire longitudinal force and friction force curve for dugoff's model are shown. For simulation, $C_i = 20000 \ N$; $C_\alpha = 2720.55422 \ \ N/rad$ and $\varepsilon_r = 001099$ are taken.

LuGre friction model

LuGe tire model is a typical dynamic model which is proposed by Canudas de Wit *et al*. (De Wit, Olsson, Johan Astrom, & Lischinsky, 1995) The LuGre model is able to capture most friction phenomena that are of interests to feedback controls. It regards the friction as reciprocity between the bristle of the interface. It has two surfaces connected by elastic bristle. A tangential force acts on the bristle when there is a relative velocity between the two surfaces. The bristle will get distortion like a spring. The bristle begins to slip when the distortion is high enough. The model considers the average deflection of the bristles.

The dynamics of the deflection z is given by the following differential equation.

$$\dot{z} = V_r - \frac{\sigma_0 |V_r|}{G(V_r)} z \tag{3.5.19}$$

where, V_r is the relative velocity between the two surfaces, $G(V_r)$ denotes the non-linear friction characteristic function which is a positive function as described by the following equation. σ_0 is the stiffness of the bristle.

$$G(V_r) = \mu_c + (\mu_s - \mu_c) e^{\left(-\left|\frac{V_r}{V_s}\right|^{\frac{1}{2}}\right)} \tag{3.5.20}$$

where μ_c is the Coulomb friction level, μ_s is the level of static friction force, and V_s is the constant Stribeck velocity. For LuGre tire model the longitudinal tire force is given by the following equation.

$$F_x = (\sigma_0 z + \sigma_1 \dot{z} + \sigma_2 V_r) F_z \tag{3.5.21}$$

Here F_z is the normal load, σ_1 is the damping coefficient and σ_2 is the viscous coefficient. In general the normal load, $F_z = m_t g$.

In the above-stated dynamics the relative velocity $V_r = R\dot{\theta} - V$, where R is the rolling radius of the tire, θ is the angular displacement, and V is the velocity of the vehicle. μ_c, μ_s, V_s and σ_2 are the static friction parameters while σ_0 and σ_1 are the dynamic friction parameters.

Burckhardt friction model

Burckhardt friction model (Patel, Edwards, & Spurgeon, 2007) is also a popular one which is widely used for the maneuvers. Comparatively it is simple and includes only static friction model. The simpler model (Park & Lim, 2008) which does not consider the side slips have been chosen for the longitudinal slip control problem. This model characterizes the simple relationship between the road friction coefficient and the longitudinal slip ratio by the following equation.

$$\mu(\lambda, C_r) = C_1\left(1 - e^{-C_2\lambda}\right) - C_3\lambda \tag{3.5.22}$$

Where, the vector C_r has three elements only. By changing the different values of C_1, C_2 and C_3 many different tire frictions can be modeled. Where C_1 is the maximum friction value, C_2 is the friction curve shape, and C_3 is the friction curve difference between the maximum value and the value at $\lambda = 1$. The table: 3.1 (Park & Lim, 2008) shows different combination of these parameters which is used for different road surface conditions.

Table 3.1 Value of different parameters for different road conditions

Surface conditions	C_1	C_2	C_3
Dry asphalt	1.2801	23.99	0.52
Wet asphalt	0.857	33.822	0.347
Dry concrete	1.1973	25.168	0.5373
Snow	0.1946	94.129	0.0464
Ice	0.05	306.39	0

Brush Model

The lateral forces and moments of the tire can be modeled by the Brush model (Ahn, Peng, & Eric Tseng, 2013) It gives a non-linear relationship between side-slip angle α and the friction coefficient μ. The tire lateral force f_y and the aligning moment of the tire τ_a are.

If $\alpha \le \alpha_{sl}$

$$f_y = -3\mu F_z l \theta_y \sigma_y \left\{ 1 - \left| \theta_y \sigma_y \right| + \frac{1}{3} \left(\theta_y \sigma_y \right)^2 \right\} \tag{3.5.23}$$

$$\tau_a = \mu F_z l \theta_y \sigma_y \left\{ 1 - 3 \left| \theta_y \sigma_y \right| + 3 \left(\theta_y \sigma_y \right)^2 - \left| \theta_y \sigma_y \right|^3 \right\} \tag{3.5.24}$$

Else,

$$f_y = -\mu F_z \operatorname{sgn}(\alpha) \tag{3.5.25}$$

$$\tau_a = 0 \tag{3.5.26}$$

Sliding slip angle defined as

$$\alpha_{sl} = \tan^{-1}\left(\frac{1}{\theta_y} \right) \tag{3.5.27}$$

Where, $\theta_y = \dfrac{2C_p l^2}{3\mu F_z}$ and $\sigma_y = \tan(\alpha)$. l is the half of the tire-road frictional coefficient, F_z is the tire normal force, C_p is the stiffness coefficient of the tire in unit length. The characteristics curves are shown in Fig 3.9 and Fig 3.10.

4 Algorithm for Existing Q-Adaptive Estimators

4.1 Chapter introduction

Model-based optimal estimators like Kalman Filter exhibits optimal performance when models (Plant model and measurement model) are accurately known to the estimators (Simon, 2006) (Zarchan, 2005) . Performance of such filters degrades when plant models are inaccurately known or unknown. In this chapter some nonlinear adaptive filters are discussed which adapt process noise automatically. The adaptation of process noise covariance improves the performance of the Estimators when the process model is uncertain or inaccurately known to the filter. The usefulness of those adaptive state estimators is analyzed, studied and evaluated with the help of case studies. Aircraft tracking scenarios have been considered for the evaluation of performance of nonlinear Q-adaptive estimators.

Q-Adaptation Vs R- Adaptation:

The knowledge of process noise covariance (Q) and the measurement noise covariance (R) has great importance to design model based optimal or sub-optimal filters. The Process and measurement noise covariances are considered to be known for such estimators for the best result. The Adaptive filters are useful when any of these noise covariances are unknown or inaccurately known to the estimators. The estimators which adapt process noise covariance Q are called Q-Adaptive filter/estimator and the estimator to adapt measurement noise covariance (R) called R-adaptive filter/estimator. Measurement noise covariance R represents the quantitative measure of the inaccuracy of the measurements. R-adaptive filters are designed to estimate the value of R when it is not known accurately. On the other hand, Q adaptive filters are designed to estimate the value of Process Noise Covariance (Q) of the system. The process noise covariance Q often represents the amount of model inaccuracies in the system.

It is often difficult to assign the process noise covariance in the estimator without performing numerical and other experiments especially when simplified process dynamics models are used in the filter. The trial and error method, called manual tuning, is often used to obtain the appropriate value of the process noise covariance (Q). In this work, we are focused to work on the state estimation of a system under model uncertainty or model mismatch. In this chapter, we have studied the possibility of employing Q adaptation schemes to improve the robustness of state estimation by nonlinear filters. The evaluation process of Q-adaptive nonlinear filters is thus carried out for a process where model uncertainty is present. We have assumed that the measurement noise covariance R to be known to the filters.

4.2 Q-Adaptive state estimators for linear systems

Process noise adaptation for optimal linear state estimator has been reviewed in (Mohamed & Schwarz, 1999) and (Almagbile, Jinling, & Weidong, 2010). The adaptive Kalman Filters are mainly deployed for three different scenarios. They are: (i) adapting process noise covariance, Q (ii) adapting measurement noise covariance, R and (iii) Adapting initial value of state error covariance, *P*. Several approaches have been reported in the literature to adapt these parameters such as fading memory based Q and R adaptive as presented in (Lee T. S., 1988) (Xia, Rao, Ying, & Shen, 1994),

Q-adaptive estimators for the linear system are summarised. The estimation process of Q or R matrices of Adaptive Kalman Filter is generally based on residual or innovation.

For a linear system, the dynamics of the state and measurement models can be expressed as

$$x_{k+1} = \Phi_k x_k + w_k \tag{4.2.1}$$

$$y_{k+1} = \mathrm{H}_{k+1} x_{k+1} + v_k \tag{4.2.2}$$

Where x_k is the state vector, Φ_k is the state transition matrix, y_k is the measurement vector, H is the observation matrix w_k and v_k are uncorrelated white noise sequence with covariance Q and R respectively. The steps of the Kalman Filters are summarized below:

State prediction: $$\hat{x}_{k+1|k} = \Phi_k \hat{x}_{k|k} \tag{4.2.3}$$

Innovation: $$v_k = y_k - \mathrm{H}_{k+1} \hat{x}_{k+1|k} \tag{4.2.4}$$

Error Covariance prediction: $$P_{k+1|k} = \Phi_k P_k \Phi_k^T + Q_k \tag{4.2.5}$$

Kalman Gain: $$K_{k+1} = P_{k+1|k} \mathrm{H}_{k+1} \left(\mathrm{H}_{k+1} P_{k+1|k} \mathrm{H}_{k+1}^T + R \right)^{-1} \tag{4.2.6}$$

Measurement update: $$\hat{x}_{k+1} = \hat{x}_{k+1|k} + K_{k+1} v_k \tag{4.2.7}$$

Error Covariance update: $$P_{k+1} = \left(I - K_{k+1} H \right) P_{k+1|k} \tag{4.2.8}$$

The scheme of Adaptive Kalman filter (Mohamed & Schwarz, 1999) is shown in Fig 4.1.

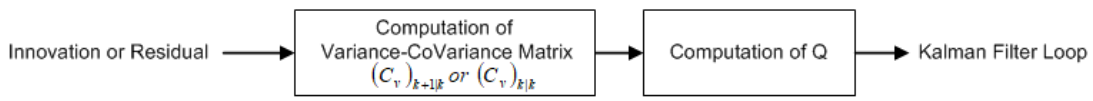

Figure 4.1 Scheme of Adaptive Kalman Filter

The adaptive scheme as shown above may be classified into two categories based on the input to the computation of Variance-Covariance matrix (i) Innovation based and (ii) Residual-based. Innovation and residual are defined as bellow

$$\nu_k = y_k - \mathrm{H}_{k+1}\hat{x}_{k+1|k} \tag{4.2.9}$$

$$\bar{\nu}_k = y_k - \mathrm{H}_{k+1}\hat{x}_{k+1} \tag{4.2.10}$$

Where ν_k is the innovation vector and $\bar{\nu}_k$ is the residual vector. Evaluation and comparative study of both the cases are given in (Almagbile, Jinling, & Weidong, 2010). In this thesis we have considered only innovation based adaptation techniques.

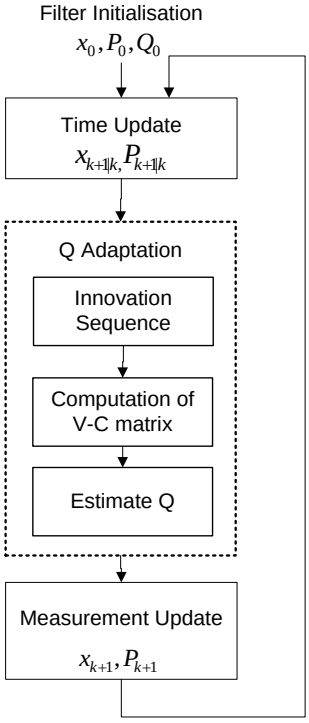

Figure 4.2 Flowchart of the adaptive filters

The Eq 4.2.5 in the Kalman Filter algorithm requires Q to be known as the prediction stage. Two popular innovation based adaptation techniques are described in the next sections.

4.2.1 Algorithm for Scaling factor based Q-adaptation

The covariance matching principle based algorithm as given in (Mehra, 1970) (Mohamed & Schwarz, 1999) (Ding, Jinling, Chris, & Doug, 2007). Variance-covariance matrix is computed through averaging inside a moving window of size *N*.

$$C_v = \frac{1}{N}\sum_{i=1}^{N} v_{k-i} v_{k-i}^T \tag{4.2.11}$$

Where, v is the innovation sequence. Based on covariance matching principle Q is estimated based on innovation.

If R and $P_{k+1|k}$ are assumed to be known, Q can be scaled by calculating the ratio between the estimated innovation covariance and predicted innovation covariance.

$$\alpha_k = \frac{trace\{C_v - R\}}{trace\{HP_{k+1|k}H^T\}} \tag{4.2.12}$$

Detailed derivation is given in (Ding, Jinling, Chris, & Doug, 2007).

Now, Q can be scaled at every epoch k as given below:

$$\hat{Q}_{k+1} = Q_k \sqrt{\alpha_k} \tag{4.2.13}$$

When the process noise covariance is a constant, and the estimation attains the steady state, the scaling factor α_k should be ideally equal or close to 1.

4.2.2 Algorithm for ML-based Q-Adaptation

The innovation based adaptive estimation approaches base on Maximum Likelihood (ML) are given in (Mehra, 1970) (Maybeck, Jensen, & A. Harnly, 1981) (Mohamed & Schwarz, 1999). Maximum Likelihood-based adaptation technique is also window based adaptation approach. This approach also assumes R and $P_{k+1|k}$ to be known. The estimated process noise covariance at every epoch is computed as:

$$\hat{Q}_{k+1} = K_{k+1} C_v K_{k+1}^T \tag{4.2.14}$$

Here, the variance-covariance matrix C_v is computed from Eq 4.2.11.

4.3 Q-Adaptive state estimators for nonlinear systems

The nonlinear suboptimal filters also suffer from the inaccurate knowledge of the process noise covariance. The approaches of the nonlinear adaptive filters are discussed in this section.

A nonlinear system may be defined as:

$$x_{k+1} = f(x_k, u_k) + w_k \tag{4.3.1}$$

$$y_k = h(x_k) + v_k \tag{4.3.2}$$

where the state vector x_k and y_k are the state and the measurement vectors of the system respectively at the instant k for input u_k. The uncorrelated white Gaussian process and measurement noise are represented as w_k and v_k with their covariances Q_k and R_k respectively.

4.3.1 Options for nonlinear non-adaptive estimations

Among numerous nonlinear filters, here some important and popular options for adaptive filters are given in this section.

4.3.1.1 Extended Kalman filter

The extended Kalman Filter (Simon, 2006) is the nonlinear extension of Kalman Filter here the $f(\cdot)$ and $h(\cdot)$ are linearized. Where F denotes the linearized system matrix obtained by taking the Jacobian $\frac{\partial(f(\hat{x}_{k|k}, u_k))}{\partial \hat{x}_{k|k}}$. The algorithm is similar to the Kalman Filter.

4.3.1.2 Unscented Kalman filter

Unscented Kalman Filter (Wan & Van Der Merwe, 2000) is one of the most popular estimators based on 'Sigma Points'.

A brief algorithm is described below. For details see (Wan & Van Der Merwe, 2000)

i. The set of sigma points χ are created by applying a sigma point selection algorithm

$$\chi_{k-1} = \left\{ \hat{x}_{k-1} \quad \hat{x}_{k-1} + \eta\sqrt{P_{k-1}} \quad \hat{x}_{k-1} - \eta\sqrt{P_{k-1}} \right\}$$

ii. The transformed set is given by instantiating each point through the process model

$$\chi_{i,k}^{-} = f(\chi_{k-1}, u_{k-1})$$

iii. The predicted mean is computed as

$$\hat{x}_{i,k}^{-} = \sum_{i=0}^{2L} W_i^{(m)} \chi_{i,k}^{-}$$

iv. And the predicted covariance is computed as

$$P_k^- = \sum_{i=0}^{2L} W_i^{(m)} \left(\chi_{i,k}^- - \hat{x}_k^-\right)\left(\chi_{i,k}^- - \hat{x}_k^-\right)^T + Q_k$$

v. Instantiate each of the prediction points through the observation model

$$y_{i,k}^- = h\left(\chi_{i,k}^-\right)$$

vi. The predicted observation is calculated by

$$\hat{y}_k^- = \sum_{i=0}^{2L} W_i^{(m)} y_{i,k}^-$$

vii. The innovation covariance is

$$P_{\hat{y}_k \hat{y}_k} = \sum_{i=0}^{2L} W_i^{(m)} \left(y_{i,k}^- - \hat{y}_k^-\right)\left(y_{i,k}^- - \hat{y}_k^-\right)^T + R_k$$

viii. The cross-correlation matrix is determined by

$$P_{x_k y_k} = \sum_{i=0}^{2L} W_i^{(m)} \left(\chi_{i,k}^- - \hat{x}_k^-\right)\left(y_{i,k}^- - \hat{y}_k^-\right)$$

ix. Finally, the update can be performed using the normal Kalman filter equations:

$$\kappa_k = P_{x_k y_k} P_{\hat{y}_k \hat{y}_k}^{-1}$$
$$\hat{x}_k = \hat{x}_k^- + \kappa_k \left(y_k - \hat{y}_k^-\right)$$
$$P_k = P_k^- - \kappa_k P_{\hat{y}_k \hat{y}_k} \kappa_k^T$$

4.3.1.3 Divided Difference Filter

Divided difference Filter (DDF) (NøRgaard, Niels K, & Ravn, 2000) is another option for nonlinear filtering.

The brief algorithm of second order Divided Difference Filter is given as follow (Notations are in the standard form)

i. Initialization: $\hat{x}_0, P_0$

ii. Computation of Cholesky factor $\hat{P}_k = \hat{S}_x(k-1)\hat{S}_x^T(k-1)$

iii. State propagation $\bar{x}_k = \frac{h^2 - n}{h^2} f(\hat{x}_{k-1}) + \frac{1}{2h^2} \sum_{p=1}^{n} \left\{ f(\hat{x}_{k-1} + h\hat{s}_{x,p}) + f(\hat{x}_{k-1} - h\hat{s}_{x,p}) \right\}$

iv. Propagation of predicted error covariance

$$\bar{P}_k = S_{x\hat{x}}^{(1)}(k)\left(S_{x\hat{x}}^{(1)}(k)\right)^T + S_{x\hat{x}}^{(2)}(k)\left(S_{x\hat{x}}^{(2)}(k)\right)^T + Q_k$$

$$S_{x\hat{x}}^{(1)}(k)_{(i,j)} = \frac{1}{2h}\left(f_i\left(\hat{x}_{k-1} + h\hat{s}_{x,j}\right) - f_i\left(\hat{x}_{k-1} - h\hat{s}_{x,j}\right)\right)$$

$$S_{x\hat{x}}^{(2)}(k)_{(i,j)} = \frac{\sqrt{h^2 - 1}}{2h}\left(f_i\left(\hat{x}_{k-1} + h\hat{s}_{x,j}\right) + f_i\left(\hat{x}_{k-1} - h\hat{s}_{x,p}\right) - 2f_i(\hat{x}_{k-1})\right)$$

v. Measurement update

$$\bar{y}_k = \frac{h^2 - n}{h^2} g(\bar{x}_k) + \frac{1}{2h^2} \sum_{p=1}^{n} \left\{ g(\bar{x}_{k-1} + h\bar{s}_{x,p}) + g(\bar{x}_{k-1} - h\bar{s}_{x,p}) \right\}$$

vi. Propagation of innovation covariance

$$P_k^y = S_{y\bar{x}}^{(1)}(k)\left(S_{y\bar{x}}^{(1)}(k)\right)^T + S_{y\bar{x}}^{(2)}(k)\left(S_{y\bar{x}}^{(2)}(k)\right)^T + R$$

$$S_{y\bar{x}}^{(1)}{}_{(i,j)} = \frac{1}{2h}\left(g_i\left(\bar{x}_k + h\bar{s}_{x,j}\right) - g_i\left(\bar{x}_k - h\bar{s}_{x,j}\right)\right)$$

$$S_{x\hat{x}}^{(2)}(k)_{(i,j)} = \frac{\sqrt{h^2 - 1}}{2h}\left(g_i\left(\bar{x}_k + h\bar{s}_{x,j}\right) + g_i\left(\bar{x}_k - h\bar{s}_{x,j}\right) - 2g_i(\bar{x}_k)\right)$$

vii. Cross-covariance

$$P_k^{xy} = \left[\bar{S}_x(k)\right]\left[S_{y\bar{x}}^{(1)}(k)\right]^T$$

viii. Gain $K_k = P_k^{xy}(P_k^y)^{-1}$

ix. State Update

$$\hat{x}_k = \bar{x}_k + K_k(y_k - \bar{y}_k)$$

$$\hat{P}_k = S_y(k)S_y^T(k) + K_k R K_k^T$$

4.3.1.4 Gauss Hermite Filter

Gauss Hermite Filter (Ito & Xiong, 2000) (Arasaratnam, Haykin, & J. Elliott, 2007) also belongs to the sigma point filtering class. A brief algorithm for Gauss Hermite filter is given below:

i. Computation of : $\hat{x}_0, P_0$

ii. Computation of Quadrature points and weights:

A symmetric tri-diagonal, defined as $J_{i,j} = 0$ and $J_{i,j+1} = \sqrt{\frac{i}{2}}$ for $1 \le i \le N-1$ for ' N 'quadrature points. Quadrature points are chosen as $q_i = \sqrt{2x_i}$ where x_i are the Eigen values of J .

Corresponding weights (w_i) of q_i is computed as $|(v_i)_1|^2$ where $(v_i)_1$ is the first element of i^{th} normalized eigenvector of J.

iii. Gauss Hermite Quadrature rule:

$$I_N = \int_{R^n} \tilde{F}(s) \frac{1}{(2\pi)^{\frac{n}{2}}} e^{-(1/2)|s|^2} ds$$

Can be expressed as

$$I_N = \sum_{i_1=1}^{N} ... \sum_{i_n=1}^{N} \tilde{F}(q_{i_1}, q_{i_2}, ..., q_{i_n}) w_{i_1} w_{i_2} ... w_{i_n}$$

In order to evaluate I_N for n^{th} order system, N^n number of quadrature points and weights are required.

iv. State propagation $\bar{x}_k = \frac{h^2 - n}{h^2} f(\hat{x}_{k-1}) + \frac{1}{2h^2} \sum_{p=1}^{n} \{ f(\hat{x}_{k-1} + h\hat{s}_{x,p}) + f(\hat{x}_{k-1} - h\hat{s}_{x,p}) \}$

v. Time update stage:

Cholesky Factor is computed as

$$S_x^+(k-1) = Cholesky\ (P_{k-1}^+)$$

Modify the quadrature points as

$$\chi_i^+ = S_x^+(k-1) q_i + \hat{x}_{k-1}$$

$$\bar{x}_k = \sum_{i=1}^{N} f(\chi_i^+) w_i$$

$$P_k^- = Q_{k-1} + \sum_{i=1}^{N} (f(\chi_i^+) - \bar{x}_k)(f(\chi_i^+) - \bar{x}_k)^T w_i$$

$\bar{x}_k$ is a priori estimate and P_k^- is a priori error covariance.

vi. Measurement update stage:

Cholesky Factor is computed as

$$S_x^-(k) = Cholesky\ (P_k^-)$$

Select sigma points as

$$\chi_i^- = S_x^-(k) q_i + \hat{x}_k$$

A priori estimate of measurement becomes

$$z_k = \sum_{i=1}^{N} g(\chi_i^-) w_i$$

The following covariance can be computed as

$$P_k^{xz} = \sum_{i=1}^{N} \left(g\left(\chi_i^-\right) - x_k\right)\left(g\left(\chi_i^-\right) - x_k\right)^T w_i$$

$$P_k^{zz} = \sum_{i=1}^{N} \left(g\left(\chi_i^-\right) - z_k\right)\left(g\left(\chi_i^-\right) - z_k\right)^T w_i$$

Filter Gain:

$$K_k = P_k^{xy}(P_k^{zz} + R)^{-1}$$

Covariance and Estimate Update

$$\hat{x}_k = \bar{x}_k + K_k(y_k - z_k)$$

$$P_k^+ = P_k^- - K_k\left(P_k^{zz} + R\right)K_k^T$$

4.3.2 Algorithm for Scaling factor based nonlinear adaptive filter

Scaling factor based adaptive EKF presented in (Almagbile, Jinling, & Weidong, 2010) . Extension to the adaptive nonlinear state estimators (such as ADDF, AGHF, AUKF etc.) is done by taking $\alpha_k = \frac{trace\{C_y - R\}}{trace\{P_y\}}$.

Where the term P_y represents the equivalent measurement covariance for the corresponding nonlinear estimators. The Variance-Covariance matrix C_v is computed from the innovation/residual of the respective nonlinear filters.

4.3.3 Algorithm for MLE based nonlinear adaptive filter

MLE based methods for Q adaptive have been summarised in (Mohamed & Schwarz, 1999) and (Almagbile, Jinling, & Weidong, 2010) KF. However, an extension to its nonlinear version can be done easily writing the same expression: $\hat{Q}_{k+1} = K_{k+1}C_v K_{k+1}^T$. Here K_{k+1} represent respective nonlinear gains of the filters. Adaptive version of GHF presented in (Dey, Sadhu, & Ghoshal, 2014). Adaptive Divided Difference filters are given in (Dey, Sadhu, & Ghoshal., 2013).

4.4 Aircraft Tracking by Q-Adaptive Estimators

State estimators, particularly nonlinear state estimators have synergistic relation with aerospace tracking problem. Performance improvement of such tracking systems over the years have been driven by better sensor systems like radars as well as improved state estimation algorithms. At the same time, new nonlinear state estimators have often been benchmarked with the help of aerospace tracking problems (Bar-Shalom, Li, & Kirubarajan, 2001) (Li & Vesselin, 2000) (Gadsden, Habibi, & Kirubarajan, 2014) (Gadsden & Hamed, 2015). State estimators can perform acceptably when the

process model is precisely defined, accurate values of measurement noise covariance are used and imperfections in the process model are taken care of by appropriate level of process noise covariance. The measurement noise covariance in these scenarios is often known with sufficient accuracy whereas the model of the process dynamics may not be known with sufficient accuracy or a simplified process model has to be used to reduce computational load. However, the often prescribed and simplified approach of using a 'large' process noise covariance (Q) to address the situation of inaccurate model and/or inaccurate knowledge about the genuine process noise, suffers from the disadvantage that the estimation tends to rely almost solely on the measurement information and consequently the estimation accuracy is likely to suffer. Similar situations have traditionally been addressed either by the use of adaptive approach or by the robust approach. In this particular case, one would consider using adaptive state estimators or robust state estimators.

Tracking of aircraft, both civil and military had been an active research and application area for state estimators (Bar-Shalom, Li, & Kirubarajan, 2001) (Nabaa & Bishop, 2000) (Yuan, Han, Duan, & Lei, 2005), since the early days of Kalman Filtering (Simon, 2006). Gadsden et al (Gadsden & Hamed, 2015) (Gadsden, Habibi, & Kirubarajan, 2014) and also Yongjian (Yang, et al., 2016) have recently revisited the maneuvering aircraft tracking problems. Gadsden et al (Gadsden & Hamed, 2015) (Gadsden, Habibi, & Kirubarajan, 2014) considered civilian air traffic control scenario and the same would be used here for ease of comparison with SVSF approach (Gadsden & Hamed, 2015) (Gadsden, Habibi, & Kirubarajan, 2014).

In the scenarios of tracking manned aircraft, the maneuver carried out by the pilot is often unpredictable. Even in an Air Traffic Control situation, depending on the traffic density and advice of the traffic controller, an aircraft may traverse curved or circuitous trajectories about which the automatic tracking algorithm may not have prior knowledge. The process dynamics therefore is not known with sufficient accuracy and simplified and or ad hoc models are often used in the estimators. In fact three different approaches are conceivable to address the problem of inaccurate knowledge about process dynamics, namely, (i) using a parameter tuning approach (Bar-Shalom, Li, & Kirubarajan, 2001) (Simon, 2006) where sufficiently 'large' process noise covariance (Q-matrix) is chosen to cover process model uncertainty, (ii) using a robust state estimators such as SVSF (Gadsden & Hamed, 2015) (Gadsden, Habibi, & Kirubarajan, 2014) and (iii) using an adaptive state estimator (Das, Dey, Sadhu, & Ghoshal, 2015) (Dey, Sadhu, & Ghoshal, 2014). The above discussion highlights how the process noise-adaptive (also called Q-adaptive) and the robust state estimators like SVSF, represent the two contrasting alternatives to overcome the lack of precise dynamic model of the process. The above also justifies the motivation of the present work viz., to compare performances of Q-adaptive nonlinear state estimators (often called filters) and the recently proposed robust variable structure filter, i.e., the SVSF, for tracking civilian aircraft in air traffic control scenarios. In

particular, for the adaptive nonlinear filter, representatives from the Q-adaptive sigma point filters, namely the Adaptive Divided Difference Filter (ADDF) and the Adaptive Gauss Hermite filter (AGHF) have been chosen.

As mentioned before, the kinematics of the tracked aircraft is thus complex but the tracker system is often constrained to use simplified models like standard Uniform Motion (UM) and Coordinated Turn (CT) models (Bar-Shalom, Li, & Kirubarajan, 2001) (Nabaa & Bishop, 2000) though the actual aircraft trajectory follows neither of the two simple models throughout its tracking time. It may be pointed out that while the UM model involves essentially linear dynamics, the CT model is essentially nonlinear.

In the section, adaptive nonlinear filters are used to estimate the position and velocity of aircraft following unknown but standard zigzag trajectories using both UM and CT models without any model switching (Bar-Shalom, Li, & Kirubarajan, 2001) or manual parameter tuning requirements. For the nonlinear CT model, this work evaluates a Q-adaptive version of second-order Divided Difference Filter (NøRgaard, Niels K, & Ravn, 2000), called the ADDF (Dey, Sadhu, & Ghoshal., 2013) and also the AGHF (Dey, Sadhu, & Ghoshal, 2014). It is shown subsequently that such adaptive filters obviate the need for manual tuning or choosing appropriate process noise covariance matrix but can provide improved performance over competing estimators. To the best of the knowledge of the authors, the ADDF, GHF and AGHF have not been evaluated with the kind of air traffic trajectories considered in this work. The present work takes the same ATC scenario (Gadsden, Habibi, & Kirubarajan, 2014) as one of two case studies to evaluate the relative performances of ADDF and AGHF) for unknown Q with, inter alia, the above mentioned robust Smooth Variable Structure Filter.

For evaluating the tracking estimators, both UM and CT models have been used. The performance of the tracking filters is presented in terms of typical true vs. estimated trajectory, and Monte Carlo simulation results like average and peak RMS errors.

We take the opportunity of comparing different state estimators to also investigate the effects of different sampling rates and different kinds of target position measurements, viz., in Cartesian format (x, y) or in the range-bearing (polar) format (r, θ).

Tracking Scenario:

The tracking scenarios of the civilian aircraft are discussed in section the 3.4.4 under chapter 3. Two tracking cases as shown in Fig 4.3 and Fig 4.4 have been considered for the evaluation of adaptive state estimators.

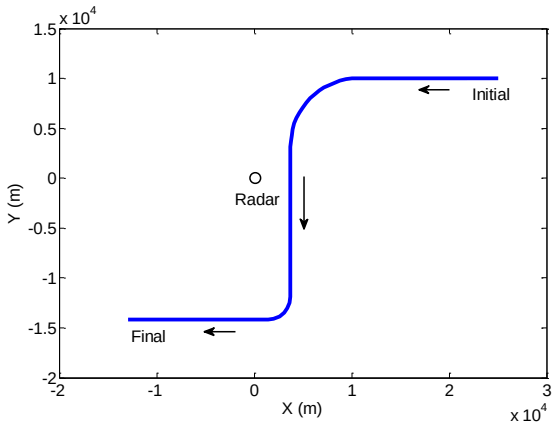

Figure 4.3 Trajectory-I

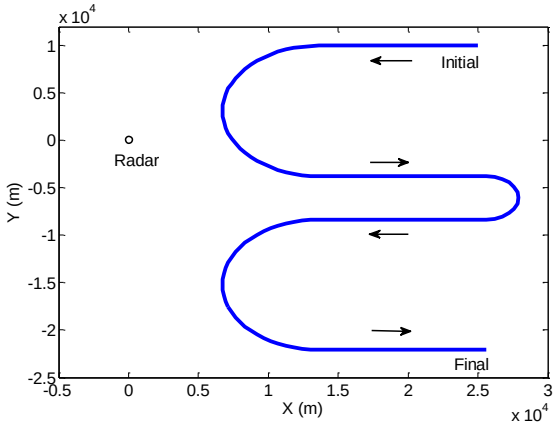

Figure 4.4 Trajectory-II

Detailed description of the Trajectory-I and Trajectory-II are given in the section 3.4.4.1 and 3.4.4.2 respectively. Truth Models to generate the trajectory are discussed in section 3.3.

Based on the measurement type, the evaluation process has been categorized into two: Linear Measurement and Polar measurement.

Simulation parameter:

The process noise covariance for the CT model is given by

$$Q_k = L_1 \begin{bmatrix} \frac{T^3}{3} & 0 & \frac{T^2}{2} & 0 & 0 \\ 0 & \frac{T^3}{3} & 0 & \frac{T^2}{2} & 0 \\ \frac{T^2}{2} & 0 & T & 0 & 0 \\ 0 & \frac{T^2}{2} & 0 & T & 0 \\ 0 & 0 & 0 & 0 & \frac{L_2}{L_1} T \end{bmatrix} \quad (4.4.1)$$

Where, L_1 and L_2 are the power spectral densities of the noise corresponding to linear velocities and angular velocities respectively. For the UM model, the fifth state variable is absent and accordingly, the 5th row and the 5th column is not required. For simulation in the case studies, values of the power spectral densities L_1 and L_2 considered are 0.16 and 0.01 respectively to maintain compatibility. Both UM and CT models have two measurements and the measurement noise covariance matrix R_k is 2 X 2.

For simulations, the Cartesian measurement the measurement noise covariance matrix is chosen as

$$R_c = 50^2 \begin{bmatrix} 1 & 0 \\ 0 & 1 \end{bmatrix} \tag{4.4.2}$$

$\rho = 0.0034e^{-x/22000}$ The corresponding measurement noise covariance for polar measurement is chosen as

$$R_p = \begin{bmatrix} 2 \times 50^2 & 0 \\ 0 & 0.1^2 \end{bmatrix} \tag{4.4.3}$$

The units of range and bearing are considered in (m) and degree $(\circ)$ respectively. For each run, initial state vector of the plant has been randomized with prescribed nominal values as given above and corrupted by an initial noise covariance P_0. For non-adaptive filters, random process noise and measurement noise sequences have been drawn from zero mean Gaussian noise sequences with prescribed covariance matrices. For the adaptive filters, the process noise covariance evolves as described in the algorithm. The performance of the tracking filters is presented in terms of time versus estimated trajectory for typical cases, Monte Carlo simulation results for RMS errors are also shown likewise. The numerical values of average (over the total run-time) RMSE and peak RMSE have been presented in appropriate tables to compare the performance of the filters with different models and methods.

The sample interval is taken as 5s for simulation of trajectory I. For trajectory II, results for two sampling intervals viz., 5s and 1s are provided. This is to investigate whether a faster sampling can substantially improve the performance. Initial error covariance P_0 is taken as $diag([50^2 \quad 50^2 \quad 100 \quad 100 \quad 1])$. RMSE plots have been provided for 500 Monte Carlo runs. True Q_k (as given in Eq 4.4.1) has been used for truth generation of the trajectory and the adaptive filters have been initialized with a typical wrong initial value (guess) as $0.01 \times Q_k$. Additional values regarding the trajectories are provided in the following sections.

4.4.1 Linear measurements (Trajectory-I)

Two-dimensional planar models: Uniform Motion and Coordinated Turn, as discussed in the section 3.3.2 are taken here for the evaluation of adaptive state estimators.

The linear measurement equation is given as:

$$\mathbf{y}_k = \begin{bmatrix} 1 & 0 & 0 & 0 & 0 \\ 0 & 1 & 0 & 0 & 0 \end{bmatrix} \mathbf{x}_k + \mathbf{v}_k \tag{4.4.4}$$

The linear measurement equation as shown in Eq 4.4.4 is considered for the nonlinear CT model. For UM model, 5th row of *H* matrix of Eq 4.4.4 should be omitted.

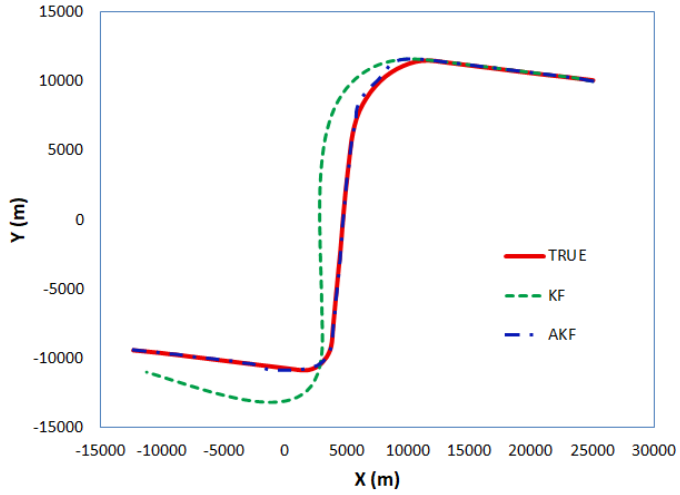

Figure 4.5 Estimation of position by KF and AKF with UM model for unknown noise ($Q_0 = 0.01 \times Q_{UM}$) for a typical MC run (with Cartesian measurements)

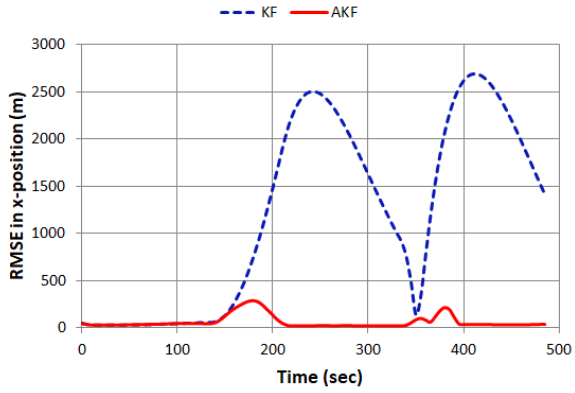

Figure 4.6 RMSE for X-position with KF and AKF via UM model where $Q_0 = 0.01 \times Q_{UM}$ for Trajectory-I

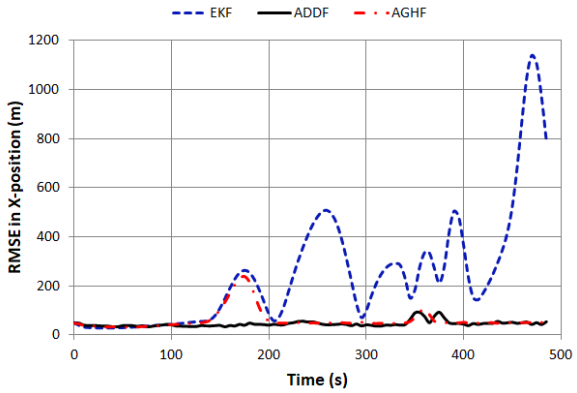

Figure 4.7 RMSE for X-position with EKF, AGHF and ADDF with CT model where $Q_0 = 0.01 \times Q_{CT}$ for Trajectory-I

Fig 4.8 represents the estimation of position of the aircraft by UM model. As UM model is linear one, simple Kalman Filter (KF) and its Q-adaptive version (AKF) are considered for state estimation. Both the filters have been initialized with the wrong value of process noise covariance ($Q_0 = 0.01 \times Q_{UM}$). The (non-adaptive) KF however, fails to track the position properly after the first turn. On the other hand, the AKF for the same scenario performs better and is able to handle the effect of model mismatch. This is evident in the plots of Fig 4.6. Table 4.1 summarises the performance of KF and AKF along with the robust SVSF (Gadsden, Habibi, & Kirubarajan, 2014).

Next, state estimation has been carried out with the EKF and ADDF and AGHF for the CT model. The simulation parameters are kept same as those taken for the case of UM model. It may be noted that the CT model with EKF performs better than the UM model with KF (as given in Table 4.1 and 4.2). However, the performance of the ADDF and AGHF has been found to be noticeably better than that of the EKF for unknown

process noise covariance (Table 4.2). Peak values of RMSE for 500 MC runs are also given in Table 4.2. It may be seen that adaptive filters (ADDF and AGHF) perform better for unknown process noise even in this metric. As expected the peak values are much larger compared to the average RMSE values.

Additionally, the average RMSE have also been compared with that for the robust SVSF (Bar-Shalom, Li, & Kirubarajan, 2001), which shows that the adaptive filters perform better even if the SVSF was tuned with true process noise.

Table 4.1 Performance comparison of Adaptive Kalman Filter with SVSF using UM model for 500 MC runs

Trajectory I UM model	**KF** $Q_0 = 0.01 \times Q_{UM}$ Composite (*X, Y*)	**AKF** $Q_0 = 0.01 \times Q_{UM}$ Composite (*X, Y*)	**SVSF** Composite (Gadsden, Habibi, & Kirubarajan, 2014)
Position error (m)	1707.8 (1195, 1220)	94.9 (64.25, 69.89)	111
Velocity error (m/sec)	55.9 (39.7, 39.4)	50.14 (35.27, 35.65)	97

Table 4.2 Performance comparison (Avg RMSE and peak RMSE) of ADDF and AGHF with EKF and SVSF for CT model for 500 MC runs for linear measurement

Trajectory I CT model	***EKF*** $Q_0 = 0.01 \times Q_{CT}$		***ADDF*** $Q_0 = 0.01 \times Q_{CT}$		***AGHF*** $Q_0 = 0.01 \times Q_{CT}$		***SVSF*** Composite (Gadsden, Habibi, & Kirubarajan, 2014)
	Average (Composite)	Peak (X,Y)	Average (Composite)	Peak (X,Y)	Average (Composite)	Peak (X,Y)	Average (Composite)
Position error (m)	528.02	(1139.14 2397.13)	82.29	(253.90, 318.98)	82.45	(238.76, 199.18)	110
Velocity error (m/sec)	41.14	(81.30, 154.17)	58.31	(196.47, 58.36)	57.14	(192.76, 58.01)	96.8

4.4.2 Polar measurements (Trajectory-I)

The polar measurement model is defined as

$$y_k = \begin{bmatrix} r_k \\ \theta_k \end{bmatrix} = \begin{bmatrix} \sqrt{\zeta_k^2 + \eta_k^2} \\ \tan^{-1}\left(\eta_k / \zeta_k\right) \end{bmatrix} + \begin{bmatrix} v_{rk} \\ v_{\theta k} \end{bmatrix} \tag{4.4.5}$$

State estimation has also been carried out with polar measurement model as given in Eq 4.4.5.

Nonlinear state estimators like ADDF and AGHF have also been used for polar measurements. Nonlinear CT model has been taken as system model. The simulation parameters are kept same as those taken for the case of the Cartesian measurement model. Performance of the estimators is evaluated for a case where process noise covariance is not known. RMSE performance for peak value and time-averaged composite value are given in Table 4.3. A total of 500 Monte Carlo Simulations were performed.

From Table 4.3, it may be noted that AGHF performs better as compared to ADDF in terms of time average RMSE. On the other hand, ADDF has shown better performance than AGHF when Peak value of RMSE is considered. Extended Kalman Filter was not considered due to the 'divided by zero' problem in the derivatives of Jacobean Matrix.

However, the performance of the nonlinear adaptive filters (ADDF and AGHF) for Polar Measurement is close to the case of Cartesian measurement.

Table 4.3 Performance comparison (Avg RMSE and peak RMSE) of ADDF and AGHF for CT model for 500 MC runs for polar measurement

Trajectory I CT model	***EKF*** $Q_0 = 0.01 \times Q_{UM}$		***ADDF*** $Q_0 = 0.01 \times Q_{CT}$		***AGHF*** $Q_0 = 0.01 \times Q_{CT}$	
	Average (Composite)	Peak (X,Y)	Average (Composite)	Peak (X,Y)	Average (Composite)	Peak (X,Y)
Position error (m)	-	-	85.52	(154.03, 208.83)	81.33	(168.51, 212.07)
Velocity error (m/sec)	-	-	56.92	(148.80, 77.52)	58.16	(166.82, 84.04)

4.4.3 Linear measurements (Trajectory-II)

In the case of Trajectory-II as defined in Fig 4.4 a faster sampling interval of T=1s is considered for the evaluation of adaptive nonlinear filters. The true trajectory along with typical runs of estimated position with EKF, ADDF and AGHF has been shown in Fig 4.8. Note that even with faster sampling, the non-adaptive EKF fails to track the trajectory when the aircraft takes a quick *'U'* turn with high turn rate. This contributes towards higher RMS error for EKF. Fig 4.9 depicts the RMSE plots of the EKF, ADDF and AGHF for Trajectory-II. The performance chart using the time-averaged RMS error metric is shown in Table 4.4, which also includes the performance of SVSF. As seen in the above figures and the table, the tracking performance of ADDF and AGHF, both being close to each other, are substantially better compared to that obtainable from the non-adaptive EKF. From Table 4.4, it is seen that the RMS position error performance of the adaptive state estimators is better compared to the SVSF which is consistent with results of Trajectory-I but the difference is less. In contrast to the results in Trajectory-I, the RMS velocity error performance is better for SVSF.

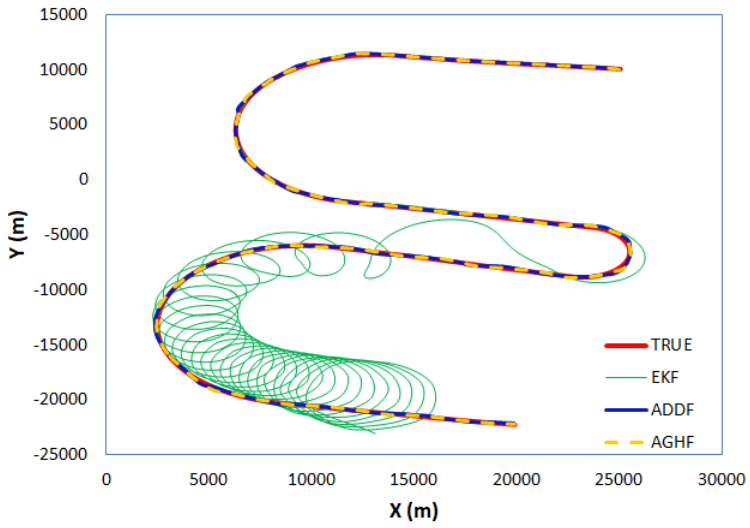

Figure 4.8 Estimation of position by EKF, AGHF and ADDF with CT model for unknown noise $Q_0 = 0.01 \times Q_{CT}$ ***(T = 1s) for a typical MC run for Trajectory – II***

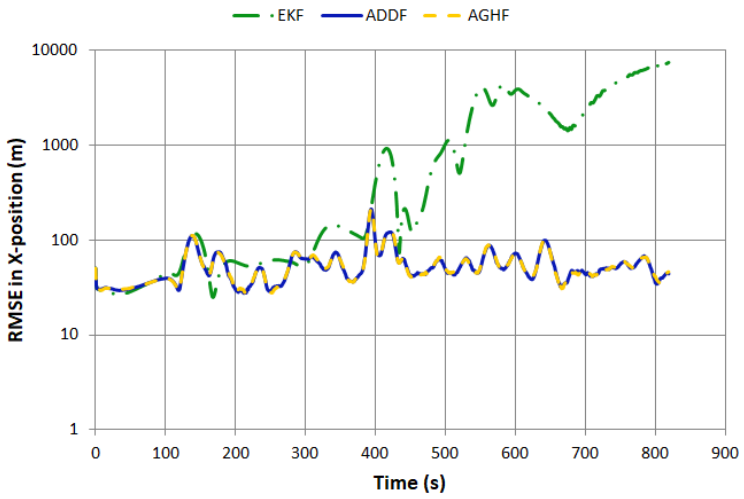

Figure 4.9 RMS position error performance of EKF, AGHF and ADDF with CT model for unknown noise $Q_0 = 0.01 \times Q_{CT}$ ***(T = 1s) for a typical MC run for Trajectory - II***

Table 4.4 Performance comparison (time-averaged RMS) of ADDF and AGHF with EKF using CT model for 500 MC runs

Trajectory-II CT model	**EKF** $Q_0 = 0.01 \times Q_{CT}$	**ADDF** $Q_0 = 0.01 \times Q_{CT}$	***AGHF*** $Q_0 = 0.01 \times Q_{CT}$	***SVSF*** ***Simulated***
Position error (m)	1986.8	85.08	85.02	92.75
Velocity error (m/sec)	479.94	75.99	76.00	65.16

4.4.4 Polar measurements (Trajectory-II)

A similar tracking performance was obtained for Polar measurement for trajectory-II. Results are not in here.

4.5 Chapter Conclusion

Using Monte Carlo simulation and two trajectories, we have evaluated performances of smooth variable structure (SVSF) based robust filters and single model adaptive nonlinear estimators. As the trajectories essentially embody nonlinear dynamics, nonlinear estimators had to be used.

Though earlier workers (Gadsden, Habibi, & Kirubarajan, 2014) benchmarked different estimation algorithms using the average RMS error as a measure, which, no doubt, provides a quick and convenient comparison between state estimators, for some practical applications the peak RMS position error measure should also be carefully considered as an off-line indicator of track loss

possibility. This is because the peak RMS position error value indicates the presence of large position errors which increases the possibility of losing track.

The relative computation time of several estimators discussed in this work is shown in Table 4.5 where it is seen that the computational efficiency of the AGHF is significantly lower compared to the other adaptive nonlinear filters. With the advent of high-speed microprocessors and parallel processing, the role of computational efficiency should be evaluated for each specific application. Here an AMD A8-7410 (2.20 GHz) Processor was used with MATLAB 2013b. Time was recorded by executing 'tic/toc' instructions.

Table 4.5 Computation Time for 500 Monte Carlo runs (Trajectory –I)

Estimator	Time elapsed (s)
EKF	16.94
AEKF	75.633
ADDF	187.00
AGHF	2.31×10^3
SVSF	64.93

From this study, some the most significant results of the present investigation are as follows.

(i) CT model-based state estimators, though marginally more computation intensive, provide better (compared to the UM model based) tracking performance for trajectories of the types considered.

(ii) Performance of the adaptive estimators even when initialized with a wrong guess value of process noise covariance provides tracking performance comparable to that obtainable with the recently introduced robust SVSF.

(iii) The AGHF is computationally more intensive by nearly an order of magnitude (more than a decade) compared to ADDF but tracking performance of this computationally intensive AGHF is very similar to that obtainable by ADDF and hence the former is not recommended for the tracking applications considered.

The salient contribution of the work presented in this chapter is a systematic evaluation and comparison of several Q-adaptive nonlinear estimators based tracking filters with robust variable structure. This may facilitate the choice of an appropriate state estimator for tracking duties. Specifically, three types of single model adaptive filters, viz., ADDF, AGHF and AKF and robust SVSF (smooth variable structure filter) and also KF and EKF have been considered.

Single model adaptive state estimators have been found to perform acceptably well when compared to recently introduced SVSF. From the abovementioned comparative evaluation, an analyst can make an informed choice and make appropriate trade-offs on the basis of estimation accuracy, algorithm complexity, tuning requirement and computational load for a given tracking scenario.

5 Sigma Point Smooth Variable Structure Filters (SPSVSF)

5.1 Chapter Introduction

This chapter serves several purposes. The primary purpose is to introduce the novel Sigma point-based Smooth Variable Structure Filter (SPSVSF), proposed in this work. The proposed SP-SVSF is based upon the Smooth Variable Structure Filter and also utilizes the benefits of using sigma point approach to deal with nonlinearity present in the system. The second purpose of this chapter is to provide a background and previous work on the Smooth Variable Structure Filter (SVSF) and especially the version with optimum boundary layer (SVSF-OBL)

The Smooth Variable Structure Filter (SVSF) has recently become popular among the robust state estimators. This chapter presents an alternative approach to estimate states by SVSF for nonlinear systems. The Traditional Smooth Variable Structure Filters are used for the continuous (smooth) system (Gadsden & Habibi, 2010). SVSF uses Jacobian for nonlinear state estimation (Gadsden, Mohammed, & Habibi, 2011). The proposed Sigma Point Variable Structure Filter (SPSVSF) utilizes the benefits of using sigma point approach to deal with nonlinearity present in the system. Thus the proposed method uses derivative free computation for the nonlinear approximation to overcome the Jacobian issue and to handle discontinuity. However, the idea of using sigma points in SVSF was presented in (Gadsden S. A., 2011). The strategy presented in (Gadsden S. A., 2011) used for combining UKF with SVSF. Whereas the present work in this chapter is to overcome Jacobian calculations in the SVSF algorithm. Monte Carlo Simulation has been carried out to evaluate the performance of the SPSVSF estimator.

The origin of the name ‘Smooth’ in SVSF came from the criteria that the estimator is applicable for a case where system model and the measurement model are continuous or smooth in nature (Habibi S. , 2007). The SVSF is applicable to both linear and nonlinear systems which are differentiable. A time-varying smoothing boundary layer is presented in (Gadsden, Mohammed, & Habibi, 2011). SVSF with time-varying smoothing boundary layer thus gives the optimal value of gain which is similar to Kalman Filter (Gadsden S. A., 2011) within the boundary layer for a linear system. However, the SVSF (with variable boundary layer) has been found to have several limitations for the nonlinear system though it is effective for robust state estimation. For the state estimation of nonlinear system, the system model and the measurement models are to be differentiable in order to obtain Jacobian for calculating the a priori estimate, the time-varying boundary layer calculation and SVSF gain. The Jacobian approximation may not be accurate for certain nonlinarites. On the other hand, there are

systems which may have discontinuities in its system or measurement model. In that case the SVSF with variable boundary layer may not be applicable to estimate the states.

The above context motivates to use a derivative-free computation of the recent version of SVSF to make the SVSF with time-varying boundary layer applicable for nonlinear and discontinuous systems. It is to be noted that the sigma point filters such as UKF, GHF and DDF are more accurate as compared to EKF for handling nonlinearities.

This chapter focuses on utilizing the sigma point formulation for the nonlinear approximation of a system for SVSF filters. Thus it minimizes the problem of nonlinear approximation and makes SVSF also applicable to discontinuous systems. However, it assumes the measurement model to be linear.

5.2 Previous work on Smooth Variable Structure State Estimators

5.2.1 Background on Smooth Variable Structure Filter (SVSF)

Recently a robust variable structure filter called Smooth Variable Structure Filter (SVSF) (Al-Shabi, Gadsden, & Habibi, 2013) (Al-Shabi, Gadsden, & S. A, 2015) (Gadsden, Habibi, & Kirubarajan, 2012) (Gadsden S. A., 2011) has been proposed and its application to air traffic control problem has been proposed in (Gadsden, Habibi, & Kirubarajan, 2014). The possibility of robust state estimation using the variable structure approach was explored in (Floquet, Edwards, & Spurgeon, 2007) (Liu, 2014) and a good tutorial exposition is provided in (Edwards & Sarah, 1998). Though the estimators cited above are in the continuous time domain and are of the type 'observer' rather than full-fledged state estimator, a good idea of robustness and convergence analysis of such estimators may be obtained therefrom.

A different kind of state estimator incorporating variable structure (often referred as VSF) was first introduced in (Gadsden, Habibi, & Kirubarajan, 2012) which, unlike earlier variable structure state estimators (with observer-structure), the VSF was formulated in a predictor-corrector structure and uses a discontinuous corrective 'gain' or, equivalently, a correction component which in Kalman filter framework would correspond to the Kalman gain multiplied by innovation. Initially the VSF concept was demonstrated using a linear plant model (Gadsden, Habibi, & Kirubarajan, 2012). In the SVSF context, the "robustness" implies that estimated (sequence of) states can be generated even with an inaccurate model of the system. Starting with a guessed initial value, the estimated sequence (trajectory) of states is forced towards the true state trajectory ('reachability phase') with a high (saturated) gain until it reaches the (time-varying) subspace termed the existence subspace (Gadsden, Habibi, & Kirubarajan, 2012) (Habibi S. , 2007) which encloses the true state trajectory as shown in Fig 5.1. Due to disturbances and uncertainties, the estimated value may switch back and forth across

the true state trajectory - a phenomenon called chattering while remaining within the existence subspace.

The VSF estimator as above was proven to ensure error convergence for bounded disturbance (even if uncertain) if the system is "consecutive bijective" and the measurement model is linear (Habibi S. , 2007). Subsequent versions of VSF permitted locally linearized approximations of the measurement equation. As the later versions of VSF required smoothness (with continuous partial derivatives of any order with respect to its arguments) of the dynamic equation the filter is called smooth variable structure filter (SVSF) (Habibi S. , 2007) (Gadsden & Habibi, 2010). The SVSF algorithm is straightforward if all the state variables are available as measurements, implying that measurement matrix (H) is non-singular. If H matrix is singular, the situation may be handled by using the pseudo inverse of H or by an auxiliary observer (Gadsden, Habibi, & Kirubarajan, 2012). Application of SVSF nonlinear plant models has been reported in (Gadsden & Habibi, 2010) (Habibi & Burton, 2007). The robustness of VSF has also been discussed in (Gadsden, Habibi, & Kirubarajan, 2012).

To reduce the effect of chattering noise (Habibi & Burton, 2002) (Al-Shabi, Gadsden, & Habibi, 2013) (Afshari, Dhafar, & Saeid, 2015) and consequent estimation error, a 'boundary layer' had been introduced in SVSF (Habibi S. , 2007) and such a version which inherits the robustness of SVSF without the encumbrance of switching noise may be called SVSF-BL for convenience. The concept of boundary layers of SVSF and the related concept of existence sub-space (Gadsden & Habibi, 2010) (Habibi S. , 2007) have been represented in Fig 5.1 which draws upon the ideas presented in (Habibi S. , 2007) and (Gadsden S. A., 2011). An SVSF-BL operates in two regimes. Outside the boundary layer, the (saturated) high gain pushes the estimated quantity to the boundary layer (despite an inaccurate process model and certain types of disturbances). Once within the boundary region, smaller (unsaturated and interpolated) gain is used resulting in smooth estimated state trajectory and estimation errors within the bounds of the width of the boundary layer due to unmodelled dynamics cannot be ruled out though. The width of the smoothing boundary layer impacts chattering and estimation accuracy. A careful or optimal choice is necessary because a narrow boundary layer would give rise to chattering whereas a very wide boundary layer would also be detrimental to estimation accuracy. Both these cases may lead to increased estimation error in the RMS sense. Cues for determining an appropriate value of boundary layer width may be obtained by measuring the amount of Chattering (Al-Shabi, Gadsden, & Habibi, 2013), however, a further improved version of SVSF (the SVSF-OBL, mentioned before) has been described in (Gadsden S. A., 2011) where an optimum boundary has been determined with the help of the process noise covariance Q, which is indicator of modeling approximation/inaccuracy. The optimal width of the boundary layer for SVSF-OBL is derived by minimizing the trace of the posterior state covariance matrix (Gadsden S. A., 2011) (Gadsden, Mohammed, & Habibi, 2011). Robustness and accuracy of the SVSF-OBL depend on the process noise and measurement noise covariance. [(Gadsden S. A., 2011), chapter 5]. However, the

knowledge of Q also helps to design a more accurate estimation within the smoothing boundary region by the use of Bayesian filters (e.g. KF, EKF, UKF, CDF (Das, Dey, Sadhu, & Ghoshal, 2015) (Simon, 2006), and cubature filter (Al-Shabi, Gadsden, & S. A, 2015)) with smooth gain.

An inaccurate knowledge of process noise covariance adversely impacts the performance of SVSF-OBL state estimators in more than one ways. Firstly, the width of the boundary layer ceases to be optimal which may lead to chattering or loss of estimation accuracy. Secondly, the state estimation algorithm used within the boundary generally makes use of the inaccurate Q (Gadsden S. A., 2011) (Gadsden, Habibi, & Kirubarajan, 2014) and therefore results in further increase of the estimation error.

Versions of SVSF-OBL which switches between SVSF-OBL and conventional Bayesian filters like those mentioned above have been proposed (Gadsden S. A., 2011) (Gadsden, Habibi, & Kirubarajan, 2014) (Gadsden & Hamed, 2015) (Gadsden, M, Ienkaran, & Saeid R., 2014).

Another variant of the SVSF uses a combined methodology of SVSF and other conventional sigma point filters to combine robustness and freedom from chattering (Al-Shabi & Hatamleh, 2014). Robustness of SVSF and 2nd order SVSF have been compared (Afshari, Dhafar, & Saeid, 2015).

A fairly comprehensive review of SVSF and its applications up to 2014 is available in (Gadsden & Hamed, 2015). An in-depth understanding about SVSF and the concept of optimal dynamic boundary layer are available in (Gadsden S. A., 2011). Some fairly recent developments have been reported in (Al-Shabi, Gadsden, & Habibi, 2013).

Various applications of the SVSF and SVSF-OBL for state estimation have been presented in (Habibi S. , 2007) (Gadsden, Mohammed, & Habibi, 2011) (Gadsden, Habibi, & Kirubarajan, 2014) which include target tracking and hydraulic actuation system.

5.2.2 Chattering in VSF and the Choice of Boundary Layer Thickness

SVSF filters may suffer from chattering (Gadsden S. A., 2011) (Al-Shabi, Gadsden, & Habibi, 2013) due to unknown process noise and other disturbances. The bounds of the amplitude of chattering in certain cases may be predicted and the same is said to be contained within an ‘existence sub-space’ (Habibi S. , 2007). SVSF with boundary layers (Gadsden & Hamed, 2015) (Gadsden S. A., 2011) (Al-Shabi, Gadsden, & Habibi, 2013) (Habibi & Burton, 2007) has been proposed to reduce such chattering. The concepts of boundary layers of SVSF and the existence sub-space (Habibi S. , 2007) have been represented in Fig 5.1 and would be further elaborated in the next section. Outside the boundary layer, a higher, saturated estimator gain is used, whereas inside the layer, a simpler estimator with smaller, unsaturated gain is generally used. The extent (thickness) of such boundary

layers should be carefully chosen so as not to allow residual chattering and at the same time, avoiding too wide a boundary layer, which may create excessive estimation error within the boundary layer.

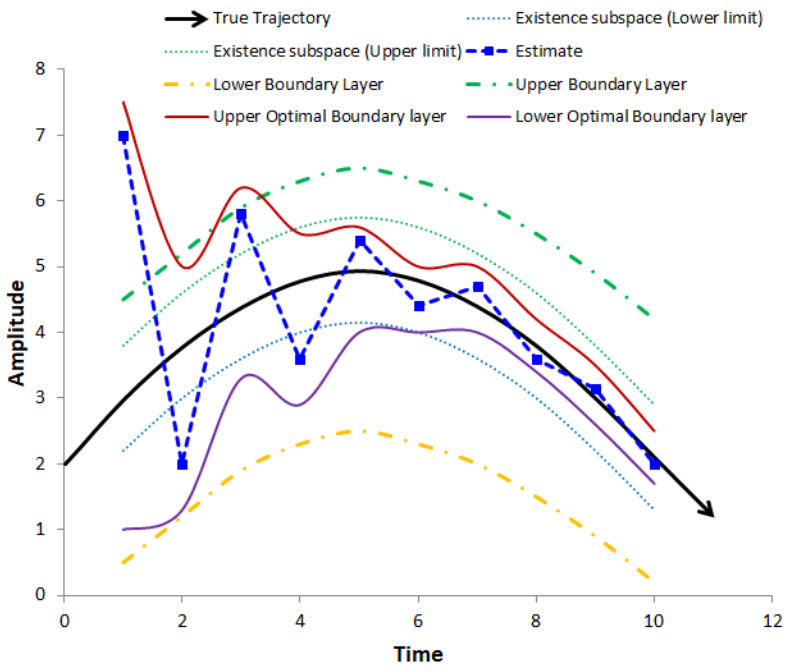

Figure 5.1 Boundary Layer Concept

This chapter proposes an improved version of SVSF-OBL by incorporating sigma points for nonlinear systems.

5.2.3 The SVSF-OBL Algorithm

The proposed ASVSF estimator is based upon a special version of SVSF proposed in ((Gadsden S. A., 2011) (Gadsden, Habibi, & Kirubarajan, 2014) envisages (to counter this by computing) an 'optimum' boundary layer thickness. From Fig 5.1, it may be seen that such an optimum boundary layer would be just wide enough to contain the existence sub-space. To distinguish the "SVSF with the optimal boundary layer" from the other versions, we may use the nomenclature SVSF-OBL where such distinction is necessary.

The algorithm/computational flow of SVSF-OBL is described below.

Though the algorithm of basic SVSF is available in several references (Gadsden S. A., 2011) (Gadsden, Habibi, & Kirubarajan, 2014) (Gadsden, Mohammed, & Habibi, 2011), a brief overview of the algorithm and certain special requirements of SVSF-OBL are pointed out here.

The most general form of SVSF requires that the functions $f(\bullet)$ and $h(\bullet)$ should be smooth and differentiable i.e., differentiable at every point of interest and the system should be observable. The SVSF (Gadsden, Habibi, & Kirubarajan, 2014) works in predictor-corrector structure with a prior estimate $\hat{x}_{k+1|k}$ (prediction) without utilizing the measurement and posterior estimates $\hat{x}_{k+1|k+1}$ (correction) taking cognizance of the measurements. The prediction step of SVSF is quite similar to the corresponding steps used for Kalman filter and updates the prior estimate of the state and also the prior error covariance $P_{k+1|k}$. The innovation ($\hat{z}_{k+1|k}$) is defined as the difference between the actual measurement y_{k+1} and the prior estimate of the measurement $\hat{y}_{k+1|k} = h(\hat{x}_{k+1|k})$. Similarly, the residual $\hat{z}_{k+1|k+1}$ is defined as the difference between the actual measurement y_{k+1} and the posterior estimate of the measurement $\hat{y}_{k+1|k+1}$.

As stated before, the SVSF-OBL state estimator assigns an optimal thickness of boundary layer in the hyperspace for a smooth estimate. Though the SVSF-OBL can be applied to more general cases, we first consider a simple form in which the measurement equation is linear and the concerned output matrix be of full rank.

In other words, the output equation is of the form

$$y_{k+1} = Hx_{k+1} + v_{k+1} \tag{5.2.1}$$

and the matrix H is invertible.

However, the condition of the output matrix being full rank (which implies that the number of measurements equals the number of state variables) may be relaxed by using appropriate observers or by using synthetic measurements as is used by (Gadsden, Habibi, & Kirubarajan, 2014). For a nonlinear output equation, one may take recourse to linearization. However, in such a case the optimality will be questionable.

The simple case of linear measurement and a full rank output matrix mentioned above, the properties of SVSF can be derived in a straightforward manner (Gadsden S. A., 2011). In the SVSF-OBL described in (Gadsden S. A., 2011) (Gadsden, Mohammed, & Habibi, 2011) the boundary layer thickness descriptor is a matrix, denoted by ψ_k which is to be calculated using the innovation ($\hat{z}_{k+1|k}$) and residual ($\hat{z}_{k|k}$) as given in (Gadsden, Mohammed, & Habibi, 2011). This boundary layer thickness matrix ψ_k is used for the calculation of SVSF gain (correction) term K_{k+1} which, in turn, is used to update the estimate analogous to the way it is done in KF in the form $\hat{x}_{k+1|k+1} = \hat{x}_{k+1|k} + K_{k+1}\hat{z}_{k+1|k}$. This expression is repeated in the detailed description of the algorithm of ASVSF.

The SVSF-OBL, however, has its own expression to update state covariance (Gadsden & Habibi, 2010) as described later.

For a discussion on the stability of SVSF and the gain, see (Al-Shabi, Gadsden, & Habibi, 2013).

5.3 Algorithm of Smooth Variable Structure Filter with Optimum Boundary Layer (SVSF-OBL)

The algorithm for SVSF given below follows descriptions of SVSF with optimum boundary layer in (Gadsden, Habibi, & Kirubarajan, 2014) (Gadsden & Hamed, 2015). Detailed derivations of the steps and the concept of the underlying theory are available in (Gadsden S. A., 2011).

A nonlinear dynamical system is described by the following equation

$$x_{k+1} = f(x_k, u_k) + w_k \tag{5.3.1}$$

$$y_{k+1} = h(x_{k+1}) + v_k \tag{5.3.2}$$

Where x_k is the state vector for input u_k and z_k represent measurement. The system has zero mean Gaussian process noise and measurement nose mentioned by w_k and v_k respectively.

The SVSF algorithm for the nonlinear system (Eq 5.3.1) and linear measurement equation $\left(y_{k+1} = Hx_{k+1} + v_k\right)$ is stated below.

i. Prediction stage:

Like the Kalman filter genre, the state and state error covariance can be predicted as follows

$$\hat{x}_{k+1|k} = f(\hat{x}_{k|k}, u_k) \tag{5.3.3}$$

$$P_{k+1|k} = FP_{k|k}F^T + Q_k \tag{5.3.4}$$

Where F denotes the linearized system matrix obtained by taking the Jacobian $\frac{\partial(f(\hat{x}_{k|k}, u_k))}{\partial \hat{x}_{k|k}}$

The innovation can be obtained as

$$\hat{z}_{k+1|k} = y_k - H\hat{x}_{k+1|k} \tag{5.3.5}$$

Innovation covariance can be represented as

$$S_k = HP_{k+1|k}H^T + R_k \tag{5.3.6}$$

ii. Smooth Boundary Layer:

The width of the boundary layer can be calculated as given in (Gadsden, Habibi, & Kirubarajan, 2014) (Gadsden & Hamed, 2015).

$$\psi_k = \left(\overline{\Lambda}_k^{-1} H P_{k+1|k} H S_k^{-1}\right)^{-1}$$

Where, $\Lambda_k = \left(\left|\hat{z}_{k+1|k}\right| + \gamma\left|\hat{z}_{k|k}\right|\right)$

γ represents the memory of VSF. It determines the convergence rate of the estimation. However, the value of γ can be chosen anything between 0 and 1 (Gadsden, Habibi, & Kirubarajan, 2014). $\overline{\Lambda}_k$ takes the diagonal values of Λ_k.

iii. Gain term:

The SVSF gain is derived as

$$K_{k+1} = H^{+} diag\left[\left(\hat{z}_{k+1|k} + \gamma\left|\hat{z}_{k|k}\right|\right) \circ sat\left(\frac{\hat{z}_{k+1|k}}{\psi_k}\right)\right] diag\left(\hat{z}_{k+1|k}\right) \tag{5.3.7}$$

The stability proof is given in (Al-Shabi, Gadsden, & Habibi, 2013)

iv. Update stage:

$$\hat{x}_{k+1|k+1} = \hat{x}_{k+1|k} + K_{k+1}\hat{z}_{k+1|k} \tag{5.3.8}$$

$$P_{k+1|k+1} = \left(I - K_{k+1}H\right)P_{k+1|k}\left(I - K_{k+1}H\right)^{T} + K_{k+1}R_{k+1}K_{k+1}^{T} \tag{5.3.9}$$

$$\hat{z}_{k|k} = y_{k+1} - H\hat{x}_{k+1|k+1} \tag{5.3.10}$$

5.4 Extended Smooth Variable Structure Filter

Extended Variable Structure Filter was presented by (Habibi S. , 2006) to deal with nonlinearity present in the system. Detailed descriptions are given in (Gadsden S. A., 2011). The version presented in (Habibi S. , 2006) did not include the optimal boundary layer. However, the below-mentioned steps include the SVSF with the optimal boundary layer.

Prediction stage:

$$\hat{x}_{k+1|k} = f(\hat{x}_{k|k}, u_k)$$

$$P_{k+1|k} = F_k P_{k|k} F_k^{\ T} + Q_k$$

$$\hat{y}_{k+1|k} = h(\hat{x}_{k+1|k})$$

Here $F_k = \left.\frac{\partial \widehat{f}}{\partial x}\right|_{\hat{x}_{k|k}, u_k}$, the linearized function of the system.

Innovation:

The innovation can be obtained as

$$\hat{z}_{k+1|k} = \mathrm{y}_{k+1} - H_k \hat{x}_{k+1|k}$$

Where $H_k = \left.\frac{\partial \hat{h}}{\partial x}\right|_{\hat{x}_{k+1|k}}$, the linearized measurement function for nonlinear system.

The Width of the Variable Boundary layer:

The expression is same as given in the section 5.3.

Gain term:

The expression is same as given in the section 5.3.

Update stage:

The expression is same as given in the section 5.3.

5.5 Sigma Point Smooth Variable Structure Filter

The sigma point SVSF actually makes use of the sigma point generation for nonlinear approximation. Here we have used the same methodology used for Unscented Kalman Filter (UKF). The SVSF discussed in previous section uses the Jacobian F_k in the prediction stage (calculation of $P_{k+1|k}$) for the estimation of the no-linear system. This proposed filter avoids the computation of derivatives for the Jacobian to make this filter used for nonlinear discontinuous system.

5.5.1 Sigma Point Generation

Sigma points are generated as per the unscented Kalman filtering (Wan & Van Der Merwe, 2000)

$$\hat{X}_{0,k|k} = \hat{x}_{k|k}$$

Where $\hat{X}$ contains sigma points. Weights $W_0^{(m)}$ and $W_0^{(c)}$ are calculated as follows:

$$W_0^{(m)} = \frac{\lambda}{n+\lambda}$$

$$W_0^{(c)} = \frac{\lambda}{n+\lambda} + \left(1 - \alpha^2 + \beta\right)$$

Where λ is the scaling parameter; α determines the distribution of sigma points; β is used to incorporate the prior knowledge of the distribution of $\hat{X}_k^-$ (for Gaussian distribution $\beta = 2$ is optimal); n is the order of the system.

$$\hat{X}_{k|k} = \left[\hat{X}_k^- \quad \hat{X}_k^- + \sqrt{(n+\lambda)P_{k+1|k}} \quad \hat{X}_k^- - \sqrt{(n+\lambda)P_{k+1|k}}\right]$$

$$W_i^{(m)} = W_i^{(c)} \frac{\lambda}{2(n+\lambda)}$$

$$\lambda = a^2(n+k) - n$$

$$W_i^{(m)} = W_i^{(c)} = \frac{\lambda}{2(n+\lambda)}$$

5.5.2 Sigma Point SVSF steps

Prediction stage:

$$\hat{x}_{k+1|k} = \sum_{i=0}^{2n} W_i \hat{X}_{k|k-1} \tag{5.5.1}$$

$$P_{k+1|k} = \sum_{i=0}^{2n} W_i \left(\hat{X}_{k|k-1} - \hat{x}_{k+1|k}\right)\left(\hat{X}_{k|k-1} - \hat{x}_{k+1|k}\right)^T + Q_k \tag{5.5.2}$$

$$\hat{Z}_{k+1|k} = h(\hat{X}_{k+1|k}, u_k) \tag{5.5.3}$$

$$\hat{y}_{k+1|k} = \sum_{i=0}^{2n} W_i \hat{Z}_{k+1|k} \tag{5.5.4}$$

Innovation:

The innovation can be obtained as

$$\hat{z}_{k+1|k} = \mathrm{y}_{\mathrm{k+1}} - \hat{y}_{k+1|k} \tag{5.5.5}$$

Width of the variable Boundary layer:

Innovation covariance is computed as

$$P_{zz|_k} = \sum_{i=0}^{2n} W_i \left(\hat{Z}_{k+1|k} - \hat{z}_{k+1|k}\right)\left(\hat{Z}_{k+1|k} - \hat{z}_{k+1|k}\right)^T + R_k \tag{5.5.6}$$

The width of the boundary layer can be calculated as given as

$$\psi_k = \left(\overline{\Lambda}_k^{-1}\left(P_{zz|_k} - R_k\right)P_{zz|_k}^{-1}\right)^{-1} \tag{5.5.7}$$

$$\text{or, } \psi_k = \left(\overline{\Lambda}_k^{-1} H_k P_{k+1|k} {H_k}^T P_{zz|_k}^{-1}\right)^{-1} + R_k \tag{5.5.8}$$

Where, $\Lambda_k = \left(\left|\hat{z}_{k+1|k}\right| + \gamma\left|\hat{z}_{k|k}\right|\right)$

γ represents the memory of VSF. It determines the convergence rate of the estimation. However, the value of γ can be chosen anything between 0 and 1

Gain term:

The SVSF gain is now given as follow. Note that the structure of the gain remained same as SVSF with variable boundary layer.

$$K_{k+1} = H_k^{-1}\left\{diag(\Lambda_k)\cdot sat(\psi_k^{-1}diag[\hat{z}_{k+1|k}])\right\}diag\left(\hat{z}_{k+1|k}\right)^{-1} \tag{5.5.9}$$

Update stage:

$$\hat{x}_{k+1|k+1} = \hat{x}_{k+1|k} + K_{k+1}\hat{z}_{k+1|k} \tag{5.5.10}$$

$$P_{k+1|k+1} = \left(I - K_{k+1}H_k\right)P_{k+1|k}\left(I - K_{k+1}H_k\right)^T + K_{k+1}R_{k+1}K_{k+1}^T \tag{5.5.11}$$

$$\hat{z}_{k+1|k+1} = y_{k+1} - H_k\hat{x}_{k+1|k+1} \tag{5.5.12}$$

5.6 Evaluation with test problem

The SPSVSF is evaluated for a nonlinear discontinuous system with linear measurement. A Case study for the discontinuous system is taken from (Sadhu, Bhaumik, Doucet, & Ghoshal, 2009) to evaluate the performance of the estimators.

The system is defined as:

$$\dot{x} = f(x) + w_k \tag{5.6.1}$$

$$y = Hx_k + v_k \tag{5.6.2}$$

Where, $f(x) = 2 - 0.001x_k\,\mathrm{sgn}(x_k)$ and $H = 1$. The system has process noise with covariance $Q_k = 1$ and measurement noise with covariance $R_k = 1$. The sampling interval is taken as 0.01s (Sadhu, Bhaumik, Doucet, & Ghoshal, 2009). Initial state error covariance, $P_0 = 2$ is considered for the simulation study. SPSVSF is evaluated for a nonlinear discontinuous system. Fig 5.2 shows the true and estimated states for single run. RMSE plot for 500 Monte Carlo runs is given in Fig 5.3.

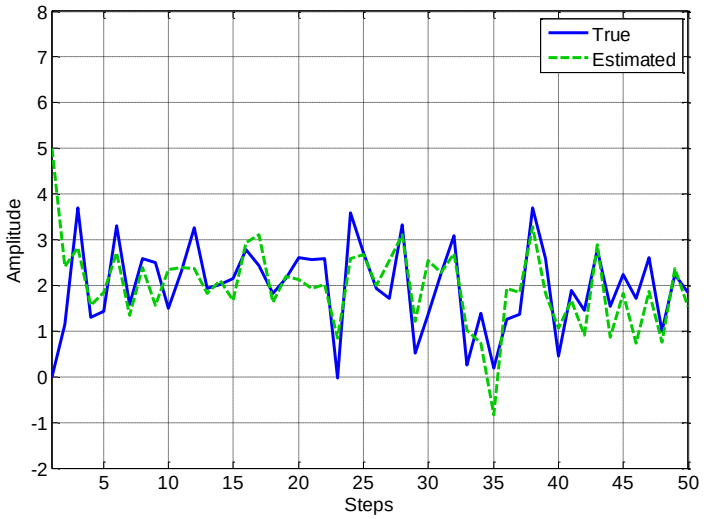

Figure 5.2 True and estimated states

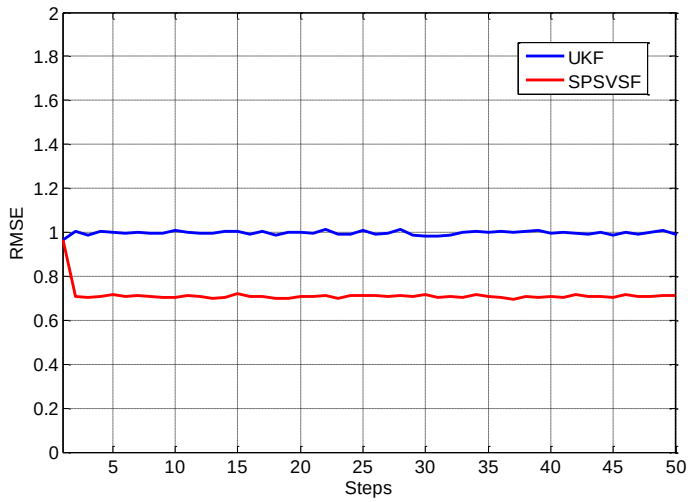

Figure 5.3 RMSE Plot of SPSVSF and UKF

Note on the study:

i. Sigma point Smooth Variable Structure Filter is presented in this chapter. From the simulation study, it is to be noted that it can estimate a discontinuous system.

ii. The measurement model is considered as linear. As the present form of SVSF gain term contains H^{-1} term, the equivalent nonlinear sigma points could not be substituted in this work.

iii. From the RMSE plot it is seen that the performance of SPSVSF is better than the UKF.

iv. For comparative study, SVSF is not included because the SVSF cannot estimate states of discontinuous system.

v. Structure of the SPSVSF gain is kept unchanged with respect to SVSF-OBL and the stability condition also did not change for the sigma point version. Only change was made to calculate the covariances with the help of sigma points as per the Unscented Transformation rules.

5.7 Chapter Conclusion

The Sigma point SVSF is presented here for the state estimation of nonlinear discontinuous system. The proposed version of the estimator has been evaluated with 1st order nonlinear discontinuous system. However, this also assumes *H* to be linear or linearized and to have full rank. This limitation may be tackled in future work.

6 Adaptive Smooth Variable Structure Filter

6.1 Chapter Introduction

This chapter proposes and describes the algorithm for an improved nonlinear adaptive state estimator called Adaptive Smooth Variable Structure Filter (ASVSF) and evaluates its performance. The proposed ASVSF extends the functionality and performance of a previously reported robust smooth variable structure filter (SVSF) with optimal boundary layer (SVSF-OBL) (Gadsden, Habibi, & Kirubarajan, 2014) (Al-Shabi, Gadsden, & Habibi, 2013). This proposed ASVSF estimator, which inherits the robustness of the SVSF, also adaptively provides an estimate of the unknown process noise covariance (and hence called adaptive SVSF or ASVSF) which is required for determining the optimal boundary layer width of SVSF-OBL. The optimal boundary layer, in turn, helps in reducing chattering noise as well as in reducing the estimation error due to the large boundary layer. Subsequent sections of this chapter would show that improvement in performance also includes the provision for accommodating unknown and time-varying process noise covariance Q, (which generally characterizes modeling uncertainty).

Any inaccuracy in the value of Q therefore would lead to lack of optimality and consequent increased RMS error. This important shortcoming is proposed to be remedied in the present work by an improved state estimator, named ‘Adaptive Smooth Variable Structure Filter (ASVSF)’, which incorporates an additional component for nonlinear adaptive estimation component for estimating the process noise covariance in every time step and uses the same for computing the optimum boundary layer. This ensures the optimality of the SVSF-OBL component without the requirement of accurate knowledge of the process noise covariance, and further, makes the proposed ASVSF state estimator capable of handling time-varying process noise that is time-varying modeling errors. Apart from making the boundary layer width optimal, the estimated value of Q also helps to reduce the estimation error within the boundary layer.

The estimation method proposed in this chapter incorporates aspects of SVSF-OBL as well as that of adaptive estimation and therefore inherits some of the good features of both. It may be noted that this type of state estimator combining the features of variable structure filter with optimum boundary layer as well as nonlinear adaptive state estimator, capable of handling unknown, time-varying modeling error, has not been previously reported.

6.1.1 Problem formulation (Generic)

The formulation of the generic nonlinear state estimation problem is given below for appreciating the proposed estimation algorithm.

$$x_{k+1} = f(x_k, u_k) + w_k \tag{6.1.1}$$

$$y_{k+1} = h(x_{k+1}) + v_{k+1} \tag{6.1.2}$$

where, x_k is the state vector and y_k is the measurement vector. The system has input u_k and the Gaussian noise can be represented by w_k and v_k having covariance matrices Q_k and R_k respectively. For the estimation algorithms to be presented, it is assumed that the measurement noise covariance R_k is known whereas the process noise covariance Q_k may not be so.

The state estimator should be able to reconstruct the state variables from the noisy measurements in an optimal manner. A state estimator is called robust if it continues to provide acceptable results when parameters of the description given in (6.1.1) and (6.1.2) are not known accurately. In particular, we are interested in robustness with respect to the process model which is parameterized by the process noise covariance matrix Q_k. In all types of state estimators there may be larger errors before the state estimator is engaged due to mismatch of initial conditions. However, it is expected that the estimate should converge towards the true value as time progresses. This property is called convergence and may be reformulated as a stability problem (Habibi S. , 2007). However, an inaccurate knowledge of process noise covariance adversely impacts the performance of SBSF-OBL state estimators in more than one ways. Firstly, the width of the boundary layer ceases to be optimal which may lead to chattering or loss of estimation accuracy. Secondly, the state estimation algorithm used within the boundary generally makes use of the inaccurate Q (Gadsden S. A., 2011) (Gadsden, Habibi, & Kirubarajan, 2014) and therefore results in further increase of the estimation error.

6.1.2 Organization of this Chapter

Rest of the chapter is organized as follows:

The next section briefly describes the background and previous work along with the context of this contribution by brief reviews of previous work on SVSF and adaptive state estimators. For the sake of continuity, the steps of SVSF-OBL over which the proposed estimator is developed are briefly described before describing the ASVSF. The algorithm of the proposed ASVSF estimator is presented in the third section.

The fourth section describes the evaluation methodology employed and two case studies involving aircraft tracking problems to establish the improved performance of the Adaptive Smooth Variable

Structure Filter (ASVSF). The truth models of the tracking problems as well as the models assumed in the filter are introduced. The simulation results are also tabulated and discussed in this section where the performance of the ASVSF is compared vis-à-vis those of SVS-OBL and a few other filters. Note that (a) the performance of the proposed ASVSF estimator is evaluated using Monte Carlo simulation and is compared with previously reported state estimators using a case of manoeuvring civilian aircraft (b) three different measures of RMS error over the trajectory have been used for comparison which demonstrates the strengths of the proposed ASVSF estimator (c) a simplified and grossly approximate process model is used in the estimator/filter for tracking and thereby generating a time-varying and unknown process noise covariance situation. The last section provides a summary and concluding discussion.

6.2 Problem Statement

6.2.1 Robust and adaptive estimators

As the rest of the chapter would indicate, the proposed estimation algorithm incorporates aspects of adaptive and robust approaches. At the outset the fundamental concepts that drive the Q-adaptive and robust approaches to estimation may be restated.

Acceptable estimation accuracy in cases where only an approximate or simplified model of the process is available may be obtained with robust and/or adaptive state estimators. Both these types of estimators tolerate deterministic as well as uncertain process parameter variation. Approximation in the process model is often represented by process noise covariance Q. The accuracy of robust estimators normally does not strongly depend on the Q matrix that means it may tolerate modeling inaccuracies. An adaptive estimator on the other hand estimates the process noise covariance Q at every estimation step and uses the same for generating the optimal estimate.

A number of nonlinear robust state estimators (Poznyak & Joel, 2001) (Hajiyev & Soken, 2014) (Habibi S. , 2007) (Gadsden & Hamed, 2015) as well as adaptive state estimators (Hajiyev & Soken, 2014) (Das, Dey, Sadhu, & Ghoshal, 2015) (Dey, Sadhu, & Ghoshal, 2014) (Dey, Das, Sadhu, & Ghoshal, 2015) have been reported in the literature.

Smooth Variable Structure Filter (SVSF) is one of the robust estimation approaches (which is briefly recalled next. The structure and algorithm for the Q-adaptive state estimator have been proposed in an earlier chapter and would be recalled in a subsequent section.

6.2.2 Outline of the Q-Adaptive Filter

The proposed ASVSF employs the concept of Q-adaptive filter over the SVSF framework to incorporate adaptivity as well as robustness within a single algorithm. The previous work on Q-

Adaptive Filter and an outline of the algorithm have already been discussed in a previous chapter. The following is provided only for the sake of continuity.

In particular, the popular scale factor based adaptation of Q-adaptive filters (Almagbile, Jinling, & Weidong, 2010) (Hajiyev & Soken, 2014) has been incorporated and the structure of the Q-adaptation scheme is shown in Fig 6.1 within the blocks bounded by dashed lines. Details of nonlinear Q-adaptive filters are discussed in chapter-4. The 3 steps of scale factor based adaptation are (i) Estimation of variance-covariance (V-C) matrix, C_v by averaging the innovation sequence through a moving window of length N. (ii) Calculation of the scaling factor α_k. (iii) Determination of the estimated value of process noise covariance from the previous estimate $\hat{Q}_{k-1}$. This value of the estimated process noise covariance matrix is used for the state estimation steps as described below.

There are two process noise adaptation techniques, viz MLE based (Mohamed & Schwarz, 1999) and scaling factor based (Almagbile, Jinling, & Weidong, 2010). Though either of the two may be used for ASVSF, the simpler, scaling factor based process noise adaptation technique has been used in this work for the adaptation and calculation of the estimated process noise covariance $\hat{Q}_k$. The algorithm for smooth variable structure filter is presented in the previous chapter.

6.3 Adaptive Smooth Variable Structure Filter (ASVSF)

6.3.1 Overview of this Contribution

The contribution of this work, which proposes augmenting the SVSF-VBL estimators with an adaptive estimator for process noise covariance, may be appreciated in the context of the previous subsection. For the SVSF-VBL estimator an accurate knowledge of the process noise covariance is required to determine the correct width of the boundary layer and hence improve the estimation performance. When the model is inaccurate or uncertain and cannot be described by a known constant value of Q, the proposed ASVSF state estimator iteratively and dynamically estimates a more accurate value of Q, by an embedded adaptive filter. Such approach can also handle time-varying Q and nonlinear systems.

The proposed estimator, called ASVFS inherits the inherent robustness of SVSF (with respect to model inaccuracy), smoothness i.e., avoidance of switching noise (for SVSF-OBL), and improved estimation accuracy by providing more accurate value of process noise covariance. The last named item i.e., reduced sensitivity to unknown process noise covariance would be particularly useful when the process noise covariance is not only unknown but also varies with time.

The difference between the root cause of robustness of SVSF and the same for ASVSF may be noted here. For the SVSF the fact that the filter performance does not depend on modeling inaccuracy (represented by the process noise covariance matrix Q) may be identified as the root cause. In the case of ASVSF, one can start with an almost wild guess about Q, which, thanks to the adaptive algorithm, recursively evolves to a near true value within a few time steps. This makes the state estimation independent of the knowledge about the process noise covariance matrix Q and hence to the extent of model inaccuracy.

6.3.2 Architecture and Algorithm of ASVSF

The system model is again represented by Eq. 6.1.1 & 6.1.2. We illustrate the concept of Adaptive Smooth Variable Structure Filter (ASVSF) using the SVSF with optimal boundary layer described above and accordingly the measurement equation is linear.

The proposed structure of ASVSF algorithm is demonstrated in Fig 6.1. It may be noted from the flowchart that the Q-adaptation steps (bounded by dashed lines) are embedded in the algorithm for SVSF with the optimal boundary layer. Further, the process noise covariance adaptation occurs before the calculation of the optimal boundary layer ψ_k. In the proposed filter, the adaptive estimate of the process noise covariance is actually used within the boundary layer region of SVSF. From the detailed steps of the SVSF (and also ASVSF), it may be noted that the boundary layer ψ_k is directly dependent on process noise covariance (symbolized by Q with appropriate suffix depending on the context) of the system. The accuracy of SVSF within the boundary layer depends on the prior knowledge of the process noise covariance of the system. If we take a closer look at the expression for the gain term K_{k+1} of the SVSF, it may be observed that the term $sat\left(\hat{z}_{k+1|k}\psi_k^{-1}\right)$ defines the linearly bounded region called the boundary layer. Thus, the accuracy of the estimator within the boundary layer may also suffer when the value of the process noise covariance is unknown. When an approximate process model is used, there would be situations where the covariance of the process noise is unknown or is varying over time as discussed earlier. The proposed ASVSF algorithm provides a mechanism to correct the inaccuracies resulting from the cases of unknown or time-varying process noise covariance by adaptively estimating the process noise covariance at every time step. Thus, the robustness property of SVSF outside the boundary layer remains unaffected whereas a more accurate optimal boundary layer width is computed and concurrently a more accurate state estimate is computed inside the boundary layer. Detailed steps are as follow.

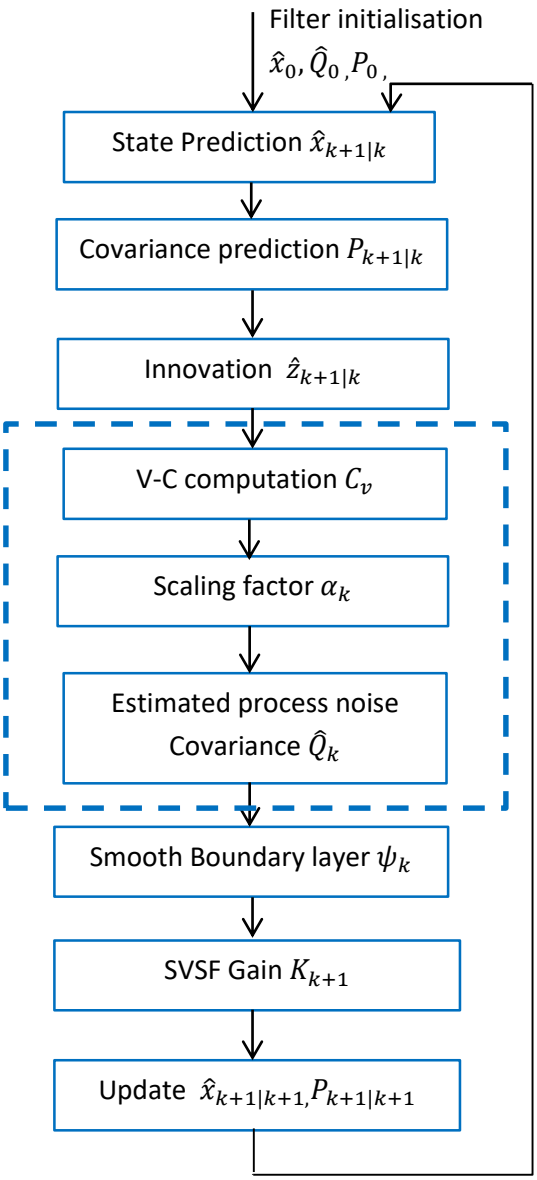

Figure 6.1 Flow chart of Adaptive SVSF

The innovation can be computed as $\hat{z}_{k+1|k} = y_k - H\hat{x}_{k+1|k}$, where y_k is the measured output of the system and $\hat{x}_{k+1|k}$ is the predicted states of the system. The covariance matrix $\hat{Q}_k$ can be estimated by averaging innovation sequence through a moving window of length N (Dey, Sadhu, & Ghoshal, 2014). The estimated variance-covariance matrix (V-C), $\hat{C}_v$ is defined as

$$\hat{C}_v = \frac{1}{N}\sum_{i=1}^{N} \hat{z}_{k+1-i|k-i}\hat{z}^T_{k+1-i|k-i} \tag{6.3.1}$$

For $k < N$, the usual practice is to truncate the window as needed. The estimated $\hat{Q}_k$ at any epoch k can be expressed as

$$\hat{Q}_k = \hat{Q}_{k-1}\sqrt{\alpha_k} \tag{6.3.2}$$

where, the scaling factor α_k denotes the ratio between calculated measurement noise covariance and its predicted counterpart (Almagbile, Jinling, & Weidong, 2010).

$$\alpha_k = \frac{trace\left\{\hat{C}_v - R_k\right\}}{trace\left\{HP_{k+1|k}H^T\right\}} \tag{6.3.3}$$

When the process noise covariance is a constant, and the estimation attains the steady state, the scaling factor α should be ideally equal or close to 1.

The steps of the ASVSF are as follows:

ASVSF estimates states of the dynamical system defined in Eq. 6.1.1-6.1.2 iteratively from predefined initial conditions. $\bar{x}_0$, P_0 and $\hat{Q}_0$ which are to be initialized appropriately before the execution. As the proposed algorithm estimates the process noise iteratively and adaptively, the results are fairly insensitive to the initial value $\hat{Q}_0$.

i. Prediction stage:

The predicted state and error covariance are to be calculated first with the help of the given model of the system.

$$\bar{x}_{k+1|k} = f(\hat{x}_{k|k}, u_k) \tag{6.3.4}$$

$$P_{k+1|k} = FP_{k|k}F^T + \hat{Q}_k \tag{6.3.5}$$

The predicted covariance $P_{k+1|k}$ is calculated with the help of linearized state matrix F and the estimated process noise covariance $\hat{Q}_k$

ii. Innovation sequence:

The innovation is thus calculated using output function and predicted sates.

$$\hat{y}_{k+1|k} = H\hat{x}_{k+1|k} \tag{6.3.6}$$

$$\hat{z}_{k+1|k} = y_k - \hat{y}_{k+1|k} \tag{6.3.7}$$

iii. Variance-covariance matrix

The variance-covariance matrix $\hat{C}_v$ for the estimation of process noise covariance is to be calculated by averaging a moving window of length N through the innovation sequence. The length of N should be chosen appropriately.

$$\hat{C}_v = \frac{1}{N}\sum_{i=1}^{N} \hat{z}_{k+1-i|k-i}\hat{z}^T_{k+1-i|k-i} \tag{6.3.8}$$

iv. Scaling factor

The estimated process noise covariance $\hat{Q}_k$ can be scaled by a factor α_k which is calculated by taking ratio between estimated process noise covariance and the predicted process noise covariance.

$$\alpha_k = \frac{trace\left\{\hat{C}_v - R_k\right\}}{trace\left\{HP_{k+1|k}H^T\right\}} \tag{6.3.9}$$

v. Innovation covariance

$$S_k = HP_{k+1|k}H^T + R \tag{6.3.10}$$

vi. Smooth boundary layer width

The smooth boundary layer ψ_k is calculated using the innovation covariance and the linearized output matrix. See (Gadsden, Mohammed, & Habibi, 2011) for full the derivation.

$$\psi_k = \left(\overline{\Lambda}_k^{-1} HP_{k+1|k}H^T S_k^{-1}\right)^{-1} \tag{6.3.11}$$

where $\overline{\Lambda}_k$ refers to forming a diagonal matrix with elements of $\Lambda_k = \left(\left|\hat{z}_{k+1|k}\right| + \gamma\left|\hat{z}_{k|k}\right|\right)$

vii. Gain calculation

The ASVSF gain can be written as (Gadsden S. A., 2011) follows

$$K_{k+1} = H^{-1}\left\{diag(\Lambda_k)\cdot sat(\psi_k^{-1}diag[\hat{z}_{k+1|k}])\right\} diag\left(\hat{z}_{k+1|k}\right)^{-1} \tag{6.3.12}$$

According to the assumptions explained earlier, H is essentially a square matrix of full rank. The situation where the system has fewer measurements than the number of states can also be addressed as per (Habibi S. , 2007).

viii. Update stage:

Finally, the estimates are to be updated with the ASVSF gain.

$$\hat{x}_{k+1|k+1} = \hat{x}_{k+1|k} + K_{k+1}\hat{z}_{k+1|k} \tag{6.3.13}$$

The state covariance is also updates as

$$P_{k+1|k+1} = (I - K_{k+1}H)P_{k+1|k}(I - K_{k+1}H)^T + K_{k+1}R_{k+1}K_{k+1}^T \tag{6.3.14}$$

Residual sequence can be updated with available measurement and the estimated states.

$$\hat{z}_{k+1|k+1} = y_{k+1} - H\hat{x}_{k+1|k+1} \tag{6.3.15}$$

ix. Process noise adaptation (update)

The estimated process noise to be scaled in every iteration by the factor α_k as calculated in Eq. 6.3.9.

$$\hat{Q}_{k+1} = \hat{Q}_k\sqrt{\alpha_{k+1}} \tag{6.3.16}$$

6.4 Evaluation of the Proposed Estimator

6.4.1 Evaluation Approach

Proofs of convergence and stability of adaptive nonlinear filters and SVSF-OBL for general nonlinear signal model are yet to be reported. Therefore, following previous workers (Hajiyev & Soken, 2014) (Al-Shabi M. , 2017) (Bhaumik, 2013) (Arasaratnam, Haykin, & Elliott, 2007) in the field of nonlinear filters, we take recourse to Monte Carlo simulation with non-trivial signal models for evaluating the performance of the new estimator.

More specifically, using suitable test problems we would like to investigate (i) whether and to what extent the proposed ASVSF estimator inherits the advantages of the SVSF when inaccurate process model is used, (ii) the ability of the ASVSF to accommodate unknown and time-varying process noise covariance, and also (iii) to compare the performance of the ASVSF, SVSF-OBL and an ordinary Kalman filter in a target tracking scenario.

Two tracking scenarios, where a target executes ‘S’ and ‘Triple U-turn’ planar test trajectories have been chosen. The scenario is characterized by nonlinear kinematics and is derived from (but is substantially more complex than) an often used example of a civil aircraft trajectory (Gadsden S. A., 2011) (Gadsden, Habibi, & Kirubarajan, 2014) (Bar-Shalom, Li, & Kirubarajan, 2001) (but closer to a UAV track). To demonstrate the efficacy of the proposed ASVSF estimator for inaccurate process model, a simpler linear dynamic model called uniform motion model (UM) is assumed in the estimators. The mismatch between the actual trajectory and the same described by the simpler kinematic model may be considered to be unknown and time-varying process noise covariance. It may

be shown that an EKF with certain inaccurate initialization will diverge for this trajectory-filter assumed kinematics combination.

The performance is evaluated with Monte Carlo studies from which the RMS error across the Monte Carlo population at each time sample may be obtained following traditional approach. For the present study, additional metrics like (i) peak RMS error, (ii) time-averaged RMS error and (iii) root of the mean square of the above RMS error (RMS of RMS) over the whole time period of the tracking problem are used as performance indicators. It may be noted that persistent peaks in the RMS error are reflected in the RMS of RMSE. Occasional peak errors however are better captured in the peak of RMSE descriptor. Performance of the proposed state estimator (ASVSF) is compared with that for SVSF and an ordinary Kalman filter.

The trajectories, as shown in the section 3.3.4, have combinations of coordinated turn (CT) and uniform motion (UM) segments. The tracking Radar assumed to be at the origin, measures the position (*x*, *y*) of the aircraft at regular intervals. The task of the estimator is to estimate the motion states, viz., position and velocity of the aircraft with the available noisy measurements. To demonstrate the robustness of the estimator, the filter uses only linear uniform motion model (described below) to estimate the motion states for the entire course of the flight. As a result of using the simplified model in the estimator, fairly severe mismatches occur at the CT segments. Such mismatches are expected to be taken care of by (enhanced) process noise covariance. As the variable structure estimators possess a fair degree of robustness, it may be expected that mismatches of the above type would be taken care of adequately.

The performance of the estimators has been evaluated with the help of Monte Carlo simulation. A total of 500 Monte Carlo runs have been performed for each study to calculate (i) the RMS error sequence ($\{e_{rms}(k)\}$) across the Monte Carlo population corresponding to each instant (ii) peak value of the RMS error sequence ($\{\sup_k[e_{rms}(k)]\}$), (iii) time average of the RMS error sequence $\frac{1}{N}\sum_{k=1}^{N} e_{rms}(k)$ and (iv) RMS of the RMS error sequence $\sqrt{\frac{1}{N}\sum_{k=1}^{N} e_{rms}^2(k)}$. The sampling interval is taken as 5s.

The SVSF-OBL convergence rate γ is chosen to be 0.1. For ASVSF, the window size *N* is taken as 35 steps.

The simulations have been carried out for two cases. In both the cases a random noise with covariance Q_{UM} is injected into the process as the truth model. Note that the ASVSF requires only an initial value of process noise covariance matrix and the estimator continually updates the process noise covariance

as per its adaptation logic. The other estimators use a constant process noise covariance. The two cases respectively are, (a) where the non-adaptive filters use Q_{UM} as the process noise whereas the same value is used as an initial estimate of process (b) here the covariance of the injected noise are unknown to the estimators and the non-adaptive and adaptive filters use $Q_0 = 0.01 \times Q_{UM}$ as the process noise and as an initial estimate of process . All RMSE plots, values of average RMSE, peak of RMSE, and RMS of RMSE in the table for position and velocity are given in composite form (viz., equivalent resultant position error and resultant velocity error).

6.4.2 Aircraft tracking Trajectory-I

Same tracking trajectory which is discussed in section 3.3.4.1 has been used here for evaluation of the proposed ASVSF (Fig 6.2). Performance of the proposed ASVSF has been compared with previously reported SVSF and traditional Kalman Filter.

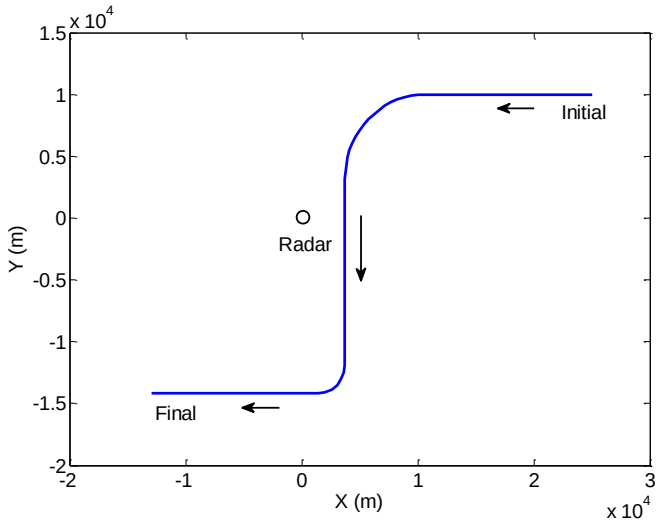

Figure 6.2 Trajectory-I (not corrupted with process noise) of the aircraft

Fig 6.3 shows the estimates by KF, SVSF and ASVSF with the true trajectory. The estimators have been initialized with a wrong guess of process noise covariance $Q_0 = 0.01 \times Q_{UM}$. The RMSE for 500 Monte Carlo runs have been plotted in Fig 6.4 and Fig 6.5 to represent the RMSE plots of position and velocity respectively for wrong initial guess.

It is to be noted that the RMSE plots show the peaks whenever the aircraft takes a turn. From the RMSE plots it is clearly seen that the ASVSF performs better than SVSF and KF. During the model mismatches the performance of ASVSF is substantially better than the other estimators.

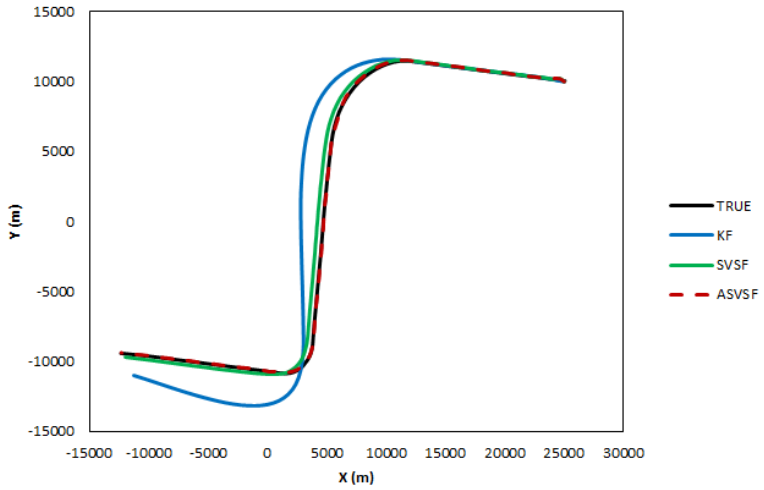

Figure 6.3 Estimation of position by KF, SVSF and ASVSF for unknown noise ($Q_0 = 0.01 \times Q_{UM}$)

Table 6.1 shows the time average RMSE performance for 500 Monte Carlo runs. The two cases have been studied: (a) with correct initial guess and (b) with wrong initial guess. For both the studies, ASVSF performs substantially better than KF and SVSF. As mentioned previously, the ASVSF takes care of process noise adaption as well as the model inaccuracy. There is almost no change in the performance of ASVSF (as compared to the other two) for initializing the estimator with wrong value.

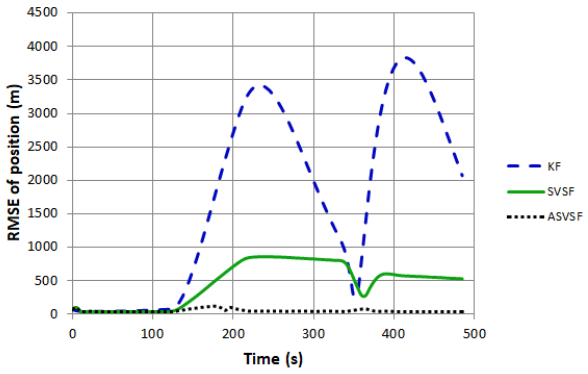

Figure 6.4 RMSE of position with KF, SVSF and ASVSF where $Q_0 = 0.01 \times Q_{UM}$

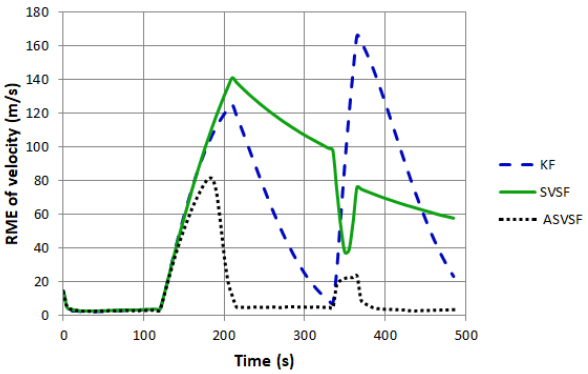

Figure 6.5: RMSE of velocity with KF, SVSF and ASVSF where $Q_0 = 0.01 \times Q_{UM}$

Table 6.1 Time average RMSE of position by KF, SVSF and ASVSF for unknown noise ($Q_0 = 0.01 \times Q_{UM}$)

Process Noise Covariance	States	KF	SVSF	ASVSF
$Q_{f\|k=0} = Q_{UM}$	Position (m)	189.6	72.93	51.99
	Velocity (m/s)	17.92	41.99	12.92
.	Position (m)	1708.5	455.17	51.94
$Q_{f\|k=0} = 0.01 \times Q_{UM}$	Velocity (m/s)	55.93	64.42	13.03

6.4.3 Aircraft tracking Trajectory-II

Trajectory-II (Fig 6.6) which takes triple 'U' turn has also been considered for the evaluation of ASVSF. The details of the trajectory are given in section 3.3.4.2.

Typical tracking trajectories including the true trajectory (with process noise) and as estimated by KF, SVSF and ASVSF are shown in Fig 6.7.

Fig 6.8 and Fig 6.9 represent the RMS error plots of position and velocity for nominal initialization of the process noise covariance. RMSE plots for wrong initialization ($Q_0 = 0.01 \times Q_{UM}$) of the process noise have been shown in Fig 6.10 and Fig 6.11.

From the plots it is seen that ASVSF can perform well even when there is a sharp turn (the 2nd turn of the trajectory) in the flight path. The wrong initial guess has almost no effect on the performance of ASVSF. Table 6.2 summarises the performance of estimators in terms of time-averaged RMSE, peak of RMSE, and RMS of RMSE. Comparative robustness performance may be visualized from Fig 6.12 and Fig 6.13 where time-averaged RMS error in position and velocity are shown against the multiplying factor for the process noise covariance.

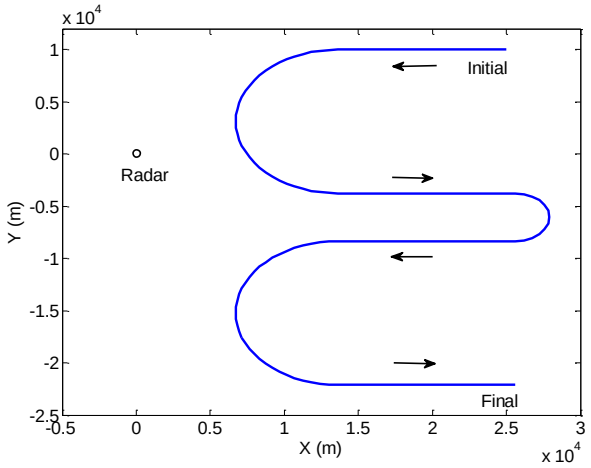

Figure 6.6 Trajectory-II (not corrupted with process noise) of the aircraft

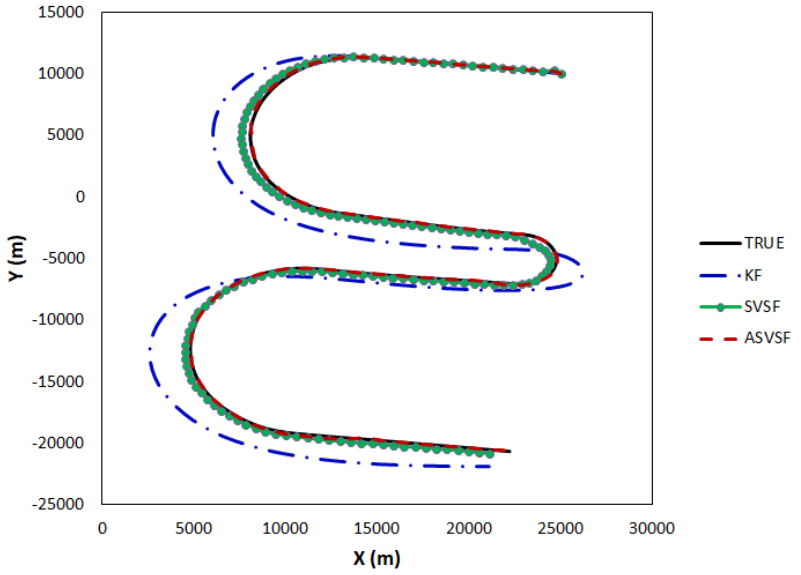

Figure 6.7 Estimation of position by KF, SVSF and ASVSF for unknown process noise ($Q_0 = 0.01 \times Q_{UM}$)

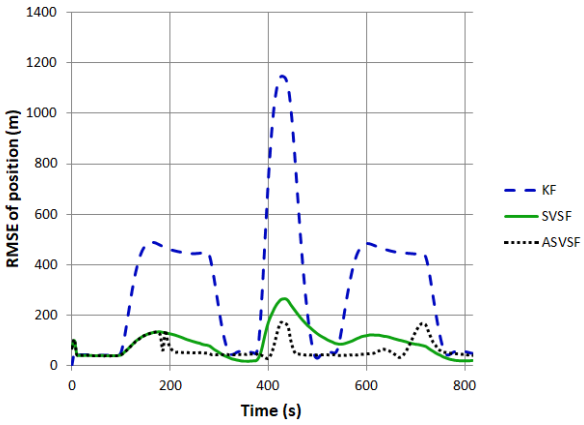

Figure 6.8 RMSE of position using KF, SVSF and ASVSF where $Q_0 = Q_{UM}$

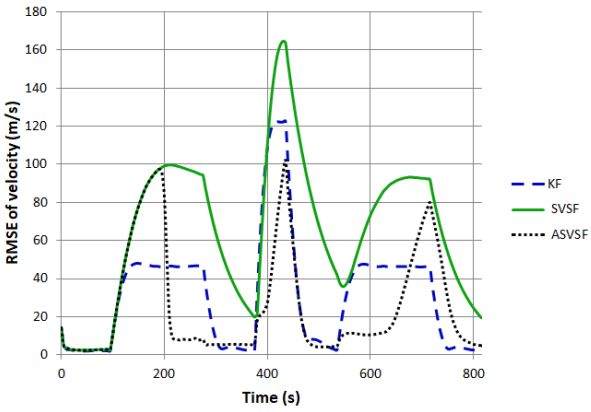

Figure 6.9 RMSE of velocity using KF, SVSF and ASVSF where $Q_0 = Q_{UM}$

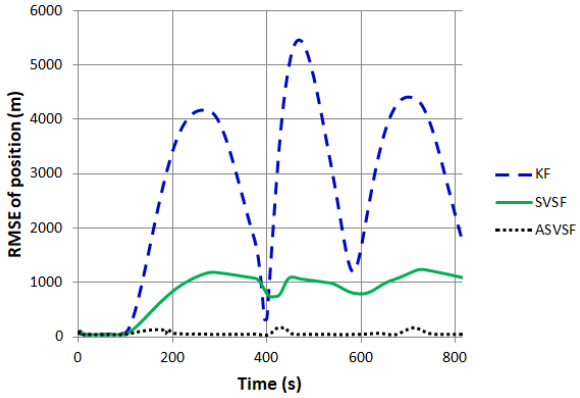

Figure 6.10 RMSE of position using KF, SVSF and ASVSF where $Q_0 = 0.01 \times Q_{UM}$

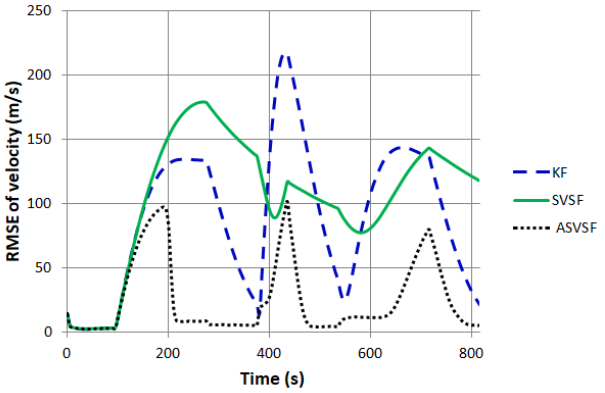

Figure 6.11 RMSE of velocity using KF, SVSF and ASVSF where $Q_0 = 0.01 \times Q_{UM}$

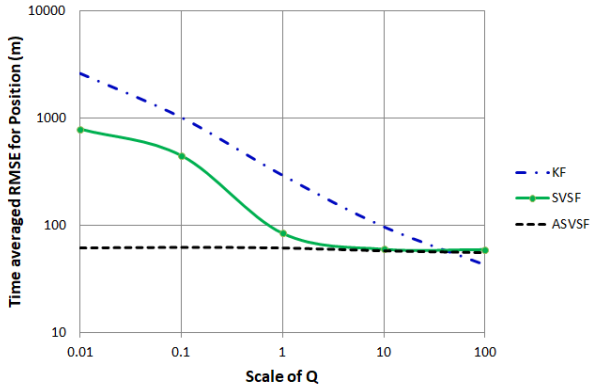

Figure 6.12 Time-averaged RMS error in position against the multiplying factor for the process noise covariance

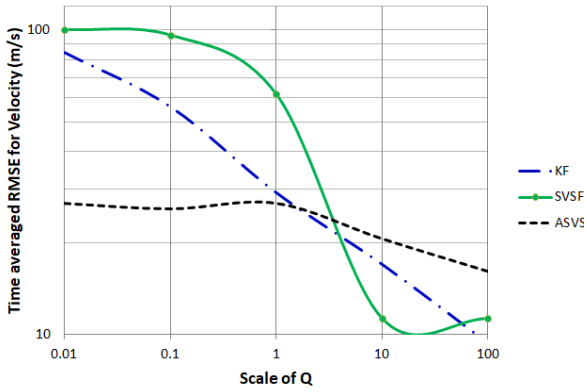

Figure 6.13 Time-averaged RMS error in velocity against the multiplying factor for the process noise covariance

Table 6.2 Performance table for 'Triple U-turn' planar Trajectory

Process noise covariance	Metric Type	Parameters	KF	AKF	SVSF	ASVSF
$Q_0 = Q_{UM}$	Time averaged RMS Error (RMSE)	Position (m)	293.95	131.56	84.76	61.97
		Velocity (m/s)	29.29	19.66	61.78	27.02
	Peak of RMSE	Position (m)	1146.1	919.03	267.45	165.31
		Velocity (m/s)	122.7	117.45	164.87	103.37
	RMS of RMSE	Position (m)	415.47	226.44	108.96	68.37
		Velocity (m/s)	43.25	31.07	75.94	38.90
$Q_0 = 0.01 \times Q_{UM}$	Time averaged RMSE	Position (m)	2610.0	242.01	792.68	61.95
		Velocity (m/s)	84.50	27.46	100.60	27.003
	Peak of RMSE	Position (m)	5461.6	2836.6	1234.2	165.14
		Velocity (m/s)	217.6	474.7	179.2	102.12
	RMS of RMSE	Position (m)	3167.5	574.73	921.34	68.64
		Velocity (m/s)	105.6	54.42	116.65	38.76

6.5 Chapter Summary and Conclusion

An algorithm for an improved state estimator, viz., ASVSF, for nonlinear systems incorporating the concepts of robustness of smooth variable structure filter (SVSF) as well as the ability to adapt unknown and time-varying process noise covariance through adaptive estimation has been proposed and evaluated by an aircraft tracking scenario where the nominal trajectory is composed of uniform motion and coordinated turn segments and the actual trajectory is also perturbed by random kinematic noise.

Recall that out of several versions of SVSF, we have used the version with optimal boundary layer (Gadsden, Habibi, & Kirubarajan, 2014) (Gadsden, Mohammed, & Habibi, 2011) i.e., SVSF-OBL. This version requires linear measurement equation with full order measurement matrix. However, in line of (Gadsden, Habibi, & Kirubarajan, 2014, we have generated the velocity measurement by the "first difference" method as discussed before.

Use of the linear UM model and linear measurement model in the filter allows us to evaluate the proposed ASVSF not only with SVSF but also with Kalman filter.

From the results in the nominal process noise case, we can make the following observations w.r.t. different variables and metrics.

- In the Average RMSE metric, in position and velocity, the proposed ASVSF exhibited the best performance.
- In the Peak RMSE metric, in position and velocity, the proposed ASVSF again provides the best result. The same is true for RMS of RMSE metric.

From the results in the off-nominal process noise case, we can make the following observations w.r.t. different variables and metrics.

- For the underestimated value of process noise covariance ($Q_0 = 0.1 \times Q_{UM}$ and $Q_0 = 0.01 \times Q_{UM}$), Average RMSE, Peak RMSE and RMS of RMSE metrices of position and velocity, indicate that the performance of the proposed ASVSF is the best.
- For the overestimated value of process noise covariance ($Q_0 = 10 \times Q_{UM}$ and $Q_0 = 100 \times Q_{UM}$), the comparative performances are more complex. Performance of the ASVSF, though good, but may not be claimed to be best for position for the different performance measures. For velocity, performance of the simple Kalman filter for higher values of Q turns out to be the best. This can be explained from the fact that for highest value of Q, information from the process model is generally ignored (Simon, 2006) (Raol & Girija, 2001)by the Kalman filter

and the velocity is most likely computed from the measurement only. Accuracy of SVSF-OBL approaches that obtainable from the ordinary Kalman filter as Q becomes very large.

Robustness of the filters was tested by the inaccurate process model in the filter and also by using off-nominal process noise covariance in the filters as shown in the comparative performances in Fig 6.12 and Fig 6.13.

- Considering the time-averaged RMS error in position first. The robustness of ASVSF is evident as the error barely changes with Q which spans four decades. However, for higher values of Q, the error in SVSF-OBL decreases and approaches that of ASVSF. This is expected as many filters perform well with over-valued process noise covariance as discussed above, and is exemplified by the ordinary Kalman filter.

- For the time-averaged RMS error in velocity, again the robustness of the proposed ASVSF would be evident while the RMS error for SVSF-OBL varies substantially with the magnitude of Q.

- Considering the accuracy and robustness from the presented results, we may see that ASVSF marginally sacrifices accuracy in favor of robustness for higher values of Q.

A number of evaluation parameters have been used to compare the performance of SVSF, the proposed ASVSF and Kalman filter. Though the filter was constrained to use a simplified uniform motion model, robustness of ASVSF ensured satisfactory tracking despite significant model inaccuracy. Considering the cases where the kinematic noise covariance is unknown and underestimated, it was shown that the proposed ASVSF outperforms the SVSF-OBL. This may be attributed to the automatic and continuous adaptation of the process noise covariance in ASVSF.

From the description of the proposed algorithm it may be inferred that the additional complexity introduced by ASVSF over standard SVSF-OBL is not significant especially in the light of improved accuracy and robustness.

As the performance of the proposed estimator was found to be encouraging, further evaluation and eventual use of the proposed state estimator in similar applications and evaluation of its performance in other nonlinear signal models may be advocated.

7 Adaptive Interacting Multiple Model Estimator

7.1 Chapter Introduction

In this chapter, an improved variant of the Interacting Multiple Model (IMM) state estimator has been proposed, its algorithm has been described and the performance of the estimator has been evaluated against the conventional IMM and other estimators.

Interacting Multiple Model (IMM) state estimator is called for where the system model is approximate and/or some deterministic inputs are unknown. Both the imperfections, clubbed together is often called "modeling inaccuracy". As discussed in earlier chapters a common example of state estimation in presence of such modeling inaccuracy is the problem of tracking a maneuvering aircraft. In such a situation the maneuver executed by the aircraft is not known to the tracker and an often a simplified (kinematic) model of the maneuvering aircraft may be employed in the tracking system. In the optimal state estimation context, the process noise covariance (Q) is often used to represent the severity of model inaccuracy. This again has been discussed before.

We have previously noted that there are two broad approaches to perform state estimation in presence of such modelling inaccuracy, namely (a) the "robust estimation" approach where the estimation performance does not depend on the process noise, exemplified by the Variable Structure Filter or (b) the "adaptation approach" where the estimator adapts to the unknown process noise covariance.

For the purpose of this discussion, we would broadly classify adaptive state estimators into two classes, viz, single model adaptive and multi-model adaptive. An example of the single model adaptive (Q-adaptive DDF) estimator was introduced and evaluated in an earlier chapter in the scenario of tracking a maneuvering civilian aircraft for air traffic control.

The flagship of multi-model adaptive estimator is of course the Interacting Multiple Model (IMM) state estimator which is widely used in aircraft tracking.

The modification of the IMM estimator proposed in this chapter primarily involves the use of Q-adaptive estimators as "sub-filters". Accordingly, the proposed estimator is referred as the "Adaptive IMM" (AIMM). This incorporation of single model adaptive estimators as sub-filters may potentially provide good estimation performance with less number of component models, especially in the context of tracking maneuvering civilian aircraft. But this remains a hypothesis which needs to be verified.

The next few sections provide a brief background for appreciating the proposed AIMM Estimator. Though a Q-adaptive DDF estimator has been used, this is not reviewed here as an elaborate exposition and evaluation thereof were carried out in an earlier chapter.

7.2 Background

7.2.1 Background of IMM Estimator

Introduced about three decades earlier (Blom & Bar-Shalom, 1988) (Bar-Shalom, Chang, & Blom, 1989) (Bar-Shalom, Rong Li, & Kirubarajan, 2001), IMM estimators have become the algorithm of choice for the above type of target tracking (Li & Jilkov, 2005) (Gadsden, Habibi, & Kirubarajan, 2010) (Mazor, A., Averbuch, & Dayan, 1998). However, interest in improving IMM estimators persists and a fair amount of improved versions has been reported in recent literature, see e.g. (Liu, Shi, & Pan, 2017)) (Zhou, Cai, Sun, & Shen Sun, 2014) (Gao, Gao, Zhong, Hu, & Gu, 2017) (Gadsden, Habibi, & Kirubarajan, 2010).

IMM state estimators fall under the broader category of Multiple Model filters which have been subdivided by (Li X.-R. , 2000) (Li & Jilkov, 2005)into three generations. The present discussion is about IMM state estimators with fixed structure, which is from the 'second generation' and probably is the most popular class of IMM. The third generation of IMM estimators are of variable structure (Jilkov, Angelova, & Semerdjiev, 1999) (Semerdjiev, Mihaylova, & Li, 1999)(Model-Group Switching) (Li X.-R. , 2000).

IMM estimators are particularly suitable for hybrid systems which can be in different 'modes' at different times, each such mode being describable by an appropriate dynamic model from the same or similar families but with unknown parameters. A typical example of such a hybrid system is the tracking problem of a maneuvering aircraft (Hwang, Balakrishnan, & Tomlin, 2006) whose trajectory may be modeled by a sequence of segments, each obeying different dynamic equations like uniform motion, coordinated turn (constant normal acceleration), constant jerk etc. As the temporal onset of such segments and the parameters of such segments like levels of normal acceleration (turning rate), jerk etc. are unknown, IMM employs a number of state estimators (called component filters or sub-filters) running in parallel and the best state estimate is obtained by an appropriately weighted sum of the estimates from such component filters. Each such component filter is generally based on an assumed (often simplified) dynamic model with designated amount of process noise covariance quantifying the extent of possible approximations involved in the model with respect to the actual dynamics. The generic structure of an IMM state estimator is shown in Fig 7.1, which is inspired by (Jwo, Chen, & Tseng, 2010) (Jwo, Hu, & Tseng, 2013).

The accuracy of the IMM estimators is often obtained by choosing a fairly large number of component estimators (Efe & Atherton, 1998). The large number may occur due to multiplicity of possible nominal dynamic models and each such nominal dynamic model may be potentially associated with a different level of process noise covariance to represent different degree of inaccuracy of such nominal dynamic models. One example of different dynamic models occur in air-traffic control situation (see for example (Patra, Sadhu, & Ghoshal, 2018) where the aircraft trajectory may be approximated as segments of flights (uniform motion, UM) and coordinated turn (CT) segments. For the uniform motion (straight line, constant velocity) segment of the trajectory in a straight line, a Kalman filter would suffice, but due to deviations and fluctuations due to unmodelled disturbances and deterministic inputs, several UM-based Kalman filters with different levels of process noise covariance may be employed. For example, a UM model with a low-level process noise covariance will satisfactorily track an aircraft moving in an almost straight line motion segment but such a filter would become strongly mismatched during a turn maneuver. Contrarily, with a larger value of covariance process noise an UM model may allow the filter to track a sharply turning target (Bar-Shalom, Rong Li, & Kirubarajan, 2001) (Efe & Atherton, 1998) but may give larger tracking error during almost straight line motion segment. For the CT motion, EKF or nonlinear filters like sigma point filters (Ristic, Arulampalam, & Gordon, 2004) would have to be used. Again, to take care of imperfections several nonlinear sub-filters with different levels of process noise covariance are needed. If both UM and CT models have three levels of covariance each, six sub-filters, would be required. This requirement of multiple sub-filters to cover the entire range of possible target motion results in increased computational burden and complexity. This is one of the perceived defects of the unmodified fixed structure IMM.

7.2.2 The significance of the Proposed IMM Variant

The proposed variant of IMM utilizes adaptive (linear and nonlinear) estimators as component filters and accordingly would be called Adaptive IMM (AIMM). The adaptive component filters in the AIMM estimator adaptively estimate the appropriate values of process noise covariance at each time instance and therefore, it may be conjectured that even with reduced number of sub-filters, an AIMM estimator may obtain similar levels of tracking accuracy as obtainable with conventional (fixed structure) IMM with a larger number of component filters seeded with different levels of process noise covariance. The above conjecture however needs to be tested by non-trivial tracking problems. Towards this, the tracking performance of the proposed Adaptive IMM state estimator would be evaluated with the help of two different aircraft tracking scenarios using three different composite performance metrics and Monte Carlo simulation. Such tracking performance would be compared with a number of standard fixed structure IMM and also a single model adaptive filter.

The next section describes the background and briefly reviews related previous work. The architecture of the proposed Adaptive IMM (AIMM) state estimator is provided in section-3. The Kinematic Models used in this work are described and the corresponding estimation methods are enumerated in section-4. The methodology for evaluation and comparison of estimator performance are described next. Results of evaluation using Monte Carlo simulation and associated discussions are provided in section-6. This is followed by the concluding comments.

7.2.3 The Basic Interacting Multiple Model State Estimator

The basic concept has been discussed in the literature (Blom & Bar-Shalom, 1988) (Blom & Bar-Shalom, 1988) (Jwo, Hu, & Tseng, Nonlinear filtering with IMM algorithm for ultra-tight GPS/INS integration, 2013) (Bar-Shalom, Rong Li, & Kirubarajan, 2001) (Bar-Shalom, Chang, & Blom, 1989) (Li X.-R. , 2000) (Mazor, A., Averbuch, & Dayan, 1998) (Simeonova & Semerdjiev, 2002) (Li & Jilkov, 2005) (Lin, 1993) (Zhou, Cai, Sun, & Shen Sun, 2014) (Zhou, Cai, Sun, & Shen Sun, 2014)

The conventional IMM algorithm (Li & Bar-Shalom, 1993) is discussed here. For a class of stochastic hybrid system with additive noise can be described as

$$x_k = f[k-1, x_{k-1}, m_k] + g[k-1, x_{k-1}, v[k-1, m_k]] \tag{7.2.1}$$

$$y_k = h[k, x_k, m_k] + w[k, m_k] \tag{7.2.2}$$

With the 'system mode' m_k is a homogeneous Markov chain with probabilities of transition given by

$$P\{m_{j,k+1} \mid m_{i,k}\} = \pi_{ij} \quad \forall m_i, m_j \in \mathrm{M} \tag{7.2.3}$$

$x_k \in R^{n_x}$ is the continuous-valued base state vector at time step k and $y_k \in R^{n_y}$ is the vector-valued noisy measurements at each time step k. $P\{\cdot\}$ denotes probability; m_k is the scalar-valued modal state at time step k. $v[k-1, m_k] \in R^{n_v}$ is the mode-dependent process noise sequence with mean $\bar{v}[k-1, m_k]$ and covariance $Q[k-1, m_k]$; and $w[k-1, m_k] \in R^{n_y}$ is the mode dependent measurement noise sequence with mean $\bar{w}[k-1, m_k]$ and covariance $R[k, m_k]$.

The algorithm is summarised below where only one execution cycle of the estimator is given. Algorithm consists of r interacting filters running in parallel. Mixing is done at the input side of the filters with their respective mixing probabilities.

The algorithm has four parts, viz interacting, filtering, model probability updation and estimate combination. Let there be *N* number of sub-filters, at the *k*-th step the *j*-th mode is symbolized by, $M_j(k)$ estimated state vector and the corresponding covariance matrix of the *j*-th sub-filter are

denoted as $\hat{x}_j(k)$ and $P_j(k)$. After the estimate combination step, the above estimates are denoted as $\hat{x}(k)$ and $P(k)$. The sequence of measurements from the time step 1 to time step *k* is denoted by Z^k. It is assumed that the mode transition probability Π matrix is known and the initial weights $w_i(0)$ are assigned.

The steps of traditional IMM estimators (Lin, 1993) are summarised below.

Interacting or Input Mixing Step:

At the $k-1$ step, prior estimates, denoted as $\hat{x}_j^0(k-1)$ and $P_j^0(k-1)$ are obtained by mixing

$$\hat{x}_j^0(k-1) = \sum_{i=1}^{N} \frac{w_i(k-1)\Pi_{ij}}{\sum_{j=1}^{n} w_i(k-1)\Pi_{ij}} \hat{x}_i(k-1) \tag{7.2.4}$$

Where $w_i(k-1)$ is the weighting of the i-th sub-filter at time step *k-1* and Π_{ij} is the corresponding element of the transition probability matrix.

$$P_j^0(k-1) = \sum_{i=1}^{N} \frac{w_i(k-1)\Pi_{ij}}{\sum_{j=1}^{n} w_i(k-1)\Pi_{ij}} [P_i(k-1) + (\hat{x}_i(k-1) - \hat{x}_j^0(k-1))((\hat{x}_i(k-1) - \hat{x}_j^0(k-1))^T] \tag{7.2.5}$$

Filtering Step:

Depending on the model/sub-filter definition, at the *k*-th step, each sub-filter carries out estimations of the following quantities $\hat{x}_j(k)$, $P_j(k)$, $P_j^-(k)$ and $B_j(k)$ as appropriate for the filter, where $P_j^-(k)$ denotes prior error covariance ($P_{k|k-1}$ in the KF/EKF notation) for the *j*-th mode and $B_j(k) = HP_j^-(k)H^T + R_k$ is the estimated measurement error covariance.

For a linear kinematic model, one would invariably use the Kalman filter steps and for a nonlinear case one may, for example use one of EKF, UKF or DDF.

Mode probability updating Step:

The weighting factor $w_j(k)$ at time step *k* is actually the probability of the *j*-th mode $M_j(k)$ given the measurement Z^k.

$$w_j(k) = \frac{\Pi(M_j(k) \mid Z^{k-1}) \sum_{j=1}^{n} w_i(k-1)\Pi_{ij}}{\Pi(Z^k \mid Z^{k-1})} \tag{7.2.6}$$

Where $\Pi(M_j(k) \mid Z^{k-1})$ is the likelihood function obtained from the innovation of the *j*-th sub-filter and $\Pi(Z^k \mid Z^{k-1})$ is the normalizing constant (Lin, 1993).

Estimate combination:

$$\hat{x}(k) = \sum_{j=1}^{N} w_j(k)\hat{x}_j(k) \tag{7.2.7}$$

$$P(k) = \sum_{j=1}^{N} \{w_j(k)\hat{x}(k) + (\hat{x}(k) - \hat{x}_j(k))(\hat{x}(k) - \hat{x}_j(k)^T)\} \tag{7.2.8}$$

It may be noted that IMM filter calls for non-trivial prior knowledge about the possible maneuvers (adequate number of modes or sub-filters), choice of appropriate sub-filters and mode transition probability matrix.

Like other nonlinear filters, the IMM filter remains an approximate filter and its optimality for a general trajectory has not been established. The standard (i.e., straightforward) implementation of the multiple model algorithms may have numerical problems in the calculation of the model probabilities in some situations (Li & Jilkov, 2005)

The structure of an interacting multiple model (IMM) algorithm of *r*-element is shown in Fig 7.1.

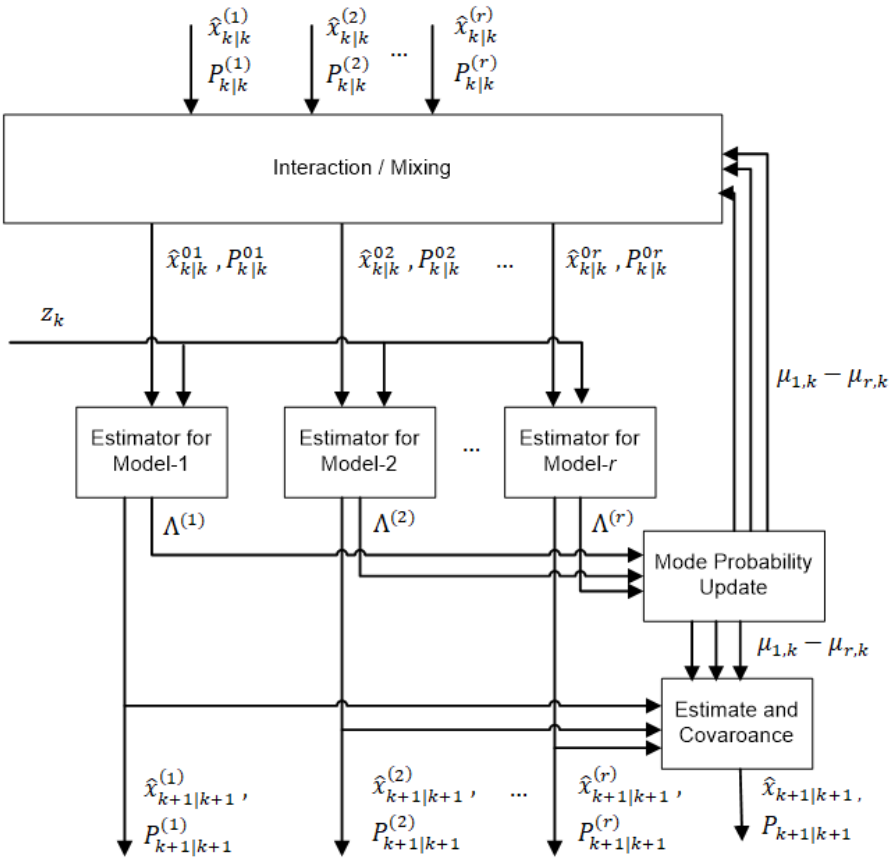

Figure 7.1 Architecture of an r-element IMM State Estimators

7.2.4 Related work on Adaptive IMM

The third generation of IMM, mentioned above are of variable structure as groups of sub-filters may be switched in and out algorithmically to obtain best state estimates and can be justifiably called as Adaptive IMM. As the Adaptive estimator proposed in this work is of fixed structure, we would restrict our attention to the fixed structure class of IMM. Over the years many improved versions of the (fixed structure) IMM have become available.

The first group of such improved IMM filter employs more powerful nonlinear estimators like UKF (Simon, 2006) (Ristic, Arulampalam, & Gordon, 2004), other sigma point filters (Van Der Merwe, Wan, & Julier, 2004) like Divided difference filter (Patra, Sadhu, & Ghoshal, 2018) (NøRgaard, Niels K, & Ravn, 2000) (Schei, 1997) and also cubature Kalman filter (Liu, Shi, & Pan, 2017))in the sub-filters, in place of EKF. The smooth variable structure filter (SVSF) a recent robust estimator based on sliding mode concepts, has been utilized as a sub-filter in an IMM framework (Gadsden, Habibi, & Kirubarajan, 2010) and its performance evaluated in an aircraft tracking scenario. Though the SVSF method is not claimed to be optimal, it is robust (as the noise covariances are not required in designing the estimator)

We would now discuss another branch of improvements which goes by the name "adaptive IMM". Models have been used in the sub-filters.

In several publications, the "adaptive" qualification has been attributed to the standard fixed structure Multi-Model estimators or IMM's in the broader sense of the term. An example is (Hide, Moore, & Smith, 2003) where the nomenclature Multiple Model Adaptive Estimation (MMAE) has been used to designate a multiple model estimation with fixed structure, employing multiple ordinary Kalman filters that run simultaneously, each using different error covariances for use in low-cost INS GPS fusion. At a given time the most appropriate model is given the highest weight using the residual probability density function.

Turn-rate Adaptivity:

This class of adaptive fixed structure IMM estimators has been designed specifically for target tracking applications. Here auxiliary estimators are used to estimate instantaneous kinematic turn rate or normal acceleration and such estimated values are plugged into state estimators with CT model. An 'adaptive' IMM for tracking maneuvering target described in (Munir & Atherton, 1995) which improved the IMM filter in (Lin, 1993) by estimating the (normal) acceleration of the target and the estimated acceleration value was fed to the alpha-beta sub-filters. In (Efe & Atherton, 1998), estimates of turn rates have been obtained by auxiliary methods and such estimates have been used in CT motion models with deterministic (known) turn rates. In a comparable work, an 'adaptive' IMM approach (Efe & Atherton, 1998) the process noise covariance level for the filter had been assigned from the estimated turn rate obtained through a 2^{nd} order Kalman filter at each sample (using an empirically obtained relation).

Sub-filter Adaptivity:

In this group, one or more sub-filters adaptively estimate the process noise covariance. In (Jwo, Hu, & Tseng, 2013) an IMM configuration called "IMM-adaptive unscented Kalman filter (IMM-AUKF)" have been evaluated for navigation sensor fusion application. Out of the bank of two parallel UKFs, one UKF is adaptively tuned with the help of an 'adaptive tuning system' (ATS). The ATS uses the normalized innovation squared value at given epoch for determining the upper bound of process noise covariance matrix. Efficacy of this adaptive estimator has been demonstrated by comparison with a non-adaptive (two model) IMM-UKF and also with a single model AUKF.

In a recent work (Gao, Gao, Zhong, Hu, & Gu, 2017) a single model adaptive UKF and a robust UKF form the two sub-filters in a fixed structure IMM and thereby pools the advantages of these two varieties of estimators. The adaptive fading UKF takes care of process model uncertainty and the measurement model uncertainty is dealt with by the robust UKF. Using the IMM estimation

formalism state estimation is achieved as a probabilistic weighted sum of the estimation results from the two sub-filters.

7.3 The Proposed AIMM State Estimator

The proposed AIMM estimator contains only a limited (say 2 or three) number of sub-filters, only 1 each for the corresponding dynamic models (Fig 7.2). Each such sub-filter is Q-adaptive and hence multiple sub-filters with the same algorithm but different values of process noise covariance are not required.

Algorithm for the Proposed AIMM Estimator:

The algorithm for proposed AIMM Estimator is stated below:

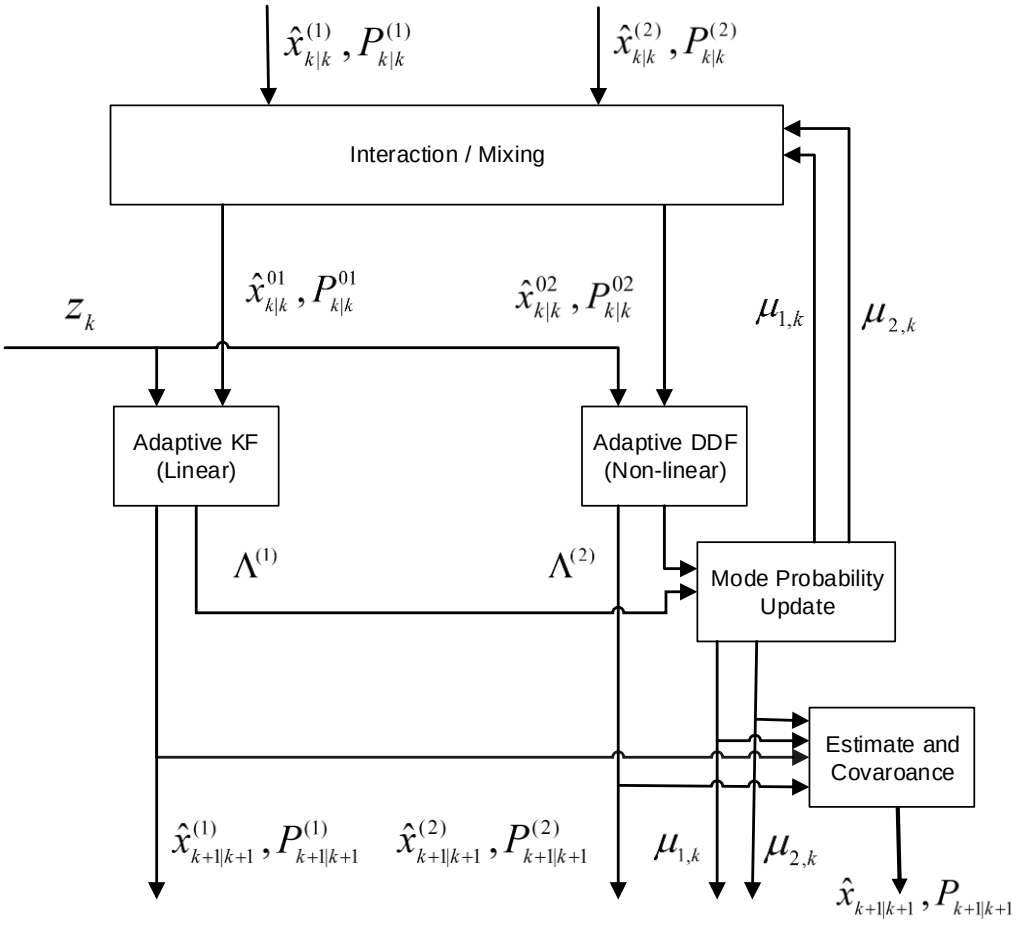

Figure 7.2 AIMM architecture

In this section adaptive version of IMM (AIMM) is formulated for automatic adaptation of process noise inside the state estimators used in IMM for better estimation accuracy for mode switched system. Thus AIMM reduces the number of filters used in IMM where filters were assigned to

different levels of process noise. Q-adaptation is applied to every individual filters used in AIMM. The below algorithm uses one linear (AKF) and one nonlinear (ADDF) filter to construct AIMM.

i. ***Initialization***

Mode transition matrix is defined as

$$\pi = \begin{bmatrix} \pi_{11} & \pi_{12} \\ \pi_{21} & \pi_{22} \end{bmatrix} \tag{7.3.1}$$

The initial value of states $\left(\hat{x}_0^{(1)}, \hat{x}_0^{(2)}\right)$, error covariance $\left(P_0^{(1)}, P_0^{(2)}\right)$, mixing probabilities $\left(\mu_{1,0}, \mu_{2,0}\right)$ and noise covariance $\left(\hat{Q}_0^{(1)}, \hat{Q}_0^{(2)}\right)$ are assigned

ii. ***For the first model***

a. Mixing

$$\bar{c}^{(1)} = \mu_{1,k}\pi_{11} + \mu_{2,k}\pi_{21} \tag{7.3.2}$$

$$\hat{x}_k^{01} = \hat{x}_k^{(1)}\mu_{1|1} + \hat{x}_k^{(2)}\mu_{2|1} \tag{7.3.3}$$

$$\mathrm{P}_k^{01} = \sum_{i=1}^{2} \mu_{i|1} P_k^{(i)} + \sum_{i=1}^{2} \mu_{i|1} \left\{ \left[\hat{x}_k^{(i)} - \hat{x}_k^{01})\right] \left[\hat{x}_k^{(i)} - \hat{x}_k^{01}\right]^T \right\} \tag{7.3.4}$$

b. Filtering (AKF)

i. Time update:

$$\hat{x}_{k+1|k}^{(1)} = f(\hat{x}_{k|k}^{(1)}, u_k) \tag{7.3.5}$$

$$P_{k+1|k}^{(1)} = F\mathrm{P}_k^{01}F^T + \hat{Q}_k^{(1)} \tag{7.3.6}$$

$$\nu_k^{(1)} = y_k - h\left(\hat{x}_{k+1|k}^{(1)}\right) \tag{7.3.7}$$

ii. Q-adaptation loop:

$$\hat{C}_\nu^{(1)} = \frac{1}{N}\sum_{i=1}^{N} \nu_{k+1-i|k-i}^{(1)} \nu_{k+1-i|k-i}^{(1)T} \tag{7.3.8}$$

$$\alpha_k^{(1)} = \frac{trace\left\{\hat{C}_\nu^{(1)} - R\right\}}{trace\left\{HP_{k+1|k}^{(1)}H^T\right\}} \tag{7.3.9}$$

iii. Measurement update:

$$K_{k+1}^{(1)} = P_{k+1|k}^{(1)}H\left(HP_{k+1|k}^{(1)}H^T + R\right)^{-1} \tag{7.3.10}$$

$$\hat{x}_{k+1}^{(1)} = \hat{x}_{k+1|k}^{(1)} + K_{k+1}^{(1)}\nu_k^{(1)} \tag{7.3.11}$$

$$P_{k+1}^{(1)} = \left(I - K_{k+1}^{(1)}H\right)P_{k+1|k}^{(1)} \tag{7.3.12}$$

iv. Q update:

$$\hat{Q}_{k+1}^{(1)} = \hat{Q}_k^{(1)} \sqrt{\alpha_k^{(1)}} \tag{7.3.13}$$

c. Mode probability update

$$\Lambda_k^{(1)} = \left[\frac{1}{(2\pi)^{\frac{n}{2}} \sqrt{\left| S_k^{(1)} \right|}} \exp\left(-\frac{\nu_k^{(1)T} S_k^{(1)-1} \nu_k^{(1)}}{2} \right) \right] \tag{7.3.14}$$

$$S_k^{(1)} = H P_{k+1|k}^{(1)} H^T + R \tag{7.3.15}$$

iii. ***For the second model***

a. Mixing

$$\bar{c}^{(2)} = \mu_{1,k} \pi_{12} + \mu_{2,k} \pi_{22} \tag{7.3.16}$$

$$\hat{x}_k^{02} = \hat{x}_k^{(1)} \mu_{1|2} + \hat{x}_k^{(2)} \mu_{2|2} \tag{7.3.17}$$

$$\mathrm{P}_k^{02} = \sum_{i=1}^{2} \mu_{i|2} P_k^{(i)} + \sum_{i=1}^{2} \mu_{i|2} \left\{ \left[\hat{x}_k^{(i)} - \hat{x}_k^{02} \right) \right] \left[\hat{x}_k^{(i)} - \hat{x}_k^{02} \right]^T \right\} \tag{7.3.18}$$

b. Filtering (ADDF):

i. Time update:

$$\bar{P}_k = \bar{S}_x \bar{S}_x^T ; \hat{P}_k = \hat{S}_x \hat{S}_x^T \tag{7.3.19}$$

$$\bar{x}_{k+1} = \frac{h^2 - n}{h^2} f(\hat{x}_k^{02}) + \frac{1}{2h^2} \sum_{p=1}^{n} \left\{ f\left(\hat{x}_k^{02} + h\hat{S}_{x,p} \right) + f\left(\hat{x}_k^{02} + h\hat{S}_{x,p} \right) \right\} \tag{7.3.20}$$

$$S_{X\hat{X},k+1}^{(1)} = \left\{ S_{X\hat{X},k+1}^{(1)}(i,j) \right\} = \left\{ \frac{1}{2h} \left(f_i\left(\hat{x}_k^{(2)} + h\hat{S}_{x,j} \right) - f_i\left(\hat{x}_k^{(2)} - h\hat{S}_{x,j} \right) \right) \right\} \tag{7.3.21}$$

$$S_{X\hat{X},k+1}^{(2)} = \left\{ S_{X\hat{X},k+1,(i,j)}^{(2)} \right\} = \left\{ \frac{\sqrt{h^2 - 1}}{2h} \left(f_i\left(\hat{x}_k^{(2)} + h\hat{S}_{x,j} \right) + f_i\left(\hat{x}_k^{(2)} - h\hat{S}_{x,j} \right) - 2 f_i(\hat{x}_k^{(2)}) \right) \right\} \tag{7.3.22}$$

$$\nu_k^{(2)} = y_k - \bar{y}_k \tag{7.3.23}$$

$$\bar{P}_{k+1} = \left[S_{X\hat{X},k+1}^{(1)} \quad S_{X\hat{X},k+1}^{(2)} \right] \left[S_{X\hat{X},k+1}^{(1)} \quad S_{X\hat{X},k+1}^{(2)} \right]^T + \hat{Q}_k^{(2)} \tag{7.3.24}$$

ii. Q-adaptation loop:

$$C_{\nu,k}^{(2)} = \frac{1}{N} \sum_{j=k-N+1}^{k} \nu_j^{(2)} \nu_j^{(2)T} \tag{7.3.25}$$

$$\alpha_k^{(2)} = \frac{trace\left\{C_{v,k}^{(2)} - R\right\}}{trace\left\{P_{k+1}^{y} - R\right\}} \tag{7.3.26}$$

iii. Measurement update:

$$\bar{y}_{k+1} = \frac{h^2 - n}{h^2} g\left(\bar{x}_{k+1}\right) + \frac{1}{2h^2}\sum_{p=1}^{n}\left\{g\left(\bar{x}_{k+1} + h\bar{s}_{x,p}\right) + g\left(\bar{x}_{k+1} - h\bar{s}_{x,p}\right)\right\} \tag{7.3.27}$$

$$S_{y\bar{X},k+1}^{(1)} = \left\{S_{y\bar{X},k+1,(i,j)}^{(1)}\right\} = \left\{\frac{1}{2h}\left(g_i\left(\bar{x}_{k+1} + h\bar{S}_{x,j}\right) - g_i\left(\bar{x}_{k+1} - h\bar{S}_{x,j}\right)\right)\right\} \tag{7.3.28}$$

$$P_{k+1}^{y} = \left[S_{y\bar{X},k+1}^{(1)}\ S_{y\bar{X},k+1}^{(2)}\right]\left[S_{y\bar{X},k+1}^{(1)}\ S_{y\bar{X},k+1}^{(2)}\right]^T + R \tag{7.3.29}$$

$$P_{k+1}^{xy} = \left[\bar{S}_{x,k+1}^{T}\right]\left[S_{y\bar{X},k+1}^{(1)}\right]^T \tag{7.3.30}$$

$$P_{k+1}^{xy} = \left[\bar{S}_{x,k+1}^{T}\right]\left[S_{y\bar{X},k+1}^{(1)}\right]^T \tag{7.3.31}$$

$$K_{k+1}^{(2)} = P_{k+1}^{xy}\left(P_{k+1}^{y}\right)^{-1} \tag{7.3.32}$$

$$\hat{x}_{k+1}^{(2)} = \bar{x}_{k+1} + K_{k+1}^{(2)}\nu_k^{(2)} \tag{7.3.33}$$

$$\hat{P}_{k+1}^{(2)} = \bar{P}_{k+1} - K_{k+1}^{(2)}P_{k+1}^{y}K_{k+1}^{(2)T} \tag{7.3.34}$$

iv. Q update:

$$\hat{Q}_{k+1}^{(2)} = \hat{Q}_k^{(2)}\sqrt{\alpha_k^{(2)}} \tag{7.3.35}$$

c. Mode probability update:

$$\Lambda_k^{(2)} = \left[\frac{1}{(2\pi)^{\frac{n}{2}}\sqrt{\left|S_k^{(2)}\right|}}\exp\left(-\frac{\nu_k^{(2)T}S_k^{(2)-1}\nu_k^{(2)}}{2}\right)\right] \tag{7.3.36}$$

$$S_k^{(2)} = P_{k+1}^{y} \tag{7.3.37}$$

iv. ***Mode selection probability update***

$$\begin{bmatrix}\mu_{1|1} & \mu_{1|2}\\ \mu_{2|1} & \mu_{2|2}\end{bmatrix} = \begin{bmatrix}\frac{\pi_{11}\mu_1}{\bar{c}^{(1)}} & \frac{\pi_{12}\mu_1}{\bar{c}^{(2)}}\\ \frac{\pi_{21}\mu_2}{\bar{c}^{(1)}} & \frac{\pi_{22}\mu_2}{\bar{c}^{(2)}}\end{bmatrix} \tag{7.3.38}$$

$$\mu_{1,k+1} = \frac{\bar{c}^{(1)}\Lambda^{(1)}}{c};\ \mu_{2,k+1} = \frac{\bar{c}^{(2)}\Lambda^{(2)}}{c} \tag{7.3.39}$$

where, $c = \bar{c}^{(1)}\Lambda^{(1)} + \bar{c}^{(2)}\Lambda^{(2)}$

v. The overall estimate and the state covariance

$$\hat{x}_{k+1} = \sum_{j=1}^{2} \hat{x}_{k+1}^{(j)} \mu_{j,k+1} \tag{7.3.40}$$

$$\mathrm{P}_{k+1} = \sum_{j=1}^{2} \mu_{j,k+1} \left[P_{k+1}^{(j)} + \left\{ \hat{x}_{k+1}^{(j)} - \hat{x}_{k+1} \right\} \left\{ \hat{x}_{k+1}^{(j)} - \hat{x}_{k+1} \right\}^{T} \right] \tag{7.3.41}$$

7.4 Kinematic Models and Estimation Methods for target tracking

Two scenarios of target tracking have been considered for the evaluation of proposed estimators. Same uniform motion and coordinated turn models which have been discussed in chapter-3 are considered here for generating truth model.

7.5 Evaluation Methodology

Specifically, the AIMM tracking estimators used in the evaluation case studies in the present contribution employ only two adaptive estimator components corresponding to the two models. One of the models is a linear dynamic UM model and uses one adaptive Kalman Filter (AKF). The other one uses a nonlinear dynamic CT model with an accompanying Adaptive Divided Difference state estimator (ADDF). Tracking performance of this two-component AIMM estimator is compared with (i) a standard IMM estimator with the same number of component filters (IMM KF-DDF), (ii) a single model ADDF estimator (iii) a standard IMM estimators with three number of component filters (IMM EKF-EKF-EKF). Monte Carlo simulation was carried out to evaluate RMSE for individual estimators.

7.5.1 Test Trajectory

Two test trajectories (Fig 4.3 and 4.4) have been considered for evaluation of the proposed estimator. The detailed description of the trajectories is given in chapter-4. All the parameters are kept same for evaluation purpose. The simulation study was performed with T=5s sampling interval. The values of *Q* and *R* are also kept same as given in Chapter-4 (for linear case).

7.5.2 Other test parameters and data

For each run, initial state vector of the plant has been randomized with prescribed nominal values as given above and corrupted by an initial noise covariance P_0. For non-adaptive filters, random process noise and measurement noise sequences have been drawn from zero mean Gaussian noise sequences with prescribed covariance matrices. The performance of the tracking filters is presented in terms of estimated trajectory versus time for typical cases; Monte Carlo simulation results for RMS errors (RMSE) are also shown likewise. The numerical values of average (over the total run-time) RMSE and peak RMSE have been presented in appropriate tables to compare the performance of the filters with different models and methods.

Initial error covariance P_0 is taken as $diag([50^2 \quad 50^2 \quad 100 \quad 100 \quad 1])$ (Gadsden, Habibi, & Kirubarajan, 2014) for both the trajectories. RMSE plots have been provided for 500 Monte Carlo runs. For the generation of the truth model, Q_{UM} and Q_{CT} (as given in Chapter 3) have been used as the value of process noise covariance for UM and CT segments of the trajectory respectively. This pair is collectively denoted as Q_{nom}. The adaptive filters have been initialized with typical non-nominal initial values as shown in the respective tables. Additional values regarding the trajectories are provided in the following sections. For adaptive versions of the estimators, the length of the window size is taken as 20 epochs.

Transition probability:

Transition probability for two modes (Bar-Shalom, Rong Li, & Kirubarajan, 2001) is given as:

$$\pi_{r=2} = \begin{bmatrix} \pi_{11} & \pi_{12} \\ \pi_{21} & \pi_{22} \end{bmatrix} = \begin{bmatrix} 0.95 & 0.05 \\ 0.05 & 0.95 \end{bmatrix}$$

Transition probability for three modes (Naidu, Gopalaratnam, & Shanthakumar, 2007) is given as:

$$\pi_{r=3} = \begin{bmatrix} 0.99 & 0.001 & 0.009 \\ 0.001 & 0.99 & 0.009 \\ 0.005 & 0.005 & 0.99 \end{bmatrix}$$

7.5.3 Evaluation Metrics

The performance of the estimators has been evaluated with the help of Monte Carlo simulation. A total of 500 Monte Carlo runs have been performed for each study to calculate (i) the RMS error sequence ($\{e_{rms}(k)\}$) across the Monte Carlo population corresponding to each instant (ii) peak value of the RMS error sequence ($\{\sup_k [e_{rms}(k)]\}$), (iii) time average of the RMS error sequence $\frac{1}{N}\sum_{k=1}^{N} e_{rms}(k)$ and (iv) RMS of the RMS error sequence $\sqrt{\frac{1}{N}\sum_{k=1}^{N} e_{rms}^2(k)}$. The sampling interval is taken as 5s.

7.6 Results & Discussions

The result is generated by Monte Carlo Simulation. Two separate sections are provided for the two tracking trajectories of the aircraft.

7.6.1 Results for Trajectory-I

The trajectory-1 is ‘s’-type trajectory of aircraft as described in chapter-4. Initial values of the states have also been randomized with the corresponding covariance matrix *P*. Fig 7.3 shows the tracking performance of the proposed AIMM in comparison with ADDF and traditional IMM (with KF and

DDF as sub-filters). As we have discussed before, the adaptive filters are initialized with the same values of the process noise covariances as assigned to the non-adaptive versions. Fig 7.4 shows the velocity profiles of the estimators. Table 7.1 contains all the performance metrics average, Peak and RMS of RMSE for all the estimators to compare performances. For completeness, the result of the IMM consist of three sub-filters (EKF) with different level of process noise ($0.01 \times Q_{CT}$, Q_{CT} and $100 \times Q_{CT}$) has also been provided in the Table 7.1.

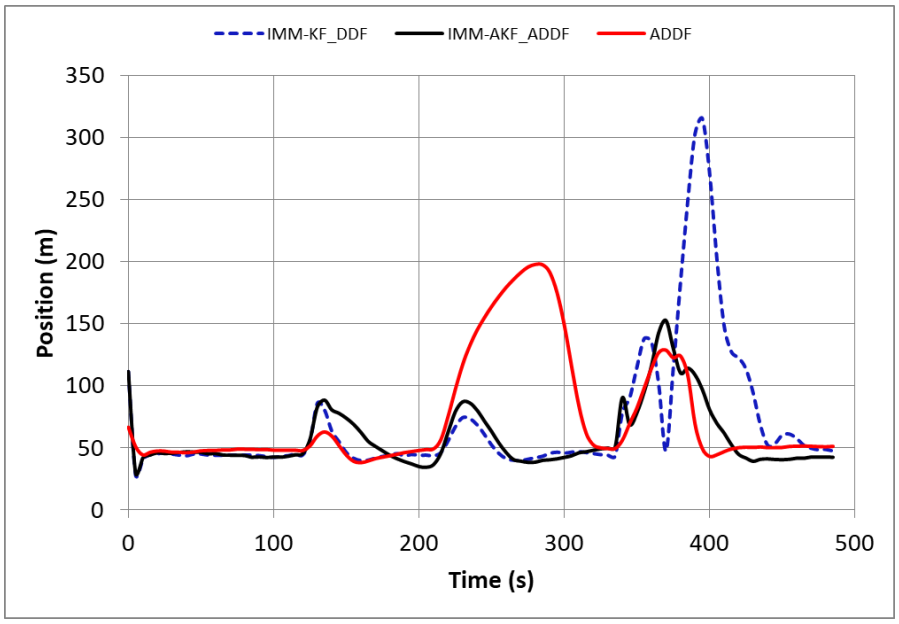

Figure 7.3 RMSE of Position

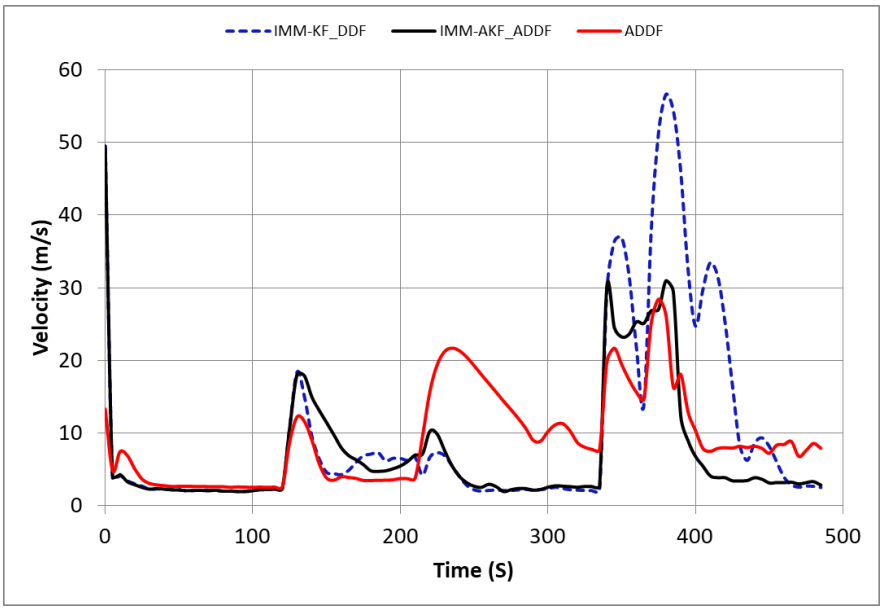

Figure 7.4 RMSE of velocity

Table 7.1 Performance table

Trajectory-I		ADDF Qf(0) = Qct	IMM-KF-DDF Qf1 = Qum Qf2 = Qct	IMM EKF-EKF-EKF Qf1 = 0.01Qct Qf2 = Qct Qf3 = 100Qct	IMM-AKF-ADDF Qf1(0) = Qum Qf2(0) = Qct
Average RMSE	Position (m)	74.96	69.74	56.13	57.21
	Velocity (m/s)	9.30	10.12	6.77	6.53
Peak RMSE	Position (m)	197.71	313.8	114.84	152.5
	Velocity (m/s)	28.43	56.29	39.13	49.49
RMSE of RMSE	Position (m)	87.96	88.14	60.46	62.94
	Velocity (m/s)	11.28	16.76	10.16	10.63

From the performance table for trajectory-I, it may be noted that:

i. Three-mode IMM (IMM EKF-EKF-EKF) performs better than two-mode IMM (IMM KF-DDF) in most cases (metric wise). It indicates that the using more number of sub-filters increase the performance of the IMM estimators.
ii. Single mode nonlinear Adaptive filter ADDF has shown better performance than two-mode IMM for all the cases.
iii. Performance of AIMM is close to the performance of three-mode IMM filter.
iv. It is to be noted that the three-mode IMM estimator is tuned with three different values of process noise. The selected range is wide to adjust the truth model of tracking scenarios. However, in the case of AIMM this tuning is not required since it adapts Q automatically.
v. The performance of AIMM can be further improved by selecting the appropriate window size and initial covariances of the process noises of the sub-filters.

7.6.2 Results for Trajectory-II

Proposed AIMM has also been evaluated for a relatively zigzag trajectory, trajectory-II (detailed description is given in Chapter-4) tracking scenario. Fig 7.5 shows the RMSE performance of the proposed estimator in comparison with traditional IMM and ADFF. Table 7.2 shows all the performance metrics to have a comparative view. Table also contains the IMM with three sub-filters having different process noise covariances.

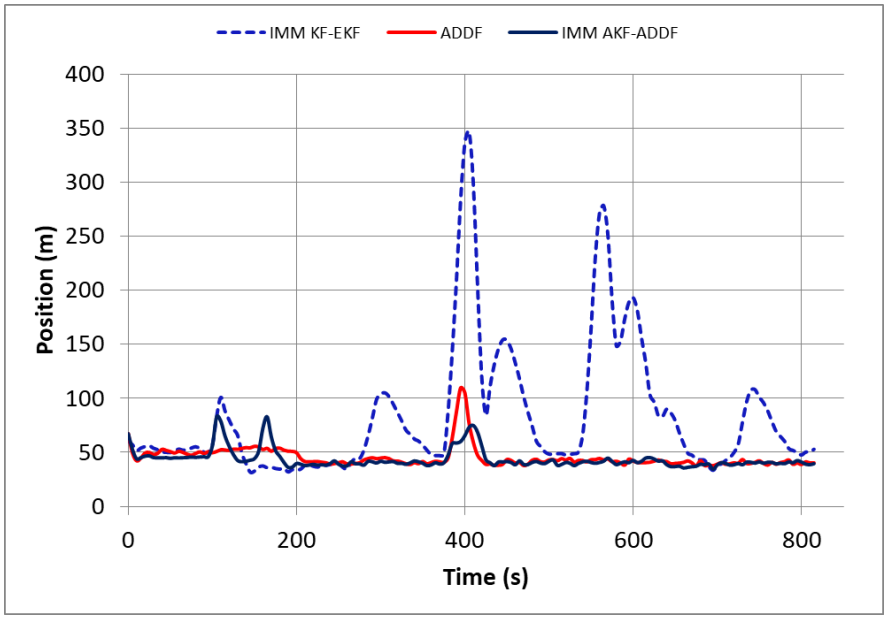

Figure 7.5 Time-averaged RMSE for position

Table 7.2 Performance table for trajectory-II

Trajectory-II		IMM- KF-EKF	ADDF	IMM EKF-EKF-EKF	IMM-AKF-ADDF
		Qf1 = Qum Qf2 = Qct	Qf(0) = Qct	Qf1 = 0.01Qct Qf2 = Qct Qf3 = 100Qct	Qf1(0) = Qum Qf2(0) = Qct
Average RMSE	Position (m)	83.29	45.28	46.63	43.78
	Velocity (m/s)	10.19	52.95	5.23	8.12
Peak RMSE	Position (m)	346.92	109.71	118.10	83.03
	Velocity (m/s)	50.10	115.61	39.39	29.15
RMSE of RMSE	Position (m)	103.47	46.32	48.81	44.68
	Velocity (m/s)	14.67	68.20	7.04	9.49

From the performance table for trajectory-II, following points may be noted:

i. Results are almost consistent for the more complex tracking scenario, trajectory-II.

ii. Unlike the previous trajectory, here IMM KF-EKF is used for two-mode IMM estimator. The results are almost similar and comparable.

iii. Three-mode IMM (IMM EKF-EKF-EKF) performs better than two-mode IMM (IMM EKF-EKF) in all cases.

iv. Single mode nonlinear Adaptive filter ADDF has shown better performance than two-mode IMM for the position. For velocity, two-mode IMM performs better.

v. Performance of AIMM is found to be better or close to the performance shown by three-mode IMM filter (except two cases).

7.7 Chapter conclusions

The structure of a modified adaptive sub-filter based IMM estimator and its algorithm is presented. It may be seen that the structure is easy to appreciate and consists of only limited number of sub-filters each being of the type Q-adaptive. The efficacy of the proposed filters for target tracking scenario has been demonstrated using two trajectories which may be encountered in air traffic control scenario. These types of air traffic control trajectories can be decomposed into uniform motion and coordinated turn segments. As a result, only two sub-filters proved to be adequate. The sub-filters automatically adapted with different process noise to compensate for modeling inaccuracies.

In air defense scenarios also the tracking trajectories are often modeled as UM, constants acceleration and sometimes constant jerk (Mehrotra & Mahapatra, 1997) (Ghosh & Mukhopadhyay, 2011) (Naidu, Gopalaratnam, & Shanthakumar, 2007). Thus it can be conjectured that only three sub-filters would be adequate to track such targets. It may be pointed out that the defense community generally demands very rigorous simulation to try a new algorithm and rejecting the existing practice that aspect is left for the future work.

It is clearly seen, that the proposed adaptive version of the IMM improves the performance over the traditional IMM for tracking scenario. It reduces the number of filters used in the traditional IMM state estimators to attain better accuracy. The proposed AIMM uses only two sub-filters, one for linear and other for nonlinear mode and it automatically adapts required process noise covariance to match required level. Thus for AIMM, the knowledge of Q for different modes of the filter is not required.

8 Discussion and Conclusions

8.1 Discussions

It may be recalled that (re-articulated) objectives of the present work had been to

(i) evaluate different existing nonlinear state estimators for (hybrid) systems with inaccurate process model.

(ii) enhance SVSF and IMM estimators so as to obtain better state estimation for nonlinear state and parameter estimation and evaluate their performance.

(iii) compare the performances of the enhanced estimators with the already reported state estimators above tune up the parameters of the state estimators for a system with model error

(iv) evaluation of such enhanced estimators for parameter estimation

Towards the above objectives a focussed and fairly comprehensive literature survey (on nonlinear state estimation, including adaptive state estimator and variable structure state estimators) had been carried out. A systematic survey of literature about estimation in aircraft tracking scenarios was also carried out. Another systematic study was carried out to obtain insight into the Q-adaptation process by performing manual tuning of Kalman filters vis a vis studying Q-adaptive nonlinear state estimators.

A ‘walk through’ of the dissertation would indicate that the stated objectives have mostly been met.

The following table compares the individual objectives and corresponding investigation done.

Table 8.1 Coverage of the objectives

No	Objective	Attainment
1	Evaluate different existing nonlinear state estimators for (hybrid) systems with inaccurate process model.	Evaluation of Adaptive nonlinear state estimators such as AEKF, AUKF, ADDF and AGHF has been carried out for aircraft tracking scenarios under model uncertainty and unknown noise statistics.

		A number of metrics and Monte Carlo simulation have been used for this purpose. Details provided immediately after this table.
2 & 3	enhance SVSF and IMM estimators so as to obtain better state estimation for nonlinear state estimation and evaluate their performance	Following modified and improved nonlinear state estimators have been proposed, characterized and evaluated (by cross-comparisons of performance) for civil aircraft tracking scenarios. These are: i. A sigma point variant of Smooth Variable Structure Filter(SVSF) ii. An adaptive version of Smooth Variable Structure Filter (ASVSF). iii. An adaptive version of Interacting Multiple Model Filter (AIMM) Again a number of metrics and Monte Carlo simulation have been used for this purpose. The results of the Monte Carlo studies have been presented graphically as well as in tabular form.
3	compare the performances of the enhanced estimators with the already reported state estimators above tune up the parameters of the state estimators for a system with model error	Performance of the proposed enhanced state estimators have been compared with (as appropriate) • Non adaptive standard nonlinear filters like EKF, UKF, DDF and GHF • Ordinary Smooth Variable Structure Filter with the optimum boundary layer. • Non adaptive nonlinear filter. • Ordinary IMM filter as available in the literature.

Different values of process noise covariances have been used for non-adaptive filters

Notes about the evaluation of non-adaptive nonlinear filters:

Trajectory tracking scenarios have been considered for evaluation and characterisation of the single model linear and nonlinear non-adaptive filters such as KF, EKF, and UKF. The performances of estimators were analysed by tuning the process noise covariance (assumed by the filter) with the help of a scaling factor. A higher process noise covariance is created simply by increasing a scalar multiplier. This is effective because in the point mass model, this amounts to increasing the covariance of the equivalent acceleration.

The objective was to systematically study and evaluate the optimal/suboptimal state estimators for a class of nonlinear hybrid system. Monte Carlo simulation had been used and three metrics, namely, average RMS error, peak RMS error and RMS of RMSE error have been used for summary evaluation in tabular form.

It was conjectured that though the time-averaged RMS error provides a quick comparison between state estimators, for practical applications the peak RMS errors should also be considered as this indirectly indicate the possibility of track loss.

It was conjectured that the encouraging results obtained from studying non-adaptive filters can be extended to other problems in this class where the hybrid nature occurs because the inputs are not known to the estimator and such inputs enforce the different modes. Subsequent studies confirm the validity of such a conjecture.

While comparing adaptive estimator with the corresponding non-adaptive estimators, the initial value of the process noise covariance of adaptive estimators were kept the same as that in the non-adaptive estimators. This was to confirm that indeed process noise covariance adaptation indeed occurs even with wild initially assumed values.

Regarding the Smooth variable structure filter (SVSF) it may be noted that (i) The SVSF with optimal boundary layer has been chosen as the version of SVSF, the longer nomenclature i.e. SVSF-OBL has been avoided to keep the discussion easier to read. (ii) Adaptive Smooth Variable Structure Filter has been proposed by the present worker to overcome the shortcomings of Smooth Variable Structure Filter with optimal boundary layer by incorporating the advantages of Process

noise adaptation technique. The proposed algorithm was evaluated with two aircraft tracking scenarios

8.2 Conclusion

The conclusion section has been subdivided into six major areas of work.

8.2.1 Evaluation of the non-adaptive nonlinear estimators in trajectory tracking scenario

- The various metrics of estimation performance, as expected were found to be strongly dependent on the process noise covariance multiplier.
- The nonlinear CT model based filters generally exhibited better performance as compared to the linear UM model.
- For the KF and the EKF, all the error descriptors viz., time averaged, peak and RMS of RMS error for both position and velocity of the aircraft were seen to decrease with increase in scaling factor λ. For the UKF, a mild minima occurs at a higher value of λ. The errors in UKF, however, tend to increase thereafter.
- A typical study says, the performance of UKF with increasing λ beyond the optimum value needs some explanation. With the high value of process noise covariance, the "sigma points" in a sigma point based nonlinear state estimator become very widely spread leading to lower estimation accuracy so much so that for very high values of λ the UKF may diverge.
- For the optimal choice of λ, the value of the descriptor metric for the position had been found to be substantially smaller compared to the square root of the corresponding measurement noise covariance. This indicates sufficient filtering despite the process model in the filter being simplistic and inaccurate.

8.2.2 Evaluation of the adaptive estimators

- It is seen that single mode adaptive state estimators including version with KF, EKF, DDF and GHF show better tracking performance compared to robust SVSF.
- Single mode Adaptive Filters have shown similar performance as obtained from Interacting Multiple Model (IMM) state estimators with high value of Q or IMM with three sub filters.
- The performance of adaptive estimators are particularly noteworthy because while SVSF results in (Gadsden, 2011) were obtained with the (known) nominal process noise covariance,

the adaptive estimators on the other hand, have been initialised with a wrong value of Q which was two decades below the true nominal value.

- It is also noted that computationally intensive AGHF provides similar tracking performance as obtainable from ADDF and hence the former is not recommended due to computational cost.
- Between the UM and CT model, the CT model (though marginally more computation intensive) performs noticeably better across all adaptive filtering algorithms with minor exception (X-velocity for ADDF).
- Performance of different versions of adaptive estimators as well as the non-adaptive EKF was evaluated. The non-adaptive EKF was observed to fail miserably to track one particular trajectory whereas the adaptive DDF and adaptive GHF tracked satisfactorily.
- ADDF or AGHF have been found to perform better than 2-element IMM estimators for peak RMS errors.
- It may be concluded that (i) performance of the adaptive estimators even starting with a wrong guess value of process noise covariance is closely comparable to that obtainable with the robust SVSF, (ii) the computationally more intensive AGHF provides similar tracking errors as obtainable from ADDF, (iii) CT model based state estimators, though marginally more computation intensive, provide better tracking performance for trajectories of the types considered. (iv) Single mode Adaptive Filters performs close to IMM estimators.

8.2.3 Adaptive Smooth variable structure Filter

- Performance of the proposed ASVSF (Average RMSE, Peak RMSE and RMS of RMSE) exhibits better performance as compared to the non-adaptive SVSF estimator.
- For off-nominal values of process noise covariance, (i) for low initial value ($Q_0 = 0.001 \times Q_{UM}$) the performance of ASVSF has again shown better than SVSF for all the metrics (ii) for over estimated value ($Q_0 = 10 \times Q_{UM}$ and $Q_0 = 100 \times Q_{UM}$), the comparative performances are more complex. Performance of the ASVSF, though good, but may not be claimed to be best for position for the different performance measures. This can be explained from the fact that for the highest value of Q, information from the process model is generally ignored by the Kalman filter and the velocity is most likely computed from the measurement only. Accuracy of SVSF-OBL approaches that obtainable from the ordinary Kalman filter as Q becomes very large.
- Robustness of the ASVSF was also tested by taking inaccurate process model in the estimator and also by using off-nominal process noise covariances in the filters. The robustness of ASVSF is evident as the error barely changes with the change of Q which spans four decades. However, for higher values of Q, the RMS error in SVSF-OBL decreases and approaches that of ASVSF. This is expected as many filters perform well with over-valued process noise covariance as discussed above, and is exemplified by the ordinary Kalman filter.

8.2.4 Adaptive Interacting Multiple Model

- Adaptive Interacting Multiple Model (AIMM) estimator was proposed to reduce the number of sub-filters used in IMM with acceptable accuracy and to avoid the manual choice of process noise Q to tune the sub-filters. Performance of AIMM was evaluated with the two different tracking scenarios.

- It is seen from Monte Carlo simulations that IMM performs better when the number of sub-filters of IMM increases. In particular, the three-mode IMM (IMM EKF-EKF-EKF) performs better than two-mode IMM (IMM KF-DDF) in most cases (metric wise).

- Performance of the AIMM estimator was found to be close to that of the carefully tuned three-mode IMM filter. The "carefully tuned" three-mode IMM estimator is to be iteratively tuned with three different values of process noise. The selected range of the process noise should be just wide enough for the given truth model of tracking scenarios. However, in case of AIMM this careful tuning is not at all required since it adapts Q automatically.

- An interesting observation was that the single mode nonlinear Adaptive filter ADDF has outperformed the two-mode IMM for all the cases.

8.3 Suggestions for Future work

i. In this work, Adaptive SVSF was proposed for linear measurement model. The algorithm can be formulated considering nonlinear measurement model.

ii. Similarly, Sigma point SVSF can also be extended for nonlinear measurement model.

iii. In air defence scenarios also the tracking trajectories are often modelled as UM, constants acceleration and sometimes constant jerk (Mehrotra & Mahapatra, 1997) (Ghosh & Mukhopadhyay, 2011) (Naidu, Gopalaratnam, & Shanthakumar, 2007). Thus it can be conjectured that only three sub-filters would be adequate to track such targets. It may be pointed out that defence community generally demands very rigorous simulation to try a new algorithm and rejecting the existing practice that aspect is left for the future work.

iv. Evaluation process of proposed ASVSF and AIMM were carried out for planner model of tracking trajectory. However, 3D models could also be considered for the evaluation process.

v. The adaptive versions of SVSF and AIMM may potentially be employed for fault detection and identification in the line suggested by (Chatterjee, Sadhu, & Ghoshal, 2015).

Appendices

This section provides some additional findings and results that are relevant to the research work but not presented in the body of the thesis.

9 Pragmatics for Process Noise Covariance Tuning

The problem of tuning single mode stochastic state estimators for a class of nonlinear systems (NLS), which are often encountered in tracking of aerospace objects, is addressed. A trajectory of maneuvering aircraft may require different dynamic equations for different segments of the trajectory and the corresponding dynamic model may be classified as nonlinear hybrid system. This contribution investigates the use of single mode (non-hybrid) state estimators (in contrast to the option of using relatively complex multiple model estimators) for the tracking duty. Any mismatch between the dynamics of the actual system and the model used in the filter is often quantified by the process noise covariance. In the case of tracking, the true process noise covariance is time-varying and unknown. Estimation problem for simpler systems with unknown process noise is typically handled in the industry by manually tuning the estimator with a suitable high value of the process noise covariance. This contribution empirically investigates whether such tuning heuristics may be extended to more complex nonlinear hybrid systems and the efficacy of such tuning for aircraft tracking tasks with single mode linear and nonlinear state estimators. A well-known trajectory for a maneuvering aircraft has been used as an example of this class of systems. To compare the performance of filters with different tuning parameters, Monte Carlo simulation and three different aggregate metrics have been employed, viz., (i) time average of RMS error, (ii) peak of RMS error, (iii) RMS of RMS error. The study shows that (i) better estimation accuracy in terms of peak of RMS position error is obtainable with an estimator using a nonlinear (CT) model rather than a linear(UM) model, (ii) the practice of using a high value of process noise covariance applies even to this simplified system model and state estimator combination for the chosen problem, (iii) performance of such a manually tuned state estimator approaches that of the IMM filter and is better than an adaptive filter (UKF) and also than the variable structure (SVSF) filter and It is argued that, use of a more sophisticated and computationally intensive estimator would be justified provided such an estimator outperforms the single mode state estimators with manual tuning.

Stochastic state estimators like Kalman filters (Simon, 2006) (Åkesson, Jørgensen, Poulsen, & Jørgensen, 2007) and its variants (Rezaie & Eidsvik, 2016) (Lefebvre, Herman Bruyninckx, & Schutter, 2004) extensions and successors provide optimal estimates of the states and are often used

for target tracking application (Rawat & Parthasarathy, 2008) (Bar-Shalom, Yaakov, & Kirubarajan, 2001) (Mehrotra & Mahapatra, 1997). Recent publications (Aalto, 2016) (Gadsden, Habibi, & Kirubarajan, 2014) (Gadola, Chindamo, & Fabrizio, 2014) (Mohan, Naik, Gemson, & Ananthasayanam, 2015) (Ananthasayanam, 2011) (Johansen & Thor, 2017) (Shambaky, 2011) and a review (Auger, et al., 2013)reveal that Kalman filter and its variants are still relevant for the industry and academia.

Kalman filter gives optimum state estimation when, among other conditions, the process noise covariance should be known (Simon, 2006) (Åkesson, Jørgensen, Poulsen, & Jørgensen, 2007).

The quantitative value of the process noise covariance, often denoted as Q represents the degree of inaccuracy or inadequacy of the process model, in a broad sense. Modeling inaccuracy may occur due to unknown values of the plant parameters and also due to unmodelled inputs as in the case of maneuvering aircraft model. The process noise covariance has a special role because it is used to represent a quantified mismatch between the actual process dynamics and the simplified process dynamics model used in the filter. Accordingly, the value of Q is not generally known a priori and the estimator performance may suffer due to the use of inappropriate value of Q. practitioners often tackle such situations by manually tuning the noise covariance parameters (Åkesson, Jørgensen, Poulsen, & Jørgensen, 2007) (Zarchan, 2005) (Ananthasayanam, 2011). While adaptive filters (Mehra, 1972) (Lee & Alfriend, 2004) (Mohamed & Schwarz, 1999) (Almagbile, Jinling, & Weidong, 2010) perform such tuning algorithmically, practitioners often perform manual tuning by adjusting Q and R.

Tracking of maneuvering targets are often modeled as a hybrid nonlinear system (Hwang, Balakrishnan, & Tomlin, 2006), which makes the state estimation problem more complex than that for ordinary (single mode, non-hybrid) systems because each mode of the hybrid system would have distinctly different dynamics. State estimators for hybrid systems may use switched multiple models and interacting multiple models (Hwang, Balakrishnan, & Tomlin, 2006) (Bar-Shalom, Yaakov, & Kirubarajan, 2001) (Li & Bar-Shalom, 1993) which lead to their complexity (as implicit or explicit determination of instantaneous modes or prior knowledge may be necessary except for simplistic cases). In this contribution, we explore the possibility of using simple single mode filters along with manual tuning for such nonlinear hybrid systems. Use of the single-model state estimator has the advantages of (i) simplicity (ii) computational efficiency and (iii) simplified tuning or adaptation procedure.

A generally accepted heuristics for manual tuning is to tune the process covariance matrix with a sufficiently large value (Simon, 2006) (Zarchan, 2005) where an inaccurate (but simple and convenient) model has been used in the estimator. While such heuristics has been demonstrated to work well in the case of linear systems, the same cannot be said about nonlinear systems and also

hybrid nonlinear systems. One more objective of this chapter is to investigate and quantify the efficacy of such manual tuning heuristics for nonlinear and hybrid system using simple or simplified process models.

It may be noted that when the plant model is linear and the covariances Q and R are known, rigorous theoretical proofs for optimal estimation are available (Simon, 2006). However, when the plant model is nonlinear and/or the noise covariances are not known, rigorous general proofs are not easy to come by (Simon, 2006). Nonlinearity may be handled by local and zonal linearization as is done respectively in extended Kalman filter (EKF) (Simon, 2006) or in the family of sigma point filters (Sadhu, Mondal, Srinivasan, & Ghoshal, 2006) which includes unscented Kalman filter (UKF) (Rezaie & Eidsvik, 2016) (Simon, 2006) (Lefebvre, Herman Bruyninckx, & Schutter, 2004) and divided difference filter (DDF) (Lefebvre, Herman Bruyninckx, & Schutter, 2004). Absence of rigorous general proof implies that application of nonlinear and adaptive filters must be evaluated by extensive simulation. For the stochastic estimators, such evaluation is usually carried out by Monte Carlo method (Zarchan, 2005).

For aircraft tracking problems where sophisticated motion models (Bishop, 2000) (Li & P. Jilkov, 2003) (Mehrotra & Mahapatra, 1997) and state estimation algorithms (Bar-Shalom, Yaakov, & Kirubarajan, 2001) (Gadsden, Habibi, & Kirubarajan, 2014) are available, the industry reportedly continues to use manually tuned (Mohan, Naik, Gemson, & Ananthasayanam, 2015) simpler tracking filters employing simple motion models. Two particular well-known motion models are uniform motion (UM) and coordinated turn (CT) described in a subsequent section. Trajectory of a civil aircraft may be considered as a hybrid system containing sequences of UM and CT segments.

For the UM model the plant model is linear and a Kalman filter suffices, whereas for the nonlinear CT model, two filters viz., EKF and UKF have been used. However, in the present contribution we have characterized the performance of state estimators (filters) with UT model (by Kalman Filter) and CT model (with nonlinear filters), taking one at a time. Finally, performance of the several types of manually tuned nonadaptive, single model state estimators have been compared with adaptive UKF (AUKF), recently introduced smooth variable structure filter (SVSF) and with interacting multiple model (IMM) estimators using adequate Monte Carlo simulation and three quantitative descriptors of estimation performances.

To the best of the knowledge of the contributors, such a comprehensive comparison, especially with SVSF, AUKF and IMM has not been reported in the literature.

9.1 Formulation of the Specific Aircraft Tracking Problem

9.1.1 Preliminaries

The general discrete nonlinear plant model is described as follows:

$$x_{k+1} = f(x_k, u_k) + w_k \tag{9.1.1}$$

$$y_k = h(x_k) + v_k \tag{9.1.2}$$

where, the state vector x_k and y_k are the state and the measurement vectors of the system respectively at the instance k for input u_k. The uncorrelated white Gaussian process and measurement noise are represented as w_k and v_k with their covariances Q_k and R_k respectively.

A wide variety of models for describing target motion with maneuver have been reported in the literature (Bishop, 2000) (Li & P. Jilkov, 2003) (Mehrotra & Mahapatra, 1997). A number of sophisticated state estimation based tracking systems (like multi-modal, interactive multiple model (Bar-Shalom, Yaakov, & Kirubarajan, 2001), adaptive estimators (Lee & Alfriend, 2004), variable structure filter (Gadsden, Habibi, & Kirubarajan, 2014)) have been suggested for tracking maneuvering aircraft.

The aircraft trajectory considered in this contribution has been used by several previous workers (Bar-Shalom, Yaakov, & Kirubarajan, 2001) (Gadsden, Habibi, & Kirubarajan, 2014) for evaluating state estimators. In the “S-shaped” trajectory the aircraft travels in a horizontal plane and such trajectory consists of three uniform motion (UM) segments and two coordinated turn (CT) segments. The nominal trajectory is shown in Fig 4.3. Appropriate dynamic models of these two segments are described subsequently.

9.1.2 The Trajectory

In the trajectory shown in Fig 4.3, the aircraft flies westward (along negative X-direction) from the initial position of [25,000m, 10,000m], with a constant velocity of 120m/s for 125s. Thereafter, it takes a coordinated turn with a turn rate of 1 degree/sec in the anti-clockwise direction for 90s and then flies southward for another 125s at a constant velocity of 120m/s. The aircraft then takes a clockwise coordinated turn for 30s at 3 degree/sec, after which it follows a straight westward path at 120m/s for 120s.

The UM segment is generally represented by a linear 4th-order model (where a simple Kalman filter would be appropriate) whereas the CT segment requires a 5^{th} order nonlinear model with the ‘turn

rate' as an additional state. For the sake of compatibility with the model in (Bar-Shalom, Yaakov, & Kirubarajan, 2001) (Gadsden, Habibi, & Kirubarajan, 2014), it is assumed that measurements of position in Cartesian coordinates are available from a tracking system.

9.1.3 Model of the Uniform Motion

The discrete state equations of the model for uniform motion are represented as (Bar-Shalom, Yaakov, & Kirubarajan, 2001).

$$\mathbf{x}_{k+1} = \begin{bmatrix} 1 & 0 & T & 0 \\ 0 & 1 & 0 & T \\ 0 & 0 & 1 & 0 \\ 0 & 0 & 0 & 1 \end{bmatrix} \mathbf{x}_k + \begin{bmatrix} 0.5T^2 & 0 \\ 0 & 0.5T^2 \\ T & 0 \\ 0 & T \end{bmatrix} \mathbf{w}_k \tag{9.1.3}$$

where, T is the sampling interval, and the state vector $\mathbf{x}_k$ is defined as

$$\mathbf{x}_k = \begin{bmatrix} \zeta_k & \eta_k & \dot{\zeta}_k & \dot{\eta}_k \end{bmatrix}' \tag{9.1.4}$$

with ζ_k and η_k representing the position of the aircraft along the X and Y direction respectively; $\dot{\zeta}_k$ and $\dot{\eta}_k$ represent the corresponding linear velocities. Here $\mathbf{w}_k$ represents the discrete equivalent of noise in the acceleration in the X and Y directions with covariance Q_{UM}.

9.1.4 Model of Coordinated Turn

The coordinated turn model contains an additional state variable, viz., the turn rate Ω, which is nominally an unknown constant (Bar-Shalom, Yaakov, & Kirubarajan, 2001). For this model, the state vector $\mathbf{x}_k$ is defined as $\mathbf{x}_k = \begin{bmatrix} \zeta_k & \eta_k & \dot{\zeta}_k & \dot{\eta}_k & \Omega \end{bmatrix}'$

$$\mathbf{x}_{k+1} = \begin{bmatrix} 1 & 0 & \frac{\sin(\Omega_k T)}{\Omega_k} & -\frac{1-\cos(\Omega_k T)}{\Omega_k} & 0 \\ 0 & 1 & \frac{1-\cos(\Omega_k T)}{\Omega_k} & \frac{\sin(\Omega_k T)}{\Omega_k} & 0 \\ 0 & 0 & \cos(\Omega_k T) & -\sin(\Omega_k T) & 0 \\ 0 & 0 & \sin(\Omega_k T) & \cos(\Omega_k T) & 0 \\ 0 & 0 & 0 & 0 & 1 \end{bmatrix} \mathbf{x}_k + \begin{bmatrix} 0.5T^2 & 0 & 0 \\ 0 & 0.5T^2 & 0 \\ T & 0 & 0 \\ 0 & T & 0 \\ 0 & 0 & T \end{bmatrix} \mathbf{w}_k \tag{9.1.5}$$

Here $\mathbf{w}_k$ represents the discrete equivalent of noise in the acceleration in the X and Y directions with covariance Q_{CT}.

9.1.5 Measurement Models

It is assumed that the tracker is stationed at the origin to measure the position along the X and Y directions. The measurement for the UM model is

$$\mathbf{y}_k = \begin{bmatrix} 1 & 0 & 0 & 0 \\ 0 & 1 & 0 & 0 \end{bmatrix} \mathbf{x}_k + \mathbf{v}_k \tag{9.1.6}$$

$\mathbf{v}_k$ represents the discrete measurement noise of the system with covariance $\mathbf{R}$. The corresponding measurement model for CT is

$$\mathbf{y}_k = \begin{bmatrix} 1 & 0 & 0 & 0 & 0 \\ 0 & 1 & 0 & 0 & 0 \end{bmatrix} \mathbf{x}_k + \mathbf{v}_k \tag{9.1.7}$$

9.1.6 Noise Covariances

The process noise covariance for the UM mode is

$$\mathbf{Q}_{UM} = \begin{bmatrix} \frac{T^3}{3} & 0 & \frac{T^2}{2} & 0 \\ 0 & \frac{T^3}{3} & 0 & \frac{T^2}{2} \\ \frac{T^2}{2} & 0 & T & 0 \\ 0 & \frac{T^2}{2} & 0 & T \end{bmatrix} .L_1 \tag{9.1.8}$$

and the measurement noise covariance are defined as (Bar-Shalom, Yaakov, & Kirubarajan, 2001)

$$\mathbf{Q}_{CT} = \begin{bmatrix} \mathbf{Q}_{UM} & \mathbf{0}_{4X1} \\ \mathbf{0}_{1X4} & \frac{L_2}{L_1} T \end{bmatrix} .L_1 \tag{9.1.9}$$

L_1 and L_2 are the power spectral densities (Bar-Shalom, Yaakov, & Kirubarajan, 2001) of corresponding continuous domain noise for linear acceleration and angular acceleration respectively. The corresponding numerical values are 0.16 and 0.01 respectively.

The measurement noise covariance values taken for this problem is (Gadsden, Habibi, & Kirubarajan, 2014)

9.2 Evaluation Approach

9.2.1 Performance Metrics

Evaluation of state estimation of nonlinear hybrid systems even with the help of numerical Monte Carlo simulation poses a few problems. Hybrid systems follow cycles of trajectories and estimation errors may vary at each point in the cycle. For objective comparison of estimators, one has to use an aggregate metric for estimation errors. Previous workers have used time average of Monte Carlo (MC) derived RMS error (Gadsden, Habibi, & Kirubarajan, 2014). As a single metric may not be able to capture the relative efficacy of different tracking algorithms, we use two additional metrics viz., peak (h-infinity norm) RMS error as obtained from Monte Carlo studies and RMS of RMS error as obtained from Monte Carlo studies.

9.2.2 Truth Model

The truth model is created from the UM and CT models as above as appropriate for each segment. To make it realistic, the UM model used for this purpose is the CT model with the turn rate set to $\Omega = 0$. This permits addition of turning rate noise even in the nominal mode. The truth model is initialized with random initial conditions drawn from random Gaussian sequences with covariance $\mathbf{P}_0 = diag([50^2 \quad 50^2 \quad 100 \quad 100])$ and mean $\mathbf{x}_0 = [25000 \quad 10000 \quad 0 \quad 0]^T$. Here the distances are in meters, velocities in meter/sec. For each instance of such trajectory defined above, random process noise drawn from random Gaussian sequences with covariance $\mathbf{Q}_{UM}$ or $\mathbf{Q}_{CT}$ as appropriate, are added.

The filter is initialized with deterministic values $\mathbf{x}_0 = [25000 \quad 10000 \quad 0 \quad 0]^T$ for the UM model. For the CT model, the initial turn rate is set as 0.

9.2.3 Estimators Evaluated

Using MC studies and the above set of descriptor metrics, we compare the performance of two types of manually tuned single model estimators (viz. the uniform motion (UM) and coordinated turn (CT) types described in the next section) with that obtainable from sophisticated state estimators like (a) Q-adaptive estimator (Lee & Alfriend, 2004) like adaptive unscented Kalman filter (AUKF) (b) smooth variable structure filter (SVSF) (c) an interacting multiple model estimator (IMM).

It may be noted that use of the CT model involves the estimation of turn rate parameter and makes the estimation problem nonlinear.

Tracking performance results for KF, EKF, UKF, AUKF and IMM were computed as a part of this present work whereas the same for SVSF was taken from (Gadsden, Habibi, & Kirubarajan, 2014).

The steps of EKF and UKF are as per their respective conventional forms given in (Simon, 2006) (Gadsden, Habibi, & Kirubarajan, 2014). The parameters for the UKF are chosen as $\kappa = 0,\ \beta = 2,\ \alpha = 0.6$ (Sadhu, Mondal, Srinivasan, & Ghoshal, 2006).

A scale factor based adaptive UKF (Lee & Alfriend, 2004) has been used in the simulation study with the same parameters as in the UKF for the kernel. The length of the adaptation window is taken as 20 samples and the AUKF estimator is initialized with $Q_0 = 100\, Q_{CT}$. We note in passing other forms of adaptation involving process noise covariance are also possible (Shambaky, 2011).

In this work, we have used a two-mode version of the IMM, with initial weights (0.5, 0.5) for each mode. Several versions of the two-mode IMM were tried out of which we have selected the following which provided the best result amongst the versions considered. The chosen version incorporates CT model and EKF for both the modes but with different process noise covariance for the modes; specifically, with nominal process noise covariance ($Q_0 = Q_{CT}$) in one mode and high process noise covariance ($Q_0 = 20\, Q_{CT}$) in the other. The value of transition probability matrix (in MATLAB notation) is chosen as [0.95, 0.05; 0.05, 0.95] as in (Bar-Shalom, Yaakov, & Kirubarajan, 2001).

9.2.4 Evaluation Specifics

The performance of the estimators has been evaluated with the help of Monte Carlo simulation with sampling interval of $T = 5s$.

For each study, 500 Monte Carlo runs have been used to calculate (i) the RMS error sequence, $\{e_{rms}(k)\}$ across the Monte Carlo population corresponding to each instant k (ii) peak value of the RMS error sequence, $\Sigma_{peak} = \sup_k [\{e_{rms}(k)\}]$, (iii) time average of the RMS error sequence, $\Sigma_{avg} = \frac{1}{N}\sum_{k=1}^{N} \{e_{rms}(k)\}$, (iv) RMS of the RMS error sequence $\Sigma_{RMS} = \sqrt{\frac{1}{N}\sum_{k=1}^{N} e_{rms}^2(k)}$. Note that the RMS error sequence is plotted against time sample k whereas the other three metrics being aggregated single numbers are tabulated. For a compact representation, the position errors in X and Y are aggregated in a single number called composite position error, being the square root of sum of squared values of the components. The composite values of velocity errors are similarly computed.

As the objective of the present work is to study the effect of varying the norm of the process noise covariance matrix, (designated as $\mathbf{Q}_{filter}$) with the help of a multiplying scalar λ so that

$\mathbf{Q}_{filter} = \lambda \mathbf{Q}_{nom}$, where $\mathbf{Q}_{nom}$ is the nominal value of the process noise covariance corresponding to the choice of UM or CT model. The scaler λ has been varied from a very low value (0.001) to a very high value (1000).

9.3 Results of Linear Model (UM) Based Filter

Note that the UM-based filter is a simple Kalman filter as both the process and the measurement models are linear. For initializing the error covariance $\mathbf{P}$ in the UM-based filter, an initial error covariance $\mathbf{P}_0$ is taken as $diag([50^2 \quad 50^2 \quad 100 \quad 100])$.

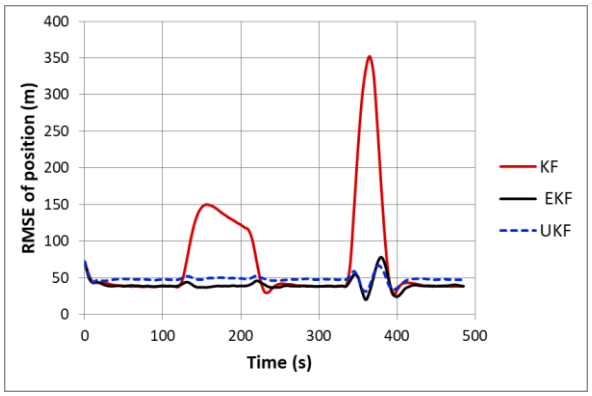

Figure 9.1 RMSE (from MC simulation) of position for λ=10

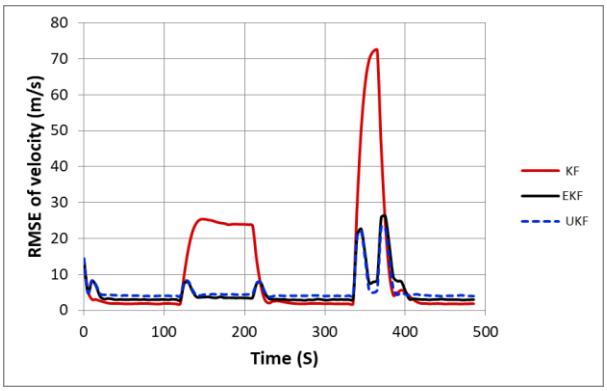

Figure 9.2 RMSE (from MC simulation) of velocity for λ=10

The aggregate performance parameters of the UM-based filter with different values of the process noise covariance (quantified by the multiplier λ) are tabulated in Table 9.1, Table 9.2 and Table 9.3 and their temporal profile are represented in corresponding figures as mentioned below.

From these we may note the following.

- Temporal variation of RMS error (position and velocity) for a specific value of multiplying factor $\lambda = 10$ is shown in components marked with KF in Fig 9.1 and Fig 9.2.
- Temporal variation of RMS error (position and velocity) for different values of multiplying factor λ is shown in Fig 9.3 and Fig 9.4. The aggregate values of the metrics shown in the tables mentioned above are computed from these. Note that larger peak errors occur during the coordinated turn segments for all such cases. We also note that the peaks reduce as λ is increased.
- For different values of multiplying factor λ as given in Table 9.1, we note that time average of RMS error (Σ_{avg}) of composite position, decreases as λ increases with no distinct minima.

The same trend is seen for time average of RMS error in the case of composite velocity. This may also be visualized from the plots marked KF in Fig 9.5 and Fig 9.6. For the position error and with $\lambda \geq 10$, we see that the values are substantially less than square root of measurement error covariance ($50\sqrt{2}$ m).

- The Table 9.2 shows that the peak of RMS error (Σ_{peak}) of composite position decreases as λ increases with no distinct minima. Though the trend for the peak of RMS composite velocity error is non-monotonic, the overall trend follows that of the position error. It may be noted that the peak values are substantially higher compared to the time-averaged values especially for higher values of λ. These may also be visualized from the plots marked KF in Fig 9.7 and Fig 9.8. We note that the high peak errors were also discernable in Fig 9.1, Fig 9.2, Fig 9.3, and Fig 9.4.

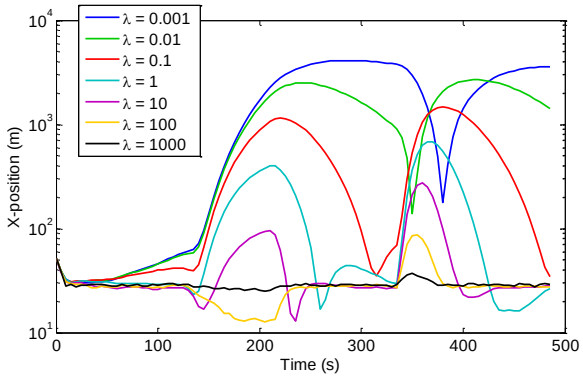

Figure 9.3 RMSE of x-position for UM-KF for different choice of λ

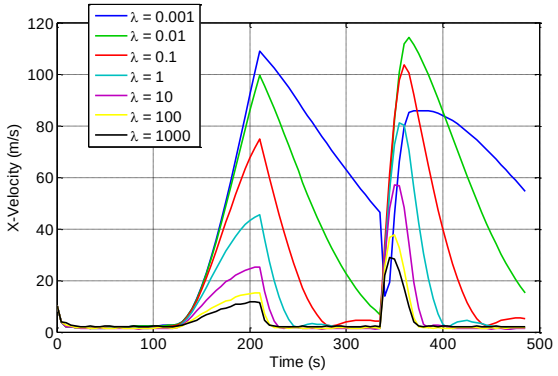

Figure 9.4 RMSE of x-velocity for UM-KF for different choice of λ

Table 9.1 Time-averaged RMS error (Σ_{avg})

Scale factor (λ)	Composite error	KF	EKF	UKF
0.001	Position (m)	2712.6	1192.6	1175.9
	Velocity (m/s)	72.7	60.8	60.2
0.01	Position (m)	1729.6	557.53	548.41
	Velocity (m/s)	56.9	44.62	44.06
0.1	Position (m)	615.02	232.72	219.97
	Velocity (m/s)	33.12	27.77	26.34
1	Position (m)	197.97	67.34	65.36
	Velocity (m/s)	18.80	10.40	9.39
10	Position (m)	74.54	39.73	47.33
	Velocity (m/s)	10.45	4.87	5.38

100	Position (m)	43.73	39.10	47.06
	Velocity (m/s)	6.36	5.07	9.21
1000	Position (m)	39.95	39.64	43.22
	Velocity (m/s)	6.12	7.65	27.06

- The Table 9.3, shows that the RMS of RMS error (Σ_{RMS}) of composite position as well as composite velocity decreases as λ increases with no distinct minima.

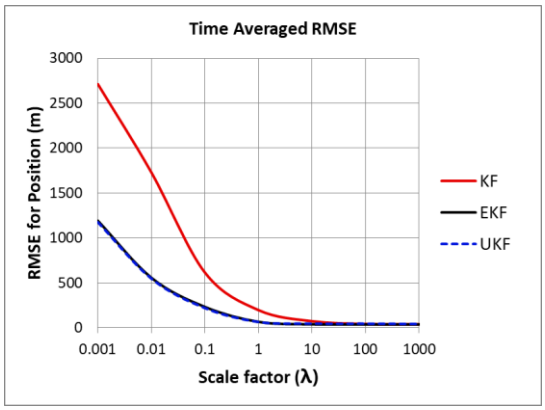

Figure 9.5 Time-averaged position RMSE for different filters

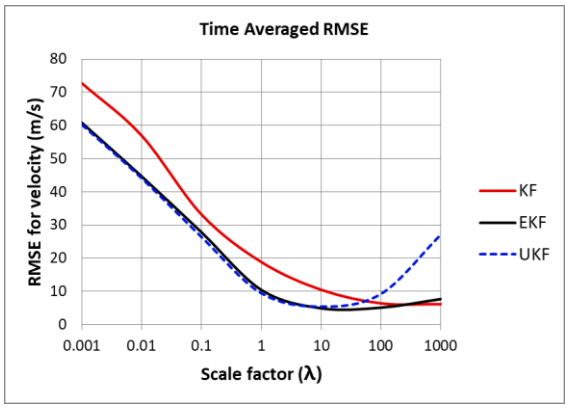

Figure 9.6 Time-averaged velocity RMSE for different filters

Table 9.2 Peak of RMS (Σ_{peak})

Scale factor (λ)	Composite error	KF	EKF	UKF
0.001	Position (m)	5534.5	5924.9	5832.3
	Velocity (m/s)	143.1	181.2	179.5
0.01	Position (m)	3833.1	2454.5	2425.1
	Velocity (m/s)	165.9	160.5	158.2
0.1	Position (m)	2021.3	1111.0	1056.2
	Velocity (m/s)	149.0	102.7	98.0
1	Position (m)	934.36	345.87	294.48
	Velocity (m/s)	116.45	59.76	55.79
10	Position (m)	353.68	77.88	71.92
	Velocity (m/s)	72.49	26.16	23.05
100	Position (m)	104.73	71.92	71.92
	Velocity (m/s)	38.00	15.45	16.11
1000	Position (m)	71.92	71.92	71.92
	Velocity (m/s)	19.75	14.38	28.42

9.4 Results of the Nonlinear Model (CT) Based Filters

Two types of CT based filters have been used viz., EKF and UKF.

For initializing the error covariance $\mathbf{P}$, an initial error covariance $\mathbf{P}_0$ is taken as $diag([50^2 \quad 50^2 \quad 100 \quad 100 \quad 1])$. Note that the turn rate is in degree/sec and the corresponding covariance element is (degree/sec)-squared. The aggregate performance of the two CT based filters with different values of the process noise covariance is also tabulated in Table 9.1, Table 9.2 and Table 9.3 and represented in corresponding figures.

From these we may note the following.

- Performance of the EKF may be seen to closely follow that of UKF except as mentioned below.
- Temporal variation of RMS error (position and velocity) for a specific value of multiplying factor $\lambda = 10$ is shown in components marked with EKF and UKF in Fig 9.2 and Fig 9.3. We note that the nonlinear (EKF and UKF) filters perform better than the linear filter for all time instances.

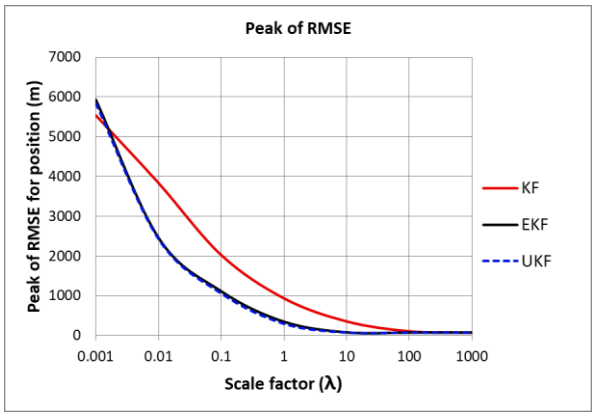

Figure 9.7 Peak of position RMSE for different filters

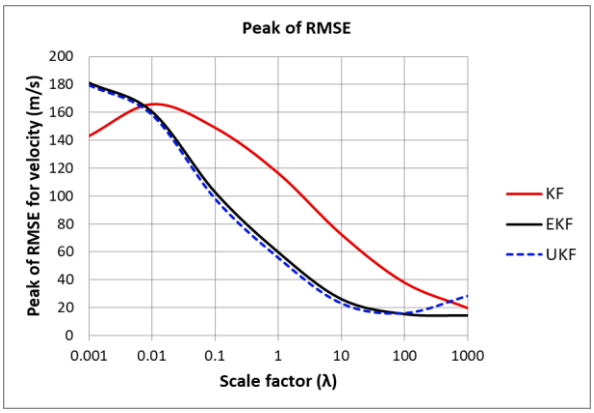

Figure 9.8 Peak of velocity RMSE for different filters

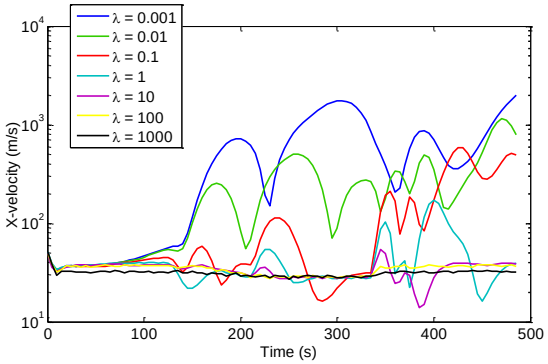

Figure 9.9 RMSE of x-position for CT-UKF for different choice of λ

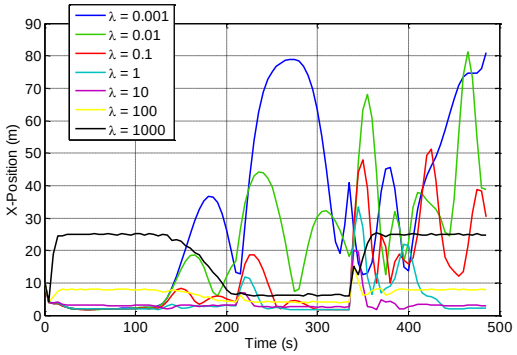

Figure 9.10 RMSE of x-velocity for CT-UKF for different choice of λ

- Temporal variation of RMS error (position and velocity) for different values of multiplying factor λ is shown in Fig 9.9 and Fig 9.10 (UKF). Note that in these cases larger peak errors occur during transition to and from coordinated turn modes for all such cases. We also note that the peaks reduce as λ is increased.

- Plots of RMS errors over the time provide insights about the areas of possible improvement. As the RMS errors tend to peak near mode transition points, it was conjectured that a multiple model may show better performance. However it turned out that the manually tuned EKF performance with adequate value of λ outperformed that of a typical IMM estimator as discussed below.

- For different values of multiplying factor λ, we note that time average of RMS error (Σ_{avg}) of composite position decreases as λ increases with no distinct minima. This may also be verified from the plots marked EKF and UKF in Fig 9.5.

- Time-averaged RMS error in the case of composite velocity also decreases monotonically with λ for $\lambda \leq 10$. However, for higher values of λ, i.e., at or beyond $\lambda = 10$, minima can be observed in EKF and UKF. This may also be visualized from the plots marked EKF and UKF in Fig 9.6. For the UKF, the minima is more distinct compared to the EKF. So for all practical purpose, $\lambda = 100$ may be considered the upper permissible limit to obtain good position error performance and reasonable velocity error performance.

Table 9.3 RMS of RMS error (Σ_{RMS})

Scale factor (λ)	Composite error	KF	EKF	UKF
0.001	Position (m)	3488.7	1799.3	1771.4
	Velocity (m/s)	87.7	81.1	80.3
0.01	Position (m)	2203.9	830.89	818.65
	Velocity (m/s)	75.1	63.60	62.94
0.1	Position (m)	875.11	386.12	359.75
	Velocity (m/s)	50.63	44.18	41.72
1	Position (m)	306.49	92.70	82.85
	Velocity (m/s)	32.27	17.33	15.64
10	Position (m)	102.30	41.23	48.34
	Velocity (m/s)	19.16	6.90	6.80
100	Position (m)	46.56	40.00	47.87
	Velocity (m/s)	10.53	5.57	9.43
1000	Position (m)	40.85	40.50	44.06
	Velocity (m/s)	7.21	7.88	27.34

- From the above figures, we note that both position error and velocity error are noticeably less compared to the Kalman filter for $\lambda \leq 10$. For the composite velocity error well past the optimum value of λ, the UKF exhibits more error compared to the Kalman filter.

- If a substantially higher value of λ is used ($\lambda > 1000$), the UKF was seen to diverge. The reason may be attributed to the fact that increasing λ increases the spread of the sigma points and at a very high value, the approximations made by the sigma points may be invalid and/or beyond the current mode. This phenomenon may be avoided by adjusting the tuning factors of the UKF with some penalty on the performance at lower value of λ.

- Further, (i) the peak of RMS error (Σ_{peak}) of composite position as well as composite velocity decreases as λ increases. (ii) During the numerical interval, $0.01 \leq \lambda \leq 100$, both position error and velocity error are noticeably less compared to the Kalman filter. (iii) The velocity error for UKF exhibits mild minima. These may also be seen from the plots marked EKF and UKF in Fig 9.6 and Fig 9.8.

- Again, the RMS of RMS error (Σ_{RMS}) of composite position decreases as λ increases with no distinct minima. RMS error in the case of composite velocity, however, exhibits a minima.

- Even for the case of RMS of RMS error, the position error is noticeably less compared to the Kalman filter for $\lambda \leq 1$. The velocity error in the range $0.01 \leq \lambda \leq 100$ is also noticeably less

compared to the Kalman filter.

- Table 9.4 provides a fairly comprehensive comparison table of filtering performance using all the three metrics and for all the filters evaluated for the same tracking scenario. Results for manually tuned filter, KF, UKF, AUKF and IMM were evaluated as part of this work whereas the results for Smooth Variable Structure Filter (SVSF) variants are taken from (Gadsden et al., 2014). For manually tuned EKF, $Q_{filter} = 100\, Q_{CT}$ has been used and the AUKF is initialized with $Q_0 = 100\, Q_{CT}$ for this comprehensive table.

- We may note that performance of the manually tuned EKF is better than the more complex filters like SVSF and AUKF and is equivalent to (actually just marginally better than) the version of the IMM estimator used for this comparison. In particular, the peak RMS error in the IMM is substantially higher compared to the manually tuned filter.

Table 9.4 RMSE Metrics for Estimators Evaluated

Composite RMS State Error		Manually tuned CT (EKF) (λ =100)	AUKF $Q_0 = 100\, Q_{CT}$	IMM EKF-EKF	UKF $Q_{filter} = 100\, Q_{CT}$	SVSF-CT
Time averaged	Position (m)	39.10	59.21	40.48	47.06	110
	Velocity (m/s)	5.07	17.38	4.79	9.21	96
Peak	Position (m)	71.92	230.12	72.05	71.92	-
	Velocity (m/s)	15.45	49.06	28.99	16.11	-
RMS of RMSE	Position (m)	40.00	66.66	41.20	47.87	-
	Velocity (m/s)	5.57	22.45	6.69	9.43	-

- While it may be argued that the performance of the IMM could have been improved by a different choice of component filters, it must be noted that choosing the component filters (adequate number of modes or sub-filters, choice of appropriate sub-filters) in an IMM calls for non-trivial prior knowledge about possible manoeuvres and mode transition probability matrix. Results for the IMM estimator presented in the table may be considered as a representative value.

- From the above results and discussion, it may be inferred that the performance of the manually tuned EKF with a CT model with a suitably high value of process noise covariance is at par or even better than other complex and sophisticated estimators.

9.5 Concluding Discussions

From the figures, the tables and discussion provided above, the following conclusions can be made:

i. All the three descriptors of estimation performance were found to be strongly dependent on the norm of process noise covariance, quantified by the multiplier λ.

ii. As expected, the nonlinear CT model-based filters generally exhibited better performance (in peak RMS position error) compared to the linear UM model.

iii. For the Kalman filter, EKF and UKF, all the error descriptors viz., time-averaged, peak and RMS of RMS error for both position and velocity were seen to decrease with increase in λ when the parameter is varied from very low value to $\lambda = 100$.

iv. The general trend obtained from this study reaffirms the industry practice of using higher process noise where the model is not known adequately because estimation errors generally tend to decrease with increasing λ.

v. Table 9.4 provides a comprehensive comparison of the various filters which underlines the strength of the manually tuned filter with high suitably high value of process noise covariance over other options.

vi. It may be noted that a higher process noise covariance created simply by increasing a scalar proved to be effective because in the point mass model, this amounts to increasing the amount of unmodelled equivalent acceleration.

vii. Overall, the manually tuned EKF turns out to be best in filtering performance and simplicity. Industry usually prefers simple solutions even if such a solution is not numerically optimum. However, the performance of simplistic single model filters surpassed the expectation and competed commendably with the IMM.

Thus the present contribution has outlined an approach with which an informed decision about the choice of filters may be made for comparable tracking problems. We advocate that a similar analysis be carried out with manually tuned simple filter before a sophisticated state estimator (like adaptive, variable structure or interacting multiple model filter) is deployed.

10 Parameter Estimation

In this chapter some of the important nonlinear problems on ballistic target tracking and road-tire friction estimation have been considered.

10.1 Ballistic Coefficient

A nonlinear Ballistic target tracking model (Zarchan, 2005) as discussed in the section 3.4.2 is considered here for a parameter estimation problem. An Q-adaptive Extended Kalman Filter was used to estimate the state of the system.

This plant model has been chosen for the characterization of the Q adaptive filters for a case where noise elements are the function of states. It would be interesting to see how Q-adaptive filters would perform under such circumstances. The expression of Q for two-dimensional system as given below.

$$Q_k = \Phi_s \begin{bmatrix} \frac{T^2}{3} & \frac{T^2}{2} + f_{22}\frac{T^2}{3} \\ \frac{T^2}{2} + f_{22}\frac{T^2}{3} & T + f_{22}T^2 + f_{22}^2\frac{T^2}{3} \end{bmatrix} \tag{10.1.1}$$

where, Φ_s is the noise spectral density of the system assumed to be on the acceleration and T is the sampling interval. And $f_{21} = \frac{-\rho g x^2}{44{,}000\,\beta}$; $f_{22} = \frac{\rho g \dot{x}}{\beta}$. Here ρ is representing the air density, β indicates drag, Q_p is the dynamic pressure $(Q_p = 0.5\rho\dot{x}^2)$, in the system having two states, position and velocity $\begin{bmatrix} x & \dot{x} \end{bmatrix}^T$. Fig 10.1 shows the elements of the process noise, Q which vary over time.

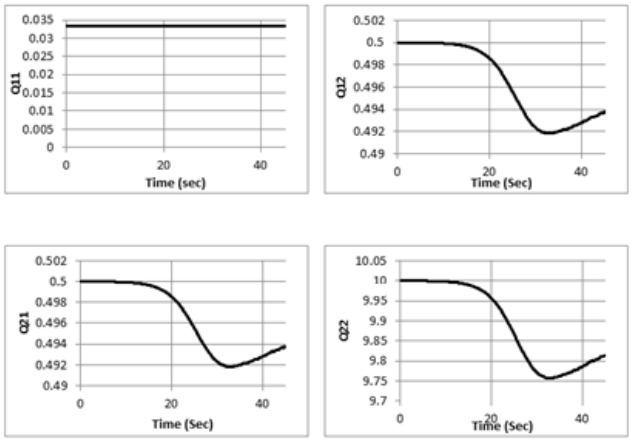

Figure 10.1 Process Noise

10.1.1 State estimation by Adaptive EKF

A scaling factor based Q adaptive EKF (Almagbile, Jinling, & Weidong, 2010) was used to evaluate the system. Position and velocity are considered for characterization of the adaptive EKF. Position is considered as the measurement. System and measurement equations are given in the section 3.4.2.

The simulation of has been carried out with the Q-adaptive Extended Kalman filter for the above-stated system. The simulation parameter is given on the Table: 10.1. The simulation time has been set to 45 seconds after which the object touches the ground

Table 10.1 Simulation Parameters

Initial altitude	200,000 Ft
Initial velocity	6000ft/s
Ballistic coefficient β	500 lb/ft^2
Gravitational constant g	32.2 Ft/sec^2
Noise spectral density Φ_s	100
Measurement noise standard deviation σ_v	25 Ft
Sampling interval, T_s	0.1s
Simulation time	45 s
Sate error covariance P_0	$diag[\ 25^2\ \ 150^2\ ]$

Estimation of the two states of the ballistic target tracking system is presented in section 3.4.2, where the process noise covariance Q has been initialised wrongly $Q_{filter|k=0} = 1000 \times Q_{plant|k=0}$. The RMSE plots of the estimation errors have been shown in the Fig. 10.4-10.5 to evaluate the performance of the filter for 10,000 Monte Carlo runs with different random noise sequences. It is observed from the simulation study that the performance of the adaptive filter for both position and velocity estimation is better as compared to the case where the adaptive cases are not adopted with a wrong value of Q (Fig 10.6-10.7). Fig 9.8 is the demonstration of the convergence of scaling factor α for estimation of Q. For the nominal study, the noise spectral density Φ_s is taken as 100 (Zarchan, 2005) for this simulation, which has been shown in Fig 9.2-9.5. However, the variation of the Φ_s would cause impact on the performance of the Q adaptation process (Fig 10.6-10.7). Three different cases with the variation of $\Phi_s$have been considered here and it is observed that with the higher value of Φ_s the convergence of α is faster. Convergence plot of α has been shown in Fig 10.8 and 10.9.

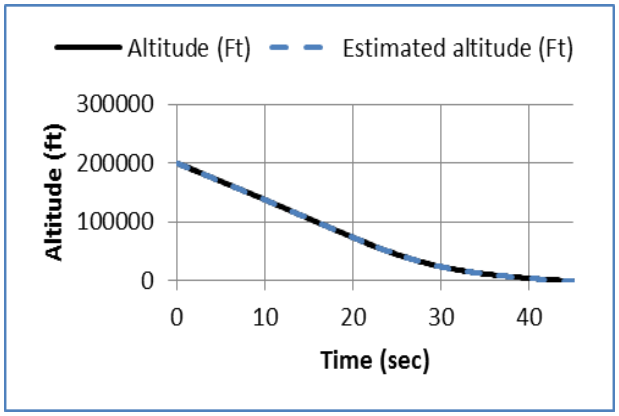

Figure 10.2 Estimation of Altitude

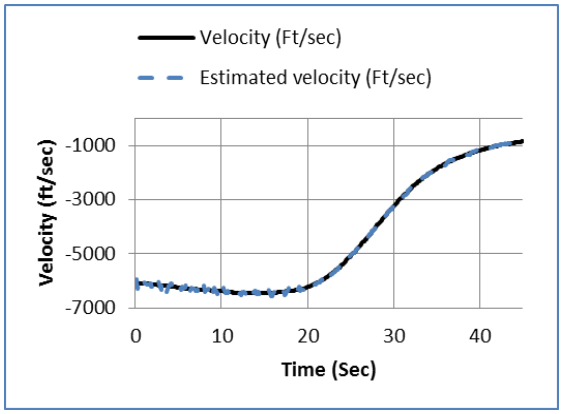

Figure 10.3 Estimation of velocity

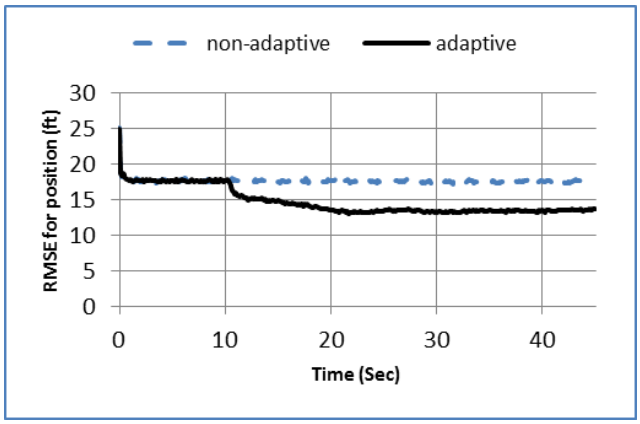

Figure 10.4 RMSE for altitude when $Q_{filter} = 1000 \times Q_{plant}$

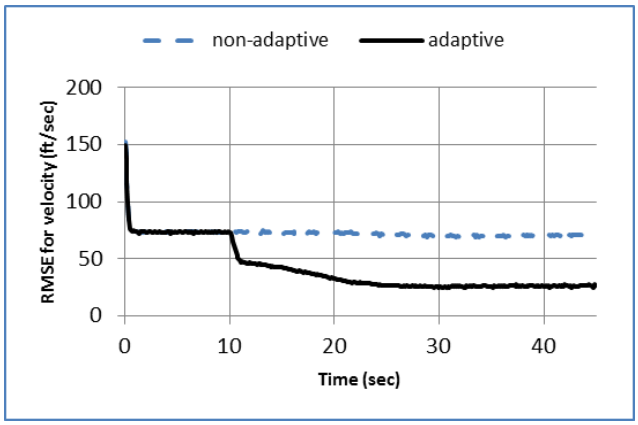

Figure **10.5** *RMSE for velocity when* $Q_{filter} = 1000 \times Q_{plant}$

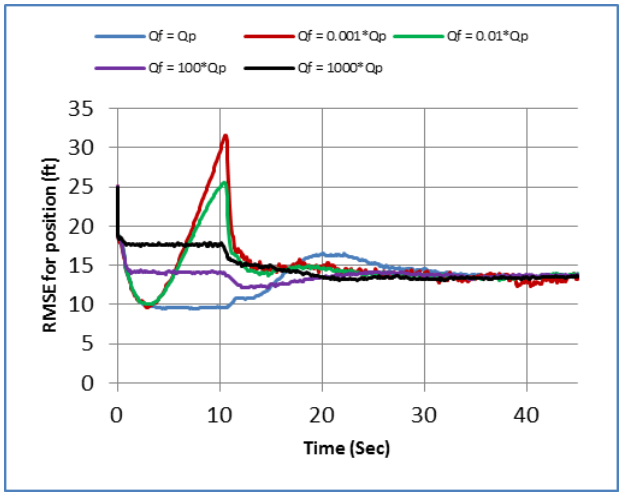

Figure 10.6 RMSE plot for position for different initial guesses of process noise

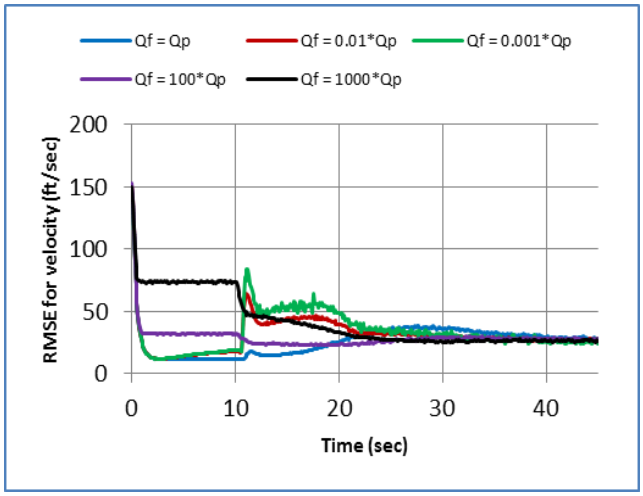

Figure 10.7 RMSE plot for velocity for different initial guesses of process noise

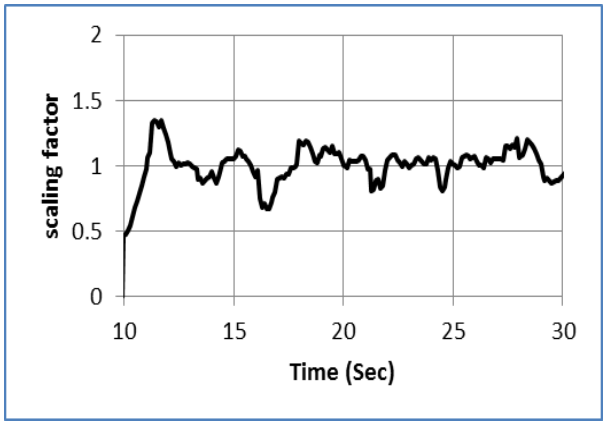

Figure 10.8 Plot of the scaling factor α for (a) $Q_{filter} = 1000 \times Q_{plant}$

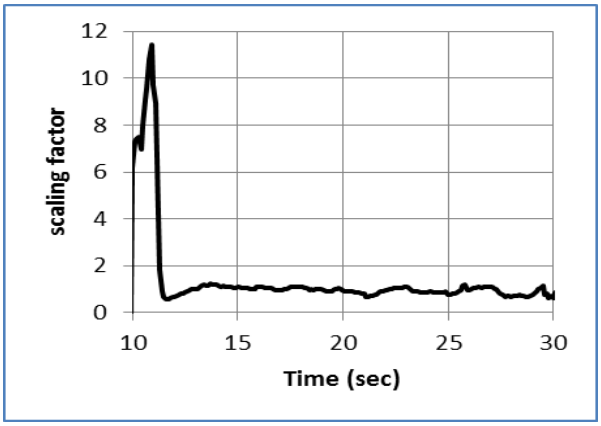

Figure 10.9 Plot of the scaling factor α for (a) $Q_{filter} = 0.001 \times Q_{plant}$

Estimation of Ballistic Coefficient:

For parameter estimation, the ballistic coefficient β has been kept unknown to the estimator. The unknown parameter is considered as the third state ($\mathrm{X} = \begin{bmatrix} x & \dot{x} & \beta \end{bmatrix}^T$). The process noise (Zarchan, 2005) is defined as

$$Q_k = \Phi_s \begin{bmatrix} 0 & 0 & 0 \\ 0 & f_d^2 \dfrac{T_s^3}{3} & f_d \dfrac{T_s^2}{2} \\ 0 & f_d \dfrac{T_s^2}{2} & T_s \end{bmatrix} \qquad (10.1.2)$$

Where, $f_d = -\dfrac{\hat{\rho} g \hat{\dot{x}}^2}{2\hat{\beta}^2}$. For simulation study, the ballistic coefficient is initialized as a random number, say 800. Fig 10.10 shows that the estimator track its true value, 500 in 20s. Fig 10.11 shows RMS error for Ballistic Coefficient after 1000 MC runs.

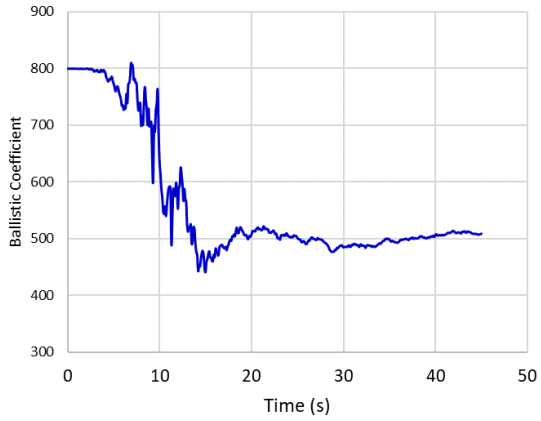

Figure 10.10 Estimated ballistic coefficient

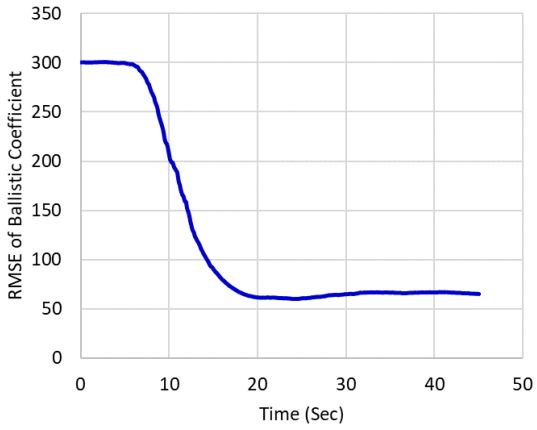

Figure 10.11 RMSE plot of ballistic coefficient

Salient observations

i. In the case of RMS position error, adaptive estimator exhibits markedly improved performance for different initial error covariance (guess) over a wide range. The above almost preclude use of non-adaptive filters where Q is unknown. However, RMSE of velocity shows anomalous behavior for cases where the guess value of Q is much smaller than the true value as the RMSE for non-adaptive estimators comes out to be smaller than the adaptive estimators.

ii. From the simulation studies of RMSE of the states, it is observed that the steady state performance of the adaptive filter for this model is consistent for all different choices of (wrong) initial guesses of Q for both position and velocity (Fig. 9.6 and 9.7). That is irrespective of the choice of the initial covariance over a wide range, the steady state RMSE error remain quite close.

iii. The initial error dynamics of the RMS error for position as well as for velocity for adaptive estimators off course change widely with different choice of the initial Q.

iv. It is interesting to notice that evolution of the scaling factor α (ideal value is unity) over iterations has a dissimilar pattern with the different choice of initial guesses of Q. If the initial guess of Q is higher than that of nominal value the plot of α over time shows an initial overshoot, which doesn't occur if the initial guess is kept lower than that of nominal one (refer to Fig. 9.8 and 9.9). In both the cases however, value of α settles down to the unity in steady state.

v. The ballistic coefficient was initially guessed wrongly as 800 whereas the exact value was considered to be 500 in the truth model (Fig 10.10 and 10.11). The Q Adaptive EKF could track the unknown parameter within 15-20s. The steady state RMSE was noted as 65.

10.2 R-Adaptive EKF for the state estimation of vehicle

The system is described in the previous section. A quarter car model has been taken (as discussed in section 3.5), to model the system and a popular LuGre friction model is considered for the modeling of anti-lock braking system. The system states and the parameter of the tire have been estimated. The main objective is to estimate the velocity of the vehicle, v which is essential to calculate the current slip value of the vehicle for anti-lock braking system. The R adaptive Extended Kalman Filer scheme has been developed to estimate the internal parameter of the tire, vehicle velocity and the wheel velocity even if the noise statistics is unknown to the filter. The angular velocity of the wheel, which is considered here as the measurement state, can easily be measured by available sensor.

10.2.1 System dynamics

The dynamics of the system can be represented as the following state-space model (K. Deng, 2006)

The quarter-car model is described in the third chapter. The longitudinal dynamics of the car is described in 3.5.2.2.

$$\dot{x} = \begin{bmatrix} \dot{z} \\ \dot{\omega} \\ \dot{v} \end{bmatrix} = f(z, \omega, v, T_b) + w$$

$$y = h(x) + v$$

Where, the states are $z, \omega \; and \; v$ which represent internal parameter of the tire, wheel speed and the vehicle velocity. The measurement vector y is considered a linear function of wheel's angular speed. Here, w and v are the process noise and the measurement noise respectively.

The system has been discretized with a sampling rate of 0.001s

$$Q = \begin{bmatrix} 10^{-6} & 0 & 0 \\ 0 & 10^{-6} & 0 \\ 0 & 0 & 10^{-4} \end{bmatrix}$$

$$R = 1$$

10.2.2 REKF Algorithm

Maximum Likelihood equation based adaptive algorithm is revisited and the same is applied to the Extended Kalman Filter for ABS. The measurement noise statistics, R is adapted by the following equation based on the innovation sequence of the measurement.

$$\hat{R}_k = C_{vk} - H_k P_k^- H_k^T$$

Where, $C_{vk} = \frac{1}{L}\sum_{i=i_0}^{k} \vartheta_i \vartheta_i^T$

H_k and P_k^- are the partial derivative matrix calculated for EKF and predicted covariance of the state matrix respectively. The C_{vk} is calculated by averaging a moving window of size L The first epoch of the estimation window is taken as $i_0 = k - L + 1.$ The estimated $\hat{R}_k$ is fed to the EKF to calculate Kalman gain for the estimation of states of the system.

10.2.3 Simulation results

The simulation study has been performed to evaluate the performance of the estimator. The simulation parameters are taken as mentioned in (K. Deng, 2006). A straight path is considered for braking with initial longitudinal velocity of the vehicle and wheel as 22.5m/s. The initial value of internal parameter of the tire is considered to be zero. The other simulation parameters of the systems are given in the table: 1. sampling interval of the filter is taken as 0.001s and window length for averaging innovation sequence is taken as 250 epochs. Fig 10.12-10.17 depict the plot of estimated states over real states and the plots of estimation error for the three states of the vehicle with the application of AEKF. The nominal value of measurement noise covariance R in the plant is taken as 1. The first set (Fig 10.18-10.21) of simulation has been performed with a random value of $R = 0.1$ in the Filter. The filter performs well while the value of *R* is wrongly initialized to the filter. However, it is also important to evaluate the performance of the filter under noise-uncertainty. The performance of AEKF has been shown in RMSE plots (Fig 10.18-10.21). In all the cases the RMSE error has been reduced by the use of adaptive one over the non-adaptive cases. Plot of estimated noise covariance R is shown in Fig 10.22, where it is initialized with the different initial values. It is seen that for all the cases noise covariance converge to its true value ($R = 1$) within finite time.

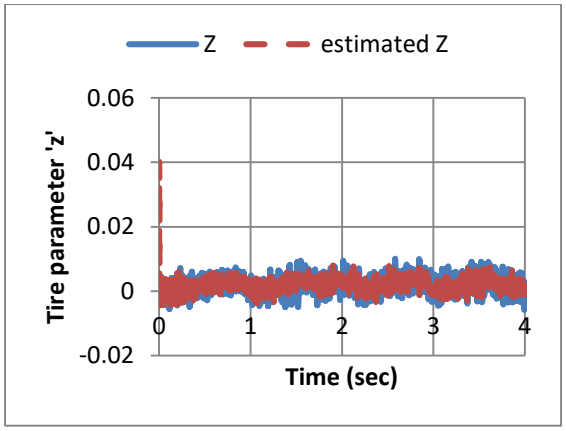

Figure 10.12 Plot of actual and estimated tire parameter

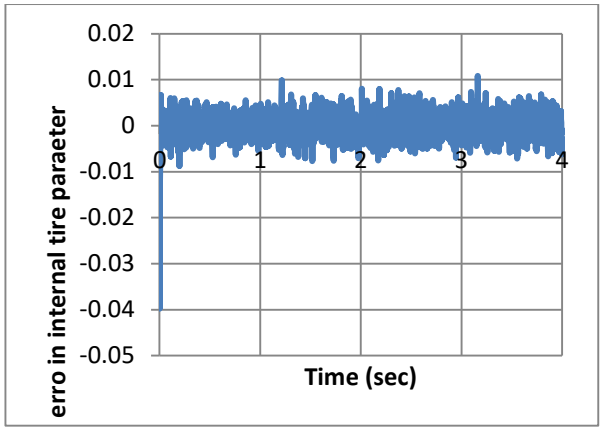

Figure 10.13 Estimation error of the tire parameter

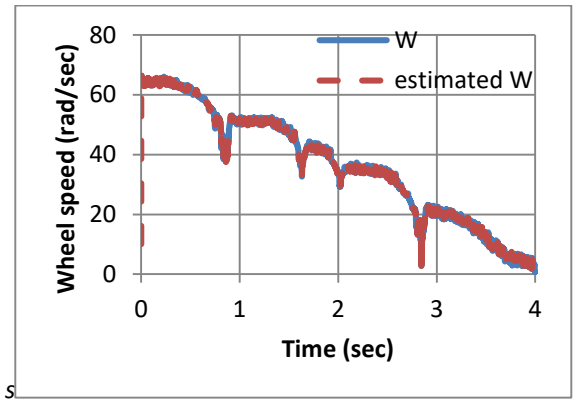

Figure 10.14 Plot of actual and estimated wheel speed

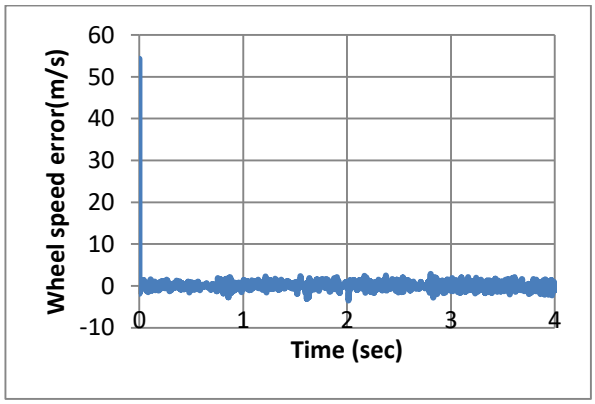

Figure 10.15 Estimation error of the wheel speed

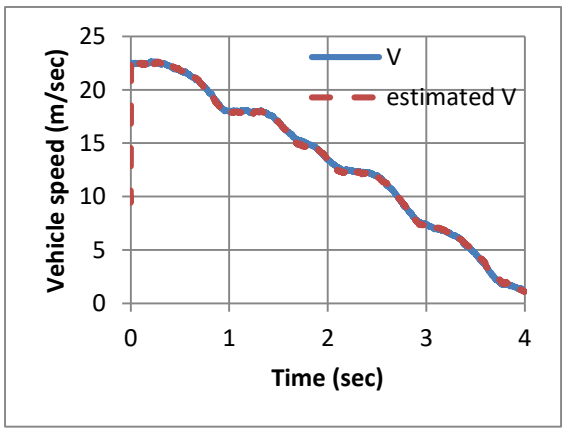

Figure 10.16 Plot of actual and estimated vehicle speed

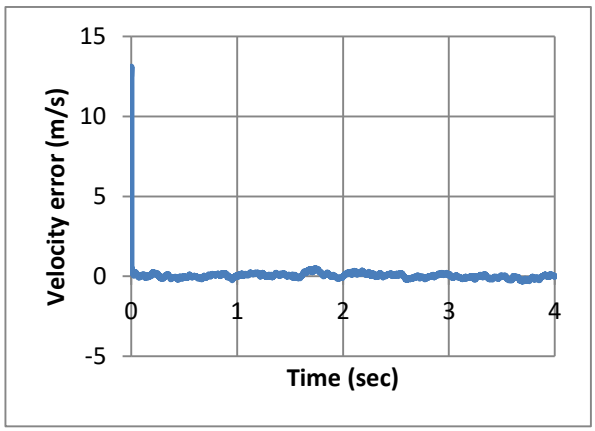

Figure 10.17 Estimation error of the vehicle speed

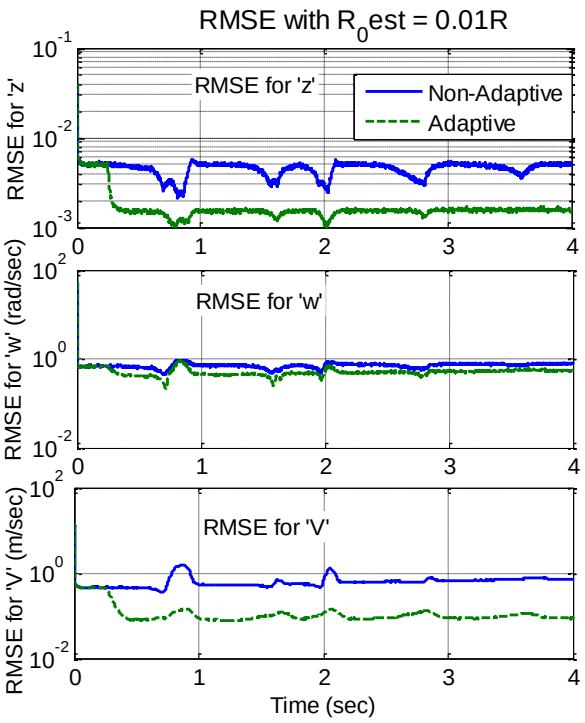

Figure 10.18 RMSE with $\hat{R}_0 = 0.01R$

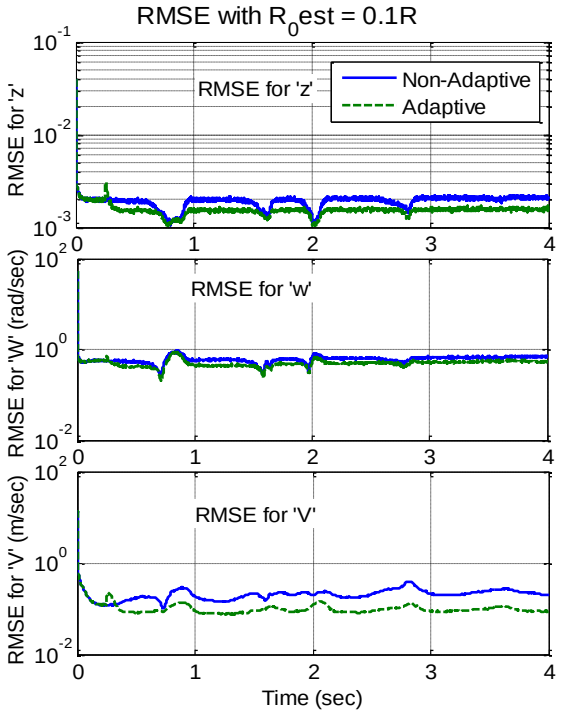

Figure 10.19 RMSE with $\hat{R}_0 = 0.1R$

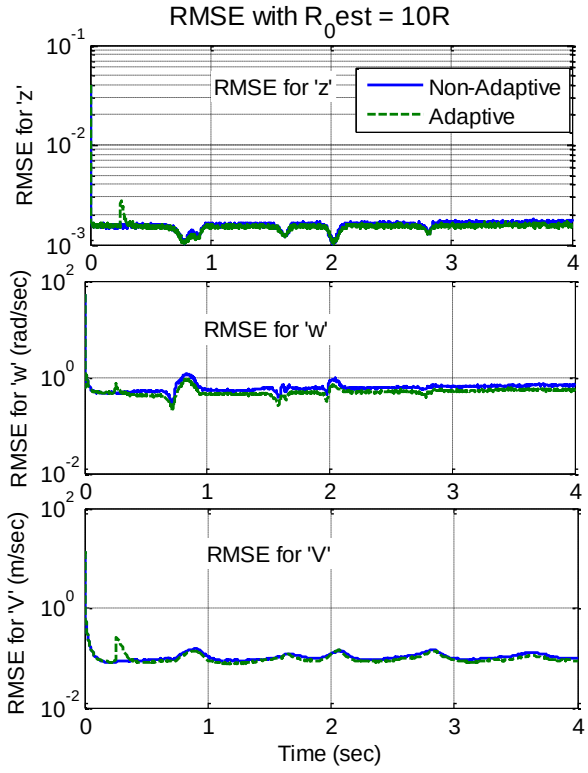

Figure 10.20 RMSE with $\hat{R}_0 = 10R$

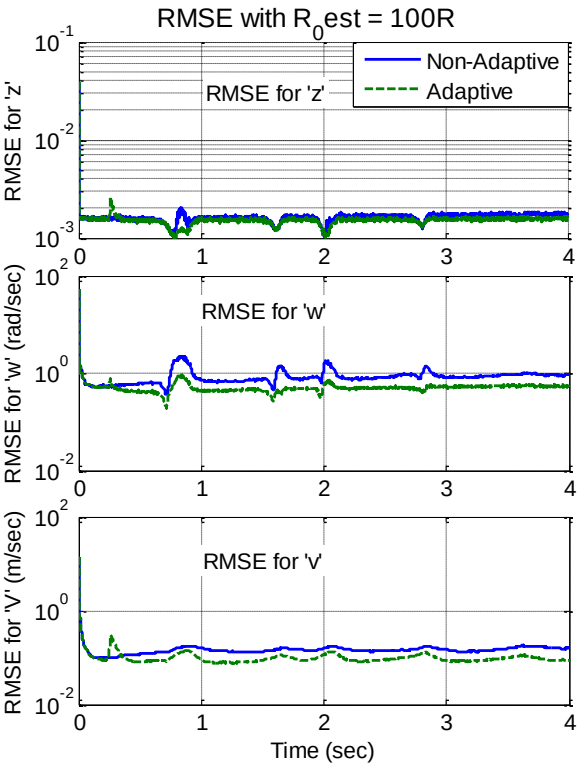

Figure 10.21 ***RMSE with*** $\hat{R}_0 = 100R$

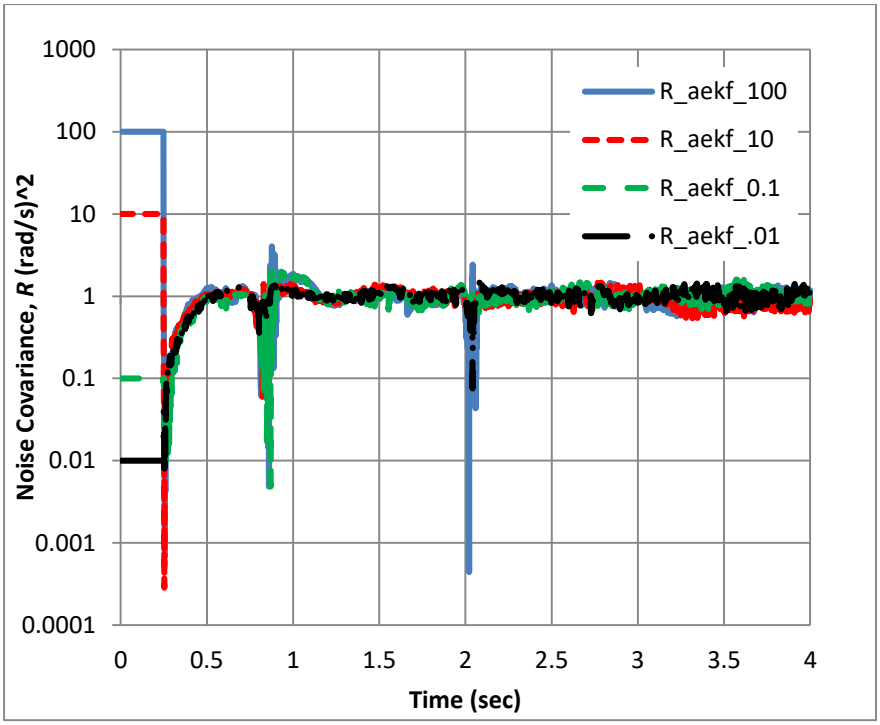

Figure 10.22 Plot of $\hat{R}_{AEKF}$ with different value of $\hat{R}_0$

10.2.4 Discussion

The states of the longitudinal dynamics of the vehicle are estimated under a braking situation in a straight path. The adaptive methodology of the estimation exhibits good performance of estimating measurement noise covariance and the states of the system as well. The RMSE of the states have been reduced in all the simulation cases with the employment of adaptive terms in the filter.

10.3 Side-slip angle and friction coefficient estimation of vehicle from Lateral dynamics

The friction coefficient is one of the important parameters of the Anti-lock Braking System (ABS). The friction coefficient between the tire and road contact surface characterizes the tire force. On the other hand, the maximum brake force which can be applied on the wheel before it gets locked depends on the friction coefficient at the contact patch. Thus, in ABS system, it is important to measure or estimate the frictional force or the friction coefficient dynamically. The characteristics of frictional force with the change in longitudinal slip. However, to estimate the friction coefficient the lateral vehicle model can also be considered. In that case, side-slip angle is another important parameter for capturing the alignment of the tire. The side-slip angle helps to estimate the friction coefficient. It can be estimated via lateral force or aligning moment of the tire.

This work considers lateral model of the vehicle with lateral acceleration, aligning moment, and yaw rate and side-slip angle given in (Ahn, Peng, & Tseng, 2013).

10.3.1 Lateral dynamics

As discussed previously in chapter 3, the friction coefficient and the side-slip angle is estimated through the Brush model. The lateral acceleration and the aligning moment of the tire are measured. The motion equation is discussed below. The symbols used here are discussed previously and carry their usual meaning. The detailed dynamics of the system is given in the section 3.5.2

Steering angle δ is the excitation of the system. The road steer input is 0.25 Hz sinusoidal with a magnitude of 0.04 rad

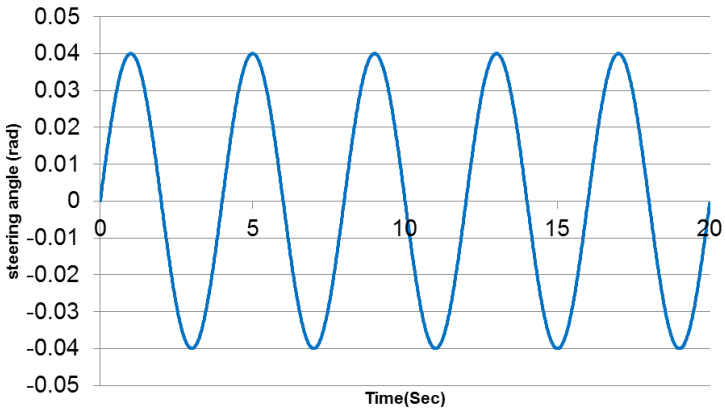

Figure 10.23 Steering input δ

10.3.2 Simulation results and discussion

The simulation study was carried out with the parameters given below. Two sets of simulation were performed. First, the state and parameters are estimated by the unscented Kalman Filter (UKF), second, adaptive scheme was applied for the UKF and the simulation s have been performed. Fig. 10.24 to 10.27 is the representation of estimation of the vehicle's lateral velocity, yaw rate and the friction coefficient. Fig 10.28 to 10.30 represent the RMSEs of the corresponding estimated states using R-adaptive UKF. RMSE plots for RAUKF was done performing 100 MC runs with $R_{truth} = \begin{bmatrix} 50 & 0 \\ 0 & 100 \end{bmatrix} R_{filter}(0) = 100 \times R.$

Table 10.2 Simulation Parameters

Sampling time	0.01s
Q	*diag* ([10^-9 10^-9 10^-5])
R	*diag*([50 100])
P	*diag*([10 10 10])
α	0.6
β	2
X_{true}	$[V_y \quad r \quad \mu]' = [0.01 \ .02 \ 0.5]'$
$X_{estimate}$	$[\hat{V}_y \quad \hat{r} \quad \hat{\mu}]' = [0.01 \ 0 \ 0.3]'$

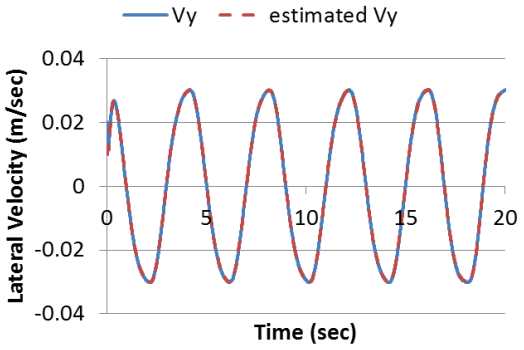

Figure 10.24 Estimation of Lateral Velocity

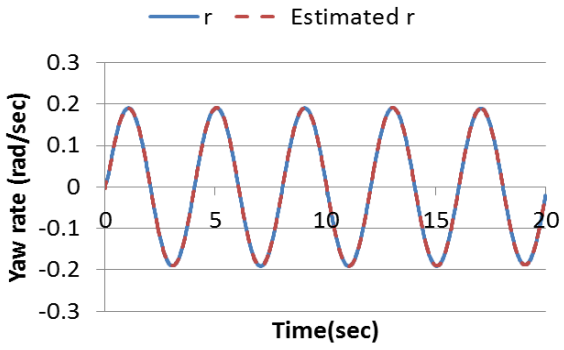

Figure 10.25 Estimation of yaw rate

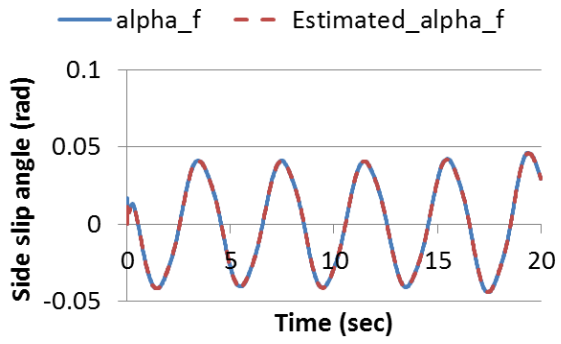

Figure 10.26 Estimation of side-slip angle

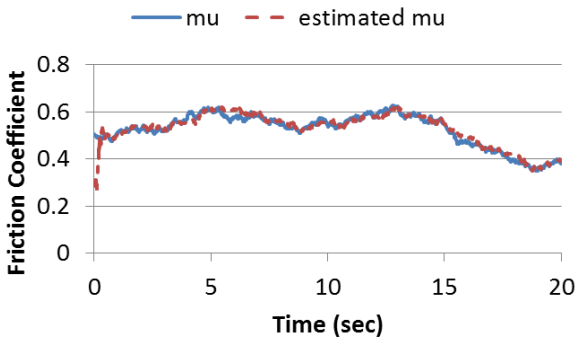

Figure 10.27 Estimation of friction coefficient

Estimation of Friction coefficient and Side-slip angle by R- adaptive UKF:

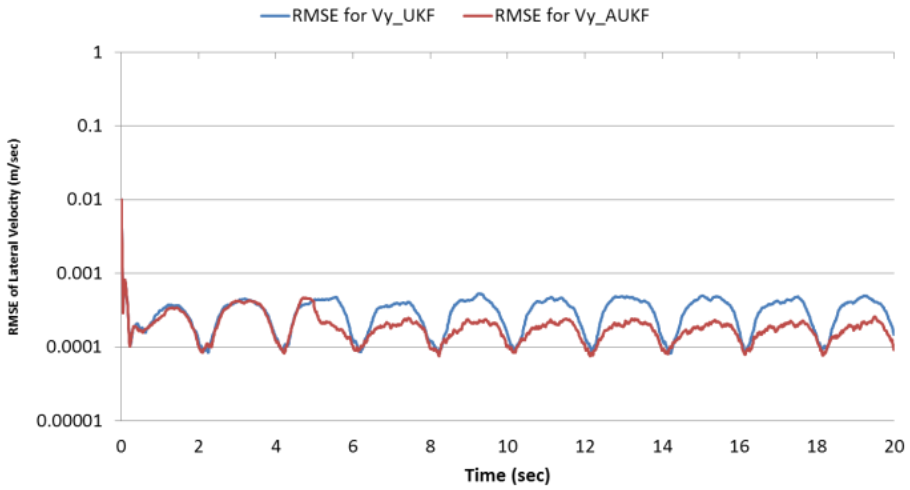

Figure 10.28 RMSE for lateral velocity $R_{filter}(0) = 100 \times R$

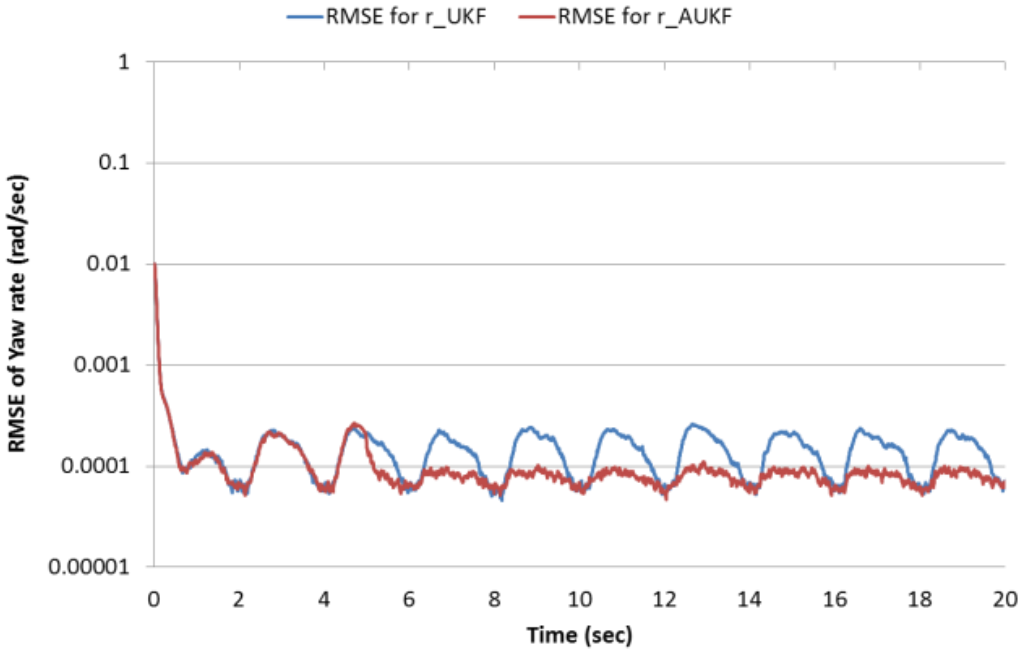

Figure 10.29 RMSE for Yaw rate $R_{filter}(0) = 100 \times R$

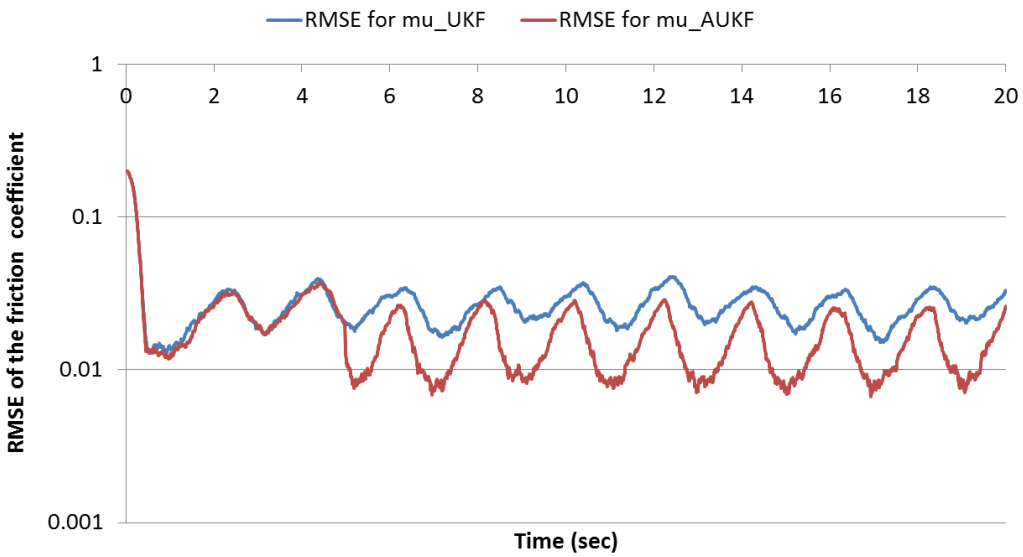

Figure 10.30 RMSE for the friction coefficient $R_{filter}(0) = 100 \times R$

10.3.3 Conclusion

Road-tire friction coefficient and side-lip are estimated by Unscented Kalman Filter. An adaptive scheme has been employed with the UKF and results are simulated with different test cases. The performance of the R-adaptive UKF based scheme is better than the non-adaptive cases.

11 Addendum

11.1 Introduction to the addendum

Based on the reviewers' comments and suggestions some results are provided in this chapter. Important observations and comments based on the result are also provided.

11.1.1 Objective of the addendum

Objective of this addendum is to provide some important results which were not included in the previous chapters. The results are obtained based on the reviewers' comments and suggestions. Some key observations from the result obtained by the estimators for different sampling intervals and initial conditions are noted.

11.1.2 Organization of the addendum

Next Section provides the plots of the width of boundary layer simulated from the actual data for a tracking scenario. Section 11.3 presents evaluation of adaptive filters for a faster sampling rate. Behaviour of EKF for trajectory tracking scenario with faster sampling rate is given in 11.4. Evaluation of Sigma Point Smooth Variable Structure Filter for a tracking scenario is provided in the section 11.5. Performance of ASVSF for different initial conditions is evaluated in 11.6. In the section 11.7 effect of sampling rate on ASVSF is presented. The last section provides the algorithms of UKF, DDF and GHF.

11.2 Boundary Layer and existence subspace for Smooth Variable Structure Filter (Response to comment 1)

In chapter 5 and chapter 6 the concept of SVSF has been discussed. The existence subspace with the boundary layer has been demonstrated in this section with the actual data for a specific case (UM model, Trajectory-I, with the same parameters as given in 3.3.4.1). For the following figure, the existing SVSF simulation program was run for a typical noise sequence. X-position of the filter has been set at 20000m initially.

The figure for existence subspace are shown by (Gadsden, 2014) to illustrate the conceptual relationship between the true value of the state variable, typical estimate of that variable and a conceptual boundary where the estimate error is bounded in long term. As the basis for drawing the so-named existence boundary in the referred publication is not provided. We can provide only an equivalent representation which shows the convergence of both estimation error and the boundary layer for one particular variable.

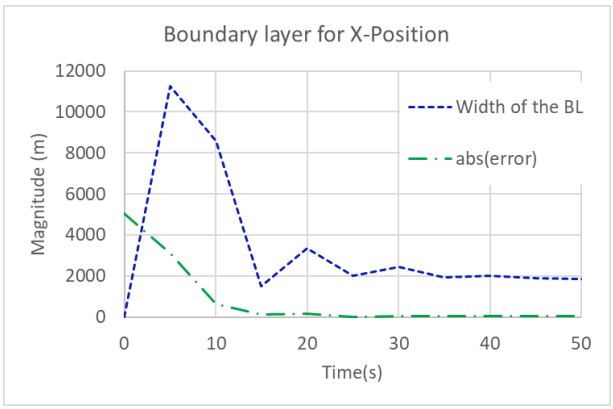

Figure 11.1 Boundary Layer and Error

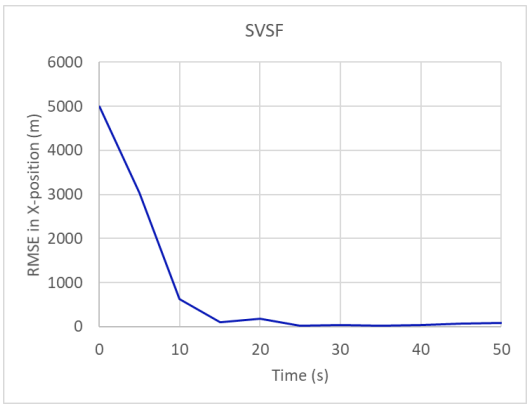

Figure 11.2 RMSE in x-position

In Fig (11.1) for a single instance the convergence of the width of the boundary layer, absolute value of error. In Fig (11.2) and Fig (11.3) we show the nature of the RMS Error vs time for SVSF and ASVSF respectively. However, such plot can be misleading as such errors may vary in a multi-segment trajectory which has both UM and CT segments. For this reason, only first segment is provided. It

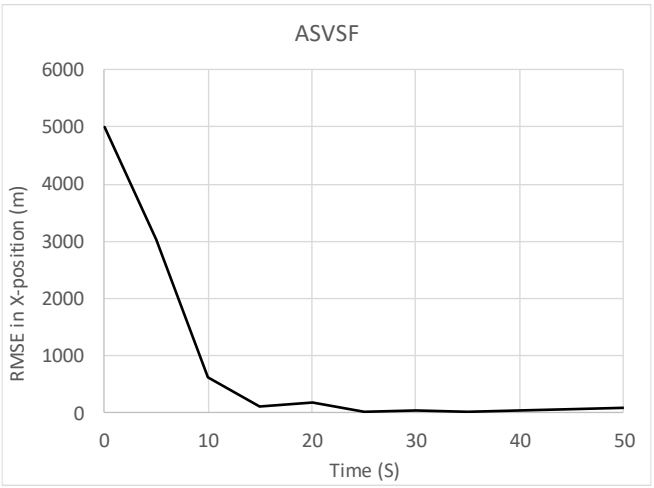

Figure 11.3 RMSE in X-position for ASVSF

should be pointed out that the results pertain to SVSF algorithm which is developed of previous worker.

11.3 Results of adaptive filters with faster sampling rate for Trajectory-I

(Response to comment 8)

Results for UM and CT model using adaptive filters for Trajectory-I are provided here. Simulation parameters are set as given in Section 4.4.1 except the sampling interval. Results are given in table 11.1 and 11.2. It is to be noted that in the section 4.4.2, the adaptive filters were already evaluated for Trajectory-II with 1s sampling rate. For completeness results for the Trajectory-I are given here.

Table 11.1 Simulation of UM Model using 1s Sampling interval

Trajectory I UM model	KF $Q_0 = 0.01 \times Q_{UM}$ COMPOSITE (X, Y)	AKF $Q_0 = 0.01 \times Q_{UM}$ COMPOSITE (X, Y)
Position error (m)	938.87 (649.425, 647.71)	38.23 (26.78, 26.88)
Velocity error (m/sec)	40.29 (27.70, 27.45)	5.15 (3.48, 3.61)

Table 11.2 Simulation of CT Model using 1s Sampling interval

Trajectory I CT model	EKF $Q_0 = 0.01 \times Q_{UM}$		ADDF $Q_0 = 0.01 \times Q_{CT}$		AGHF $Q_0 = 0.01 \times Q_{CT}$	
	Average (Composite)	Peak (X,Y)	Average (Composite)	Peak (X,Y)	Average (Composite)	Peak (X,Y)
Position error (m)	43.05	(100.05 , 146.92)	42.28	(235.99, 108.23)	37.48	(30.85, 29.50)
Velocity error (m/sec)	4.75	(30.42,40.66)	14.40	(69.75, 80.57)	14.93	(10.83, 10.47)

Observations: Faster sampling implies faster measurement updates to the estimators. With 1s sampling interval both non-adaptive (KF and EKF) and adaptive state estimators (AKF, ADDF and AGHF) improve their performance as compared to the 5s sampling rate. However, the result of adaptive filters can further be improved by choosing proper window size.

11.4 Performance of EKF with CT model for faster sampling rate (Response to comment 9)

Section 4.4.3 presents the analysis of the performance of adaptive filters for Trajectory-II. It was seen in Fig 4.8 that EKF have failed to track the aircraft trajectory after it takes the second U-turn. However, the Adaptive filters could effectively perform for the same scenario. In this section performance of the EKF is observed for a sampling rate faster than 1s.

Fig 11.4 shows the estimate of position for 0.1s sampling interval. Table 11.3 provides results for two different sampling intervals (0.1s and 0.01s).

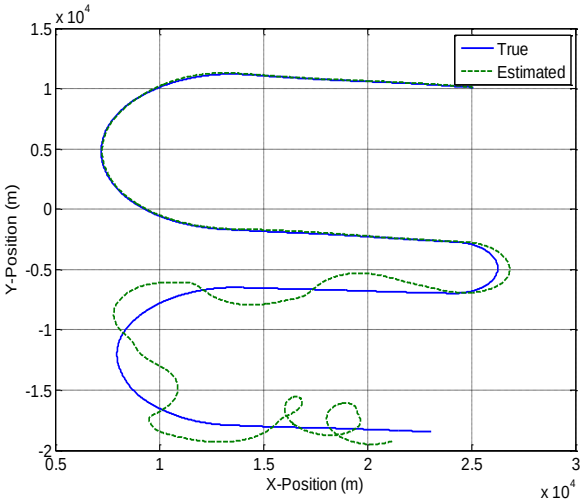

Figure 11.4 Estimation of position by EKF with CT model using T=0.1s

Table 11.3 Simulation of CT Model with 0.1s and 0.01s Sampling interval for EKF

Trajectory II	EKF $T = 0.1s$		EKF $T = 0.01s$	
CT Model	Average Composite (X,Y)	Peak Composite (X,Y)	Average Composite (X,Y)	Peak Composite (X,Y)
Position error (m)	676.69 (470.39, 452.53)	2492.8 (2260.6,1507.6)	105.84 (67.44,77.37)	345.44 (296.25, 330.92)
Velocity error (m/sec)	85.73 (55.53, 60.20)	605.9 (475.2, 442.3)	7.50 (3.51,3.51)	52.66 (36.07, 52.28)

Observation: Though it shows a poor tracking performance for a maneuver with high turn rate with faster sampling rate it improves the performance.

11.5 Evaluation of Sigma Point Smooth Variable Structure Filter (SPSVSF) in tracking scenario (Response to comment 13)

In chapter 5, SPSVSF was evaluated by a test case as given in section 5.6. Here the same algorithm is evaluated for the tracking scenario as discussed for Trajectory-I. Sampling interval is taken as 1s. Fig. 11.5 shows the RMSE plot for SPSVSF. For completeness, results obtained by SVSF with 1s sampling interval are also provided for comparative study (Table 11.4).

Table 11.4 Simulation of UM Model using 1s Sampling interval for SPSVSF

Trajectory I UM Model	SPSVSF		SVSF	
	Average Composite (X,Y)	Peak Composite (X,Y)	Average Composite (X,Y)	Peak Composite (X,Y)
Position error (m)	53.24 (35.29, 36.16)	160.25 (146.63,84.98)	64.08 (41.86,43.27)	210.51 (182.68, 115.59)
Velocity error (m/sec)	14.27 (9.58, 9.82)	78.78 (56.22, 63.59)	17.78 (11.97,12.28)	89.38 (62.64, 69.76)

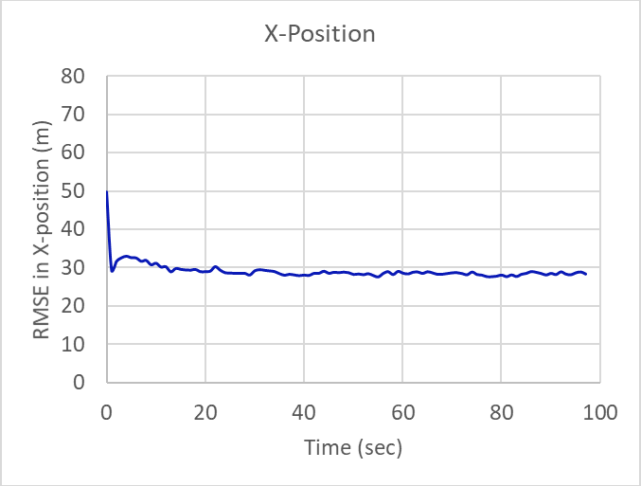

Figure 11.5 RMS E plot of X-position for SPSVSF

11.6 Evaluation of ASVSF with different values of initial process noise (Response to comment 15)

Adaptive Smooth Variable Structure Filter (ASVSF) is presented in chapter 6. Performance was evaluated for only $Q_{f|k=0} = 0.01 \times Q_{UM}$. In this section ASVSF is evaluated with different initial values of

Table.11.5 Initial Process Noise Covariance of ASVSF

Process Noise Covariance	States	ASVSF (Composite)
$Q_{f\|k=0} = Q_{UM}$	Position (m)	51.99
	Velocity (m/s)	12.92
$\cdot Q_{f\|k=0} = 0.01 \times Q_{UM}$	Position (m)	51.94
	Velocity (m/s)	13.03
$Q_{f\|k=0} = 10 \times Q_{UM}$	Position (m)	52.11
	Velocity (m/s)	12.91
$Q_{f\|k=0} = 100 \times Q_{UM}$	Position (m)	52.30
	Velocity (m/s)	13.24

process noise covariance. Table 11.5 shows the performance (time average RMSE) of ASVSF for four such cases.

Note: As expected the RMSE values does not change with the different Q levels. An Adaptive estimator is expected to estimate the state variables when the value of Q is unknown or is wrongly guessed. Hence, it is demonstrated that ASVSF performance remains insensitive to the initial guess value of Q over a wide range.

11.7 Effect of sampling rates for ASVSF (Response to comment 16)

Chapter 6 provides the evaluation of ASVSF for aircraft tracking scenario using 5s sampling interval. Here the effect of faster sampling rates has been studied. Same Trajectory (Trajectory-I) was taken as given in Chapter 6. Other simulation parameters are kept unchanged.

Table.11.6 Effect of sampling interval ASVSF

Trajectory-I $Q_{f\|k=0} = Q_{UM}$	ASVSF $T = 1s$		ASVSF $T = 0.1s$	
	Average Composite (X,Y)	Peak Composite (X,Y)	Average Composite (X,Y)	Peak Composite (X,Y)
Position error (m)	40.60 (28.86, 28.70)	70.78 (50.05,50.05)	42.17 (29.80,29.82)	80.78 (55.56, 58.71)
Velocity error (m/sec)	16.06 (11.31, 11.42)	35.80 (25.04, 25.59)	287.31 (203.03,202.92)	402.32 (278.53, 290.31)

Table 11.6 provides results for two different cases (T=1s and T=0.1s).

Note: It is interesting to note that the performance of ASVSF does not improve with the faster sampling rate. Rather, velocity estimation got worsen for the case of 0.1s sampling interval. This is because of the additional unmodelled noise coming from the generation of synthetic measurement for velocity terms.

11.8 Algorithm of UKF, DDF and GHF (Response to comment 4)

11.8.1 Unscented Kalman filter

A brief algorithm is described below. For details see (Wan & Van Der Merwe, 2000)

i. The set of sigma points χ are created by applying a sigma point selection algorithm

$$\chi_{k-1} = \left\{ \hat{x}_{k-1} \quad \hat{x}_{k-1} + \eta\sqrt{P_{k-1}} \quad \hat{x}_{k-1} - \eta\sqrt{P_{k-1}} \right\}$$

ii. The transformed set is given by instantiating each point through the process model

$$\chi_{i,k}^{-} = f\left(\chi_{k-1}, u_{k-1}\right)$$

iii. The predicted mean is computed as

$$\hat{x}_{i,k}^{-} = \sum_{i=0}^{2L} W_i^{(m)} \chi_{i,k}^{-}$$

iv. And the predicted covariance is computed as

$$P_k^{-} = \sum_{i=0}^{2L} W_i^{(m)} \left(\chi_{i,k}^{-} - \hat{x}_k^{-}\right)\left(\chi_{i,k}^{-} - \hat{x}_k^{-}\right)^T + Q_k$$

v. Instantiate each of the prediction points through the observation model

$$y_{i,k}^{-} = h\left(\chi_{i,k}^{-}\right)$$

vi. The predicted observation is calculated by

$$\hat{\mathrm{y}}_{\mathrm{k}}^{-} = \sum_{i=0}^{2L} W_i^{(m)} y_{i,k}^{-}$$

vii. The innovation covariance is

$$P_{\hat{y}_k \hat{y}_k} = \sum_{i=0}^{2L} W_i^{(m)} \left(y_{i,k}^{-} - \hat{\mathrm{y}}_{\mathrm{k}}^{-}\right)\left(y_{i,k}^{-} - \hat{\mathrm{y}}_{\mathrm{k}}^{-}\right)^T + R_k$$

viii. The cross-correlation matrix is determined by

$$P_{x_k y_k} = \sum_{i=0}^{2L} W_i^{(m)} \left(\chi_{i,k}^{-} - \hat{x}_k^{-}\right)\left(y_{i,k}^{-} - \hat{\mathrm{y}}_{\mathrm{k}}^{-}\right)$$

ix. Finally, the update can be performed using the normal Kalman filter equations:

$$\kappa_k = P_{x_k y_k} P_{\hat{y}_k \hat{y}_k}^{-1}$$
$$\hat{x}_k = \hat{x}_k^{-} + \kappa_k \left(y_k - \hat{\mathrm{y}}_{\mathrm{k}}^{-}\right)$$
$$P_k = P_k^{-} - \kappa_k P_{\hat{y}_k \hat{y}_k} \kappa_k^T$$

11.8.2 Divided Difference Filter

Divided difference Filter (DDF) (NøRgaard, Niels K, & Ravn, 2000) is another option for nonlinear filtering.

The brief algorithm of second order Divided Difference Filter is given as follow (Notations are in the standard form)

i. Initialization: $\hat{x}_0, P_0$

ii. Computation of Cholesky factor $\hat{P}_k = \hat{S}_x(k-1)\hat{S}_x^T(k-1)$

iii. State propagation $\bar{x}_k = \frac{h^2-n}{h^2} f(\hat{x}_{k-1}) + \frac{1}{2h^2}\sum_{p=1}^{n}\left\{f(\hat{x}_{k-1}+h\hat{s}_{x,p}) + f(\hat{x}_{k-1}-h\hat{s}_{x,p})\right\}$

iv. Propagation of predicted error covariance

$$\bar{P}_k = S_{x\hat{x}}^{(1)}(k)\left(S_{x\hat{x}}^{(1)}(k)\right)^T + S_{x\hat{x}}^{(2)}(k)\left(S_{x\hat{x}}^{(2)}(k)\right)^T + Q_k$$

$$S_{x\hat{x}}^{(1)}(k)_{(i,j)} = \frac{1}{2h}\left(f_i\left(\hat{x}_{k-1}+h\hat{s}_{x,j}\right) - f_i\left(\hat{x}_{k-1}-h\hat{s}_{x,j}\right)\right)$$

$$S_{x\hat{x}}^{(2)}(k)_{(i,j)} = \frac{\sqrt{h^2-1}}{2h}\left(f_i\left(\hat{x}_{k-1}+h\hat{s}_{x,j}\right) + f_i\left(\hat{x}_{k-1}-h\hat{s}_{x,p}\right) - 2f_i(\hat{x}_{k-1})\right)$$

v. Measurement update

$$\bar{y}_k = \frac{h^2-n}{h^2} g(\bar{x}_k) + \frac{1}{2h^2}\sum_{p=1}^{n}\left\{g(\bar{x}_{k-1}+h\bar{s}_{x,p}) + g(\bar{x}_{k-1}-h\bar{s}_{x,p}\right\}$$

vi. Propagation of innovation covariance

$$P_k^y = S_{y\bar{x}}^{(1)}(k)\left(S_{y\bar{x}}^{(1)}(k)\right)^T + S_{y\bar{x}}^{(2)}(k)\left(S_{y\bar{x}}^{(2)}(k)\right)^T + R$$

$$S_{y\bar{x}}^{(1)}{}_{(i,j)} = \frac{1}{2h}\left(g_i\left(\bar{x}_k+h\bar{s}_{x,j}\right) - g_i\left(\bar{x}_k-h\bar{s}_{x,j}\right)\right)$$

$$S_{x\hat{x}}^{(2)}(k)_{(i,j)} = \frac{\sqrt{h^2-1}}{2h}\left(g_i\left(\bar{x}_k+h\bar{s}_{x,j}\right) + g_i\left(\bar{x}_k-h\bar{s}_{x,j}\right) - 2g_i(\bar{x}_k)\right)$$

vii. Cross-covariance

$$P_k^{xy} = \left[\bar{S}_x(k)\right]\left[S_{y\bar{x}}^{(1)}(k)\right]^T$$

viii. Gain $K_k = P_k^{xy}(P_k^y)^{-1}$

ix. State Update

$$\hat{x}_k = \bar{x}_k + K_k(y_k - \bar{y}_k)$$

$$\hat{P}_k = S_y(k)S_y^T(k) + K_k R K_k^T$$

11.8.3 Gauss Hermite Filter

Gauss Hermite Filter (Ito & Xiong, 2000) (Arasaratnam, Haykin, & J. Elliott, 2007) also belongs to the sigma point filtering class. A brief algorithm for Gauss Hermite filter is given below:

i. Computation of : $\hat{x}_0, P_0$

ii. Computation of Quadrature points and weights:

A symmetric tri-diagonal, defined as $J_{i,j} = 0$ and $J_{i,j+1} = \sqrt{\frac{i}{2}}$ for $1 \le i \le N-1$ for ' N 'quadrature points. Quadrature points are chosen as $q_i = \sqrt{2x_i}$ where x_i are the Eigen values of J .

Corresponding weights (w_i) of q_i is computed as $\left|(v_i)_1\right|^2$ where $(v_i)_1$ is the first element of i^{th} normalized eigenvector of J .

iii. Gauss Hermite Quadrature rule:

$$I_N = \int_{R^n} \tilde{F}(s) \frac{1}{(2\pi)^{\frac{n}{2}}} e^{-(1/2)|s|^2} ds$$

Can be expressed as

$$I_N = \sum_{i_1=1}^{N} \ldots \sum_{i_n=1}^{N} \tilde{F}\left(q_{i_1}, q_{i_2}, \ldots, q_{i_n}\right) w_{i_1} w_{i_2} \ldots w_{i_n}$$

In order to evaluate I_N for n^{th} order system, N^n number of quadrature points and weights are required.

iv. State propagation $\bar{x}_k = \frac{h^2 - n}{h^2} f(\hat{x}_{k-1}) + \frac{1}{2h^2} \sum_{p=1}^{n} \left\{ f(\hat{x}_{k-1} + h\hat{s}_{x,p}) + f(\hat{x}_{k-1} - h\hat{s}_{x,p}) \right\}$

v. Time update stage:

Cholesky Factor is computed as

$$S_x^+(k-1) = Cholesky\left(P_{k-1}^+\right)$$

Modify the quadrature points as

$$\chi_i^+ = S_x^+(k-1) q_i + \hat{x}_{k-1}$$

$$\bar{x}_k = \sum_{i=1}^{N} f\left(\chi_i^+\right) w_i$$

$$P_k^- = Q_{k-1} + \sum_{i=1}^{N} \left(f\left(\chi_i^+\right) - \bar{x}_k\right)\left(f\left(\chi_i^+\right) - \bar{x}_k\right)^T w_i$$

$\bar{x}_k$ is a priori estimate and P_k^- is a priori error covariance.

vi. Measurement update stage:

Cholesky Factor is computed as

$$S_x^-(k) = Cholesky\left(P_k^-\right)$$

Select sigma points as

$$\chi_i^- = S_x^-(k) q_i + \bar{x}_k$$

A priori estimate of measurement becomes

$$z_k = \sum_{i=1}^{N} g\left(\chi_i^-\right) w_i$$

The following covariance can be computed as

$$P_k^{xz} = \sum_{i=1}^{N} \left(g\left(\chi_i^-\right) - x_k\right)\left(g\left(\chi_i^-\right) - x_k\right)^T w_i$$

$$P_k^{zz} = \sum_{i=1}^{N} \left(g\left(\chi_i^-\right) - z_k\right)\left(g\left(\chi_i^-\right) - z_k\right)^T w_i$$

Filter Gain:

$$K_k = P_k^{xy}(P_k^{zz} + R)^{-1}$$

Covariance and Estimate Update

$$\hat{x}_k = \bar{x}_k + K_k(y_k - z_k)$$

$$P_k^+ = P_k^- - K_k\left(P_k^{zz} + R\right)K_k^T$$

Bibliography

Aalto, A. (2016). Convergence of discrete-time Kalman filter estimate to continuous time estimate. *International Journal of Control, 89*(4), 668-679.

Afshari, H. H. (2014). *The 2nd-Order Smooth Variable Structure Filter (2nd-SVSF) for State Estimation: Theory and Applications.* PhD Thesis, McMaster University.

Afshari, H. H., Dhafar, A.-A., & Saeid, H. (2015). Robustness comparison of some state estimation methods with an explicit consideration of modeling uncertainties. *2015 IEEE 28th Canadian Conference on Electrical and Computer Engineering (CCECE)*, (pp. 925-931).

Ahmadi, M., Khayatian, A., & Karimaghaee, P. (2012). Attitude estimation by divided difference filter in quaternion space. *Acta Astronautica, 75*, 95-107.

Ahn, C., Peng, H., & Tseng, H. E. (2013). Robust Estimation of Road Frictional Coefficient. *IEEE Transactions on Control Systems Technology, 21*(1), 1-13.

Åkesson, B. M., Jørgensen, J. B., Poulsen, N. K., & Jørgensen, S. B. (2007). A tool for kalman filter tuning. *In Computer Aided Chemical Engineering*, 859-864.

Al -Shabi, M., & Habibi, S. (2010). Iterative Smooth Variable Structure Filter for Parameter Estimation. *ISRN Signal Processing*.

Almagbile, A., Jinling, W., & Weidong, D. (2010). Evaluating the performances of adaptive Kalman filter methods in GPS/INS integration. *Journal of Global Positioning Systems, 9*(1), 33-40.

Al-Shabi, M. (2017). Sigma-point Smooth Variable Structure Filters applications into robotic arm. *2017 7th International Conference on Modeling, Simulation, and Applied Optimization (ICMSAO)*, (pp. 1-6).

Al-Shabi, M., & Hatamleh, K. (2014). The Unscented Smooth Variable Structure Filter Application into a Robotic Arm. *ASME 2014 International Mechanical Engineering Congress and Exposition.* Canada: American Society of Mechanical Engineers.

Al-Shabi, M., Gadsden, S. A., & Habibi, S. R. (2013). Kalman filtering strategies utilizing the chattering effects of the smooth variable structure filter. *Signal Processing, 93*(2), 420-431.

Al-Shabi, M., Gadsden, S. A., & S. A, W. (2015). The cubature smooth variable structure filter estimation strategy applied to a quadrotor controller. *SPIE Defense+ Security. International Society for Optics and Photonics*, 94741I-94741I.

Alspach, D. H. (1972). Nonlinear Bayesian estimation using Gaussian sum approximations. *IEEE transactions on automatic control, 17*(4), 439-448.

Amodeo, M., Antonella, F., Riccardo, T., & Claudio, V. (2010). Wheel slip control via second-order sliding-mode generation. *IEEE Transactions on Intelligent Transportation Systems, 11*(1), 122-131.

Ananthasayanam, M. (2011). Kalman filter design by tuning its statistics or gains? *Int. Conf. of Data Assimilation*, (pp. 1–102).

Anderson, B. D., & Moore, J. B. (1979). *Optimal Filtering.* NY: Prentice Hall.

Angelova, D., Simeonova, I., & Semerdjiev, T. (2003). Monte Carlo algorithm for ballistic object tracking with uncertain drag parameter. *International conference on large-scale scientific computing* (pp. 112-120). Berlin: Springer.

Antonov, S., Fehn, A., & Kugi, A. (2011). Unscented Kalman filter for vehicle state estimation. *Vehicle System Dynamics, 49*(9), 1497-1520.

Anwar, S. (2006). Anti-lock braking control of a hybrid brake-by-wire system. *Institution of Mechanical Engineers, Part D: Journal of Automobile Engineering, 220*(8), 1101-1117.

Arasaratnam, I., & Haykin, S. (2009). Cubature kalman filters. *IEEE Transactions on automatic control, 54*(6), 1254-1269.

Arasaratnam, I., Haykin, S., & Elliott, R. J. (2007). Discrete-time nonlinear filtering algorithms using Gauss–Hermite quadrature. *Proceedings of the IEEE, 95*(5), 953-977.

Attari, M., Gadsden, S. A., & Habibi, S. R. (2013). Target Tracking Formulation of the SVSF as a Probabilistic Data Association Algorithm. *American Control Conference (ACC)*, (pp. 6328-6332). Washington, DC.

Auger, F., Hilairet, M., Guerrero, J. M., Monmasson, E., Orlowska-Kowalska, T., & Katsura, S. (2013). Industrial applications of the Kalman filter: A review. *IEEE Transactions on Industrial Electronics, 60*(12), 5458-5471.

B., R., Farina, A., Benvenuti, D., & Arulampalam, M. S. (2003). Performance bounds and comparison of nonlinear filters for tracking a ballistic object on re-entry. *IEE Proceedings-Radar, Sonar and Navigation, 150*(2), 65-70.

Baffet, G., Charara, A., & Lechner, D. (2007). Experimental evaluation of a sliding mode observer for tire-road forces and an extended Kalman filter for vehicle sideslip angle. *IEEE Conference on Decision and Control* (pp. 3877-3882). IEEE.

Baffet, G., Charara, A., & Lechner, D. (2009). Estimation of vehicle sideslip, tire force and wheel cornering stiffness. *Control Engineering Practice, 17*(11), 1255-1264.

Bar-Shalom, Y., Chang, K. C., & Blom, H. A. (1989). Tracking a maneuvering target using input estimation versus the interacting multiple model algorithm. *IEEE Transactions on Aerospace and Electronic Systems, 25*(2), 296-300.

Bar-Shalom, Y., Rong Li, X., & Kirubarajan, T. (2001). *Estimation with applications to tracking and navigation: theory algorithms and software.* John Wiley & Sons.

Bar-Shalom, Yaakov, X. L., & Kirubarajan, T. (2001). *Adaptive Estimation and Maneuvering Targets: Estimation with Applications to Tracking and Navigation: Theory, Algorithms and Software.*

Bhaumik, S. (2013). Cubature quadrature Kalman filter. *IET Signal Processing, 7*(7), 533-541.

Bishop, R. H. (2000). Validation and comparison of coordinated turn aircraft maneuver models. *IEEE Transactions on Aerospace and Electronic Systems, 36*(1), 250-259.

Bisht, S. S., & Singh, M. P. (2014). An adaptive unscented Kalman filter for tracking sudden stiffness changes. *Mechanical Systems and Signal Processing, 49*(1-2), 181-195.

Blom, H. A., & Bar-Shalom, Y. (1988). The interacting multiple model algorithm for systems with Markovian switching coefficients. *IEEE transactions on Automatic Control, 33*(8), 780-783.

Brookner, E. (1998). *Tracking and Kalman filtering made easy.* New York: Wiley.

Brown, R. G., & Hwang, P. Y. (1992). *Introduction to random signals and applied Kalman filtering* (Vol. 3). New York: Wiley.

Cao, E., & Kai, J. (2016). Adaptive unscented Kalman filter for input estimations in Diesel-engine selective catalytic reduction systems. *Neurocomputing, 205*, 329-335.

Chatterjee, S., Sadhu, S., & Ghoshal, T. K. (2015). Fault detection and identification of non-linear hybrid system using self-switched sigma point filter bank. *IET Control Theory & Applications, 9*(7), 1093-1102.

Crouse, D. (2015). Basic tracking using nonlinear continuous-time dynamic models [Tutorial]. *IEEE Aerospace and Electronic Systems Magazine, 30*(2), 4-41.

Dakhlallah, J., Glaser, S., Mammar, S., & Sebsadji, Y. (2008). Tire-road forces estimation using extended Kalman filter and sideslip angle evaluation. *American Control Conference* (pp. 4597-4602). IEEE.

Das, M., Dey, A., Sadhu, S., & Ghoshal, T. K. (2015). Adaptive central difference filter for non-linear state estimation. *ET Science, Measurement & Technology, 9*(6), 728-733.

Das, M., Sadhu, S., & Ghoshal, T. K. (2013). An adaptive sigma point filter for nonlinear filtering problems. *International Journal of Electrical, Electronics and Computer Engineering, 2*(2), 13-19.

De Wit, C. C., Olsson, H., Johan Astrom, K., & Lischinsky, P. (1995). A new model for control of systems with friction. *IEEE Transactions on automatic control, 40*(3), 419-425.

Dey, A., Das, M., Sadhu, S., & Ghoshal, T. K. (2015). Adaptive divided difference filter for parameter and state estimation of non-linear systems. *IET Signal Processing, 9*(4), 369-376.

Dey, A., Das, M., Sadhu, S., & Ghoshal, T. K. (2015). Adaptive unscented information filter for multiple sensor fusion. *Michael Faraday IET International Summit 2015*, (p. 94).

Dey, A., Sadhu, S., & Ghoshal, T. K. (2013). Joint estimation of parameters and states of nonlinear systems using adaptive divided difference filter. *Int. J. Electr. Electron. Comput. Eng, 2*(2), 7-12.

Dey, A., Sadhu, S., & Ghoshal, T. K. (2014). Adaptive divided difference filter for nonlinear systems with unknown noise. *Control, Instrumentation, Energy and Communication (CIEC)* (pp. 573-577). IEEE.

Dey, A., Sadhu, S., & Ghoshal, T. K. (2014). Adaptive Gauss Hermite filter for parameter varying nonlinear systems. *International Conference on Signal Processing and Communications (SPCOM)* (pp. 1-5). IEEE.

Dey, A., Sadhu, S., & Ghoshal., T. K. (2013). Joint estimation of parameters and states of nonlinear systems using adaptive divided difference filter. *Int. J. Electr. Electron. Comput. Eng,, 2*(2), 7-12.

Ding, W., Jinling, W., Chris, R., & Doug, K. (2007). Improving adaptive Kalman estimation in GPS/INS integration. *The Journal of Navigation, 60*(3), 517-529.

Doumiati, M., Victorino, A., Charara, A., & Lechner, D. (2010). A method to estimate the lateral tire force and the sideslip angle of a vehicle: Experimental validation. *American Control Conference (ACC)* (pp. 6936-6942). IEEE.

Dróżdż, K., & Szabat, K. (2016). Application of Unscented Kalman Filter in adaptive control structure of two-mass system. *IEEE International Conference on Power Electronics and Motion Control Conference (PEMC)*, (pp. 1150-1154).

Dugoff, H. (1969). *Tire performance characteristics affecting vehicle response to steering and braking control inputs.* Final report.

Edwards, C., & Sarah, S. (1998). *Sliding mode control: theory and applications.* CRC Press.

Efe, M., & Atherton, D. P. (1998). Maneuvering target tracking with an adaptive Kalman filter. *37th IEEE Conference on Decision and Control. 1*. IEEE.

Farina, A., Benvenuti, D., & Ristic, B. (2002). Estimation accuracy of a landing point of a ballistic target. *Fifth International Conference on Information Fusion* (pp. 2-9). IEEE.

Farina, A., Ristic, B., & Benvenuti, D. (2002). Tracking a ballistic target: comparison of several nonlinear filters. *IEEE Transactions on aerospace and electronic systems*, 854-867.

Felter, S. C. (1990). An overview of decentralized Kalman filter techniques. *In Southern Tier Technical Conference*, (pp. 79-87).

Floquet, T., Edwards, C., & Spurgeon, S. K. (2007). On sliding mode observers for systems with unknown inputs. *International Journal of Adaptive Control and Signal Processing, 21*(8-9), 638-656.

Gadola, M. D., Chindamo, M. R., & Fabrizio, P. (2014). Development and validation of a Kalman filter-based model for vehicle slip angle estimation. *Vehicle System Dynamics, 52*(1), 68-84.

Gadsden, A., Habibi, S. R., & Kirubarajan, T. (2012). The Smooth Particle Variable Structure Filter. *Transactions of the Canadian Society for Mechanical Engineering, 36*(2), 177-194.

Gadsden, S. A. (2011). *Smooth variable structure filtering: theory and applications.* PhD Thesis.

Gadsden, S. A., & Habibi, S. (2009). Target tracking using the smooth variable structure filter. *ASME dynamic systems and control conference (DSCC)*, (pp. 1-7).

Gadsden, S. A., & Habibi, S. R. (2010). A new form of the smooth variable structure filter with a covariance derivation. *49th IEEE Conference on Decision and Control (CDC) IEEE*, (pp. 7389-7394).

Gadsden, S. A., & Hamed, H. A. (2015). A Review of Smooth Variable Structure Filters: Recent Advances in Theory and Applications. *ASME 2015 International Mechanical Engineering Congress and Exposition* (pp. 1-8). American Society of Mechanical Engineers.

Gadsden, S. A., & Lee, A. S. (2017). Advances of the smooth variable structure filter: square-root and two-pass formulations. *Journal of Applied Remote Sensing* .

Gadsden, S. A., El Sayed, M., & Habibi, S. R. (2011). The continuous-time smooth variable structure filter. *23rd Canadian Congress of Applied Mechanics (CANCAM).* Vancouver, British Columbia.

Gadsden, S. A., Habibi, S. R., & Kirubarajan, T. (2010). A novel interacting multiple model method for nonlinear target tracking. *2010 13th Conference on Information Fusion (FUSION)* (pp. 1-8). IEEE.

Gadsden, S. A., Habibi, S., & Kirubarajan, T. (2014). Kalman and smooth variable structure filters for robust estimation. *IEEE Transactions on Aerospace and Electronic Systems, 50*(2), 1038-1050.

Gadsden, S. A., M, A.-S., Ienkaran, A., & Saeid R., H. (2014). Combined cubature Kalman and smooth variable structure. *Signal Processing*, 290-299.

Gadsden, S. A., Mohammed, S., & Habibi, S. R. (2011). Derivation of an optimal boundary layer width for the smooth variable structure filter. *Proceedings of the 2011 American Control Conference. IEEE*, (pp. 4922-4927).

Gadsden, S., Al-Shabi, M., Arasaratnam, I., & Habibi, S. (2014). Combined cubature Kalman and smooth variable structure filtering: A robust nonlinear estimation strategy. *Signal Processing*, 290-299.

Gandhi, M. A., & Mili, L. (2010). Robust Kalman filter based on a generalized maximum-likelihood-type estimator. *IEEE Transactions on Signal Processing, 58*(5), 2509-2520.

Gao, B., Gao, S., Zhong, Y., Hu, G., & Gu, C. (2017). Interacting multiple model estimation-based adaptive robust unscented Kalman filter. *International Journal of Control, Automation and Systems, 15*(5), 2013-2025.

Ghosh, S., & Mukhopadhyay, S. (2011). Tracking reentry ballistic targets using acceleration and jerk models. *IEEE Transactions on Aerospace and Electronic Systems, 47*(1), 666-683.

Grewal, M. S. (2011). *Kalman filtering.* Springer Berlin Heidelberg.

Habibi, S. (2006). The Extended Variable Structure Filter. *Journal of Dynamic Systems, Measurement, and Control, 128*(2), 341-351.

Habibi, S. (2007). The Smooth Variable Structure Filter. *Proceedings of IEEE, 95*(5), 1026-1059.

Habibi, S. (2008). Parameter estimation using a combined variable structure and kalman filtering approach. *Journal of Dynamic Systems, Measurement, and Control, 130*(5).

Habibi, S. R., & Burton, R. (2002). The variable structure filter. *ASME International Mechanical Engineering Congress and Exposition*, 157-165.

Habibi, S. R., & Burton, R. (2007). Parameter identification for a high-performance hydrostatic actuation system using the variable structure filter concept. *Journal of Dynamic Systems, Measurement, and Control, 129*(2), 229-235.

Habibi, S., Burton, R., & Chinniah, Y. (2002). Estimation Using a New Variable Structure Filter. *The American Control Conference*, (pp. 2937-2942). Anchorage.

Hagh, Y. S., Asl, R. M., & Cocquempot, V. (2017). A hybrid robust fault tolerant control based on adaptive joint unscented kalman filter. *ISA transactions, 66*, 262-274.

Hajiyev, C., & Soken, H. E. (2014). Robust adaptive unscented Kalman filter for attitude estimation of pico satellites. *International Journal of Adaptive Control and Signal Processing, 28*(2), 107-120.

Han, J., Kim, D., & Sunwoo, M. (2009). State-of-charge estimation of lead-acid batteries using an adaptive extended Kalman filter. *Journal of Power Sources, 188*(2), 606-612.

Han, J., Song, Q., & and He, Y. (2009). Adaptive unscented Kalman filter and its applications in nonlinear control. *INTECH Open Access Publisher*.

He, H., Xiong, R., Zhang, X., Sun, F., & Fan, J. (2011). State-of-charge estimation of the lithium-ion battery using an adaptive extended Kalman filter based on an improved Thevenin model. *EEE Transactions on Vehicular Technology, 60*(4), 1461-1469.

Hide, C., Moore, T., & Smith, M. (2003). Adaptive Kalman filtering for low-cost INS/GPS. *The Journal of Navigation, 56*(1), 143-152.

Hong-Quan, Q., & Shao-Hong, L. (2008). The model set multiple hypotheses IMM algorithm for maneuvering target tracking. *9th International Conference on Signal Processing*, (pp. 2302-2305).

Huang, X., & Wang, J. (2013). Robust sideslip angle estimation for lightweight vehicles using smooth variable structure filter. *ASME Dynamic Systems and Control Conference.* California.

Hwang, I., Balakrishnan, H., & Tomlin, C. (2006). State estimation for hybrid systems: applications to aircraft tracking. *IEE Proceedings-Control Theory and Applications, 153*(5), 556-566.

Imsland, L., Grip, H. F., Johansen, T. A., Fossen, T. I., Kalkkuhl, J. C., & Suissa, A. (2007). Nonlinear observer for vehicle velocity with friction and Road bank angle adaptation-validation and comparison with an extended Kalman filter. *SAE Technical Paper, 2007-01-0808*.

Ito, K., & Xiong, K. (2000). Gaussian Filters for Nonlinear Filtering Problems. *IEEE Transactions On Automatic Control, 45*(5).

Jetto, L., Longhi, S., & Venturini, G. (1999). Development and experimental validation of an adaptive extended Kalman filter for the localization of mobile robots. *IEEE Transactions on Robotics and Automation, 15*(2), 219-229.

Jia, B., Xin, M., & Cheng, Y. (2013). High-degree cubature Kalman filter. *Automatica, 49*(2), 510-518.

Jiang, Z., Song, Q., He, Y., & Han, J. (2007). A Novel Adaptive Unscented Kalman Filter for. *46th IEEE Conference on Decision and Control*, (pp. 4293-4298).

Jilkov, V. P., Angelova, D. S., & Semerdjiev, T. A. (1999). Design and comparison of mode-set adaptive IMM algorithms for maneuvering target tracking. *IEEE Transactions on Aerospace and Electronic Systems, 35*(1), 343-350.

Jitendra K, T. (1982). Detection and estimation for abruptly changing systems. *Automatica, 18*(5), 607-615.

Johansen, T. A., & Thor, I. F. (2017). The exogenous Kalman filter (XKF). *International Journal of Control, 90*(2), 161-167.

Julier, S. J. (2002). The scaled unscented transformation. *American Control Conference. 6.* IEEE.

Julier, S. J., & Uhlmann, J. K. (1996). *A general method for approximating nonlinear transformations of probability distributions.* Robotics Research Group, Department of Engineering Science, University of Oxford.

Julier, S. J., & Uhlmann, J. K. (1997). A new extension of the Kalman filter to nonlinear systems. *Int. symp. aerospace/defense sensing, simul. and controls, 3*(26).

Julier, S., Uhlmann, J., & Durrant-Whyte, H. F. (2000). A new method for the nonlinear transformation of means and covariances in filters and estimators. *IEEE Transactions on automatic control, 45*(3), 477-482.

Jwo, D.-J., Chen, M.-Y., & Tseng, C.-H. (2010). Interacting multiple model adaptive unscented kalman filters for navigation sensor fusion. *27th international congress of the aeronautical sciences*, (pp. 1-10).

Jwo, D.-J., Hu, C.-W., & Tseng, C.-H. (2013). Nonlinear filtering with IMM algorithm for ultra-tight GPS/INS integration. *International Journal of Advanced Robotic Systems, 10*(5), 222.

Kalman, R. E. (1960). A new approach to linear filtering and prediction problems. *Journal of basic Engineering, 82*(1), 35-45.

Kalman, R. E. (1961). New results in linear filtering and prediction theory. *Journal of basic engineering, 83*(1), 95-108.

Kiani, M., & Pourtakdoust, S. H. (2014). Adaptive Square-Root Cubature–Quadrature Kalman particle Filter for satellite attitude determination using vector observations. *Acta Astronautica, 105*(1), 109-116.

Kirubarajan, T., & Bar-Shalom, Y. (2003). Kalman filter versus IMM estimator: when do we need the latter? *EEE Transactions on Aerospace and Electronic Systems, 39*(4), 1452-1457.

Köppen, T., Küpper, T., & Makarenkov, O. (2017). Existence and stability of limit cycles in control of anti-lock braking systems with two boundaries via perturbation theory. *International Journal of Control, 90*(5), 974-989.

Lee, D. J., & Alfriend, K. T. (2004). Adaptive sigma point filtering for state and parameter estimation. *AIAA/AAS Astrodynamics specialist conference and exhibit.*

Lee, T. S. (1988). Theory and application of adaptive fading memory Kalman filters. *IEEE transactions on circuits and systems, 35*(4), 474-477.

Lefebvre, Herman Bruyninckx, T., & Schutter, J. D. (2004). Kalman filters for non-linear systems: a comparison of performance. *International journal of Control, 77*(7), 639-653.

Lefebvre, T., Bruyninckx, H., & Schuller, J. D. (2002). "Comment on" A new method for the nonlinear transformation of means and covariances in filters and estimators"[with authors' reply].". *IEEE Transactions on Automatic Control, 47*(8), 1406-1409.

Lefebvre, T., Bruyninckx, H., & Schutter, J. D. (2004). Kalman filters for non-linear systems: a comparison of performance. *International journal of Control, 77*(7), 639-653.

Li, W., Sun, S., Jia, Y., & Du, J. (2016). Robust unscented Kalman filter with adaptation of process and measurement noise covariances. *Digital Signal Processing, 48*, 93-103.

Li, X. R. (1994). Multiple-model estimation with variable structure: Some theoretical considerations. *Proceedings of the 33rd IEEE Conference on Decision and Control* (pp. 1199-1204). IEEE.

Li, X. R. (1998). Optimal selection of estimate for multiple-model estimation with uncertain parameters. *IEEE Transactions on Aerospace and Electronic Systems, 34*(2), 653-657.

Li, X. R., & Jilkov, V. P. (2001). Survey of maneuvering target tracking: III. Measurement models. *Signal and Data Processing of Small Targets, 4473*.

Li, X. R., & Jilkov, V. P. (2005). Survey of maneuvering target tracking. Part V Multiple-model methods. *IEEE Transactions on Aerospace and Electronic Systems, 41*(4), 1255-1321.

Li, X. R., & P. Jilkov, V. (2001). Survey of maneuvering target tracking: II. Ballistic target models. *Signal and Data Processing of Small Targets, 4473*.

Li, X. R., & P. Jilkov, V. (2003). Survey of maneuvering target tracking. Part I. Dynamic models. *IEEE Transactions on aerospace and electronic systems, 39*(4), 1333-1364.

Li, X. R., & Vesselin, P. J. (2000). Survey of maneuvering target tracking: dynamic models. *International Society for Optics and Photonics, AeroSense 2000.* nternational Society for Optics and Photonics.

Li, X. R., & Zhang, Y. (2000). Numerically robust implementation of multiple-model algorithms. *IEEE Transactions on Aerospace and Electronic Systems, 36*(1), 266-278.

Li, X.-R. (2000). Engineer's guide to variable-structure multiple-model estimation for tracking. *Multitarget-multisensor tracking: Applications and advances, 3*, 499-567.

Li, X.-R., & Bar-Shalom, Y. (1993). Design of an interacting multiple model algorithm for air traffic control tracking. *IEEE Transactions on Control Systems Technology, 1*(3), 186-194.

Li, X.-R., & Bar-Shalom, Y. (1996). Multiple-model estimation with variable structure. *IEEE Transactions on Automatic control, 41*(4), 478-493.

Lin, H.-J. A. (1993). Investigation of IMM tracking algorithm for the maneuvering target tracking. *The First IEEE Regional Conference on Aerospace Control Systems.* IEEE.

Liu, C. P. (2011). Unscented extended Kalman filter for target tracking. *Journal of Systems Engineering and Electronics, 22*(2), 188-192.

Liu, W., Shi, P., & Pan, J.-S. (2017)). State estimation for discrete-time Markov jump linear systems with time-correlated and mode-dependent measurement noise. *Automatica, 85* , 9-21.

Liu, W.-J. (2014). Adaptive sliding mode observer design for a class of uncertain systems. *International Journal of Adaptive Control and Signal Processing, 28*(12), 1341-1356.

Magill, D. (1965). Optimal adaptive estimation of sampled stochastic processes. *IEEE Transactions on Automatic Control, 10*(4), 434-439.

Maybeck, P. S., Jensen, R. L., & A. Harnly, D. (1981). An adaptive extended Kalman filter for target image tracking. *IEEE Transactions on Aerospace and Electronic System*, 173-180.

Mazor, E., A., Averbuch, B.-S. Y., & Dayan, J. (1998). Interacting multiple model methods in target tracking: a survey. *IEEE Transactions on aerospace and electronic systems, 34*(1), 103-123.

Mehra, R. (1970). On the identification of variances and adaptive Kalman filtering. *EEE Transactions on automatic control, 15*(2), 175-184.

Mehra, R. (1972). Approaches to adaptive filtering. *EEE Transactions on automatic control, 17*(5), 693-698.

Mehra, R., Seereeram, S., Bayard, D., & Hadaegh, F. (1995). Adaptive Kalman filtering, failure detection and identification for spacecraft attitude estimation. *4th IEEE Conference on Control Applications* (pp. 176-181). IEEE.

Mehrotra, K., & Mahapatra, P. R. (1997). A jerk model for tracking highly maneuvering targets. *IEEE Transactions on Aerospace and Electronic Systems, 33*(4), 1094-1105.

Meng, J., Luo, G., & Gao, F. (2016). Lithium polymer battery state-of-charge estimation based on adaptive unscented Kalman filter and support vector machine. *IEEE Transactions on Power Electronics, 31*(3), 2226-2238.

Meng, Y., Gao, S., Zhong, Y., Hu, G., & Subic, A. (2016). Covariance matching based adaptive unscented Kalman filter for direct filtering in INS/GNSS integration. *Acta Astronautica, 120*, 171-181.

Mirzaeinejad, H., & Mirzaei, M. (2010). A novel method for non-linear control of wheel slip in anti-lock braking systems. *Control Engineering Practice, 18*(8), 918-926.

Mohamed, A. H., & Schwarz, K. P. (1999). Adaptive Kalman filtering for INS/GPS. *Journal of geodesy , 73*(4), 193-203.

Mohan, M. S., Naik, N., Gemson, R., & Ananthasayanam, M. (2015). *Introduction to the Kalman Filter and Tuning its Statistics for Near Optimal Estimates and Cramer Rao Bound.* Indian Institute Of Technology Kanpur, India, Department Of Electrical Engineering.

Moose, R. L., Vanlandingham, H. F., & McCabe, D. H. (1979). Modeling and estimation for tracking maneuvering targets. *IEEE Transactions on Aerospace and Electronic Systems, 3*, 448-456.

Munir, A., & Atherton, D. P. (1995). Maneuvring target tracking using different turn rate models in the interacting multiple model algorithm. *4th IEEE Conference on Decision and Control. 3*, pp. 2747-2751. IEEE.

Nabaa, N., & Bishop, R. H. (2000). Validation and comparison of coordinated turn aircraft maneuver models. *IEEE Transactions on aerospace and electronic systems, 36*(1), 250-259.

Naidu, V. P., Gopalaratnam, G., & Shanthakumar, N. (2007). Three model IMM-EKF for tracking targets executing evasive maneuvers. *45th AIAA Aerospace Sciences Meeting and Exhibit.* AIAA.

Nam, K., Hiroshi, F., & Yoichi, H. (2012). Lateral stability control of in-wheel-motor-driven electric vehicles based on sideslip angle estimation using lateral tire force sensors. *IEEE Transactions on Vehicular Technology, 61*(5), 1972-1985.

NøRgaard, M., Niels K, P., & Ravn, O. (2000). New developments in state estimation for nonlinear systems. *Automatica, 36*(11), 627-1638.

Ogata, K., & Yang, Y. (2002). *Modern control engineering* (Vol. 4). India: Prentice hall.

Park, K.-S., & Lim, J.-T. (2008). "Wheel slip control for ABS with time delay input using feedback linearization and adaptive sliding mode control. *International Conference on Control, Automation and Systems* (pp. 290-295). IEEE.

Partovibakhsh, M., & Liu, G. (2015). An Adaptive Unscented Kalman Filtering Approach for Online Estimation of Model Parameters and State-of-Charge of Lithium-Ion Batteries for Autonomous Mobile Robots. *IEEE Transactions on Control Systems Technology, 23*(1), 357-363.

Patel, N., Edwards, C., & Spurgeon, S. K. (2007). Tyre/Road Friction Estimation-a Comparision of Two Observers. *IEEE International Conference on Control Applications, 2007. CCA 2007* (pp. 1365-1370). IEEE.

Patra, N., Sadhu, S., & Ghoshal, T. K. (2016). Pragmatics for tuning aircraft tracking estimators. *IEEE International Conference on Power Electronics, Intelligent Control and Energy Systems (ICPEICES).* IEEE.

Patra, N., Sadhu, S., & Ghoshal, T. K. (2018). Adaptive state estimation for tracking of civilian aircraft. *IET Science, Measurement & Technology*.

Patra, N, Sadhu, S (2015). Adaptive Extended Kalman Filter for the state estimation of Anti-Lock Braking System. *India Conference (INDICON), 2015 Annual IEEE*.

Patra, N, Sadhu, S & Ghoshal T. K. (2016). Adaptive state estimation for ballistic object tracking with nonlinear model and state dependent process noise. *Power Electronics, Intelligent Control and Energy Systems (ICPEICES).* IEEE

Pitre, R. R., Jilkov, V. P., & Li, X. R. (2005). A comparative study of multiple-model algorithms for maneuvering target tracking. *Signal Processing, Sensor Fusion and Target Recognition XIV*, 549-561.

Poznyak, A. S., & Joel, C. M. (2001). Variable structure robust state and parameter estimator. *International Journal of Adaptive Control and Signal Processing, 15*(2), 179-208.

Rahimi, A., Dev Kumar, K., & Alighanbari, H. (2015). Enhanced adaptive unscented Kalman filter for reaction wheels. *IEEE Transactions on Aerospace and Electronic Systems, 51*(2), 1568-1575.

Rahimi, A., Dev Kumar, K., & Alighanbari, H. (2017). Fault estimation of satellite reaction wheels using covariance based adaptive unscented Kalman filter. *Acta Astronautica, 134* , 159-169.

Rajamani, R. G., Piyabongkarn, D., & Lew, J. Y. (2012). Algorithms for real-time estimation of individual wheel tire-road friction coefficients. *IEEE/ASME Transactions on Mechatronics, 17*(6), 1183-1195.

Raol, J. R., & Girija, G. (2001). Evaluation of adaptive Kalman filtering methods for target tracking applications. *AIAA Guidance, Navigation and Control Conference. 4106.* Montreal, Canada: AIAA.

Rawat, K. T., & Parthasarathy, H. (2008). Manoeuvring target tracking with coordinated-turn motion using stochastic non-linear filter. *International Journal of Control, 81*(7), 1102-1113.

Rezaie, J., & Eidsvik, J. (2016). A skewed unscented Kalman filter. *International Journal of Control, 89*(12), 2572-2583.

Ristic, B., Gordon, N., & Arulampalam, S. (2004). *Beyond the kalman filter: Particle filters for tracking applications.* Artech House London.

Sadhu, S., Bhaumik, S., Doucet, A., & Ghoshal, T. K. (2009). Particle-method-based formulation of risk-sensitive filter. *Signal Processing, 89*(3), 314-319.

Sadhu, S., Mondal, S., Srinivasan, M., & Ghoshal, T. K. (2006). Sigma point Kalman filter for bearing only tracking. *Signal processing*, 3769-3777.

Sage, A., & Husa, G. (1969). Algorithms for sequential adaptive estimation of prior statistics. *1969 IEEE Symposium on Adaptive Processes (8th) Decision and Control, 8*, p. 61.

Sarmavuori, J., & Sarkka, S. (2012). Fourier-hermite kalman filter. *IEEE Transactions on Automatic Control, 57*(6), 1511-1515.

Schei, T. S. (1997). A finite-difference method for linearization in nonlinear estimation algorithms. *Automatica, 33*(11), 2053-2058.

Sebsadji, Y., S., G., S., M., & J, D. (2008). Road slope and vehicle dynamics estimation. *American Control Conference* (pp. 4603-4608). IEEE.

Semerdjiev, E., Mihaylova, L., & Li, X. R. (1999). An adaptive IMM estimator for aircraft tracking. *International Conference on Information Fusion.*

Sepasi, S., Ghorbani, R., & Yann Liaw, B. (2014). A novel on-board state-of-charge estimation method for aged Li-ion batteries based on model adaptive extended Kalman filter. *Journal of Power Sources, 245* , 337-344.

Shambaky, E. H. (2011). Improving the performance of Kalman filter by updating the covariance matrix of the process noise random vector. *Survey Review, 43*(323), 598-613.

Shi, Y., Han, C., & Liang, Y. (2009). Adaptive UKF for target tracking with unknown process noise statistics. *Information Fusion, 2009. FUSION'09. 12th International Conference on* (pp. 1815-1820). IEEE, 2009.

Simeonova, I., & Semerdjiev, T. (2002). Specific features of IMM tracking filter design. *Information and Security, 9*, 154-165.

Simon, D. (2006). *Optimal state estimation: Kalman, H infinity, and nonlinear approaches.* John Wiley & Sons.

Smith, D. E., & Starkey, J. M. (1995). Effects of model complexity on the performance of automated vehicle steering controllers: Model development, validation and comparison. *Vehicle System Dynamics, 24*(2), 163-181.

Soken, H. E., & Hajiyev, C. (2009). Adaptive unscented Kalman filter with multiple fading factors for pico satellite attitude estimation. *4th International Conference on Recent Advances in Space Technologies* (pp. 541-546). IEEE .

Song, Q., & He, Y. (2009). Adaptive unscented Kalman filter for estimation of modelling errors for helicopter. *2009 IEEE International Conference on Robotics and Biomimetics (ROBIO).*

Stallard, D. V. (1982). Process-noise-adaptive Kalman filters for tracking. *Guid. Control Conf, 1*, pp. 57-65.

Tsai, C., & Kurz, L. (1983). An adaptive robustizing approach to Kalman filtering. *Automatica, 19*(3), 279-288.

Unsal, C., & Kachroo, P. (1999). Sliding mode measurement feedback control for antilock braking systems. *IEEE Transactions on Control Systems Technology, 7*(2), 271-281.

Utkin, V. I. (1993). Sliding mode control design principles and applications to electric drives. *IEEE transactions on industrial electronics, 40*(1), 23-26.

Van Der Merwe, R., Wan, E., & Julier, S. (2004). Sigma-point Kalman filters for nonlinear estimation and sensor-fusion: Applications to integrated navigation. *AIAA Guidance, Navigation, and Control Conference and Exhibit.*

Villagra, J., D'Andréa-Novel, B., Fliess, M., & Mounier, H. (2011). A diagnosis-based approach for tire–road forces and maximum friction estimation. *Control engineering practice, 19*(2), 174-184.

Wan, E. A., & Van Der Merwe, R. (2000). The unscented Kalman filter for nonlinear estimation. *Adaptive Systems for Signal Processing, Communications, and Control Symposium AS-SPCC* (pp. 153-158). IEEE.

Wang, H., Kirubarajan, T., & Bar-Shalom, Y. (1999). Precision large scale air traffic surveillance using IMM/assignment estimators. *IEEE Transactions on Aerospace and Electronic Systems, 35*(1), 255-266.

Wang, S., Habibi, S., & Burton, R. (2008). A comparative study of a smooth variable structure filter and the extended Kalman filter. *Trans. CSME, 32*(3-4), 353-369.

Wu, L., Ma, J., & Tian, J. (2010). A self-adaptive unscented Kalman filtering for underwater gravity aided navigation. *Position Location and Navigation Symposium (PLANS) 2010* (pp. 142-145). IEEE.

Xia, Q., Rao, M., Ying, Y., & Shen, X. (1994). Adaptive fading Kalman filter with an application. *Automatica, 30*(8), 1333-1338.

Xiang, J., Su, H., & Chu, J. (2005). On the design of Walcott-Zak sliding mode observer. *American Control Conference.* IEEE.

Xie, L., & Chai Soh, Y. .. (1994). Robust Kalman filtering for uncertain systems. *Systems & Control Letters* , 123-129.

Xie, L., Chai Soh, Y., & Souza, C. E. (1994). Robust Kalman filtering for uncertain discrete-time systems. *IEEE Transactions on automatic control, 39*(6), 1310-1314.

Xiong, R., H., H., F., S., & K, Z. (2013). valuation on state of charge estimation of batteries with adaptive extended Kalman filter by experiment approach. *IEEE Transactions on Vehicular Technology, 62*(1), 108-117.

Xiong, R., X., G., C. C., M., & F, S. (2013). A robust state-of-charge estimator for multiple types of lithium-ion batteries using adaptive extended Kalman filter. *Journal of Power Sources, 243*, 805-816.

Yaakov, B.-S., X, -R. L., & Kirubarajan, T. (2001). *Estimation with Applications To Tracking and Navigation.* Wiley-Interscience .

Yang, Yongjian, Fan, X., Zhuo, Z., Wang, S., Nan, J., & Huang, J. (2016). AFAKF for manoeuvring target tracking based on current statistical model. *IET Science, Measurement & Technology, 10*(6), 637-643.

Yuan, X., Han, C., Duan, Z., & Lei, a. M. (2005). Comparison and choice of models in tracking target with coordinated turn motion. *2005 7th International Conference on Information Fusion IEEE*, *2*, pp. 1497-1502.

Zarchan, P. (2005). *Progress In Astronautics and Aeronautics: Fundamentals of Kalman Filtering: A Practical Approach* (Vol. 208). AIAA.

Zhang, W., Shi, W., & Ma, Z. (2015). Adaptive unscented Kalman filter based state of energy and power capability estimation approach for lithium-ion battery. *Journal of Power Sources, 289*, 50-62.

Zhou, W. d., Cai, J. n., Sun, L., & Shen Sun, C. (2014). An improved interacting multiple model algorithm used in aircraft tracking. *Mathematical Problems in Engineering*.

Zong, C.-f., Song, P., & Hu, D. (2011). Estimation of vehicle states and tire-road friction using parallel extended Kalman filtering. *Journal of Zhejiang University-SCIENCE A, 12*(6), 446-452.